CHALMERS TEKNISKA HÖGSKOLA

CHALMERS UNIVERSITY OF TECHNOLOGY
GÖTEBORG
SWEDEN

Modelling of Solids and Metal Transport from Small Urban Watersheds

by
GILBERT SVENSSON

Chalmers University of Technology
Department of Sanitary Engineering
Göteborg 1987

PREFACE

Stormwater quantity and quality has been a major research subject at the Department of Sanitary Engineering, Chalmers University of Technology since around 1970. The research started at the department but later became an integrated part of the research effort made by the Urban Geohydrology Research Group, which was formed in 1972.

The work presented in this report is based on a study made between 1978 and 1982. The project was in practice a continuation of an earlier study on the quality of runoff from mixed urban watersheds made between 1975 and 1977. The reason for starting a new project in 1978, looking at small urban watersheds, was the difficulties we had to generalize our findings. It was my belief that it would be possible to predict urban runoff quality from detailed knowledge of runoff quality from small watersheds. Another reason for the project was the need for an urban runoff quantity simulation model. At the onset of this work, urban runoff quantity modelling had left its infant stage and was widely used in practice. However, the analysis of urban drainage systems will be incomplete as long as the runoff quality modelling is lacking or based on very simple assumptions.

This thesis deals with the modelling of solids and heavy metal (cadmium, copper and lead) transport in runoff from small urban watersheds. The model has developed within the framework of this thesis, but has not reached a commercial level. It is written in common FORTRAN and is available at the Gothenburg University Computing Centre.

It is my hope that the results of my work will be useful for the ongoing work to improve urban drainage simulation models.

Göteborg in September 1987

Gilbert Svensson

ACKNOWLEDGEMENTS

This work has been supported by grants from the Swedish Council for Building Research. This support is gratefully acknowledged since it made the field investigations and data collection possible.

During the progress of this work, many people have been involved and I would like to thank them all. A special mention is made here to:

My supervisor Peter Balmér supported me all the way, always a good reader and discussor.

In the beginning of the work the cooperation with my colleague Per-Arne Malmqvist was invaluable.

Sven Lyngfelt and Anders Sjöberg from the Department of Hydraulics contributed to the thesis by their criticism of my way of handling the hydraulics.

The field observations and data collection had not been possible without the assistance from Bengt Carlsson, Börje Sjölander and Claes Wångsell.

The laboratory experiment were partly made as a diploma thesis by Arne Lund and Roger Ström.

The laboratory work was carefully undertaken by our own laboratory and the innumerable analyses were made by Evy Axén, Gabriella Kaffehr and Mona Zanders.

Alicja Janiszewska, always willing to help, digitized all of the recorded charts and drew some of the figures.

The data processing and computer programme development were made easier with Håkan Strandner's guidance.

During the process of evaluating all the data Doug Lumley was always willing to help in finding the possibilities of the Statistical Analysis System (SAS) and Tell-a-Graph at the Gothenburg University Computing Centre. He also commented on the language in the thesis.

The word processing was done by Inger Hessel, always patient and never complaining about the different formats of the text being transmitted to the word processor from the computing centre, from desk top computers and from portables.

Thanks, to all of you.

Gilbert Svensson

SUMMARY

This thesis deals with the problem of modelling solids and heavy metals concentrations in urban runoff. A solids transport model has been developed which is based on sediment transport theories and a metals transport model based on investigations of solids associated metals in urban runoff. The developed models were verified with data from a database consisting of some thirty observed storm events. The observations were made for a roof, a parking lot and a street. The verification showed good agreement between observed and simulated concentrations as well as observed and simulated masses.

The concern for stormwater quality and its impact on receiving waters started to grow around 1970 and there are several assessments of stormwater quality from this period. The well known Sartor & Boyd study in USA dates back to 1972 and in Sweden there are the studies of Söderlund & Lehtinen (1970) and Lisper (1974). These studies established knowledge of the level of concentration of different substances found in stormwater. It was realized that stormwater could transport considerable amounts of pollutants to receiving water bodies. The two main reasons for stormwater being an important transport path for pollutants are:

- During the passage of rainwater or snow through the atmosphere and over urban surfaces there is an uptake of soluble substances, which will be transported by the runoff.

- Raindrops hitting a surface are a very good erosive agent thus creating the possibility of the runoff transporting particulate substances accumulated from atmospheric fallout and local sources.

Urban runoff quality modelling started parallel to the studies of pollutant concentration levels. The models were either based

on a pollutant buildup function for the urban surfaces and an exponential washoff function during runoff, or a constant concentration for each substance linked to the stormwater flow. Later, several attempts were made to develop more deterministic models, thus reducing the need for calibration evident in the early models. These models are not, however widely used. Still, the buildup-washoff concept dominates among the models used.

The main objectives of the present study were to obtain more basic knowledge of the washoff and transport of pollutants from urban watersheds and to improve the simulation models for stormwater quality.

The substances choosen to study in the runoff from three different types of areas (a roof, a parking lot and a street) were: suspended solids, cadmium, copper, lead and zinc. In all, five events from the roof, nine from the parking lot and 15 from the street were recorded. Discrete samples were taken with a time resolution of three to five minutes. A comparison between the studied watersheds and some mixed watersheds, which had been investigated earlier, showed that the concentration levels met the expected levels. The solids associated metal concentrations varied both within storms and between different storms. The dissolved metal concentrations were lower and varied less than the solids associated concentrations for lead and for those events with a high pH-value also for cadmium and copper. The dissolved fraction had a marked increase at lower pH-values for cadmium and copper. The solids associated metal concentrations were also analysed for different particle size fractions and found to be highly correlated to the surface area of the solids. A model with the particle diameter as the independent variable was investigated and was shown to fit the observed solids associated metal concentrations.

A solids transport model for one surface, based on sediment transport theories for non-urban surfaces, was developed. The main features of the model are the balancing of the solids

detachment rate by the transport capacity for different particle size fractions and the mass balance for the surface load of solids. This model was partly verified with data from a small laboratory surface without any rainfall impact.

The model was extended to be able to simulate surface runoff and solids transport from two surfaces connected to one gutter. The length of the gutter was the same as the width of the surfaces. This improved model was, with respect to solids transport, basically the same as the first developed model. Using the database of observed storms from the street and the parking lot, this model was verified and found to simulate both masses and concentrations in agreement with those observed.

The next step in the model development was to incorporate the solids associated metals model into the solids transport model, thus creating a model for the simulation of solids and metal transport in urban runoff. Once again the database of observed storms was used for the verification of the metals transport model. For all the verifications, storms were used which had not been used earlier for model development. The simulation of the metals transport proved to be good as long as the simulation of the solids transport was good. The transported load had to be balanced by the surface load of the catchment, otherwise too high concentrations and thus, too high loads were simulated.

The following conclusions were drawn from the work presented here:

- Solids concentration curves for urban runoff can be simulated using theories on sediment transport in open channels.

- The sediment transport rate is determined by either the detachment rate or the transport capacity.

- The transport capacity of solids is strongly dependent on particle size.

- The solids supply of a surface can be a limiting factor for the tranport of some particle size fractions.

- A first flush effect is logical and is caused by small particles which are readily transported but limited in supply.

- There is a linear relationship between the solids associated metal concentrations and the surface area of the particles.

It should be investigated if the sediment detachment and transport equations of the model presented can be simplified.The model presented should also be tested for larger catchments with a simplified areal description. An integration of the developed model in an urban drainage planning and analysis model has to be done to make the model suitable for practical applications.

TABLE OF CONTENTS

1. INTRODUCTION

1.1 The urban water cycle

Urban areas, that is areas where the man made environment dominate over the natural environment, are from a hydrological point of view still a part of the hydrological cycle. Comparing a rural area to an urban area in terms of precipitation, evapotranspiration and runoff shows less evapotranspiration, more runoff and less ground water production in an urban area. The runoff process is much more rapid in urban areas, giving higher maximum flows and thus having a high potential of transporting particulate substances and substances bound to particles. The interaction between urban areas and the atmosphere is outlined in Fig. 1.1, which shows that there is not only a deposition of substances from the atmosphere but also an uptake of substances produced within the area.

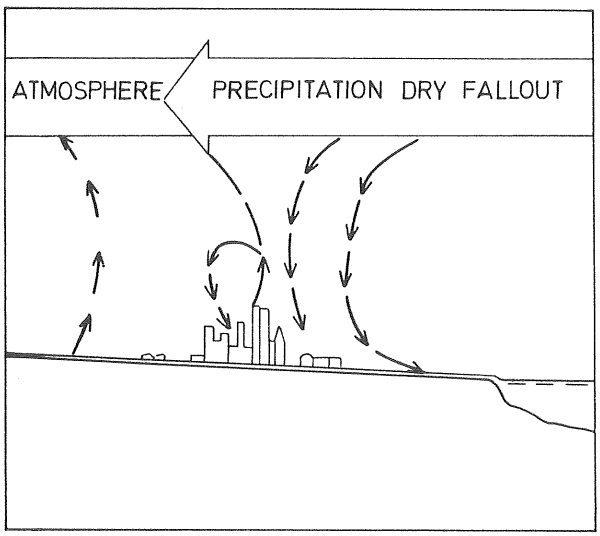

Figure 1.1 Interactions between the atmosphere and an urban area.

The local hydrological cycle is to a great extent disturbed by man made structures. In sewered areas the water balance is more or less controlled by man. In principle there are two water cycles in urban areas: One is concerned with the production and distribution of drinking water, which becomes sewage during the passage through the urban area with the later being discharged into a receiving water. The other is the rainfall-runoff process which is a part of the natural hydrological cycle. Both are outlined in Fig. 1.2, where some interactions between the two systems are also marked. For example the yearly storm water volume is of the same order of magnitude as the yearly infiltrated volume of ground water due to leaky sewers for many urban areas in Sweden.

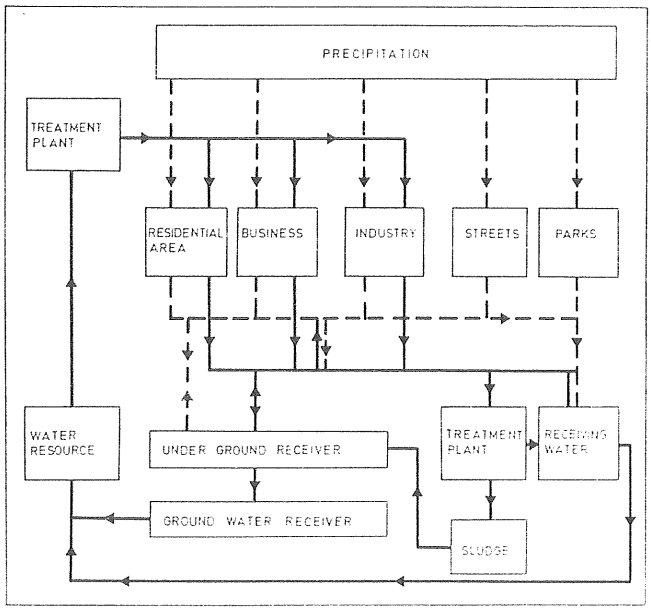

Figure 1.2 Water cycles of urban areas.

This thesis will deal only with the rainfall runoff process in urban areas and the transport of substances by stormwater. Stormwater transports considerable amounts of physical, chemical and biological substances to the receiving waters via wastewater treatment plants, combined sewer overflows and storm sewer

outfalls. To a minor extent ground water aquifers also receive stormwater through exfiltration from sewers and infiltration or percolation of stormwater into the ground.

To get an impression of the magnitudes of the mass flows in the urban rainfall runoff process, an example from the City of Lund in the southern part of Sweden, (Hogland, 1986), is shown in Fig. 1.3.

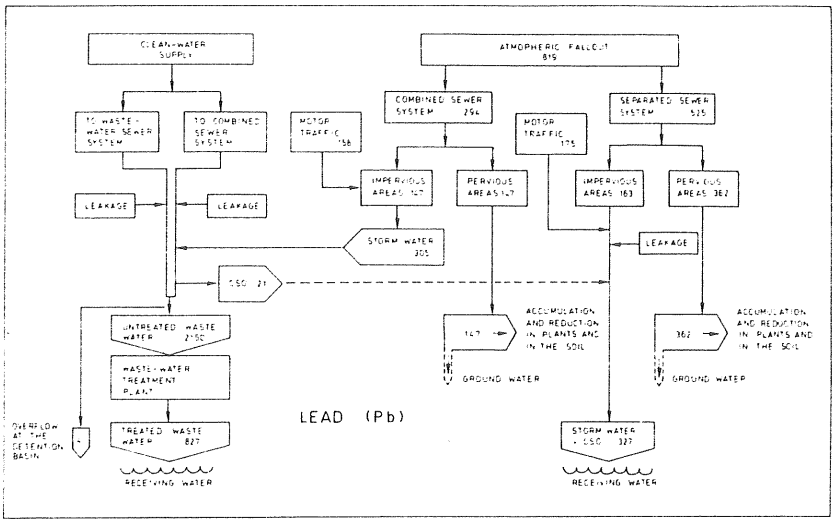

Figure 1.3 Yearly mass balance of Pb for the City of Lund, after Hogland (1986).

1.2 The recognition of storm water as an important transport path for urban pollution

The sources of the substances found in storm water can be divided into atmospheric sources and surface bound sources. Both can be further subdivided, as by Malmqvist (1983). A reproduction of this subdivision is made in Fig. 1.4

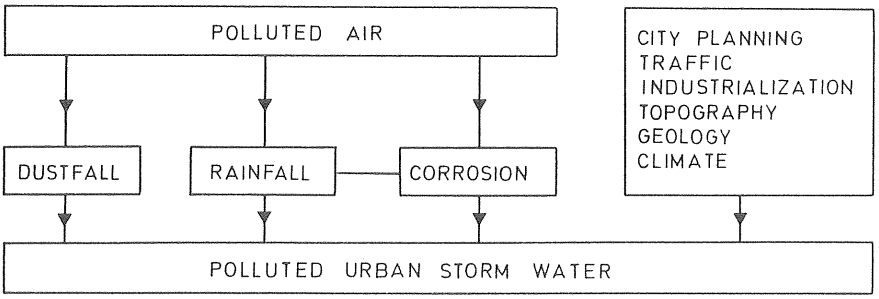

Figure 1.4 Factors influencing the quality of storm water, (after Malmqvist (1983)).

There are two main reasons why storm water is an important transport path of substances in the urban environment. The first is the fact that rainfall or snow passes through the atmosphere over an urban area and hits every part of the area at least some times every year. As water is a good solvent for many substances this causes a transport of soluble substances from the atmosphere and from urban surfaces by the runoff. The second reason is that raindrops, when hitting a surface, are a very good erosive agent, thus creating the possibility of transporting particulate substances. However, this cannot be done without the runoff having a sufficient transport capacity, which will vary with the runoff intensity, the topology of the area etc. Saying that the transport capacity varies within an area, implies that a substance can be transported from one part of an area to another, not necessarily reaching the receiving water during a single rainfall event.

An outline of the transport paths in a sewered urban catchment is shown in Fig. 1.5. All parts of the area accumulate substances between runoff events. During runoff, however, some parts will be washed, thus having less accumulated substances after the runoff event and some parts will act as a sink, thus having more accumultated substances after the event. An example of a part acting as a sink is a catch basin, which not only accumu-

late substances, but also affects the composition of the storm water through processes going on between runoff events, (Morrison (1985)).

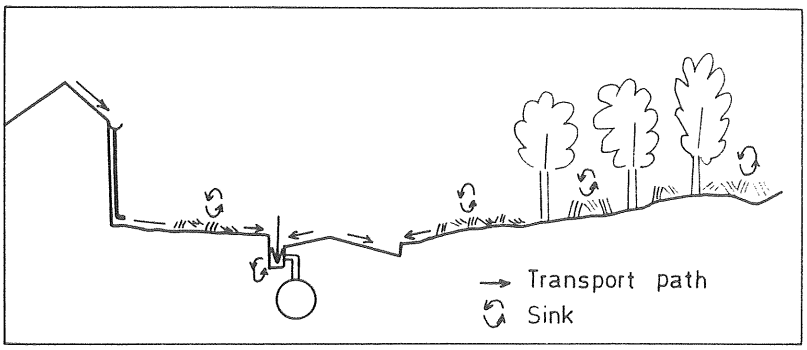

Figure 1.5 Transport paths and sinks for substances found in storm water.

1.3 Effects of storm water discharges

The physical, chemical and biological substances in stormwater may be harmful to the aquatic life in receiving waters. Looking at background concentrations of receiving waters, stormwater most often increases these concentrations, thus stormwater can be regarded as a polluter. However, wether the stormwater is harmful or not depends on the concentration levels and if they are critical for aquatic life or not.

When discussing concentration levels it is essential to distinguish between acute toxic effects and long term effects. The acute toxic effects are related to soluble or weakly bound substances, which are available for organisms and can be taken up rapidly. The long term effects are related to substances, which tend to accumulate in organisms and in plants.

The discussed effects of storm water on the aquatic life are the primary effects of storm water discharges. A secondary effect on the receiving water is the combined sewer overflow, where the flow increase during a storm event causes the overflow, and the mixture of sewage and stormwater overflowed causes the environmental effect. Similary stormwater discharges to sewage treatment plants often disturb the treatment process, thus effecting the quality of the effluent from the treatment plant.

1.4 Scientific and engineering needs of understanding the transport of substances by stormwater

The reason of studying transport of substances by storm water is mainly the environmental effects of stormwater discharges, which must be taken seriously. Even if acute toxic effects seldom are reported, storm water discharges are responsible for the poor water quality of many small streams and rivers. One of the most crucial substances in the industrialized world is cadmium, which is known to accumulate in plants and in organisms. The acceptable human intake of cadmium without permanent effects is known and can be reached during the next century if the use of cadmium is not reduced.

From a scientific point of view the interactions between storm water and surfaces or basins during the passage through an urban area is of interest. Basic knowledge of these interactions is the only source of understanding, when effects are seen in a receiving water, a treatment plant or in a ground water aquifer, which calls for an explanation.

From an engineering point of view a basic knowledge of availability and transport mechanisms for different substances is essential. The engineering task is to reduce the pollution of receiving waters and to choose the most appropriate receiving water for the pollution load under both technical and economical restrictions. To solve this problem, the engineer needs reliable tools for the simulation of transport of pollutants by storm water.

2. STORMWATER QUALITY MODELLING - A BACKGROUND

2.1 Assessment of stormwater quality

It was not until around 1970 the quality of the urban runoff was discussed and looked upon as a potential polluter of rivers and lakes. The two main reasons for this was: Firstly the concern of the quality of the receiving waters which had improved treatment of wastewater and made possible construction of many new wastewater treatment plants. Secondly the separation of stormwater and sanitary sewage. The technique of transporting stormwater and sanitary sewage in separate pipes developed parallel to the more extensive treatment of the wastewater.

In Sweden the first paper on stormwater quality dates to 1950 and was authored by Åkerlindh (Åkerlindh (1950)). His paper discusses the impact on receiving waters from urban runoff with respect to organics and nutrients.

The next step came not until the late sixties when Söderlund and Lehtinen made investigations of the quality of runoff from several urban areas with respect to organics, nutrients and heavy metals, Söderlund et al, (1970).

The investigation of Söderlund were followed by Lïsper, who investigated a heavily polluted highway in Göteborg, Lisper (1974).

Typical for these early studies were that they established knowledge of the levels of concentration of different substances found in stormwater.

A compilation of the data from Söderlund´s and Lisper´s work was made by Malmqvist and Svensson (Malmqvist et al, 1974), which was the first Swedish assessment of the stormwater quality.

In USA the interest in stormwater quality dates to the same time, the late sixties. An investigation from Chicago made by the American Public Works Association (APWA (1969)) looked not only at the stormwater quality but also the accumulation of solids on the urban surfaces. The accumulated solids were regarded as the main source of stormwater pollution.

This study was later followed by the well known investigation by Sartor and Boyd, (Sartor et al. (1972)) who reported on data from ten cities.

The established knowledge of stormwater quality in the early seventies was based on these early investigations. It was recognized that stormwater in general had lower concentration of nutrients and organics than treated wastewater but higher concentrations of certain heavy metals as for example Pb, Cu and Zn.

2.2 The early stormwater quality simulation models

Following the early investigations in the USA, models developed there tend to be based on some buildup function for the accumulation of solids on urban surfaces and an exponential washoff function. For example the Stormwater Management Model (SWMM), whose first version was presented 1971, (Metcalf & Eddy, Inc. et al. (1971)). This was a single event model for the design and analysis of combined and separated sewer networks.

Later the SWMM was followed by the Storage, Treatment, Overflow, Runoff-Model (STORM), which is a model for continous simulation of urban runoff, (Roesner et al. (1979)).

Both models used a linear buildup function according to Eq. (2.1) and an exponential washoff function according to Eq. (2.2).

$$P = at \tag{2.1}$$

$$P_0 - P = P_0(1 - e^{-krt}) \tag{2.2}$$

In Europe the NIVA-model was developed in Norway with a first version presented in 1972, Lindholm (1978). The model was developed for the analysis of combined sewer networks and included a quality model based on constant concentrations for the sanitary sewage and a power function of the discharge for the urban runoff according to Eq. (2.3).

$$P = aq^b \tag{2.3}$$

In Germany the Dorsch Consult Developed the Quantity, Quality Simulation model (QQS) in the mid seventies. A model for the continous simulation of urban runoff impact on receiving waters, Geiger (1975). The quality modelling concept of QQS was to use unit pollutographs for the calculation of urban runoff concentrations of different substances. The unit pollutographs are derived for different land uses and a calibration technique is applied to achieve as accurate unit pollutographs as possible.

Parallel to the work with model development the investigations of urban runoff and combined sewer overflow quality continued.

In Sweden Malmqvist investigated the stormwater pollutant sources (Malmqvist (1983)) and made a compilation of all investigations in the Scandinavian countries. Hogland made a mass balance for the city of Lund including both combined and separate sewers, Hogland (1986).

In Munich an extensive investigation of combined sewer runoff was made, Geiger (1984).

The Nationwide Urban Runoff Program (NURP), EPA (1983) in the USA has compiled urban runoff quality data from some 30 cities.

It has been realized that the simulation of urban runoff quality includes so many uncertainties that a credible result demands some means of calibration, which have been achieved by the compilation of urban runoff quality data in several countries.

2.3 Towards a more deterministic modelling concept

In the late seventies several attempts were made to build more physically based urban runoff quality models. The main reason was the evident need for calibration of the early models for each application.

The idea was to apply sediment transport models for rural areas to urban areas. Simons et al., (1977b) presented this idea followed by Sutherland et al. (1979). Sutherland made a complete model for urban solids transport but did not include other substances than the carrier, the solids. Price et al. (1978) made a similar attempt for solids.

These deterministic models have however not been widely used because of the lack of data on substances attached to the solids.

A summary by Huber (1986) on operational urban runoff quality models does not include any of these more physically based models but only the buildup-washoff type of models, see Table 2.1.

Table 2.1 Operational urban runoff quality models (from Huber (1986)).

Model	Year originated	Number of Pollutants	Simulation type	Reference
DR3M-QUAL	1982	4	C, SE	Alley et al. (1982)
FHWA	1981	13	SE	Dever et al. (1983)
HSPF	1976	10	C, SE	Johansson et al. (1980)
QQS	1975	2	C, SE	Geiger (1975)
STORM	1974	6	C	Roesner et al. (1974)
SWMM	1971	10	C, SE	Huber et al. (1981)

C = continous simulation
SE = single event simulation

Including the operational models used in Scandinavia, i.e. the MOUSE-model (Lindberg et al. (1986) and the NIVANETT-model (Lindholm (1978)) does not make any change. These are also based on constant or runoff related concentrations, which have to be calibrated.

3 THE PRESENT STUDY

3.1 Objectives

The main objectives of this study were to obtain more basic knowledge of the washoff and transport of pollutants from urban surfaces during storm runoff. Most of the research that was carried out before this study was initiated in 1977, had been of the black box type. That is, establishing relationships between input and output without trying to describe the underlying physical and chemical processes. This technique can be proven very successful but is based on large databases, which represent the variation of climatic factors and physical and chemical area specific factors. Since the build-up of these databases was very slow and costly, it was thought to be interesting to look into the processes involved in the washoff and transport of pollutants with surface runoff.

An important objective was not only to gain more knowledge of the above mentioned processes but also to express this knowledge in mathematical forms. The study should contribute to the process of improving simulation models for storm water quality. The latter objective was in fact a first priority objective, but it was believed not possible to fulfill without the former objective.

The study was planned to contain laboratory experiments with particle transport by surface flow and field observations of surface runoff quantity and quality for small uniform watersheds. Parallel to the laboratory work and field observations the construction of a process based simulation model was made.

3.2 Operation and limitations

The restrictions of the study both in time and money made it neccessary to limit the study to substances in storm water,

which were believed to be important from an environmental point of view. The substances which were choosen are: Suspended solids, cadmium, lead, copper and zinc.

The work was divided into six parts, some of which could be carried out parallel and some sequentially. The order they are presented below gives roughly the chronological order.

A laboratory study was made to investigate the possibility of using particle erosion-transport equations primarily developed for naturally vegetated surfaces. To this part a small laboratory surface was constructed with a surface cover similar to an asphalt surface. Experiments were made with particles in the same size range as particles found on urban surfaces and were evaluated by a simple erosion-transport model.

The main part, considering time and money, was the field observations of rainfall intensity and runoff from three small uniform catchments. Three typical types of areas were included: A part of a street, a parking lot and a roof. Approximately 80 % of the runoff volume in an urban area comes from these three types of areas. The observations were made from June to November during two years and included rainfall intensity, surface flow and discrete sampling throughout the storm events.

Parallel to the field observations, the physico-chemical laboratory work was carried out. The work included separation of the samples into a solid phase and a dissolved phase. The analyses made for both phases were solids concentration, metal concentration, pH and conductivity. To separate the two phases both filtration and centrifugation were used. Some storms were treated more extensive and the samples separated into the two phases for different particle size ranges.

Based on the laboratory particle transport experiments and the analysis of the field observations, relationships were established between; a) particle transport and hydraulic parameters

and b) particle concentrations for different particle sizes and metal concentrations. This was the base of the simulation model for particle and metal transport with surface runoff. The appropriateness of the model was evaluated with the data from the field observations.

4. PARTICLE TRANSPORTATION WITH SURFACE RUNOFF

4.1 Approach to the problem

4.1.1 Surface runoff

Surface runoff can be characterized as a shallow gravity flow. The runoff is produced by rainfall andthe water depth is governed by the slope and the roughness of the surface. A natural drainage area consists of areas or planes with different slopes and roughnesses. For this reason it is neccessary to divide the drainage area into several planes each of them with uniform slope and roughness. The problem is then reduced to treating a plane with uniform slope and roughness. Each plane has two inflows: The rainfall evenly distributed over the plane and the upstream inflow. The only outflow is the downstream one. These planes are linked together in a certain way which has to be described by the model. The links will either be non-point, that is one plane discharges to another or physically existing as open channels or closed conduits.

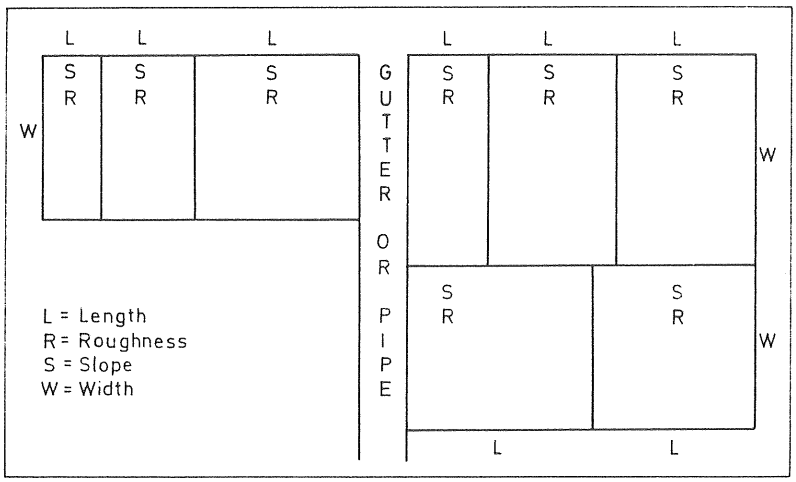

Figure 4.1 Outline of an urban catchment as a surface runoff model sees it.

There are several different techniques used to convert rainfall to runoff. One theory which realistically represents the physics of surface runoff is the kinematic wave theory, see for example Lyngfelt (1985). This theory is an approximation of the equations of continuity and momentum and has successfully been used to simulate surface runoff, Lyngfelt (1985).

4.1.2 Sediment transportation with surface runoff

Sediment transportation with surface runoff is a process of particle detachment and particle transport by erosive agents. The particles will be detached partly by rainfall and partly by overland flow. Once detached the particles will be transported downstream with the overland flow. Each particle will either continue to be transported or begin to settle depending on the flow conditions. If a particle begins to settle, it will be transported downslope again when the flow conditions have changed and are favourable for transport instead of settling.

In theory each individual particle has its own critical flow conditions which governs when the particle begins to settle. In practise, however, it is necessary to lump the particles together into groups, which will be characterized by the geometric means of the individual particle sizes and the density.

The total particle yield is a function of supply and transport capacity. The supply for transport is governed by detachment by raindrops and by flow. The transport capacity is governed by the flow conditions. From time to time during a stormevent conditions will change between supply and transport as the governing factor.

4.1.3 Application to urban areas

Sediment transport with surface runoff from areas of unprotected soil is an important problem in many countries. Considerable research effort has been put into this problem and as a result

theories have been established which describe sediment transport with surface runoff, river flow and channel flow, (Kinori et al. (1984)).

The total solids load in stormwater from urban areas originate however seldom from unprotected soil but from impervious urban surfaces. Several processes are involved, as illustrated in Fig.4.2, in the transport. The total yield from an urban area is of a different magnitude compared to the yield from a rural area. Still, a physically based theory for sediment transport will be applicable to both problems.

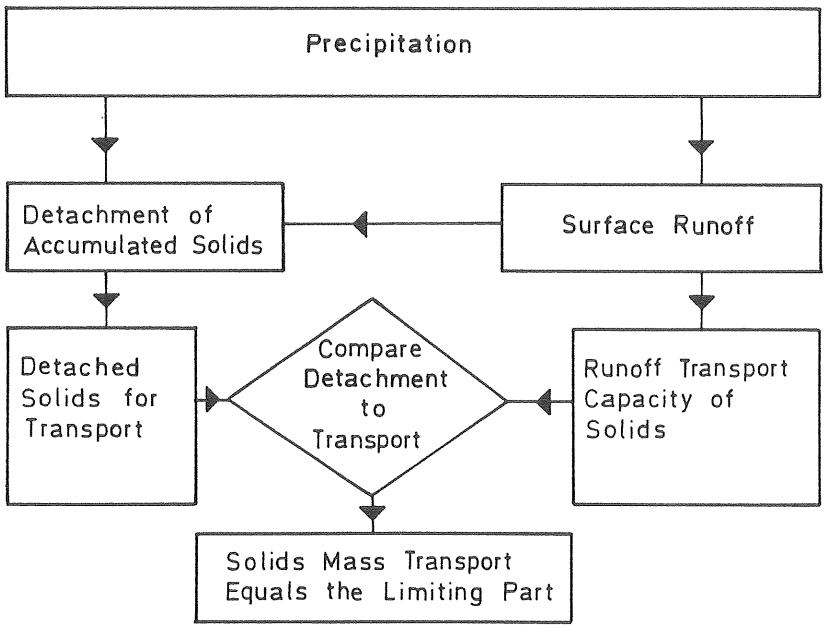

Figure 4.2 Processes involved in the particle transport by surface runoff in urban areas.

The analogy between the two problems is obvious. Surface runoff caused by rainfall is the erosive agent in both cases. The most important difference is the distribution of particles over the ground and the total mass of the load. In the urban case the particle load is limited and unevenly distributed over the surfaces while the rural case has an unlimited supply of particles which are more or less evenly distributed over the surfaces.

The processes involved in the particle transport by surface runoff for urban areas, illustrated in Fig. 4.2, are: Transport capacity, flow detachment and detachment by raindrops. Limiting factors are the available supply and armoring effects of the surface.

4.2 Basic principles of surface runoff

4.2.1 Rainfall and initial losses

Rainfall is ususally denoted by i. The rainfall intensity is time and space dependent and should therefore be written, $i(t,x)$, where t is the elapsed time from the beginning of the rainfall and x a coordinate. However, the space dependent variation is normally ignored for small urban catchments, why the rainfall intensity is written, $i(t)$.

For sewered urban areas the runoff from the impervious surfaces produces the major part of the runoff. Only at special occasions, for example at snowmelt or a long period of rainfall, does the runoff from the impervious surfaces pay an important role in the rainfall-runoff process. The runoff process for pervious surfaces will not be further discussed in this thesis.

The rainfall losses for the impervious surfaces will be limited to wetting of the surface and ponding. These losses have been estimated from several investigations to be less than 1 mm of rainfall, Arnell (1982). The effective rainfall, i_e, can then be written:

$$i_e(t) = i(t) - i_p(t) \qquad (4.1)$$

where $i_p(t)$ is the intensity of ponding and wetting of the surface.

4.2.2 Surface runoff

The surface runoff is denoted by q_r. The runoff is time dependent, and is written as $q_r(t)$. Fig. 4.3 shows a section of a small catchment with an upstream inflow, $i_u(t)$, and a $q_r(t)$, which will vary with the x-coordinate along the surface.

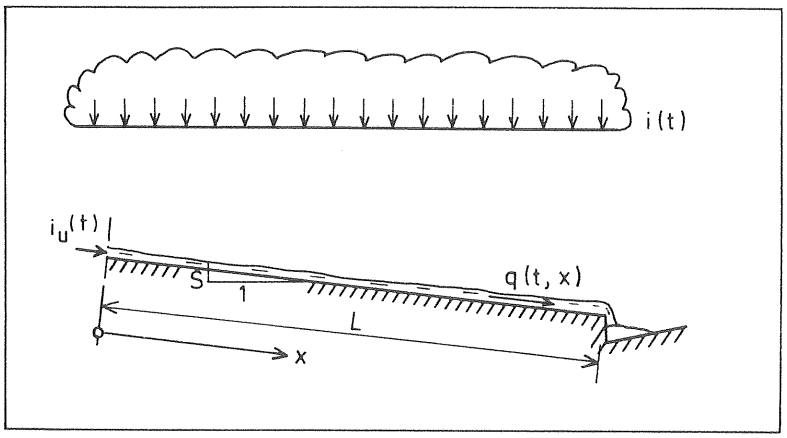

Figure 4.3 Schematic view of a surface runoff area.

Since $q_r(t)$ equals $i_u(t) + i_e(t)$ and the term $i_u(t)$ is zero for a surface with no inflow from upslope, the average runoff can be written:

$$q_r(t) = \int_0^L i_e(t)\ dx = i_e(t)\ L \qquad (4.2)$$

The runoff volume, the yield, is calculated through the integration of Eq. (4.3) for the duration of the rainfall.

$$Y_w = W\int_0^D q_r(t)\ dt = WL\int_0^D i_e(t)\ dt \qquad (4.3)$$

Y_W = the runoff volume
W = the width of the area
L = the length in direction of slope
D = the duration of rainfall

However, this concept does not take into account the traveltime over the surface. It is a fair approximation for small surfaces, i.e. short length in the direction of slope.

A more general expression for the surface runoff has to take the traveltime into account. A most commonly used set of equations is the kinematic wave approximation of the equation of motion. This was presented by Lighthill and Witham (1955) and has later been discussed by Woolhiser and Liggett (1967) and Lyngfelt (1985). The kinematic wave equations are written:

$$\frac{\partial q_r}{\partial x} + \frac{\partial y}{\partial t} = i_e + i_u \qquad (4.4)$$

$$S_f - S_0 = 0 \qquad (4.5)$$

where y is the water depth, S_f the friction slope (i.e. the slope of the water surface) and S_0 the bottom slope.

Eq. (4.5) is the uniform flow form of the momentum equation, which also can be written:

$$q_r = K\sqrt{S_0}\ y^b \qquad (4.6)$$

K = friction parameter
b = exponent dependent on the friction relation used

For a segment of an overland flow catchment as shown in Fig. 4.3, but with no upstream inflow, the continuity equation (Eq. 4.5) can be written:

$$\frac{\partial q_r}{\partial x} + \frac{\partial y}{\partial t} = i_e \qquad (4.7)$$

using that the only lateral inflow is the rainfall excess.

The roughness parameter, K, in Eq. (4.6) equals 1/n using the Manning formula and equals $(8g/f)^{\frac{1}{2}}$ using the Darcy-Weissbach formula. Now rewriting the momentum equation (Eq. 4.6) using either of the two friction relations gives:

The Manning formula

$$q_r = \frac{1}{n}\sqrt{S_0}\ y^{5/3} \qquad (4.8a)$$

n = Manning roughness coefficient

and the Darcy-Weissbach formula

$$q_r = \sqrt{\frac{8g}{f}S_0}\ y^{3/2} \qquad (4.8b)$$

g = acceleration of gravity
f = Darcy Weissbach friction factor

4.2.3 Channel flow

The kinematic wave equations given in Chap. 4.2.2 are also applicable to channel flow. But for channel flow it is more appropriate to talk of the flow rate, Q. That is the cross sectional area is defined by the channel shape and the water depth, thus giving the total flow.

The continuity and momentum equations are then written:

$$\frac{\partial Q}{\partial x} + \frac{\partial A}{\partial t} = q_r \qquad (4.9)$$

$$S_f - S_c = 0 \qquad (4.10)$$

Using the Manning formula to express the friction relation gives:

$$Q = \frac{1}{n}\sqrt{S_c}\; y^{5/3}\; B \qquad (4.11a)$$

B = channel width
S_C = channel slope

and using the Darcy-Weissbach formula gives:

$$Q = \sqrt{\frac{8g}{f}S_c}\; y^{3/2}\; B \qquad (4.11b)$$

For a prismatic channel, B is the physical width and y is the depth. However, for triangular channels, as for example a gutter will be, the corresponding width and depth has to be calculated from the geometry of the channel.

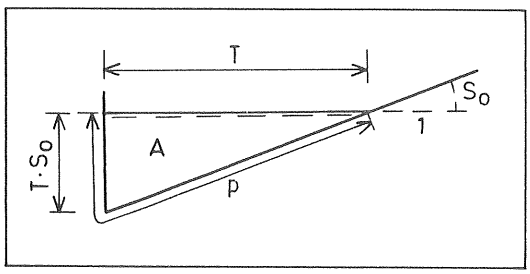

Figure 4.4 A triangular channel, as for example a gutter.

Using the notations in Fig. 4.4 the wetted perimeter and the area of the channel can be written:

$$P = TS_0 + \sqrt{T^2 + (TS_0)^2} \qquad (4.12)$$

T = channel width of water surface
P = wetted perimeter

$$A = T^2 \frac{S_0}{2} \qquad (4.13)$$

A = cross section area

Thus the hydraulic radius, R will be:

$$R = \frac{A}{P} = T \frac{S_0}{2(S_0 + \sqrt{1 + S_0^2})} \qquad (4.14)$$

Now the friction relation can be expressed in terms of the channel sidewall slope, S_0. Using the Manning or the Darcy-Weissbach formula to express the momentum equation gives:

a) The Manning formula for channel flow:

$$Q = \frac{1}{n}\sqrt{S_c}\ R^{2/3}\ A \qquad (4.15)$$

Inserting (4.14) and rearranging gives

$$Q = \frac{1}{n}\ (\frac{1}{2})^3\ (\frac{\sqrt{S_0}}{S_0 + \sqrt{1 + S_0^2}})^{2/3}\ \sqrt{S_c}\ A^{4/3} \qquad (4.16)$$

which can be used to calculate the flow, knowing the cross sectional area, for a gutter.

b) The Darcy-Weissbach formula for channel flow:

$$Q = \sqrt{\frac{8g}{f}} \sqrt{R} \sqrt{S_c} \; A \qquad (4.17)$$

Inserting Eq. (4.14) and rearranging gives

$$Q = \sqrt{\frac{8g}{f}} \; (\frac{1}{2})^{1/4} \; (\frac{\sqrt{S_0}}{S_0 + \sqrt{1 + S_0^2}})^{1/2} \; \sqrt{S_c} \; A^{5/4} \qquad (4.18)$$

Eq. (4.17) and (4.18) are the friction relation of a triangular channel with one vertical sidewall and one sidewall with the slope S_0, the same slope as of the connecting catchment.

4.2.4 The transformation of a rainfall hyetograf to an overland flow hydrograf

The transformatioon of rainfall to runoff using the kinematic wave equations can be made using different numerical methods. The difference between the metods have been discussed elsewhere, for example Lyngfelt (1985). Here a finite difference method, (Li et al (1975) and Simons et al (1977)), is applied to discuss the properties of the hydrograph when the water leaves the surface and enters the gutter and when it leaves the gutter.

Fig. 4.5 gives a schematic view of the transformation process. The hydrographs at the end of the surface, q(t) and at the end of the gutter, Q(t) will be discussed with respect to slope and rainfall intensity.

Using an area with a slope length, L=35 m and a width W=12.5 m and varying the rainfall intensity and the slope of the surface, shows the range of water depths and velocities which are normally present at runoff, see Fig. 4.6.

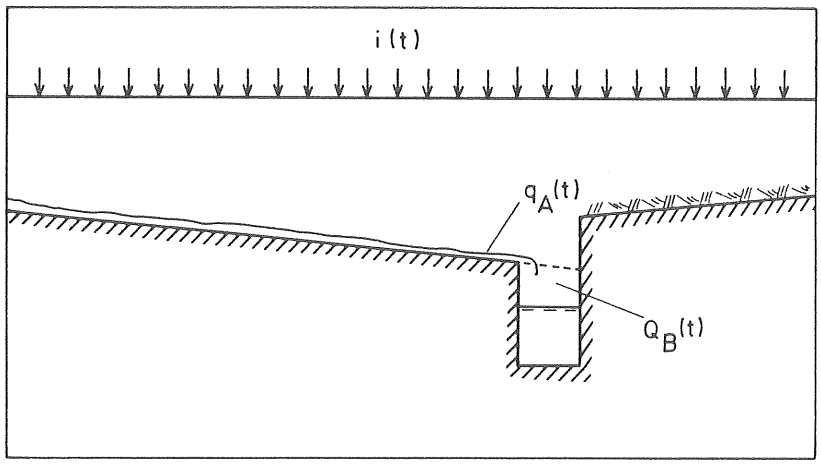

Figure 4.5 Schematic view of the transformation of rainfall to runoff.

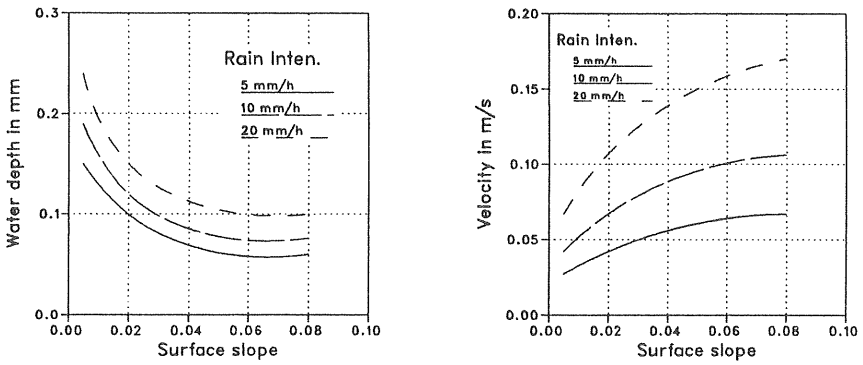

Figure 4.6 Water depths and velocities present at surface runoff with a slope length of 35 m.

The same demonstration can be done for the gutter, as shown in Fig. 4.7. The rainfall intensity was 10 mm/h through these calculations.

To demonstrate the variation in velocity throughout a runoff event the rain event in Fig. 4.8 has been choosen. The runoff is calculated for the same catchment (one plane and a gutter) but only for one set of slopes (S_o=0.01 and S_c=0.02).

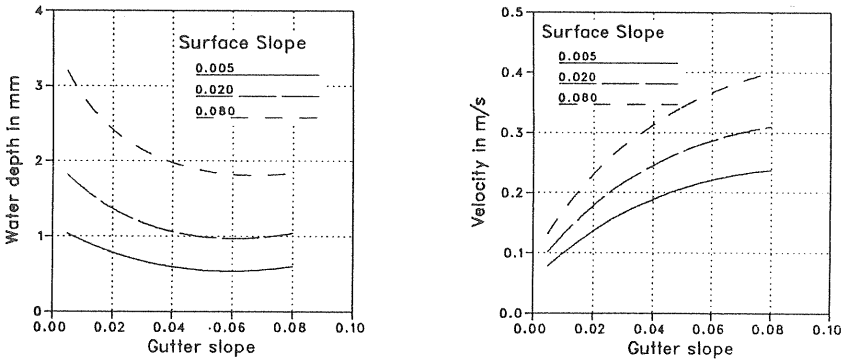

Figure 4.7 Water depths and velocities present at gutter flow with a gutter length of 12.5 m.

Looking at the hydrographs at the entrance to the gutter and at the outlet gives evidence of the continous process of decreasing the peak flows and increasing the duration of runoff. Fig. 4.8 shows that the peak is decreased with a factor of 0.3 over the surface but only slightly reduced while passing the gutter.

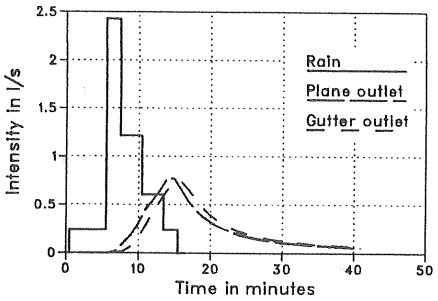

Figure 4.8 Hydrographs for overland flow and gutter flow for one rainfall event.

The velocities, shown in Fig 4.9, are relatively small for the surface thus giving the largest reduction of the peak over the surface.

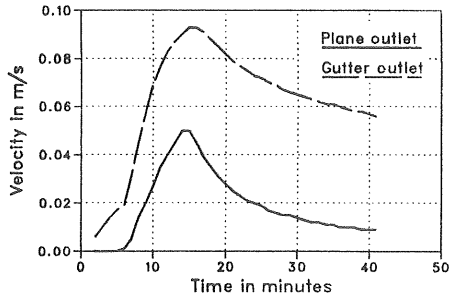

Figure 4.9 Velocities at the entrance of the gutter and at the outlet for the rainfall event in Fig. 4.8.

By these examples it is shown that the velocity is sensitive to both slope and rainfall intensity. Thus, for a specific plane and a specific gutter, the velocity is only sensitive to the rainfall intensity.

4.3 Basic principles of sediment transport with surface runoff

4.3.1 Detachment of sediment

The amount of sediment of an impervious urban surface available for transport is dependent on the detachment of particles by raindrops and by overland flow. Only particles which have been detached from the sediment supply will be available for transport during runoff.

The nonporous volume per unit of time of sediments available for transport, V_{sa} can be written as the sum of the volume per unit of time detached by raindrops, V_{sr}, and the volume per unit of time detached by overland flow, V_{sf}, according to Eq. (4.19).

$$V_{sa} = V_{sr} + V_{sf} \tag{4.19}$$

Detachment of particles by raindrops

Raindrops are a primary source of kinetic energy for detaching soil from a surface with a sediment supply. The erosive capacity can be directly related to a power function of the rainfall intensity, given among others by Meyer (1971). Other factors are the sediment supply conditions with respect to erodibility and the distribution of the sediments over the surface.

The equation of the detachment by raindrops can be written:

$$V_{sr} = D_r i^a LW(1 - \phi)A_s \qquad (4.20)$$

where D_r is a constant describing erodibility of the sediment supply, Φ is the porosity of the sediments and A_s is the fraction of the surface area which is covered with sediments. The power constant, a, has been discussed by Meyer (1971), who suggests a value of 2.0.

To make it possible to interpret the detachment coefficient by a physical property, a rainfall intensity constant, i_d, is introduced. When the rainfall intensity equals i_d, the detached non porous volume will equal the detachment coefficient for a unit area with sediment. Eq. (4.20) can then be written:

$$V_{sr} = D_r \left(\frac{i}{i_d}\right)^2 LW(1 - \phi)A_s \qquad (4.21)$$

The detachment coefficient, D_r, is then the depth to which the rainfall intensity i_d penetrates the sediment layer per unit of time.

Meyer (1971) suggests values of D_r in the range of 0.02 to 0.03. This means a penetration depth of 20 to 30 mm/h at the unit rainfall intensity, i_d = 25.4 mm/h.

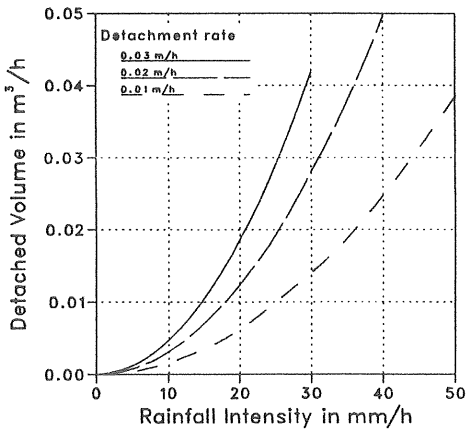

Figure 4.10 The detached volume by raindrops for a unit area as a function of rainfall intensity and detachment rate.

In Fig. 4.10 the detached volume by raindrops is shown for different values of D_r.

Detachment of particles by overland and gutter flow

The detached volume by flow, per unit time, V_{sf}, is dependent on the transport capacity of the flow. If the transport capacity for a particle size is zero or if the transport capacity is occupied by particles detached by rainfall, there will be no detachment by flow.

The expression for the detachment rate by flow can be written:

$$V_{sf} = D_f (V_{st} - V_{sr}) \qquad (4.22)$$

where V_{st} is the total sediment transport capacity of the flow and D_f is the detachment coefficient for flow. The detachment coefficient ranges between 0 and 1.0. If, for example, the sediments always are loose it should be unity and if the sediments are protected in some way it should be zero. In between, D_f depends on the surface roughness, the flow conditions and the

soil erodibility. However difficult to estimate from a theoretical discussion, it should be empirically determined.

4.3.2 Overland flow particle transport

There are two overland flow particle transport mechanisms, a) a balance between lift forces and settling forces which, if the lift forces dominate, yields a suspended load and b) shear stress from the flow acting on the sediment layer which transports particles near the sediment layer.

Taking particle size as a charachteristic parameter, the sediment yield of the surface flow can be divided into three groups. The wash load, which consists of the finer size fractions, is kept in suspension from the moment the particles are detached from the sediment layer. This means that the wash load is seldom limited by transport capacity but by availability. The suspended load consists of coarser particles in suspension. As the flow conditions changes the suspended load will change. The bed load consists of the coarsest particles. These are transported along the sediment layer and are really never suspended.

Sediment transport with runoff from impervious urban areas is accounted for mainly by the wash load and the suspended load, which is the total suspended load. From a transport point of view the bed load is not very important, but the mechanisms near or in the sediment layer related to bed load transport make particles available to be suspended.

An outline of the three forms is made in Fig. 4.11.

The bed load transport

According to modern concepts of bed load transport mechanisms, particles on the sediment layer will begin to move when a critical shear stress level is reached. However, the first attempts to establish a relationship between the movement of the bed and some hydraulic parameters, have related the movement to

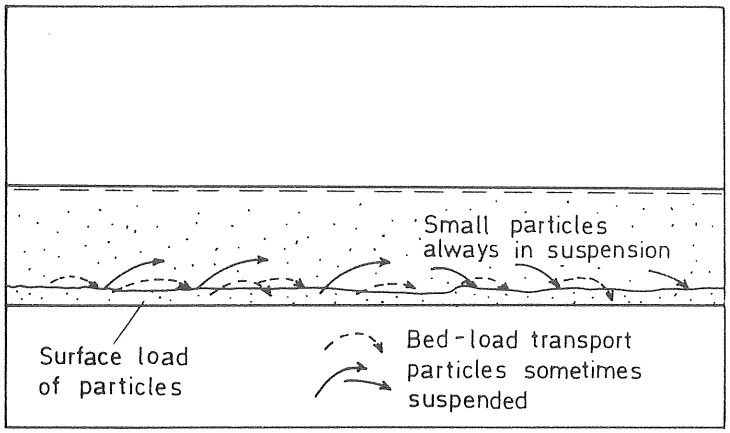

Figure 4.11 Outline of different particle transport mechanisms during surface runoff.

the mean velocity. A critical velocity was introduced for the incipient motion of particles and Hjulström (1935) presented a graph showing the relation between critical velocity, V_c, and the particle size. The graph is reproduced in Fig. 4.12, which also demonstrates the border zone between transportation and deposition.

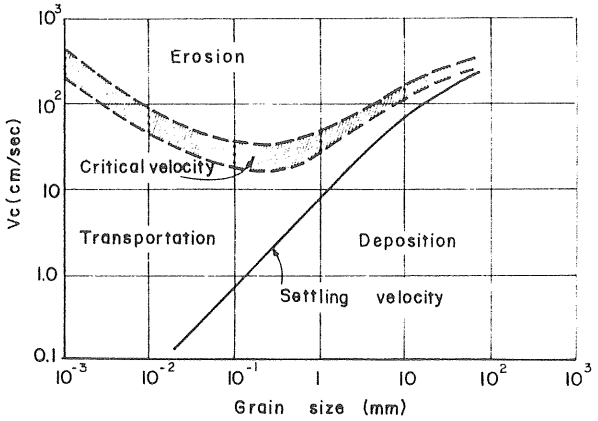

Figure 4.12 Critical velocity of incipient motion, after Hjulström (1935).

An example of the critical shear stress approach is the widely used Shields' diagram for incipient motion, shown in Fig. 4.13.

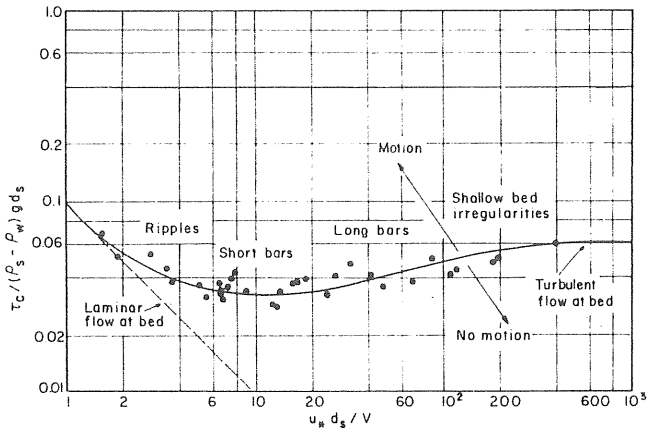

Figure 4.13 Shields' diagram of incipient motion, after Shields (1936).

According to the related development of particle incipient motion concepts, the early bed load transport rate equations were based on the critical velocity concept.

The Schoklitsch formula (1934), Eq. (4.23), is one example of the early formulas developed, which is in good agreement with formulas based on the critical shear stress concept.

$$M_s = 7000 \frac{S^{3/2}}{d_s^{1/2}} (q - q_c) \qquad (4.23)$$

M_S = bed load discharge (kg/s,m)
q_S = critical flow (l/s,m)
d_S = particle diameter (mm)
S = hydraulic gradient

The equation was developed for a wide stream which is why the discharges are related to the unit width of the bed and further the particle size is expressed in mm. For particles with a

specific density of 2.65, Schoklitsch gives the expression of q_c as:

$$q_c = 1.94\ 10^{-5} \frac{d_s}{S^{4/3}} \qquad (4.24)$$

Fig. 4.14 is a reproduction of a comparison made by Shulits (1968) between the Schoklitsch formula and later developed formulas.

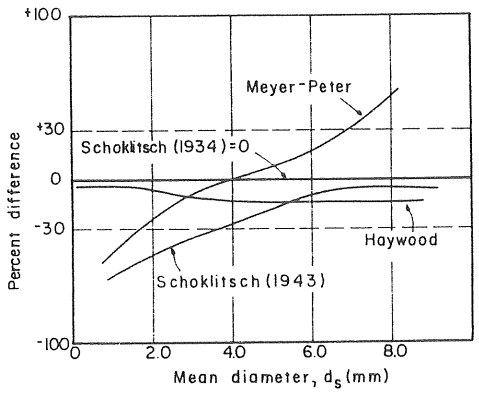

Figure 4.14 Comparison between different bed load transport rate formulas, after Shulits (1968).

However, the shear stress type of bed load equations have been favoured more and more. There have been several developed, but one of the most used is the Meyer-Peter and Müller (1948) formula. Also, the Meyer-Peter and Müller formula has been applied to surface runoff from land surfaces by Simons et al. (1978).

The original formula is given by the authors as:

$$A_b\left(\frac{\gamma}{g}\right)^{1/3}\left(\frac{\gamma_s-\gamma}{\gamma_s}\right)^{2/3} q_{sb}^{2/3} = \left(\frac{q_b}{q}\right)\left(\frac{n_g}{n_b}\right)^{3/2}\gamma y S - B_s(\gamma_s-\gamma)d_s \qquad (4.25)$$

A_b = constant
B_s = constant
n_b = Manning coefficient for bed roughness
n_g = Manning coefficient for grain roughness
q_b = bed load discharge
q_{sb} = suspended bed load discharge
γ = specific weight of water
γ_s = specific weight of sediments

The factor q_b/q was introduced to take into account the effects of the side walls in small channels and the factor can be eliminated for surface flow. The bed roughness coefficient, n_b and the grain roughness coefficient, n_g can also be set equal for overland flow. The original formula now can be rewritten in the more common form:

$$q_{sb} = K_b(\tau - \tau_c)^{3/2} \qquad (4.26)$$

K_b = constant, Eq. (4.29)
τ = shear stress
τ_c = critical shear stress

where

$$\tau = \gamma y S \qquad (4.27)$$

$$\tau_c = B_s(\gamma_s - \gamma)d_s \qquad (4.28)$$

$$K_b = \left[\frac{1}{A_b\left(\frac{\gamma}{g}\right)^{1/3}\left(\frac{\gamma_s-\gamma}{\gamma_s}\right)^{2/3}}\right]^{3/2} \qquad (4.29)$$

The two coefficients A_b and B_s are often used as calibration constants for different streams, but Meyer-Peter and Müller suggested: A_b=0.25 and B_s=0.047.

The suspended load transport

The part of the sediment load carried in suspension is influenced by two forces. Gravitational forces cause the particles to constantly fall towards the bottom. This force is however balanced by turbulence forces. Using diffusion theory it can be shown that the upward turbulent diffusion rate is proportional to the concentration gradient, dc/dy. The settling rate is proportional to the settling velocity, w, of the particles. Balancing these two rates by setting them equal gives the expression:

$$k_1 w + k_2 \frac{dc}{dy} = 0 \qquad (4.30)$$

where k_1 and k_2 are constants.

Integrating Eq. (4.30) and introducing the relative depth y/d and a reference level, y=a, at some distance from the bed gives the following expression, which was first introduced by Rouse (1937).

$$\frac{c}{c_a} = \left(\frac{d-y}{y}\,\frac{a}{d-a}\right)^z \qquad (4.31)$$

where c_a is the concentration at the distance a from the bottom $z = w/\kappa\, u_*$. The exponent z is a function of the settling velocity, w, the shear velocity, u_* and the von Karman constant, κ, which has a value of 0.40 for clear water. The variables used are also shown in Fig. 4.15.

To obtain the suspended sediment discharge, q_{ss} the concentration profile given by Eq. (4.31) has to be integrated from the reference level, y=a, to the water surface. That is:

$$q_{ss} = \int_a^d cu\, dy \qquad (4.32)$$

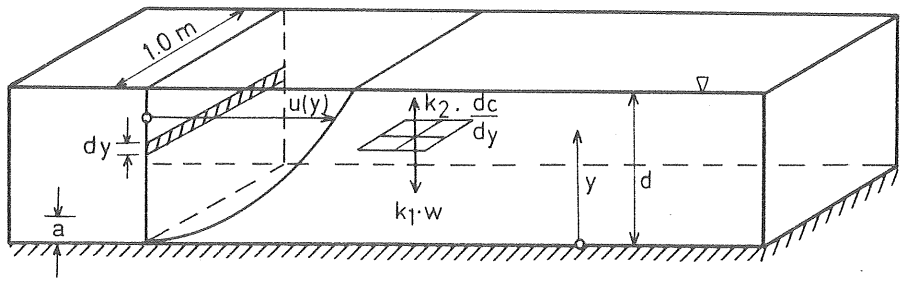

Figure 4.15 Diffusion and settling forces acting on particles in suspension.

Assuming a logarithmic velocity distribution (Einstein (1950) according to Eq. (4.33):

$$\frac{u}{u_*} = 5.75 \log(30.2\frac{y}{k_s}) \qquad (4.33)$$

k_s = roughness height
u_* = $(g\ y\ S)^{0.5}$ = shear velocity due to grain roughness

Eq. (4.32) can be rewritten:

$$q_{ss} = \int_a^d c_a(\frac{d-y}{y}\ \frac{a}{d-a})^z\ 5.75\ u_*\ \log(30.2\ \frac{y}{k_s})\ dy \qquad (4.34)$$

Introducing dimensionless ratios of the depths, $y'_a = a/d$ and $y' = y/d$ Eq. (4.34) becomes:

$$q_{ss} = \int_{y'_a}^1 cu\ dy' \qquad (4.35a)$$

$$q_{ss} = 5.75\ c_a\ u_*\ d\ (\frac{y'_a}{1-y'_a})^z \left[\log(\frac{30.2d}{k_s}) \int_{y'_a}^1 (\frac{1-y'}{y'})^z dy' + 0.434 \int_{y'_a}^1 (\frac{1-y'}{y'})^z \ln y'\ dy' \right] \qquad (4.35b)$$

Finally to be able to solve this integral numerically, Einstein (1950) transformed it to the following expression which consists of two integrals. Einstein solved these separately and presented the results in graphs. Li (1974) has later given a numerical method of solving these integrals.

$$q_{ss} = 11.6\, u_* \, c_a \, a \, (2.303 \log(\frac{30.2d}{k_s})\, I_1 + I_2) \tag{4.36}$$

$$I_1 = 0.216 \, \frac{y'^{(z-1)}_a}{(1-y'_a)^z} \int_{y'_a}^{1} (\frac{1-y'}{y'})^z dy' \tag{4.37}$$

$$I_2 = 0.216 \, \frac{y'^{(z-1)}_a}{(1-y'_a)^z} \int_{y'_a}^{1} (\frac{1-y'}{y'})^z \ln y' dy' \tag{4.38}$$

Total sediment transport capacity

The total sediment transport rate, q_{st}, is the sum of the bed load transport rate and the suspended sediment transport rate, which can be written:

$$q_{st} = q_{sb} + q_{ss} \tag{4.39}$$

According to Einstein (1950) there has to be some movement of particles near the bed to get a suspended load. He formulated the relationship as a relation between the bed load transport rate and the concentration at the reference level, y=a:

$$c_a = \frac{q_{sb}}{11.6\, u_* \, a} \tag{4.40}$$

The meaning of this is that if there is no bed load transport there can be no suspended sediment transport.

4.4 A simple model for overland flow particle transport

The simple model treats one watershed, which is described by its size, slope in the direction of flow, surface roughness and particle load on the surface, see Fig 4.16. The particle load is

described by its particle size distribution curve, which is divided into a limited number of particle size intervals, each represented by its geometrical mean value.

The particles are transported by the overland flow, which is calculated from the average rainfall intensity for the watershed using the equations given in Chap. 4.2.2. The flow calculations give the average depth and the average velocity, which are used for the particle transport calculations.

The particle transport is based on a continuity equation which literally can be expressed as: The change in particle transport over the surface has to be balanced by the change of particle mass both in the water and on the surface plus the lateral inflow of particles during one time increment. The equations for the particle transport capacity are given in Chap. 4.3.2.

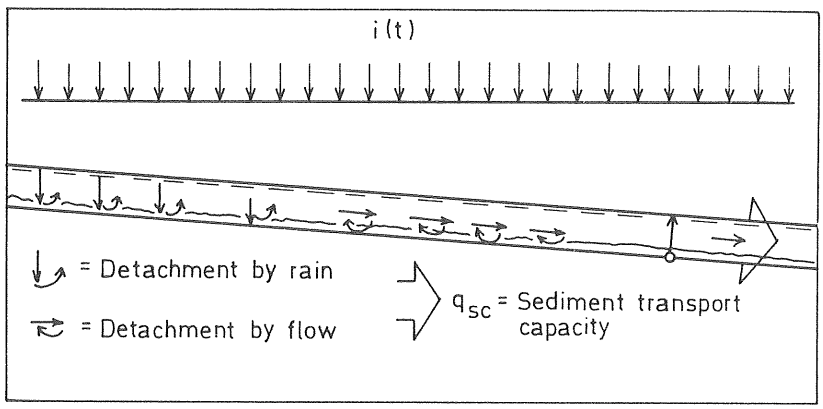

Figure 4.16 An outline of the simple surface runoff particle transport model.

However, the transport capacity can be limited by the sediment supply, both according to detachment of particles from the surface and to the total supply. The expressions for the detachment of particles by flow and raindrops are given in Chap. 4.3.1. As for total supply the accumulated transport has to be compared to the original supply on the surface.

All the calculations are made separately for each particle size interval, represented by its geometrical mean value. A flow chart for the calculations is given in Fig. 4.17, describing the loop which is run through as many times as there are particle sizes. The calculations are based on a computer programme originally published by Simons et al (1977a).

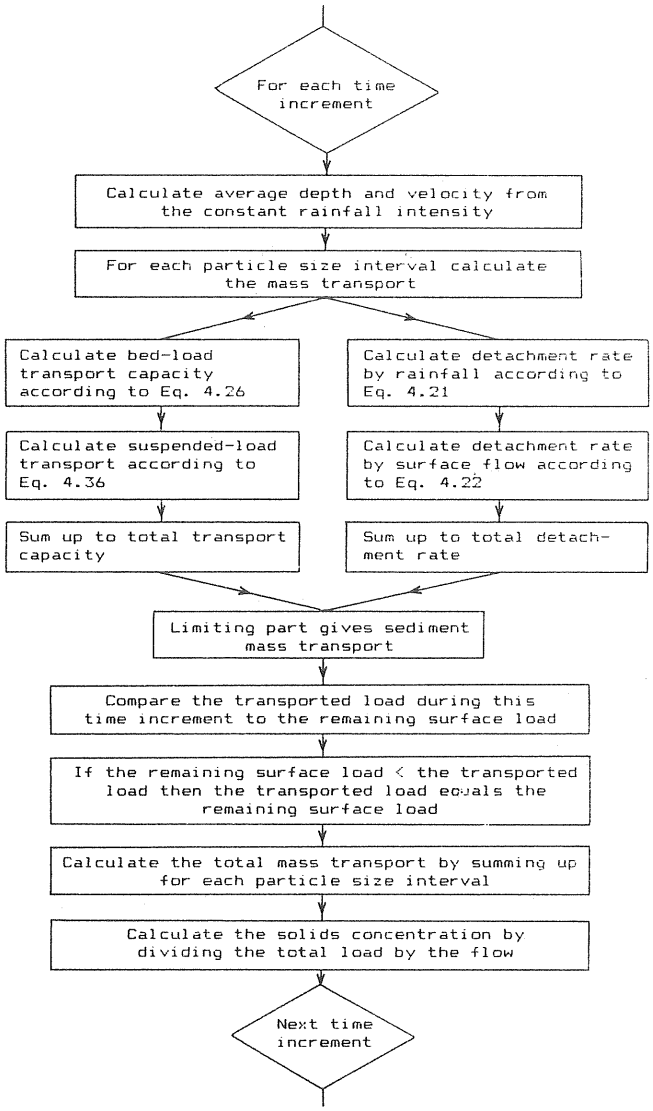

Figure 4.17 Flow chart for the simple surface runoff particle transport model.

To obtain some knowledge of the sensitivity of the model to changes in the input parametres, numerical experiments with the model were carried out. The parametres choosen for the experiments were: Slope, detachment coefficients of rain and flow (Eq. (4.21) and Eq. (4.22)), and surface roughness coefficient.

As seen from Fig. 4.18, the model is sensitive to variations in slope, detachment by rain and surface friction. The model responds positively to an increase in the detachment by rain or the slope. The slope is easily obtained for a surface but the detachment by rain coefficient has to be experimentally verified. Negative responses are obtained for the surface friction and thus the shear stress coefficient. The former can be estimated for impervious urban surfaces with good accuracy, the latter however, has to be derived from experiments.

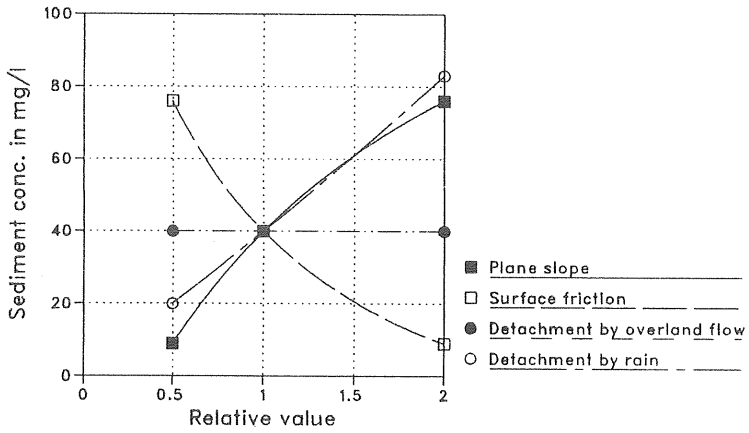

Figure 4.18 Sensitivity analysis for slope, surface friction, detachment by rain, and detachment by flow.

5 LABORATORY INVESTIGATION

5.1 Aim of the investigation

This experimental work was made to improve the understanding of the detachment and transport of particulate matter with surface runoff.

It was believed that the simple one-plane particulate transport model derived in Chap. 4 could be verified by a simple laboratory setup. Furthermore the experiments would give an understanding of the sensitivity of transport due to changes in slope, surface roughness, particle size and water depth.

5.2 A small physical model of an urban surface

5.2.1 The experimental setup

The experimental setup is shown in Fig. 5.1. The area was 4.3 m^2 and the length from where the water entered the surface to the outfall was 3.50 m. The slope of the plane could be changed from 0.055 m/m to a horisontal plane. The surface was made of Mazonite covered by a polyester resin.

The water was supplied from a storage tank. It then passed through a broadcrested curved weir in order to obtain a short transition zone. The actual flow was measured by a rotameter with a range of 0 to 1.20 l/s. The outfall was formed as a channel with a higher capacity than the maximum incoming flow to avoid backwater effects.

The Mazonite surface was supported by a large number of beams at a distance of approx. 100 mm from each other. This made it possible to avoid deflections of the surface, which otherwise could have affected the water depths.

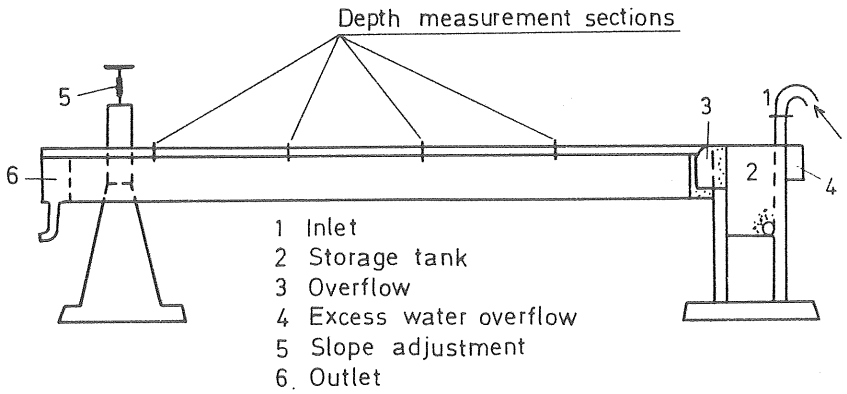

Figure 5.1 The laboratory setup.

The surface was made to simulate an urban asphalt surface by mixing the polyester resin with fine gravel. Only the fractions between 1.6 mm and 3.2 mm were used and evenly distributed over the surface. Throughout all the experiments the surface functioned well and gravel losses were negligable.

5.2.2 Instrumentation and measurement equipment.

At the inlet a rotameter measured the flow which was passed through the weir at a constant head. The inlet, is shown in Fig. 5.2 as well as the inflow distribution pipe.

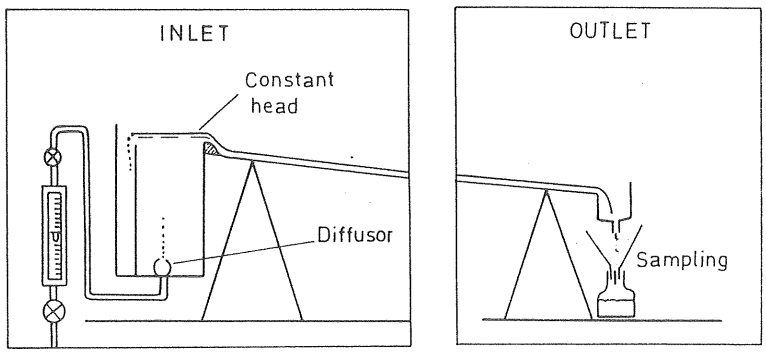

Figure 5.2 Details of the inlet and outlet of the experimental laboratory setup.

At the downstream end the overland flow could be measured and samples taken at the outlet pipe from the channel, shown in Fig. 5.2.

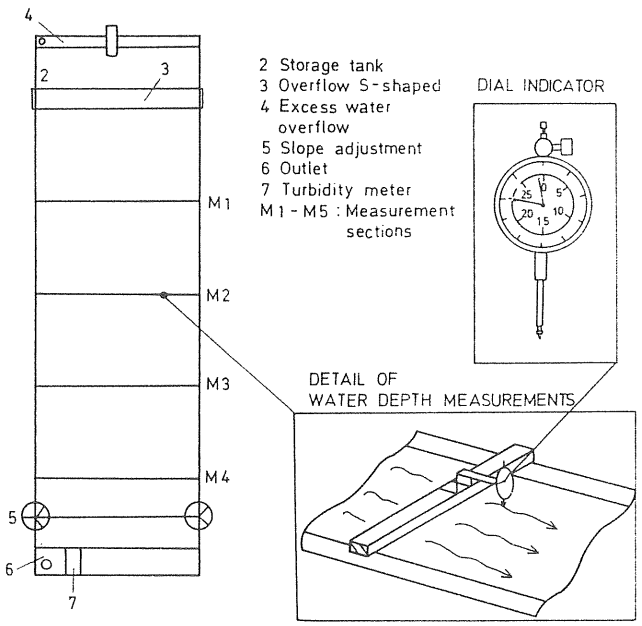

Figure 5.3 Locations of water depth measurements.

Water depths were measured at 15 to 20 locations distributed over the surface, see Fig. 5.3. The water depth at each location was measured as the distance from the bottom surface to the water surface. Two measurements were consequently taken at each location. A dial indicator designed to measure small deflections was used to measure the surfaces levels. The dial indicator was fixed to a transverse beam which could be moved from one section to another. A detail is shown in Fig. 5.3.

The sediment concentration in the surface runoff was measured by filtering a sample taken at the outlet from the downstream channel. The filter was a standard filter for suspended solids.

5.2.3 Hydraulic properties of the laboratory surface

It is essential to be sure that stationary conditions can be achieved at the laboratory surface for later experiments. The surface was observed at three different slopes ranging from 0.001 to 0.055 and at three different flows for each slope.

During each experiment water depths were taken at 15 to 20 locations distributed over the surface. The flow was constant during each experiment.

From these experiments it was possible to calculate the friction factor for the surface. Also the Reynolds' number and the Froude number were calculated.

The fricton factor was calculated according to the Darcy-Weissbach equation, which for stationary overland flow is written (Eq. (4.8b)):

$$q_r = \sqrt{\frac{8g}{f} S_0}\ y^{3/2} \qquad (5.1)$$

To calculate f it can be rewritten as:

$$f = 8g \frac{y^3 S_0}{q_r^2} \qquad (5.2)$$

The water depth used for the calculations is the arithmetic mean of all the observed depths for each flow. The hydraulic properties of the experiments are tabulated in Table 5.1, where the Reynolds' number is calculated according to $Re = q_r / \nu$ and the Froude number according to $F = q_r / y \sqrt{gy}$.

Table 5.1 Hydraulic properties of the laboratory experiments for a surface without sediments.

q_r	S_0	F	Re	f	Depth Measurements			
					y	σ	N	k/y
l/s,m					mm	mm		mm
0.11	0.001	0.083	100	1.041	5.59	0.98	15	0.36
0.46	0.001	0.233	392	0.147	7.24	0.76	15	0.27
0.82	0.001	0.273	712	0.107	9.72	0.84	15	0.21
0.26	0.027	0.512	228	0.823	2.99	0.32	15	0.67
0.46	0.027	0.671	392	0.478	3.58	0.37	15	0.56
0.82	0.027	0.786	712	0.349	4.80	0.46	15	0.42
0.26	0.055	0.610	228	1.181	2.66	0.35	15	0.75
0.46	0.055	0.738	392	0.806	3.36	0.45	15	0.60
0.82	0.055	0.975	712	0.463	4.16	0.55	15	0.48

σ = standard deviation

Looking at the depths along the surface, Fig. 5.4 to 5.6 illustrate the depth profiles. Except for the 0.001 slope the depths correspond to stationary flow with the water surface parallel to the bottom. The 0.001 slope shows a retardation at the upper half of the surface, which gives an increase in the water depth.

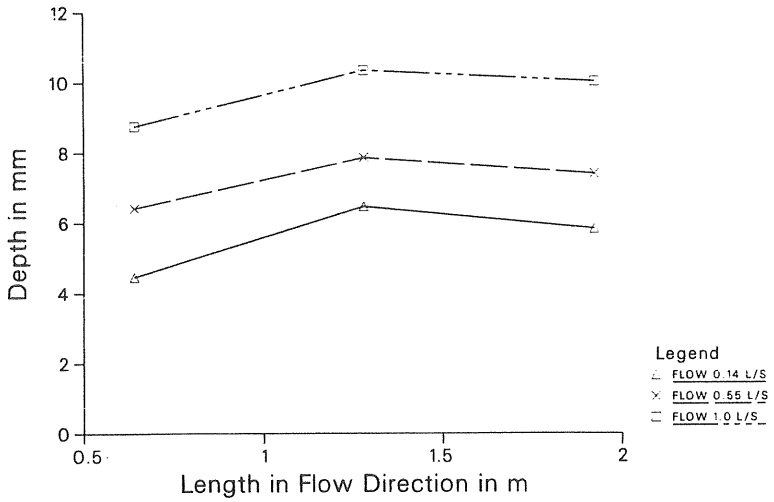

Figure 5.4 Depth profile for the 0.001 slope.

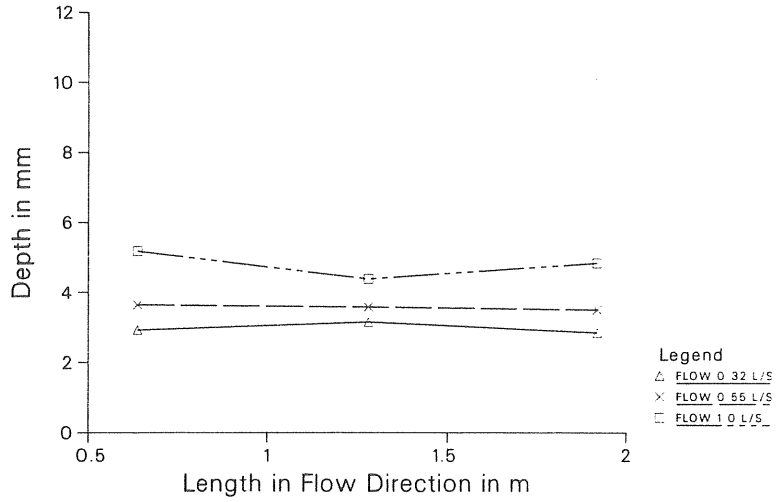

Figure 5.5 Depth profile for the 0.027 slope.

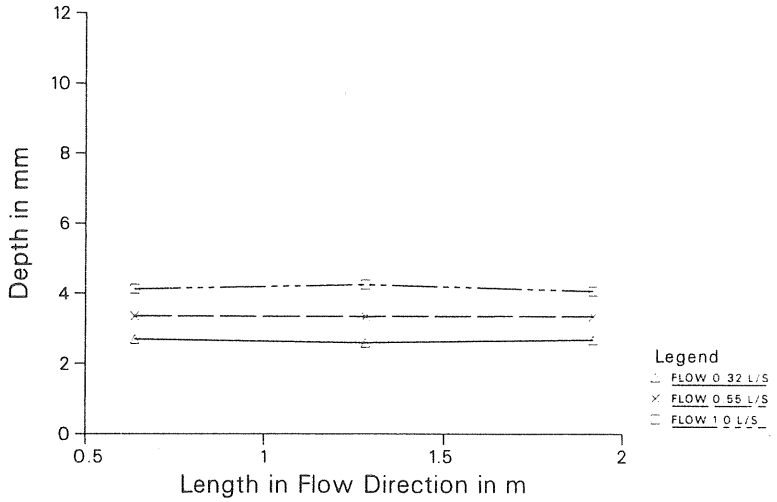

Figure 5.6 Depth profile for the 0.055 slope.

Depth flow relationships of the three slopes are shown in Fig. 5.7. They are all straight line relationships, which was expected according to the Darcy-Weissbach equation (Eq. (5.1)).

Using these average depths, i.e. a single depth corresponding to a single flow for each slope, the friction factor f was calcu-

lated according to Eq. (5.2). The variations of the friction factor are illustrated in Fig. 5.8.

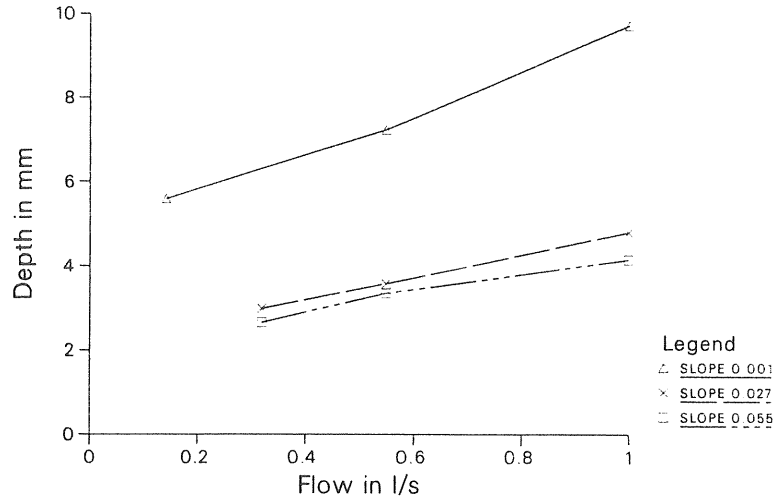

Figure 5.7 Depth-Flow relationship for the laboratory surface.

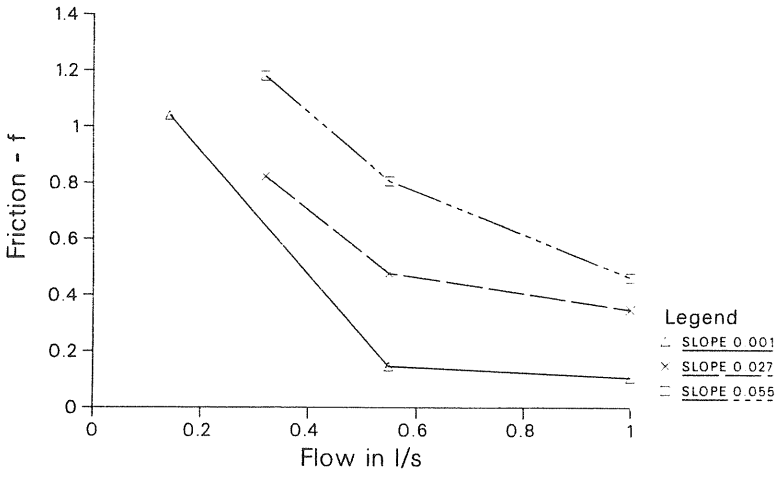

Figure 5.8 The friction factor f variation for the laboratory surface.

The variation of the friction factor f with the Reynolds' number has been investigated by many amongst them Nittim (1977). Nittim investigated an asphalt surface without a rainfall, only surface runoff. His results are illustrated in Fig. 5.9 together with the results from the CTH laboratory surface.

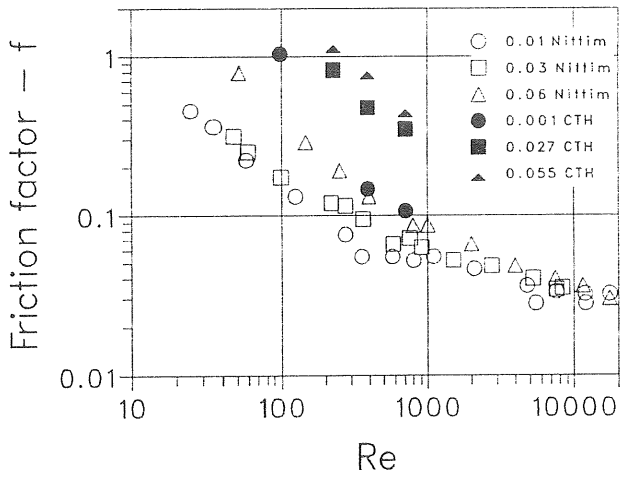

Figure 5.9 The friction factor variation with Reynolds' number of an asphalt surface, Nittim (1977) and of the laboratory surface.

Compared to Nittim's observations the friction factor is higher for the laboratory surface. The surface was built up with gravel of the diameters between 1.6 mm and 3.2 mm. The relative roughness of the surface is calculated to be between 0.21 and 0.75 which is less than that for Nittim's asphalt surface.

Phelps (1975) made similar experiments. The surface was covered with glass spheres and the tests made for relative roughnesses between 0.23 and 0.55. Phelps' results are illustrated in Fig. 5.10 and compared with those from the laboratory surface.

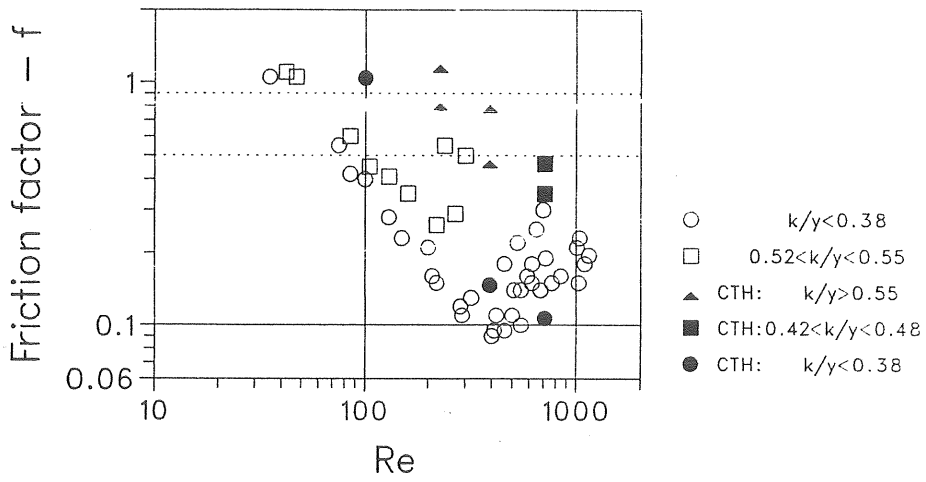

Figure 5.10 Effects on the friction factor by the relative roughness. Data from Phelps (1975) and the CTH laboratory surface.

The results from the CTH laboratory surface show the same pattern as do the results of Phelps.

5.3 Experiments with sediment transport

5.3.1 Experimental scheme

Experiments with the laboratory surface have been made for three slopes and two or three runoff intensities for each slope. The runoff intensities have been varied between 197 mm/h and 820 mm/h and thus the cross-sectional mean velocity have been in the range 0.063 - 0.177 m/s.

The runoff intensities may appear high but they correspond to the intensities achieved for a surface 50 metres downstream of a catchment with a precipitation intensity in the range 15 - 60 mm/h.

The hydraulic conditions of the experiments are tabulated in Table 5.2.

Table 5.2 Hydraulic conditions of the experiments of the laboratory surface with sediments.

Q l/s	i mm/h	S_o	y mm	v m/s
0.55	451	0.001	7.2	0.063
0.90	738	0.001	9.7	0.076
0.32	262	0.027	3.0	0.082
0.24	197	0.055	2.1	0.094
0.55	451	0.027	3.6	0.125
0.55	451	0.055	3.4	0.134
1.00	820	0.027	4.8	0.171
0.90	738	0.055	4.2	0.177

Each experiment was preceded by the distribution of 300 g of a particulate material over the surface. The material was distributed in dry phase over a dry surface. In between the experiments all remaining material was washed off the surface and the surface dried to achieve the same initial conditions for all experiments. The particle sizes of the material were approximately evenly distributed between 2 and 150 µm. An illustration of the particle sizes is given in Fig. 5.11.

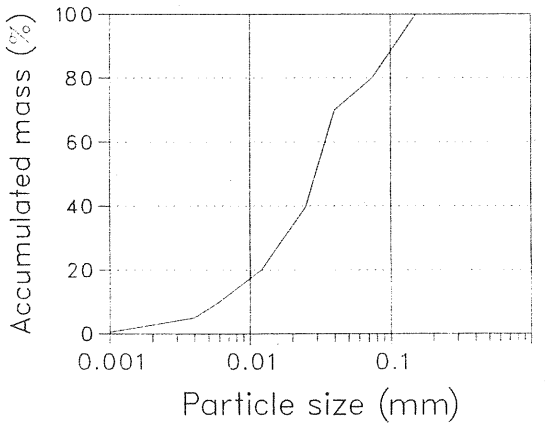

Figure 5.11 Particle size distribution for the material used in all experiments.

The experiments began by flushing of the surface at the predetermined discharge and then waiting for the water to reach the outlet. At this moment the runoff was defined to start and time set to zero. The time elapsed from the start of the flushing to the start of the runoff varied between 20 and 60 seconds depending on slope and discharge.

Sampling of the sediment concentration began a few seconds after the start of the runoff to avoid sampling before steady state conditions were reached.

The experiment ended when the output concentration had reached a nearly constant level, which was checked with a turbidimeter.

5.3.2 Observed sediment transport at the experiments

Since each experiment was carried out at stationary conditions it would be expected to get a constant sediment transport rate as a result. The basis for this expectation is an unlimited supply of particles in each particle size fraction or a sediment of only one particle size. These experiments were made using a graded sediment according to Fig. 5.11. The supply of each particle size fraction is of importance when examining the resulting sediment concentration curves.

The supply of sediment for certain particle size fractions is calculated in Table 5.3 from Fig. 5.11 and the total amount of particulate material, 300 grams, used for each experiment.

Table 5.3 Supply of sediment for each particle size fractions.

Particle sizes (mm)	0 - 0.004	0.004 - 0.006	0.006 - 0.012	0.012 - 0.025	0.025 - 0.040	0.040 - 0.074	0.074 - 0.150
Supply (g)	15	15	30	60	90	30	60

The observed sediment concentrations are drawn in Fig. 5.12 and Fig. 5.13 and sorted by the mean velocity. In Fig. 5.12 the concentrations for velocities less than 0.1 m/s are shown and in Fig. 5.13 the concentrations for velocities greater than 0.1 m/s.

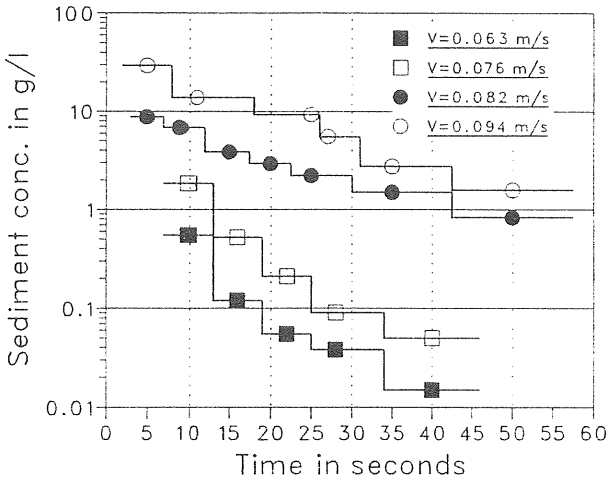

Figure 5.12 Observed sediment concentrations for velocities less than 0.1 m/s.

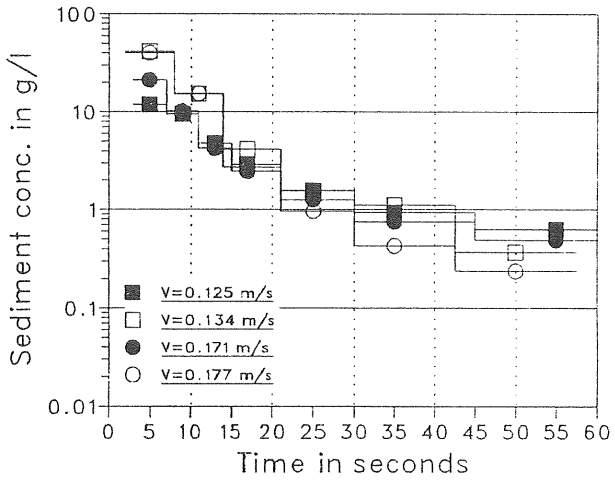

Figure 5.13 Observed sediment concentrations for velocities greater than 0.1 m/s.

To illustrate the importance of the sediment supply Table 5.4 has been made. The two finest fractions of sediment which had a supply of 15 grams each, will be removed completely within the times given in Table 5.4.

Table 5.4 Times in seconds to remove all particles of less than 0.006 mm diameter at different transport capacities.

Discharge (l/s)	Transport capacity (g/l)		
	0.1	1.0	10.0
0.5	300	30	3
1.0	150	15	1.5

The reason for the rapid decrease in sediment concentrations, especially for the experiments shown in Fig. 5.13, is a lack of supply according to Table 5.4. The constant concentrations at the end of each experiment should correspond to the transport capacity of those particle sizes left.

5.4 Verification of the basic equations for sediment transport

5.4.1 Constants and variables used at the verifications

The verifications were made using the FORTRAN-programme described in Chap. 4.4. The constants described here refer to the equations for sediment transport given in Chap. 4.3.

The physical conditions; i.e. slope, slope length, width and runoff intensity were modeled as close as possible to those of the experiments.

The value of the friction factor, f, was evaluated from each experiment, (Table 5.1). These values were used to calculate the values of K_g, (Eq. (4.6)), using the Reynolds'number of each particular experiment.

A summary of the the constants and variables of each experiment used to verify the model is given in Table 5.5.

Table 5.5 Summary of constants and variables for the verifications.

Q (l/s)	q_r (l/s,m)	S_o	Re	f	K_g	ν (m/s)
0.30	0.25	0.001	215	0.650	139	
0.55	0.46	0.001	392	0.147	58	0.063
0.90	0.82	0.001	712	0.107	76	0.076
0.32	0.26	0.027	228	0.823	187	0.082
0.55	0.46	0.027	392	0.478	187	0.125
1.00	0.82	0.027	712	0.349	250	0.171
0.32	0.26	0.055	228	1.181	269	0.094
0.55	0.46	0.055	392	0.806	316	0.134
1.00	0.82	0.055	712	0.463	330	0.177

The detachment of overland flow, D_f, (Eq. (4.22)) and the parameter B_s (Eq. (4.28)) of the expression for critical shear stress have to be evaluated from the experimental data. The values are given in Table 5.6.

Table 5.6 Evaluated values of the parameters D_f and B_s for the laboratory surface.

Detachment by overland flow D_f	Shields criteria B_s
0.01	0.10

5.4.2 Comparison between simulated and observed depths, masses and concentrations

The simulated and observed data have been compared with respect to water depths, transported sediment masses and sediment concentrations, Fig. 5.14, Fig.5.15 and Fig. 5.16. The comparison between simulated and observed depths for the laboratory surface, shown in Fig. 5.14, gives evidence of a well working model with regard to surface runoff. Simulating realistic depths, thus simulating realistic velocities is necessary to be able to simulate the sediment washoff from the surface.

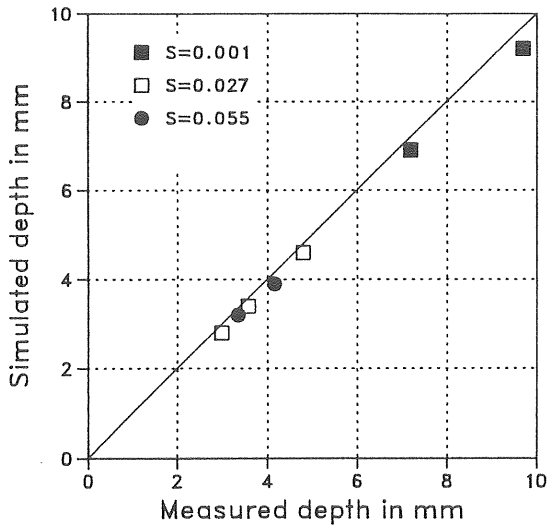

Figure 5.14 Simulated water depths compared to observed for the laboratory surface.

A straight forward comparison between observed and simulated sediment masses, shown in Fig. 5.15, implies that the model overestimates the sediment masses washed off the surface.

The simple model, described in Fig. 4.18, however, balances the transport capacity and the detachment rate and determines the transporting rate from the smallest of the two. With respect to the laboratory experiments, these were made without any rainfall over the surface. This means that the detachment rate will be the same as the detachment rate by overland flow, Eq. (4.22). The equation says that if there is no detachment of sediments by rain, the detachment by flow will be a linear function of the sediment transport capacity. The detachment coefficient, D_f, which is in the range between 0 and 1.0, tells which fraction of the transport capacity, that will equal the detachment rate.

The experimental procedure with a distribution of dry sediments over a dry surface makes it likely to beleive that D_f should be close to 1.0, when the flushing of water over the surface

started. This means a sediment transporting rate equal to the sediment transport capacity. When the sediments after a few seconds were wetted the detachment coefficient should decrease to a more realistic value for natural surfaces.

The conclusion is, that for the experiments, with respect to sediment transport, should the first part of the flushing be governed by the transport capacity and the later part be governed by the detachment rate. In between the two parts there has to be a transition zone between the two phases.

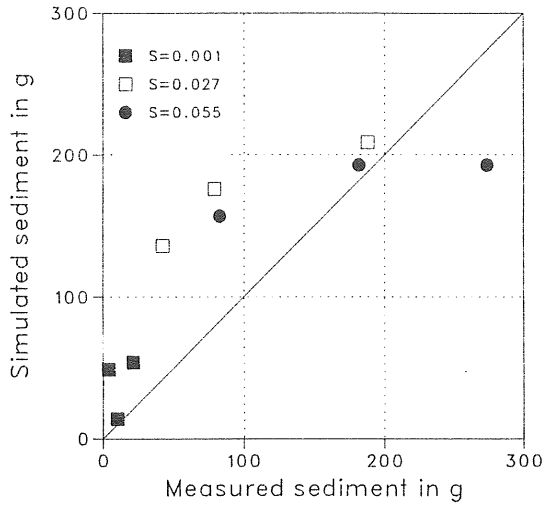

Figure 5.15 Comparison between simulated and observed sediment masses during the phase when transport capacity is governing

A comparison between observed and simulated sediment concentrations is expected to show an overestimation of the simulated concentration since in practice not all sediments will be detached and thus not will be available for transport. The concentration versus time graphs shown in Fig. 5.16 are all in agreement with this assumption. Graphs for all the experiments are shown in Appendix 4.

The detached sediment concentration, shown in Fig. 5.16 and in Appendix 4, is close to the observed concentration during the later part of the flushing for a majority of the experiments.

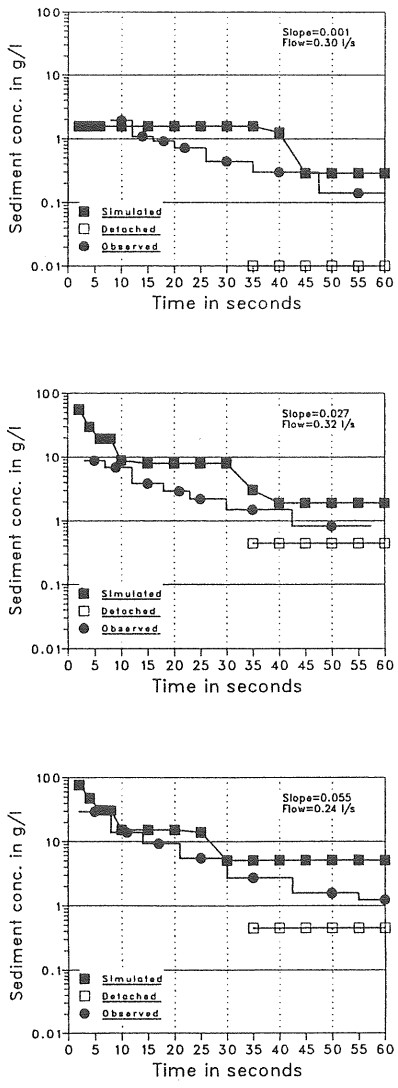

Figure 5.16 Simulated and observed sediment concentrations for the 0.001, 0.027 and 0.055 slopes.

The verification of the simple one-plane model for sediment transport was successful in the following respects:

- The sediment transport capacity equations were proven to give realistic concentrations, as shown by the first phase of each experiment

- The detachment rate with a D_f = 0.01 gave a good agreement with the observed concentration for the later phase of the flushing of the surface

However, the simulated concentrations are not in agreement with the observed concentrations throughout the whole flushing event. The reason for this is the difficulties to estimate a D_f-value for the transition zone between the two phases.

6 FIELD INVESTIGATIONS

6.1 Aim and limitations of the field experiments

The field experiments were carried out to obtain a better understanding of the chemical processes and transport mechanisms involved in the transport of pollutants during surface runoff.

Also the data obtained from the field observations should serve as a database for the verification of different pollutant transport models.

It was believed that the pollutant transport is a two phase transport with a solid phase and a dissolved phase. The experiments were consequently directed towards the observation of solids transport and pollutants associated with solids.

The study was however limited to the observation of suspended solids and certain heavy metals (lead, cadmium, copper and zinc) which from an environmental point of view are most interesting.

The investigations were carried out during 1979 and 1980, with a first period between August and November, 1979 and a second period between June and November, 1980.

6.2 Catchment characteristics and instrumentation

The catchments, all situated within the University grounds were:

* A roof area; a 170 m^2 roof connected to one downpipe

* A parking lot; a 450 m^2 car park connected to one catch basin

* A street area; a 1200 m^2 part of a street connected to one catch basin

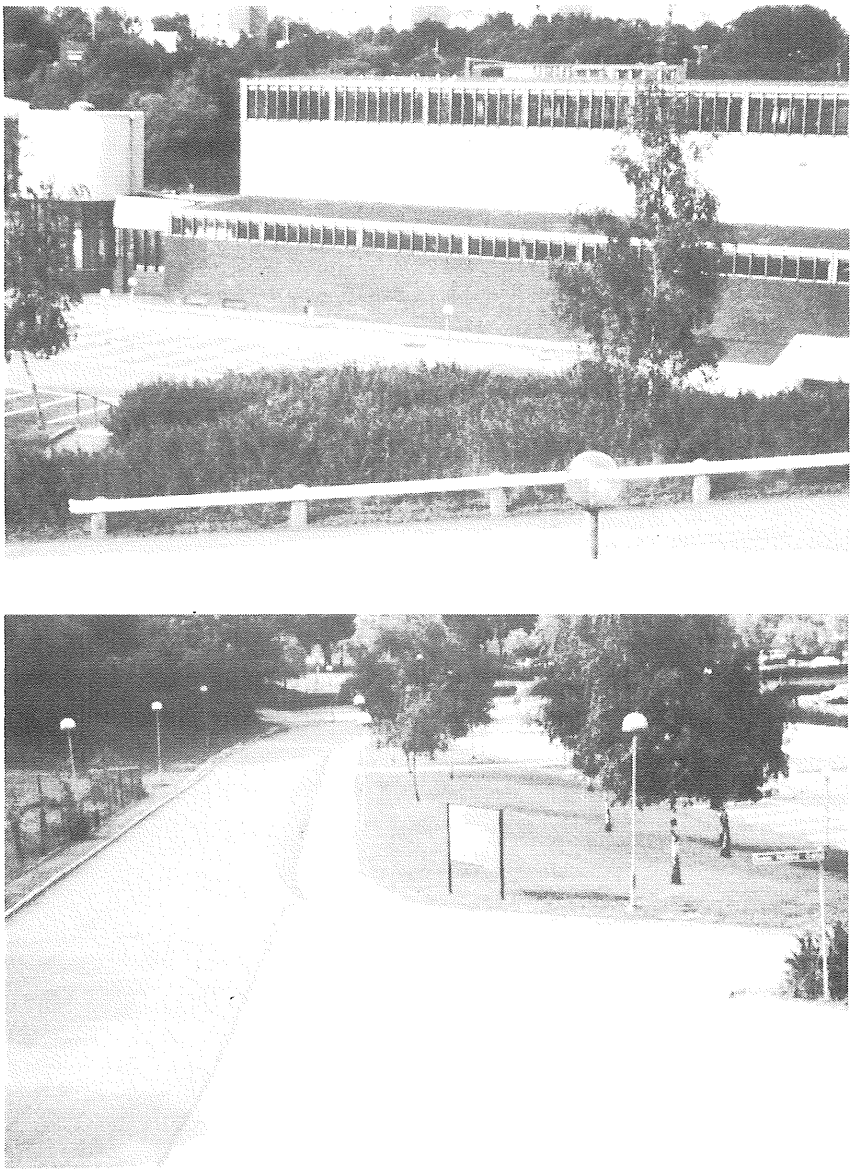

Figure 6.1 Photographs of the catchment areas.

Rainfall intensity, stormwater flow and heavy metal concentrations were observed for all three catchments. Rainfall and runoff were observed continously and the concentrations were obtained from discrete samples.

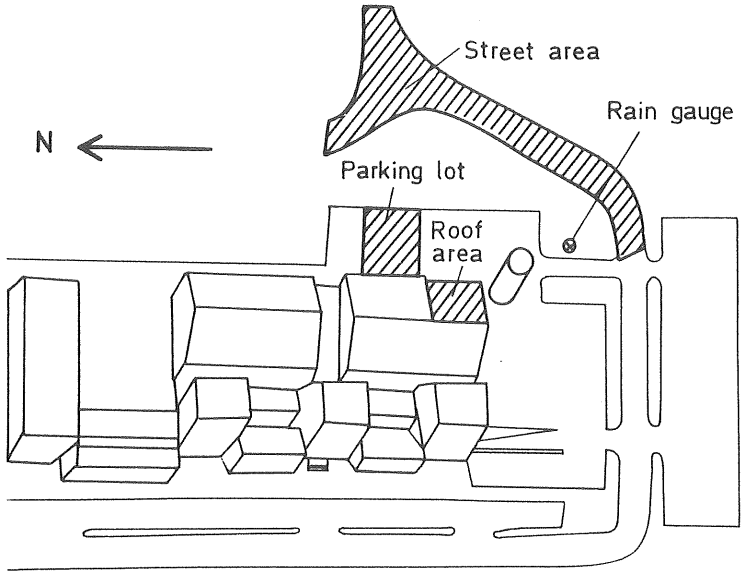

Figure 6.2 Map of the University grounds showing the catchments.

6.2.1 The Roof Area

The roof catchment, see Fig. 6.3, is a part of the roof of the hydraulics laboratory. The runoff is collected in a roof gutter at the downstream end and is connected to the storm sewer by a vertical pipe passing through the hydraulics laboratory.

It is a rather flat roof. The pollutants washed off by the runoff originate from atmospheric fallout. The only materials that the runoff came in contact with was the asphalt roof and the PVC-downpipe.

Table 6.1 Catchment characteristics of the roof area.

Area (m^2)	170
Impervious Area (%)	100
Average Slope (m/m)	0.050

A flow measuring device was connected to the downpipe inside the hydraulics laboratory.

Sampling was made prior to the water passing through the flow measuring device. The sampler was activated by a rise in flow.

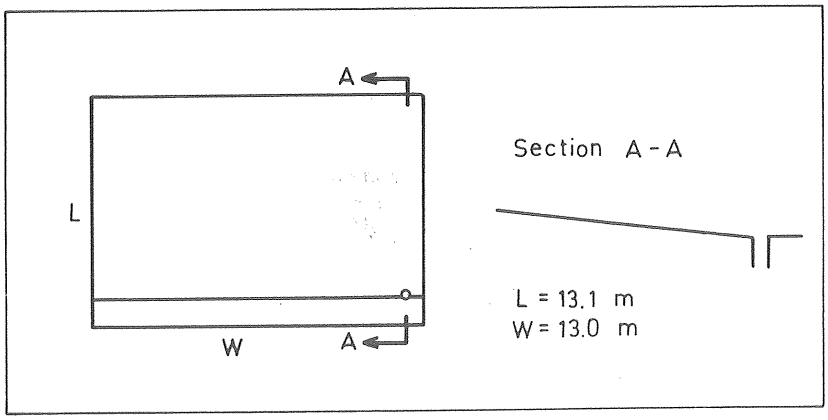

Figure 6.3 Outlay of the roof catchment.

6.2.2 The Parking Lot

The parking lot, see Fig 6.4, is comprised of an asphalt car park and road and a cobble stone sidewalk. The runoff from the surface drains to a roadside gutter which drains to one catch basin.

Pollutants washed off by the runoff may originate from corrosion of metals, from vehicular sources, deposited road dust and road surface material in addition to general atmospheric fallout.

Table 6.2 Catchment characteristics of the parking lot.

Area (m^2)	450
Impervious Area (%)	100
Average Slope (m/m)	0.018

A flow measuring device was installed in the catch basin and all the runoff was made to pass the device before leaving the basin. The sampling was made just below the inlet grating prior to the runoff entering the flow measuring device.

The samples flowed under gravity to the basement of the hydraulics laboratory, where they were collected.

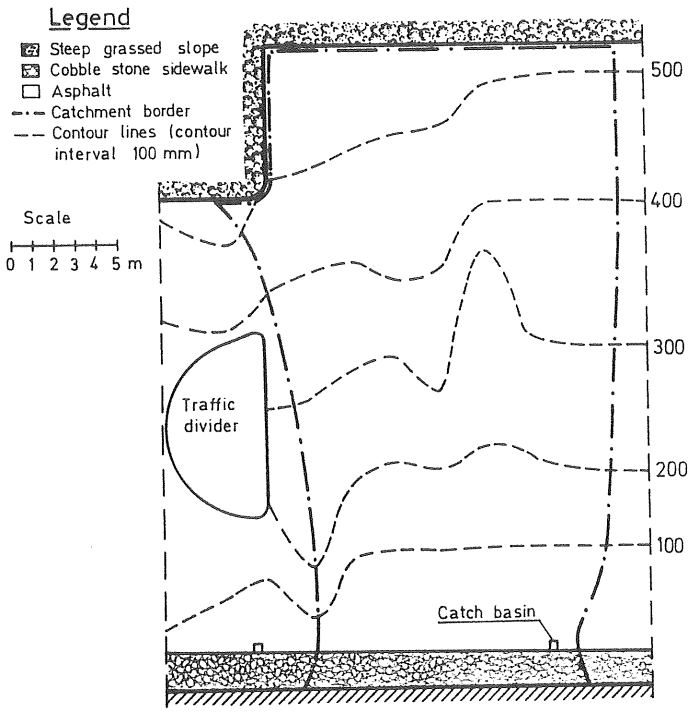

Figure 6.4 Outlay of the parking lot catchment.

6.2.3 The street area

The street area, see Fig. 6.5, is a part of a street through the University ground. One catch basin drains the 1200 m^2 street catchment which is rather steep compared to the other two catchments. The street is covered with asphalt.

Pollutants washed off the surface during runoff may originate from vehicular sources, deposited road dust, road material and general atmospheric fallout.

Table 6.3 Catchment characteristics of the street area.

Area (m^2)	1200
Impervious Area (%)	100
Average Slope (m/m)	0.060

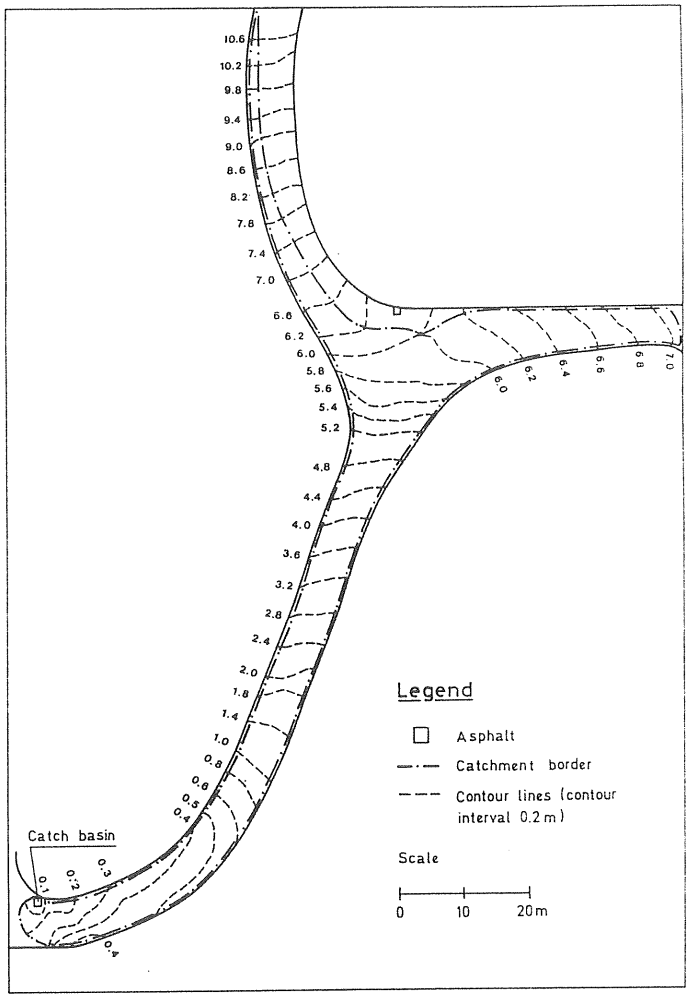

Figure 6.5 Outlay of the street catchment.

In a grassed area approximately three metres from the catch basin, a sampling device chamber was buried in the ground. The chamber was connected to the catch basin through a 50 mm PVC-pipe. The sampled water flowed by gravity through a rubber hose inside the PVC-pipe.

The flow measuring device was installed in the catch basin and the runoff was sampled prior to the water passing through the flow measuring device.

6.2.4 Flow Measuring Device

Three identical flow measuring devices developed by the University of Lund, Sweden, (Falk et al (1979)), were used. The runoff, passing through a 30 degree V-notch weir, was monitored and the V-notch height measured by the decrease in resistance between two electrodes submerged in a saline solution. The electrode chamber is separated from the V-notch by a durable moving rubber membrane, thus causing the saline solution to vary with the V-notch water level. The device is shown in Fig. 6.6.

The V-notch heights for all the three catchments were recorded on the same 12-channel chart recorder, which was placed in the basement of the hydraulics laboratory. A calibration curve was made for the V-notch height against the flow passing through. The relationship between measured height and flow was plotted and an equation derived (Eq. (6.1)). The same equation has been used for all three devices.

$$Q = 303.9h^{2.295} \quad (r^2 = 0.99) \tag{6.1}$$

Q=Flow (l/s)
h=V-notch height (mm)

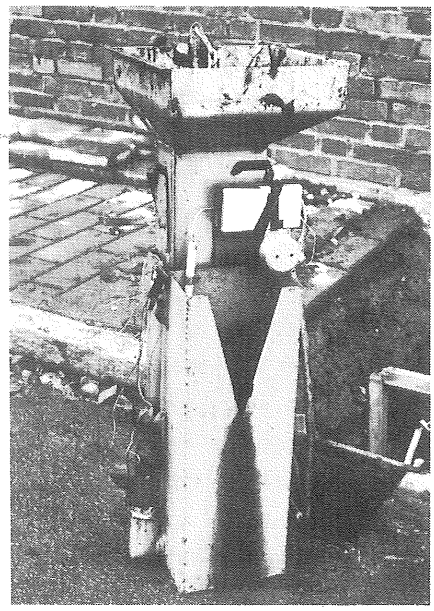

Figure 6.6 Catch basin flow measuring device. (Photo Thomas Ericsson)

6.2.5 Rainfall measurements

One raingauge was installed between the parking lot and the street area. The location is seen in Fig. 6.2. The observed rainfall intensities from this raingauge have been used for all three catchments. A second raingauge at a distance of 100 metres from the catchments was used if the first instrument had failed for some reason.

The gauge works on the tipping bucket principle and was developed by the University of Lund, Falk et al (1979). The volume resolution is 0.035 mm per tipping with a funnel area of 0.0423 m^2. The allowable intensities are between 0.035 mm/min and 4.2 mm/min.

The calibration curve for the raingauge is expressed as a relationship between the number of tippings per minute and the rain intensity. The following nonlinear equation expresses the relationship for the instrument used:

$$i = 0.03537 N_t^{1.0262} \qquad (6.2)$$

i = rainfall intensity (mm/min)
N_t = number of tippings per minute

The accumulated rainfall volume was recorded by the same 12-channel chart recorder as was used for the runoff flows. The procedure of recording the accumulated rainfall volume instead of the digital reading of the intensity was choosen to make it possible to record all signals on one chart. By this means no time lag between the recordings from the different catchments would be introduced. However, this made intensities below 0.05 mm/min difficult to read.

6.2.6 Data collection

The runoff flows (i.e. the V-notch heights) and the rainfall intensities were recorded on the same 12-channel chart recorder placed in the basement of the hydraulics laboratory.

The signals from the sensors were transferred by cable and each piece of equipment was calibrated to account for the length of the cable. An outlay of the data collection system is shown in Fig 6.7.

The chart recorder had a turn around time of one minute. Three channels were however used for each signal to obtain a 20 second interval between each dot for a single signal. Charts were taken out at either a speed of 240 mm/h giving a resolution of 3 dots per 4 mm or a speed of 150 mm/h with a resolution of 6 dots per 5 mm. The height of the chart was either 250 mm, which means that the scale factor between the V-notch height and the chart height was about 1, or 150 mm yielding a scale factor of

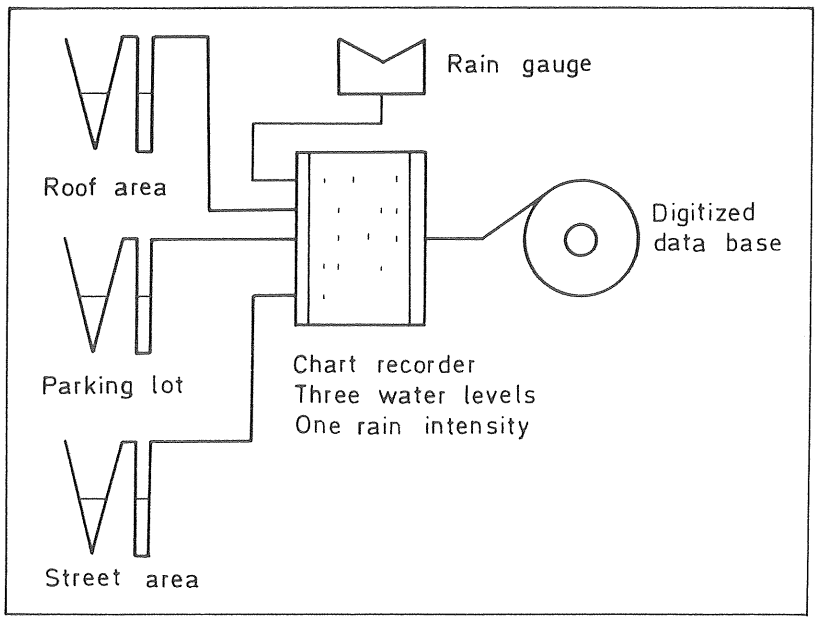

Figure 6.7 The Data collection system.

0.75. To allow for evaporation from the flow measuring device during dry periods the chart zero-level was offset by +10%.

Rain intensities were recorded as the accumulated rainfall volume with 225 mm recorded height corresponding to 10.4 mm rainfall height.

6.2.7 Sampling device

Sampling of water was made prior to the runoff passing the flow measuring device (Fig. 6.8). A special spoon sampler was constructed to sample water from the runoff before entering the catch basin just below the inlet grating. The sample was transported by gravity through a rubber hose to a sample collector with 24 bottles (Fig. 6.9), each of the volume of one litre.

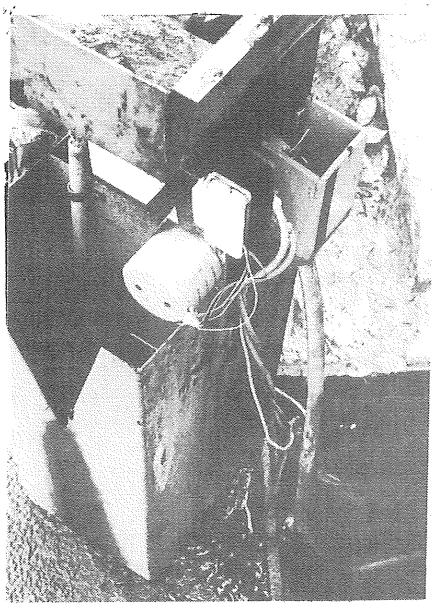

Figure 6.8 Spoon sampler for installation in a catch basin. (Photo Thomas Ericsson.)

The spoon sampler was motor driven. Two sampling intervals were used. During 1979 a 25 ml sample was taken every fifth of a second thus filling up a bottle in three minutes. During 1980 the samples were taken every ten seconds and the bottles were shifted every five minutes.

The sampling procedure was activated by a level sensor. When the V-notch level raised above the zero-level the sampling began and continued until either the 24 bottles were filled or the V-notch starting level was reached again.

The materials used for the equipment were stainless steel for the spoon sampler, natural rubber for the hoses and polyethylene for the bottles. The natural rubber hoses were choosen because of evidence that metal leached from the polyethylene hoses that were originally used.

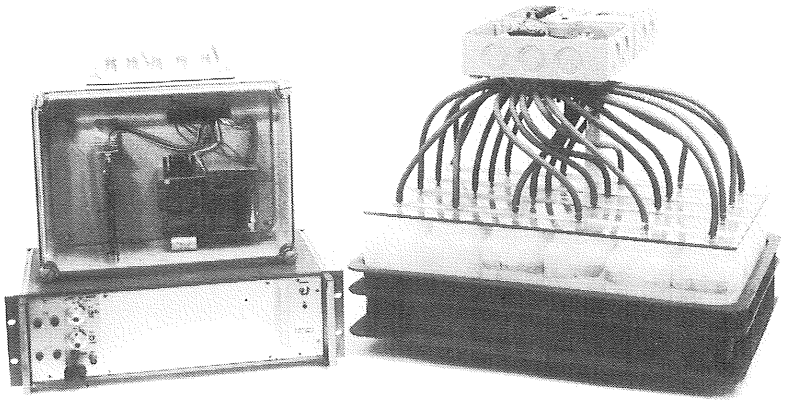

Figure 6.9 Sampling collector with 24 bottles. (Photo Thomas Ericsson.)

6.3 Experimental procedures

During the observation periods the rainfall gauge and the flow measuring device were running continously. The equipment was maintained regularly. The maintenance included cleaning of the spoon sampler, the V-notch and the rubber hose to the sample collector. The V-notch zero-level was checked and if needed the chart recorder was readjusted. The normal procedure was to first check the zero-level and than to close the V-notch and fill up with water to the maximum level. Occasionally the flow calibration curve was checked with water from a fire hydrant or with tap water at one V-notch level.

The sample equipment was triggered for sampling in the beginning of each week and samples taken from the first occuring storm. The samples were taken to the laboratory for analysis less than 12 hours after they had been filled. During some events, the full bottles were immediately replaced with empty ones making it possible to sample longer storms.

6.4 Analytical work

6.4.1 Developement of an analysis scheme

A programme for physico-chemical analyses was developed to give concentrations of suspended solids and heavy metals both solids associated metals and metals in free form.

Each sample was analysed for the total concentrations of:

pH
conductivity
suspended solids
turbidity
lead
cadmium (Parking lot and Street area)
copper
zink (Roof Area)

A centrifuge was used to separate the solids from the liquid phase. After this separation the liquid phase was analysed for:

lead
cadmium
copper

The solids associated metal concentrations were calculated as the difference between the total concentration and the liquid phase concentration.

6.4.2 Physico-chemical analyses

All analyses work was carried out at the laboratory of the Department of Sanitary Engineering, Chalmers University of Technology.

pH
pH was analysed according to the Swedish Standard SIS 028122, an electropotentiometric method in which a pH meter with a combination electrode is used.

Conductivity

Conductivity was analysed according to SIS 028123, using a Tetramatic, 4-electrode meter.

Turbidity

Turbidity was analysed using a Turner Nephelometer instrument which gives the turbidity in Nephelometric Turbidity Units (NTU).

Suspended solids

Suspended solids were analysed according to the gravimetric method SIS 028112. In this method, the sample is filtered through a fiberglass filter which is dried at 105 ^{o}C and weighed.

Lead, Cadmium, Copper and Zinc

These heavy metals were analysed by atomic-absorption spectrophotometry. The water samples were concentrated by evaporation 5 times because of the generally low concentrations of these metals. Detection limits varied but were usually around 25 µg Pb/l, 0.2 µg Cd/l, 10 µg Cu/l and 10 µg Zn/l.

6.4.3 Separation of solids from the liquid phase

The separation of solids from the liquid phase was made by using a centrifuge. Two samples of 30 ml each were taken from the stormwater sample and then centrifuged for 30 minutes at a speed of 9000 r/minute. The two parallel samples were both analysed for Pb, Cd and Cu in the liquid phase. The result was given as the arithmetic mean of the analysed concentrations.

6.5 Data processing

The data processing has produced a database of all observed storms. It consists of a time series of rainfall intensities, runoff flows and concentrations for the physico-chemical properties for each storm observed.

The database was developed in three steps, beginning with digitizing of the recorded charts. The digitized data was taken care of by a FORTRAN-programme which produced rainfall and runoff intensities with a time resolution of one minute. Accumulated rainfall and runoff volumes were also calculated.

The second step was to produce physico-chemical concentrations at the same time resolution of one minute as the hydrographs. This meant that a concentration of a sample was always assigned to several consecutive timesteps. The shortest time resolution of the concentrations was three minutes and in general between three and nine minutes depending on where in a storm the sample was taken.

The third step was to merge the hydrographs with the concentrations, which was done by another FORTRAN-programme. In the same step mass flows of suspended solids and heavy metals were also calculated.

As a summary for each storm a written output and a plot was produced.

A separate dataset was produced for the concentrations of dissolved and solids associated metals. This was completed with pH, suspended solids concentrations and accumulated solids.

Another separate dataset was produced for the concentrations of the fractioned samples.

All subsequent analysis of the datasets was made using the Statistical Analysis System (SAS) programme available at the Gothenburg University Computing Centre.

6.6 Results

6.6.1 Summary of observed storms

The Roof area

A summary of the observed runoffs from the roof is shown in Fig. 6.10 and Fig. 6.11. Tables with time series data from each storm are found in Appendix 1.

The storms are of medium intensity and a major part of each storm has been covered by sampling both with regard to volume and duration.

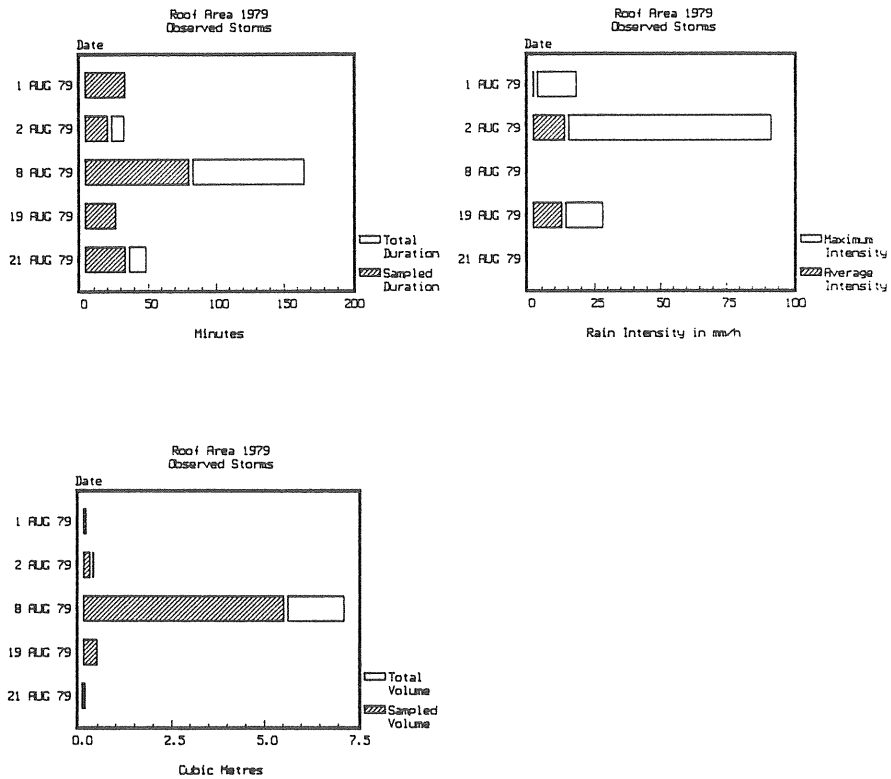

Figure 6.10 Summary of rain intensity, runoff volume and runoff duration for observed storms from the roof area.

The concentrations shown in Fig. 6.11 for the roof area are low for both solids and metals. This was expected since the major source of metals and solids for the roof is deposits from the air.

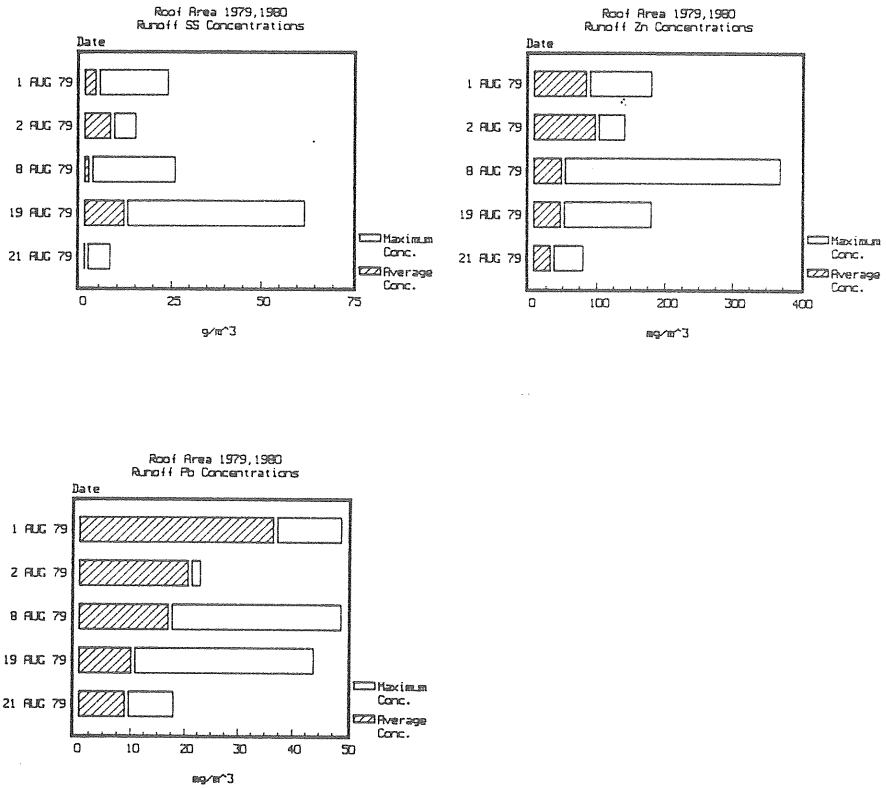

Figure 6.11 Maximum and average SS, Pb, Cu and Zn concentrations for each observed runoff from the roof area.

The Parking lot

A summary of the observed runoffs from the parking lot is shown in Fig. 6.12 and Fig. 6.13. Tables with time series data for each storm are found in Appendix 1.

The storms are of low intensity with one exception, the storm 2 Sep. 79 which has both a high average intensity and a high maximum intensity. The storms have for the most part been covered by sampling both regarding volume and duration. In general a smaller part of each of the longer and/or larger runoffs have been covered by sampling.

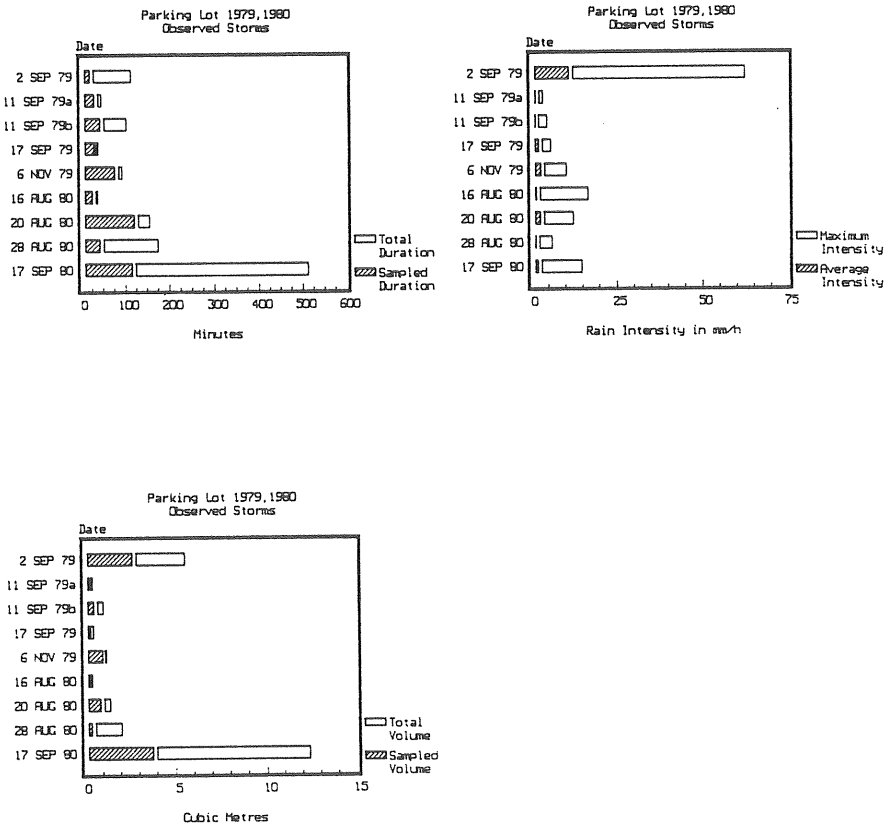

Figure 6.12 Summary of rain intensity, runoff volume and runoff duration for observed runoffs from the parking lot.

The high rainfall intensities of 2 Sep. 79 correspond to high SS concentrations but not to high metal concentrations. The opposite situation is seen for 11 Sep. 79a and 28 Aug. 80 where the metal concentrations are high but both SS concentrations and rainfall intensities are low.

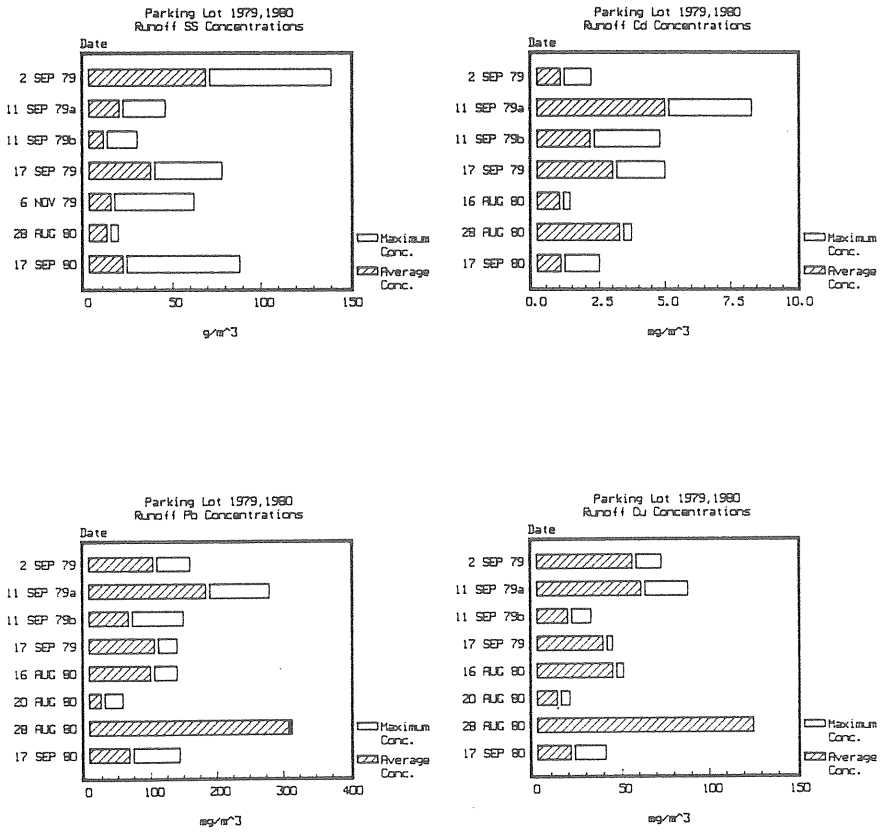

Figure 6.13 Maximum and average SS, Pb, Cd and Cu concentrations for each observed runoff from the parking lot.

The Street area

A summary of the observed runoffs from the street area is shown in Fig. 6.14 and Fig. 6.15. Tables with time series data for each storm are found in Appendix 1.

The storms are of low to medium intensity. The storms have for the most part been covered by sampling both regarding volume and duration. In general a smaller part of each of the longer and/or larger runoffs have been covered by sampling.

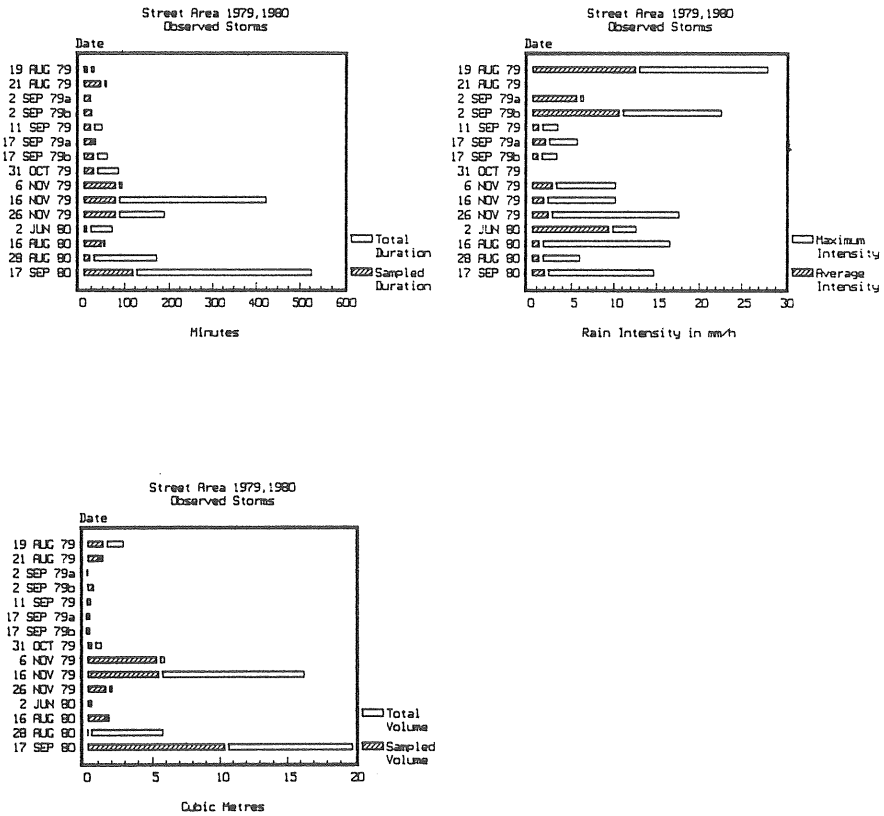

Figure 6.14 Summary of rain intensity, runoff volume and runoff duration for observed runoffs from the street area.

The high metal and SS concentrations cannot be explained simply by high rainfall intensities. The average rainfall intensities are in the same order of magnitude as those for the parking lot. However, the street area is much steeper than the roof or the parking lot. Sediments of the same particle size are transported at lower intensities at the street than at the two other areas.

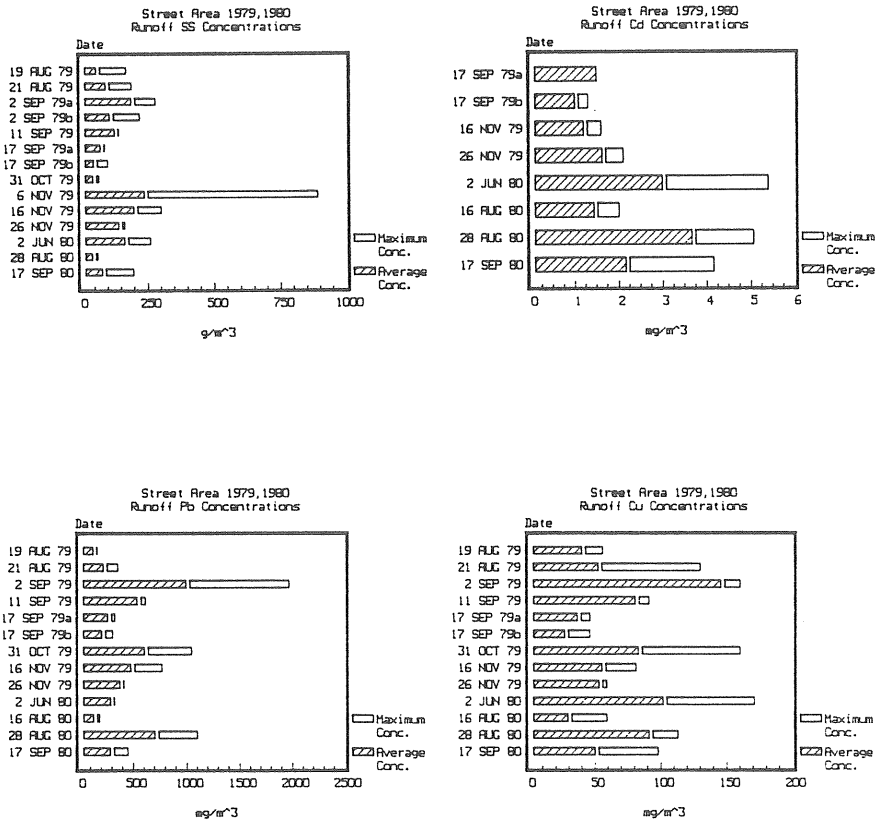

Figure 6.15 Maximum and average SS, Pb, Cd and Cu concentrations for each observed runoff from the street area.

6.6.2 Comparison with other areas

The small watersheds at the Chalmers University Site has been compared to other areas in Göteborg, which have been reported earlier by Malmqvist (1983). A mixed watershed, for example a residential area contains several of these small watersheds and one would expect the small watersheds to show larger variations than a mixed watershed.

A short characterization of the mixed watersheds is given in Table 6.4.

Table 6.4 Characterization of some mixed watersheds in Göteborg. (Malmqvist (1983)).

	Vegagatan	Mellby-leden	Bergsjö-svängen	Floda
Total area, (ha)	5.8	15.6	4.8	18.0
Impermeable area, (ha)	3.1	6.1	2.2	3.5
Roof area, (ha)	1.0	1.6	1.1	1.5
Street area, (ha)	2.1	4.5	1.1	2.0
Copper areas, (m^2)	1250	1700	5	0
Population density, (p/ha)	250	115	85	22

Both Vegagatan and Mellbyleden have more streets than roofs and thus the small street watershed should correspond to these areas with respect to lead. Neither of the small watersheds have any copper surfaces, thus they should correspond to the copper concentrations of Bergsjösvängen and Floda.

As shown in Table 6.5 the lead levels of the street corresponds to those of Vegagatan while the lead levels of the parking lot corresponds to those of Bergsjösvängen. The lead level of the roof is lower than for any of the mixed watersheds which also would be expected. The copper levels of all three Chalmers watersheds corresponds to those of Bergsjösvängen and Floda.

Table 6.5 Comparison between the Chalmers watersheds and some mixed watersheds in Göteborg.

Area		SS (mg/l)	Pb (µg/l)	Cd (µg/l)	Cu (µg/l)	Zn (µg/l)
Roof-CTH	mean	4.7	17	n.a.	23	55
	max	12	37		29	97
Parking Lot-CTH	mean	49	128	1.7	57	n.a.
	max	69	308	5.0	126	
Street-CTH	mean	122	321	1.9	55	n.a.
	max	237	999	3.7	146	
Vegagatan	mean	100	340	n.a.	260	390
	max	650	1680		960	2220
Mellby-leden	mean	58	120	5.2	170	290
	max	680	670	-	700	940
Bergsjö-svängen	mean	53	150	n.a.	26	230
	max	310	570		110	750
Floda	mean	68	63	n.a.	23	170
	max	1050	340		89	470

n.a. = not analyzed

6.6.3 The separation between dissolved and solids associated metals for the street area

The analysis of dissolved and solids associated metals is based on five events from the street area. Two events from the parking lot and two from the roof area were also analysed with respect to dissolved and solids associated metals. It has not however been possible to create separate datasets for these areas due to lack of data. The analysis is thus limited to the street area.

A summary of some properties of the analysed events is given in Table 6.6.

Looking at a 18 year long time series of rain events from Göteborg (Arnell et al. (1979)), the September event belongs to a class of events which 80 % of all events during one year belong to. The November events belong to a class which 18 % of

all events belong to. The June event belongs to a class of events which only 2 % of all events belong to.

Table 6.6 Description of the analysed events with respect to rainfall intensities and volumes.

Date	Mean intensity (mm/h)	Max. intensity (mm/h)	Volume (mm)
17 Sep 79	1.43	5.7	2.2
6 Nov 79	2.80	10.2	4.0
16 Nov 79	1.80	10.2	13.6
26 Nov 79	2.32	17.6	3.9
2 Jun 80	9.42	12.6	1.4
16 Jun 80	-	-	-

An impression of what each event represents is given by the following figures. The metal concentrations for consecutive time intervals during each runoff are given in Fig. 6.16 (the event 26 Nov. 79) and Fig 6.17 (the event 16 Nov. 79).

Graphs for all the events are shown in Appendix 5.

As shown in Fig. 6.16, the dissolved fraction of the total metal concentration is relatively small for all metals and is almost constant throughout the runoff event. This is typical when the pH-value is higher than 6.0, which it is during the entire event.

The event 16 Nov. 79 in Fig. 6.17 is showing another pattern which is typical at lower pH-values. The dissolved fractions is much higher, especially for cadmium and copper. The dissolved lead fraction is to a minor extent affected by the lowering of the pH-value.

The concentrations vary in general both within events and between events. Dissolved concentrations appear to vary less than solids associated concentrations.

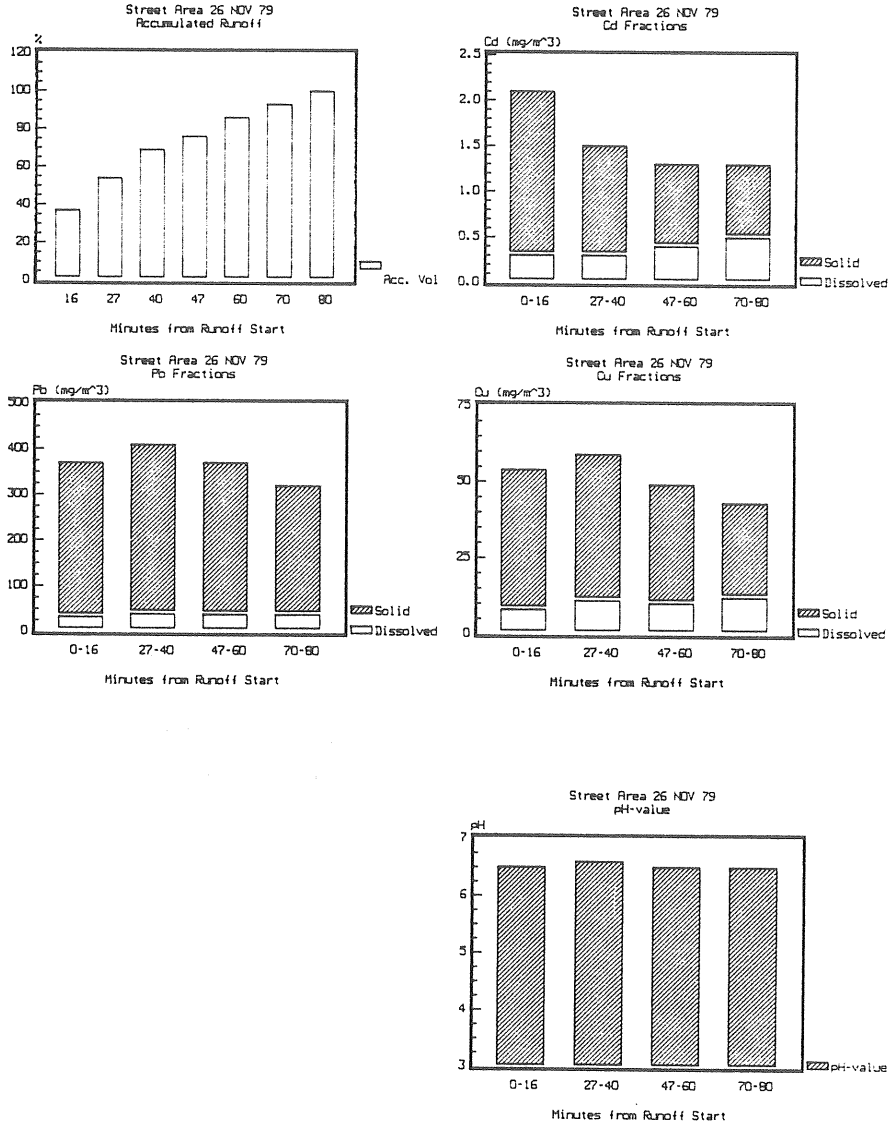

Figure 6.16 Accumulated volume, pH and dissolved and solids associated concentrations of Pb, Cd and Cu for the event 26 Nov. 79.

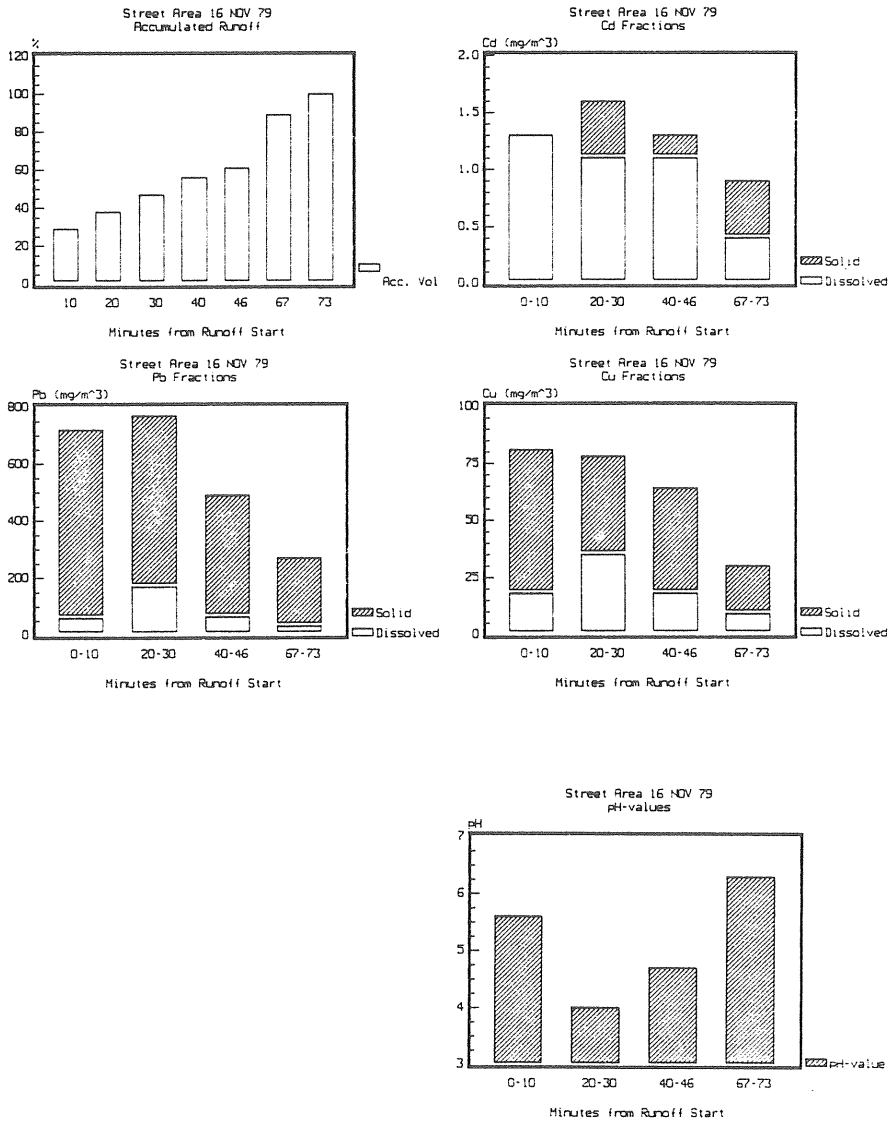

Figure 6.17 Accumulated volume, pH and dissolved and solids associated concentrations of Pb, Cd and Cu for the event 16 Nov. 79.

The arithmetic mean of all concentrations given in Table 6.7 and Table 6.8 summarizes these experiences. The standard deviation can be regarded as a measure of the variation.

Table 6.7 Arithmetic means and standard deviations of dissolved Pb, Cd and Cu concentrations for six events from the street area.

	Pb (µg/l)	Cd (µg/l)	Cu (µg/l)
Arithmetic mean	65.1	0.94	27.2
Standard deviation	44.3	0.41	21.6
Number of samples	22	17	22

Table 6.8 Arithmetic means and standard deviations of solids associated Pb, Cd and Cu concentrations for six events from the street area.

	Pb (µg/l)	Cd (µg/l)	Cu (µg/l)
Arithmetic mean	490	0.72	37.4
Standard deviation	890	0.63	37.2
Number of samples	22	17	22

Compared to the variations of the solids associated metals the dissolved concentrations will be regarded as constant for modelling purposes.

To explain the variations of the solids associated concentrations these have to be converted to weight per weight concentrations, that is µg metal per mg solids. This derived variable is given in Table 6.9 together with the solids concentrations.

Table 6.9 Solids associated metals expressed as weight per weight, solids loads and solids concentrations. Data from street area.

Date	Time (min)	Pb (µg/mg)	Cd (µg/mg)	Cu (µg/mg)	SS (mg/l)	Accumulated SS (g)
17SEP79	6	3.39	-	0.29	82	0.20
17SEP79	13	2.90	0.0011	0.24	87	6.80
17SEP79	27	3.29	0.0069	0.28	72	12.80
17SEP79	43	2.07	-	0.30	99	15.00
17SEP79	50	3.90	-	0.33	63	20.00
17SEP79	67	4.05	-	0.46	39	25.00
6NOV79	6	4.97	0.0027	0.20	890	0.10
6NOV79	23	2.67	0.0050	0.12	120	900.00
6NOV79	80	2.56	0.0044	0.20	250	1220.00
16NOV79	10	2.36	0.0000	0.23	280	550.00
16NOV79	30	2.00	0.0017	0.14	300	860.00
16NOV79	46	2.03	0.0010	0.22	210	1100.00
16NOV79	73	2.08	0.0043	0.18	115	1470.00
26NOV79	16	2.17	0.0115	0.29	156	36.00
26NOV79	40	2.39	0.0077	0.31	155	140.00
26NOV79	60	2.94	0.0080	0.35	113	190.00
26NOV79	80	3.00	0.0085	0.33	94	220.00
2JUN80	5	1.03		0.27	260	3.90
2JUN80	10	1.79	0.0069	0.25	130	21.00
16JUN80	15	2.92	0.0250	0.00	12	-
16JUN80	45	3.00	0.0083	0.13	24	-
16JUN80	75	3.92	0.0125	0.04	24	-

Simple plots of solids associated metal against SS show that there is some relationship between these two variables. Examples of this kind of plots are shown in Fig. 6.18.

A new variable name is now introduced, MESS (i.e. PBSS, CDSS, CUSS, ZNSS) which is the solids associated metal expressed as weight per weight.

The data implies that high solids concentrations do not correspond to an increase of solids associated metals. Through regression analysis relationships between MESS and different expressions derived from the SS concentration have been investi-

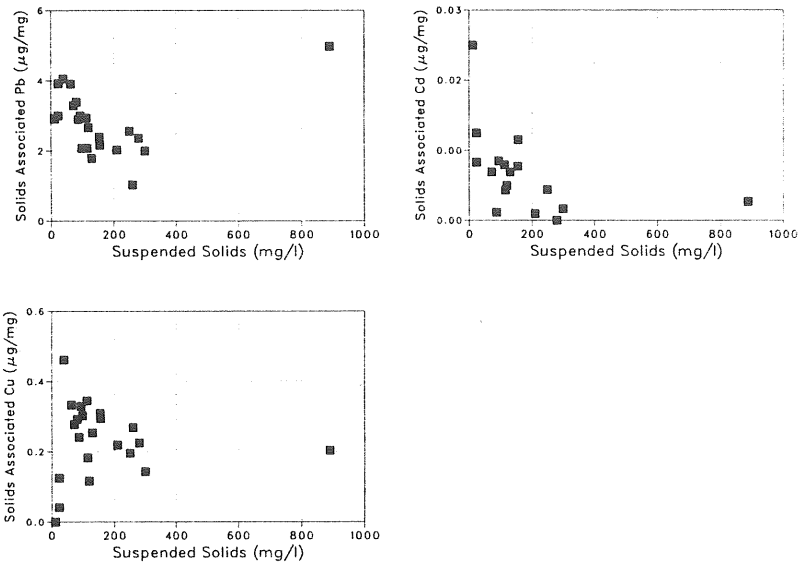

Figure 6.18 Plots of solids associated metals against SS.

gated. The models and the r^2 values are given in Table 6.10. The best fits are obtained with models which include accumulated SS (ASS), but still there are large variations around the regression line.

Table 6.10 Regression analysis of relationships between MESS and SS or ASS.

Metal	Model	r^2	N
PBSS	A+B*log(SS)	0.05	17
PBSS	A+B*ASS	0.32	14
PBSS	A+B*log(ASS)	0.50	14
CDSS	A+B*log(SS)	0.56	14
CDSS	A+B*ASS	0.15	13
CDSS	A+B*log(ASS)	0.10	13
CUSS	A+B*log(SS)	0.05	17
CUSS	A+B*ASS	0.45	14
CUSS	A+B*log(ASS)	0.25	14

Other models have been investigated but those reported in Table 6.10 are the best set of models with the original data.

It was observed however that high SS concentrations did not contribute as much as lower SS concentrations to the solids associated metals. The original SS concentrations were for this reason recalculated according to Eq. (6.3). The background of this equation was that it was observed that SS concentrations exceeding approximately 400 mg/l did not contribute to the solids associated concentrations.

$$SS = SS - \frac{SS^{1.92}}{1000} \tag{6.3}$$

A continued regression analysis with ASS as the independent variable gave the equations in Table 6.11. These are the equations which give the best fits using this approach.

Table 6.11 Regression equations of MESS as a function of ASS or log(ASS).

Metal	Model	r^2	N
PBSS	6.33-0.64*log(ASS)	0.64	13
CDSS	0.0087-3.5E-6*ASS	0.42	10
CUSS	0.367-1.5E-4*ASS	0.62	13

Plots of the regression equation and observed MESS against ASS are shown in Fig. 6.19.

Another approach is to look at mechanisms related to the surface area of the particles. The solids associated metal concentration, MESS (µg/mg), can be expressed as a constant metal load per unit area, MESSA (µg/mm^2), times a variabel X, as in Eq. (6.4).

$$MESS = MESSA \times X \tag{6.4}$$

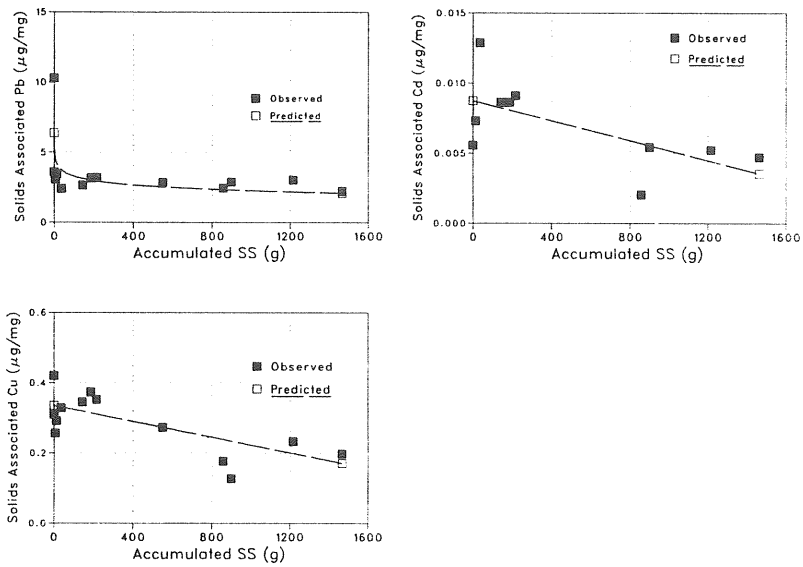

Figure 6.19 Plots of regression equations for MESS as a function of ASS or log(ASS).

Dimension analysis of the equation, gives the variable X the dimension of (mm^2/mg), which is the particle specific area, SA. Eq. (6.4) is then written:

$$MESS = MESSA \times SA \qquad (6.5)$$

The specific area does not vary for samples of the same particle size distribution, which would be the case for solids from, for example, a street surface. However, when the solids are transported, the particle size distribution will vary according to the transport capacity of different particle sizes. Samples of storm water runoff will have different particle size distributions depending on the transport capacity. The SS concentrations of the storm water are related to the transport capacity since an increase of transport capacity gives an increase of SS concentration.

A relationship between SS and SA can be derived. Assuming that all particles are spheres gives the following expression for the specific area (SA) as a function of particle size diameter.

$$SA = 3.34 \frac{1}{d} \qquad (6.6)$$

SA = specific area (mm^2/mg)
d = particle size diameter (mm)

The events in Table 6.9 can be used to simulate, with the solids transport model, the SS-loads of different particle size fractions for the same time intervals as in Table 6.9. The surface area in each of these fractions can be calculated with Eq. (6.6) thus giving the specific area of the composite sample.

Plotting this calculated specific area against SS gives Fig 6.20. A trend curve which is of the form $k/\sqrt{SS}$ is drawn together with the plotted points. Choosing a k-value of 4000 is giving the plotted line in Fig. 6.20.

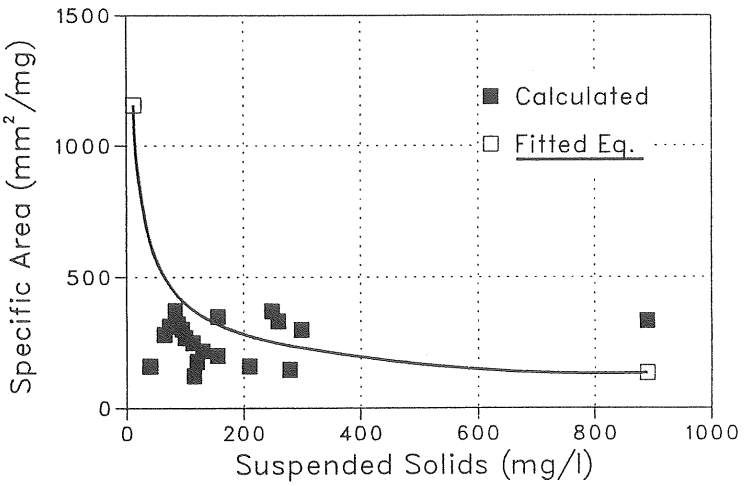

Figure 6.20 Plot of specific area against SS with a trend curve $SA=4000/\sqrt{SS}$.

Now regression lines can be made for the solids associated metals as a function of specific area, Eq. (6.5), using the calculated values of SA. The regression analysis gave the models reported in Table 6.12, using the SA-values derived by simulations with the solids transport model.

Table 6.12 Regression equations of solids associated metals as a function of simulated specific area using the events in Table 6.9.

Metal	Model	r^2	N
PBSS	0.0097*SA	0.85	19
CDSS	0.000019*SA	0.71	14
CUSS	0.00092*SA	0.85	19

The regression analysis gave the models reported in Table 6.13, using the SA-values derived by calculations with SA=4000√SS.

Table 6.13 Regression equations of solids associated metals as a function of specific area, calculated with SA=4000√SS.

Metal	Model	r^2	N
PBSS	0.0052*SA	0.78	22
CDSS	0.000017*SA	0.86	17
CUSS	0.00060*SA	0.83	20

According to Eq. (6.5), the estimate of the regression parameter should be interpreted as the metal load per unit area, MESSA ($\mu g/mm^2$). In other words, if solids associated metals are plotted against specific area and a straight line fits the points, the metal load per unit area could be estimated with the slope of the line.

The observed values of MESS are plotted against calculated and simulated specific area together with the regression lines of Table 6.13 in Fig. 6.21. The models in Table 6.12 were not used

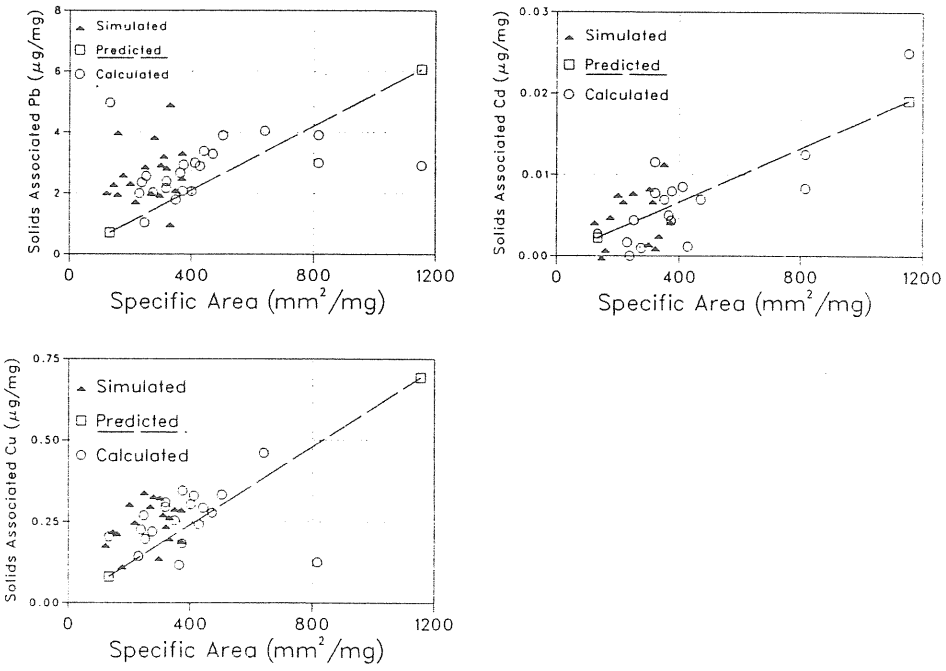

Figure 6.21 Plot of observed MESS against specific area. A regression line of the form: k*SA is fitted to the points.

for the further model development since the simulated specific areas were dependent on the quality of the solids transport model.

6.6.4 Solids associated metals dependent on particle size for the parking lot

The dataset of solids associated metals and particle sizes contains three stormwater runoffs from the parking lot. The concentrations are arithmetic means of three parallell samples taken from a container with a mixed sample from the entire runoff. The procedure for the separation of a sample into different particle size fractions is described in Chap. 6.4.

The particle size fractions are represented by the geometrical mean particle sizes: 0.010, 0.025, 0.050, 0.100, 0.200 mm.

Describing the solids associated metals in terms of weight per weight concentrations is giving the bar charts in Fig. 6.22. A marked tendency is the decrease of solids associated metals with the increase of particle size. This is consistent with the discussion in Chap. 6.6.3 where it was found that increasing specific area, that is smaller particle size, gave higher weight per weight concentrations.

The solids associated concentrations can be described in terms of weight per specific area of the particles if the specific areas are known, see Eq. (6.6).

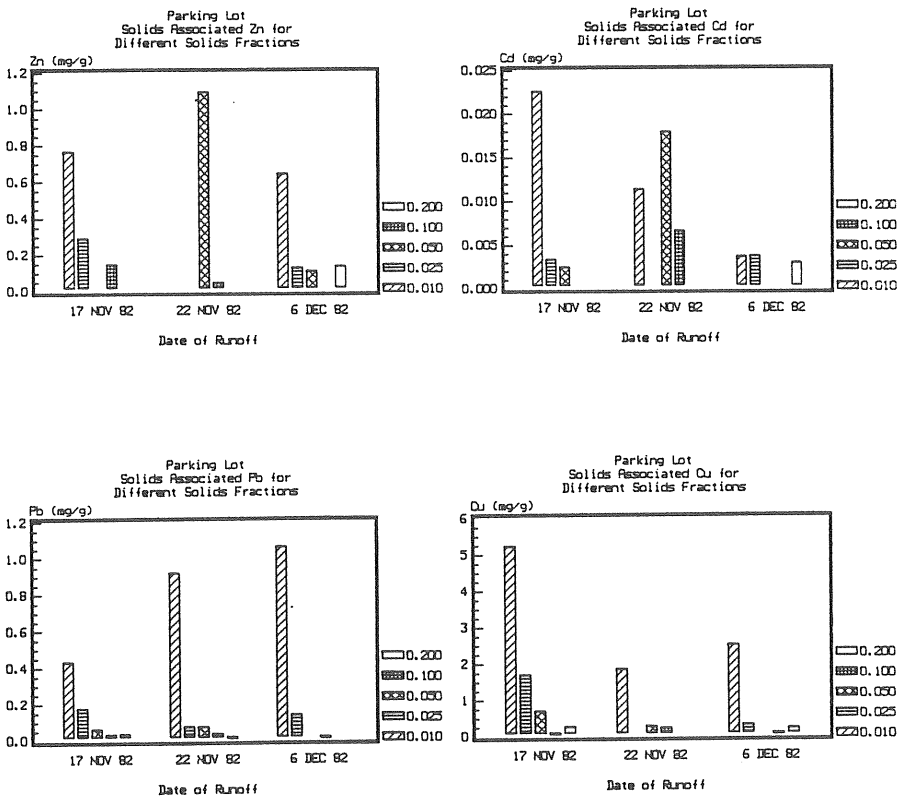

Figure 6.22 Solids associated metals concentrations in mg/g for three stormwater runoffs from the parking lot.

The metals concentrations in weight per unit area of the particles are given in the charts in Fig. 6.23. There are variations between particle sizes and between storms, but no clear tendency is evident. A most believable assumption is that the concentrations are constant and that the variation is due to sampling and analyzing errors.

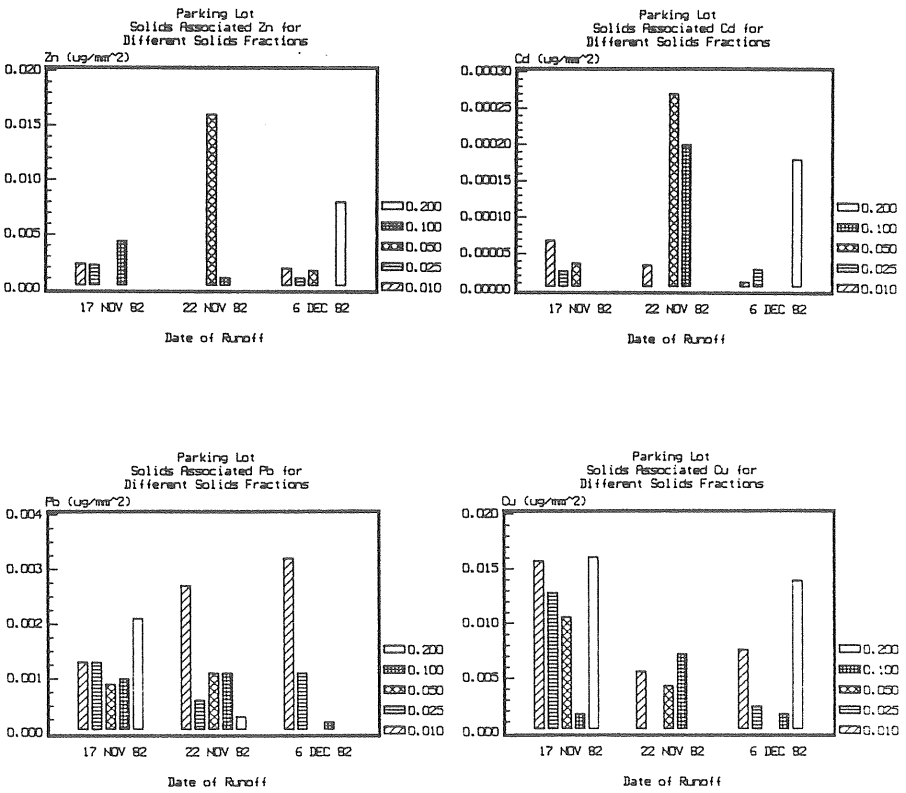

Figure 6.23 Solids associated metals concentrations in $\mu g/mm^2$ for three stormwater runoffs from the parking lot.

The arithmetic means of the concentrations per unit area have been calculated for all samples and fractions together. These can be compared to the constant concentrations per unit area

calculated in Chap. 6.6.3. There are differences between the two datasets but the street concentrations fall within the range of the concentrations of the parking lot. Considering lead a higher concentration is expected for the street than for the parking lot. (See Table 6.14)

Table 6.14 Means and standard deviations of solids associated metals concentrations in $\mu g/mm^2$.

	Pb	Cd	Cu	Zn
		($\mu g/mm^2$)		
Arithmetic mean	0.0011	0.000057	0.0066	0.0022
Standard deviation	0.0009	0.000087	0.0059	0.0025
Number of samples	15	15	15	10
Calculated from street data	0.0052	0.000017	0.0006	-

A regression analysis of the data, assuming that the solids associated concentration is an inverse function of the particle size diameter, was made. The analysis gave fairly good r^2 values except for cadmium. The regression equations are reported in Table 6.15.

Table 6.15 Regression equations of solids associated metals as functions of particle size, d (μm).

Metal	Model	r^2	N
PBSS	7.19 * 1/d	0.84	15
CDSS	0.126* 1/d	0.53	15
CUSS	29.4 * 1/d	0.77	15
ZNSS	6.69 * 1/d	0.94	10

Since the solids associated concentration is the product of the load per unit area and the specific area, the load per unit area can be calculated from the estimated constant of the regression equations in Table 6.15. Using Eq. (6.6) as the expression of specific area, the loads per unit area are calculated to the values reported in Table 6.16.

Table 6.16 Three estimates of metal load per unit area derived from data from the street area and the parking lot.

	Pb	Cd	Cu	Zn
		($\mu g/mm^2$)		
Parking lot, samples for different size fractions				
Estimated from regression Eq.	0.0022	0.000038	0.0088	0.0020
Arithmetic mean	0.0011	0.000057	0.0066	0.0022
Street area, samples for mixed size fractions				
Calculated	0.0052	0.000017	0.0006	-

These three estimates of load per unit area have been used to calculate the three curves which are plotted together with the original data in Fig. 6.24.

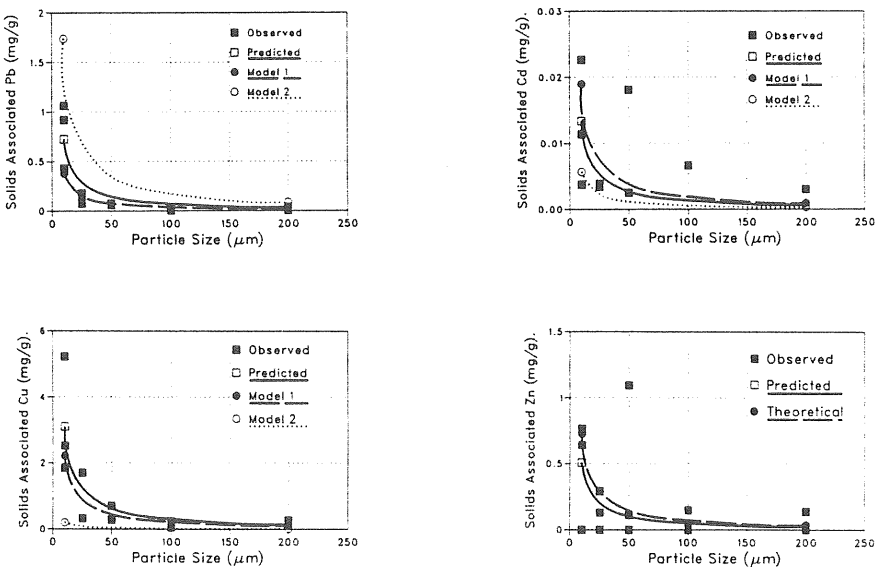

Figure 6.24 Solids associated metal as function of particle size. Predicted is the regression equation, Model 1 is based on the arithmetic mean and Model 2 is based on data from the street area.

6.6.5 A model for solids associated metals.

The different expressions for solids associated metal concentrations derived in Chap. 6.6.3 and Chap. 6.6.4 are in principal of two types. One based on pure regression analysis and one based on a deterministic model which has been evaluated by regression analysis. The pure regression equations naturally fits the observed data best. The deterministic based equations are however more general, since they reflect a real relationship between the variables and can be used for deterministic modelling. The quality of the deterministic based equations must be evaluated and found acceptable. If this is the case, a deterministic based equation will be preferred to a regression equation even if the regression equation fits the observed data better.

The analyses in the two previous chapters has given a logical based equation for the calculation of solids associated metals concentrations. The form is given in Eq. (6.7) and includes the specific area and the metal load per unit area of solids.

$$MESS = MESSA \times SA \tag{6.7}$$

MESS = solids associated metal (µg/mg)
MESSA = metal load per unit area (µg/mm^2)
SA = specific area (mm^2/mg)

The metal load per unit area has to be known and is regarded a constant. Values of MESSA have been evaluated both out of data from the street area and the parking lot. These are tabulated in Table 6.16.

There are two methods of calculating MESS demonstrated. In Chap. 6.6.3, SA is calculated for a sample of several particle size fractions and then multiplied with MESSA. The other method, demonstrated in Chap. 6.6.4, is to calculate MESS for each particle size fraction and then sum up for a mixed sample. SA is calculated for each particle size fraction.

The former method will probably give better results, when verified with the stormwater runoffs not included in the analysis in Chap. 6.6.3. The reason is that this method is based on a much larger data base than the latter method.

Both methods are verified and evaluated in Chap. 8 with the part of the data base that has not been included in the analyses so far.

7. AN IMPROVED MODEL FOR THE SIMULATION OF SEDIMENT TRANSPORT WITH SURFACE RUNOFF

7.1 Introduction

7.1.1 Modelling concept

A model appropriate for urban areas has to describe the most frequent surfaces fairly well. Most of the urban surfaces which contribute to stormwater runoff, i.e. connected to a storm water pipe system, can be described by two planes and a channel. A simple example is the pavement, the street surface and the gutter. An outline of this model concept is made in Fig. 7.1.

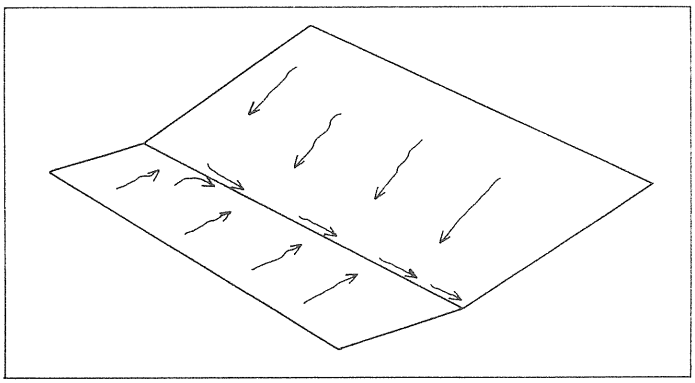

Figure 7.1 Simplified sub-catchment description of an urban area.

The model also has to have the ability to transform a historical rainfall to runoff with a resolution in time of about one minute. The reason to this is that the time of concentration for these sub-catchments can be as little as 2-3 minutes.

The sediment transport cannot be simulated without accounting for different particle sizes, as has been shown in Chap. 5. To match the findings of Chap. 6 concerning metal transport, each particle size fraction has to be treated separately.

The simple model presented in Chap. 4 has the ability of treating different particle size fractions separately but not the ability of treating a channel nor the ability of handling a variable rainfall intensity over time.

A model with the desired features was developed for rural areas at the Colorado State University, see Simons et al. (1977). This model has been further developed and applied to urban areas in the framework of this thesis. Below is a description of the model with references to the description of surface runoff and sediment transport theory in Chap. 4.

7.1.2 Verification of the improved model

The aim of this chapter is to verify the improved sediment transport model. Data on sediment transport with surface runoff (see Chap. 6) collected for the street area and the parking lot is used for the verifications. The database of observed storm events is divided into one part for calibration of some constants and one part for verification purposes.

7.2 Description of the sediment transport model

The model has the ability to describe two planes and a channel, The surface runoff from the planes feeds the channel, which is supposed to be connected to a catch basin. An outline of the physical characteristics described by the model is given in Fig. 7.2.

Each plane is described by its length in the direction of flow, L and its slope, S_0. The channel is described by its length, W, which also determines the width of the planes, and its slope, S_c. The cross section of the channel is given by the slope of one of the planes and a vertical border of the other plane, which is explained in detail in Fig. 7.2.

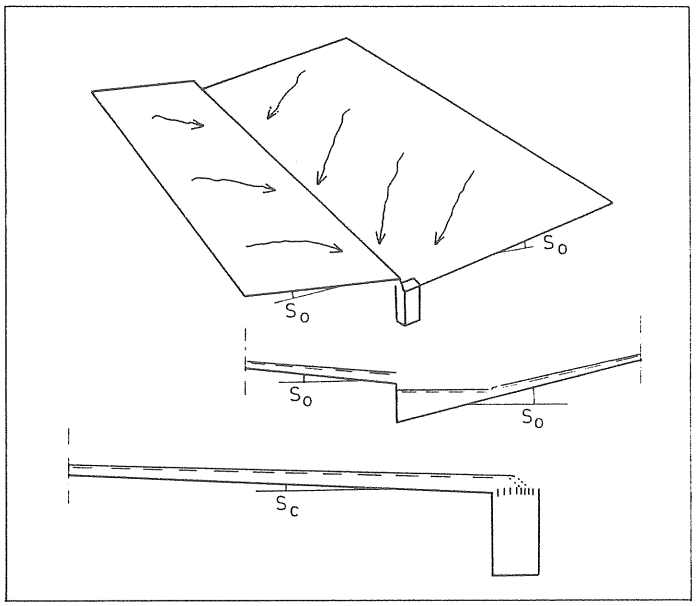

Figure 7.2 Particle transport model sub-catchment description.

The sediment yield from the sub-catchment is modeled in principal in the following way. Sediment rests on the two planes and will do so until it is made available for transport by rain detachment and flow detachment. The detached sediment is calculated separately for each given particle size fraction. However, there has to be some transporting capacity to produce a sediment yield from the planes. The transporting capacity is calculated from the surface flow and properties of the sediment. Depending on which of the two, i.e. the detached sediment volume for each size fraction or the transporting capacity, that is limiting, the yield is calculated from the smallest of them.

The yield from each plane together with what is detached by channel flow is calculated as the total detached sediment, thus available for transport by channel flow. The transporting capacity of the channel flow is calculated and compared to the total detached sediment. The sediment yield of the sub-catchment is again the smallest of the two.

A short description of the processes involved is given in Fig. 7.3. The processes are:

Overland flow, which is calculated according to Eq. (4.7) and Eq. (4.8)

Gutter flow, which is calculated according to Eq. (4.9) and Eq. (4.18).

Detachment by rain, which is described in Chap. 4.3.1. The equation is Eq. (4.21).

Detachment by flow, that is both overland flow and gutter flow. The equation used is Eq. (4.22).

Transporting capacity, which is calculated in the same manner for the planes and the gutter. The equations are described in Chap. 4.3.2 and are Eq. (4.26) for bed load and Eq. (4.36) for suspended load.

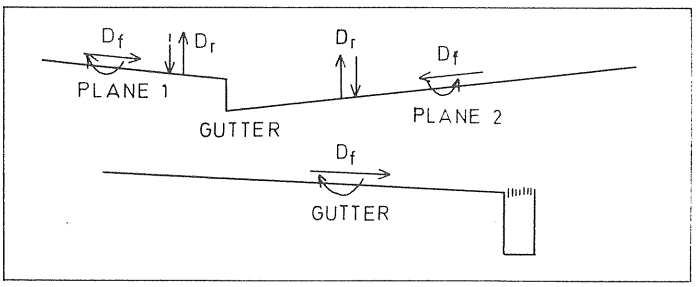

Figure 7.3 Processes included in the sediment transport model.

A flowchart for the model is given in Fig. 7.4. It should be noted that all calculations are made for each given particle

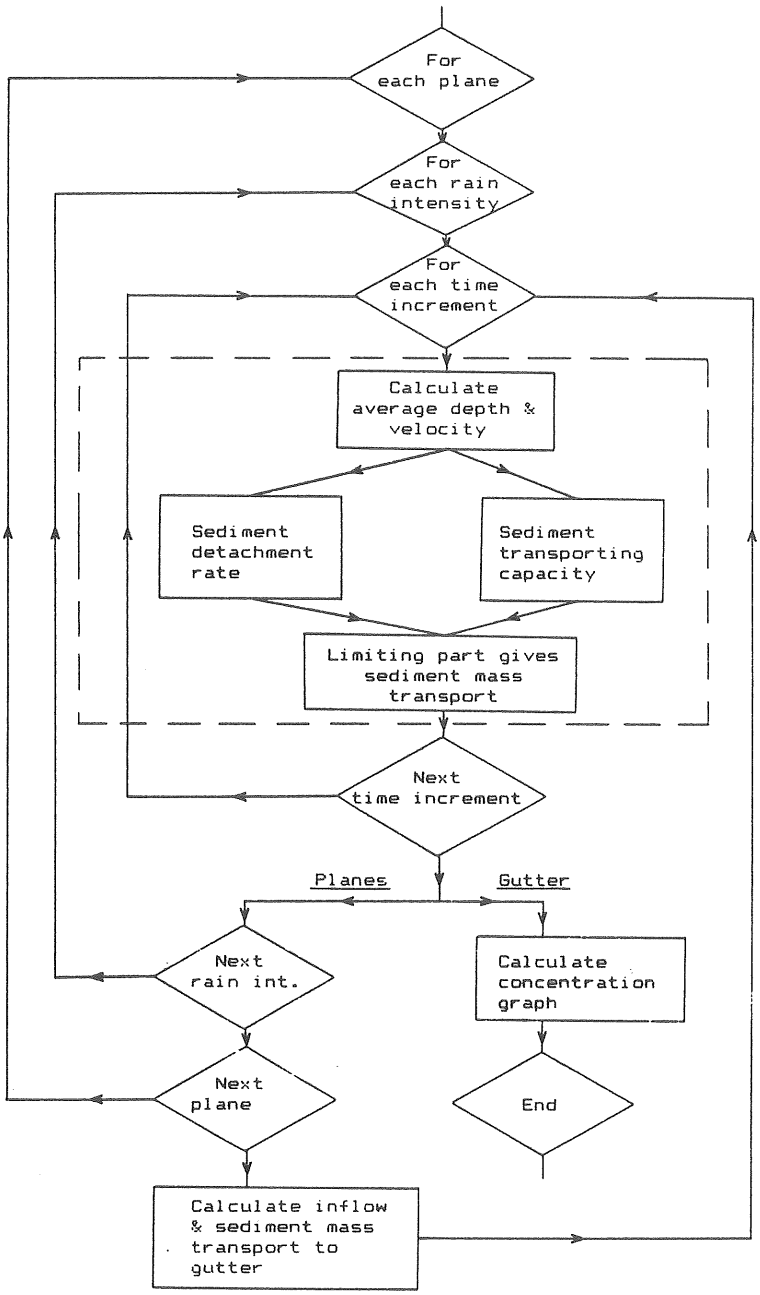

Figure 7.4a A flowchart for the sediment transport model.

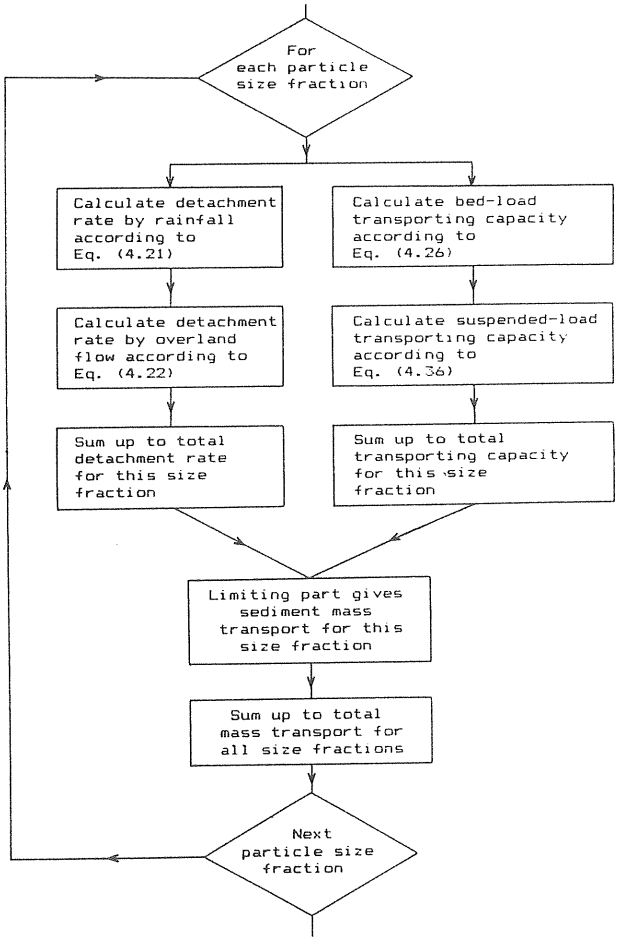

Figure 7.4b A detailed flow chart for the detachment and transport part of the sediment transport model.

size fraction, that is the geometrical mean of the particle size range. The time resolution is one minute, that is both sediment and water is routed over the surfaces and through the gutter with a time resolution of one minute.

7.3 Calibration of some model constants

Most of the variables and constants used in the model correspond to a physical property, as for example slope, length and width of the planes, surface roughness, density of the particles etc.

However, there are some constants which cannot be obtained from data about the catchment. These have to be derived from experiments and may therefore be regarded as calibration constants. In the absence of experimental data, data from the literature can be used.

The constants, whose values must be determined are:

The detachment by rain constant, D_r, in Eq. (4.21).
The detachment by flow constant, D_f, in Eq. (4.22).
The critical shear stress constant, B_s, in Eq. (4.28).

From the database of runoffs from the street catchment and the parking lot, three runoffs were choosen for calibration of the detachment and critical shear stress constants. The three runoffs were all from the street and belonged to the same group of runoffs as those used for the developement of the model for solids associated metals.

Table 7.1 gives the values of the calibration constants and in Fig. 7.5 simulated sediment volumes are compared to observed volumes.

Table 7.1 Values of the detachment and critical shear stress constants used for all simulations.

Detachment by			Critical shear stress	
Rain	Overland flow	Channel flow	Plane	Channel
D_r	D_f	D_f	B_s	B_s
0.001	0.0001	0.003	0.10	0.10

As seen from Fig. 7.5 the simulated sediment volumes are in good agreement with those observed.

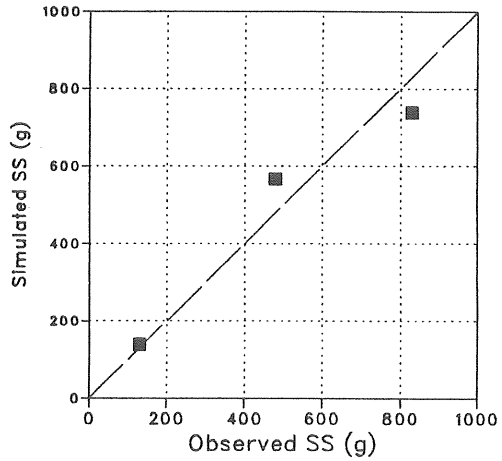

Figure 7.5 Simulated sediment volumes for the street catchment compared to observed volumes for three diffferent runoffs.

7.4 Sensitivity analysis

A sensitivity analysis was made for the constants in Table 7.2. Each constant was varied in the range 0.1-10 and the others were held at the given value.

Table 7.2 Constant values used for the sensitivity analysis.

Plane slope	0.010
Channel slope	0.010
Channel friction	0.40
Detachment by overland flow	0.0001
Detachment by rain	0.001
Detachment by channel flow	0.003
Channel shear stress	0.10

All simulations were made with a constant rainfall intensity of 10 mm/h. The response was recorded as the runoff sediment concentration. Fig. 7.6 shows the variations in runoff sediment concentration when changing the constants one by one. The figure shows, that with regard to the planes the runoff sediment concentration is most sensitive to the detachment by rain constant. With regard to the channel, the sediment concentration is most sensitive to the channel shear stress constant. Also if

the slope becomes too flat, i.e. slopes less than 0.01, the sediment concentration decreases rapidly.

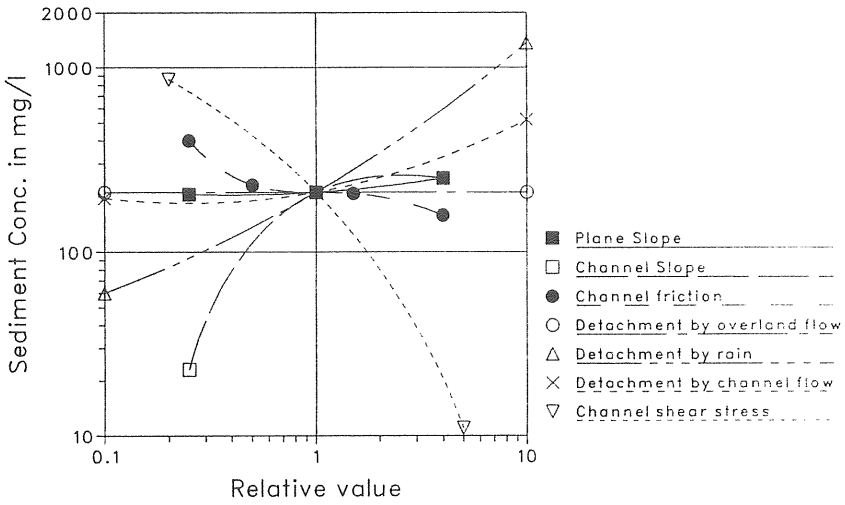

Figure 7.6 Sensitivity of the sediment transport model.

It is also found from the figure, that with regard to the planes, the detached sediment volume determines the yield, while the transport capacity determines the yield from the channel.

7.5 Verification for selected rainfalls

A set of six runoff events were choosen for the verification, four from the street catchment and two from the parking lot. In Table 7.3 some characteristics for these rainfalls are described.

Table 7.3 Description of selected rainfalls used for the verification of the simulation of sediment yield.

Date	Rainfall Characteristics			Type
	Volume (mm)	Mean Intensity (mm/h)	Max. Intensity (mm/h)	
2SEP79	0.30	5.60	6.40	Street
11SEP79	0.30	1.19	3.40	Street
6NOV79	3.70	2.80	10.20	Street
28AUG80	0.50	1.25	6.00	Street
6NOV79	3.40	2.80	10.20	Parking lot
17SEP80	4.80	1.90	14.70	Parking lot

Simulated sediment yield was compared to observed sediment yield with respect to total mass, time from the beginning of the runoff to the peak and peak value. The results are shown in Fig. 7.7, Fig. 7.8 and Fig. 7.9.

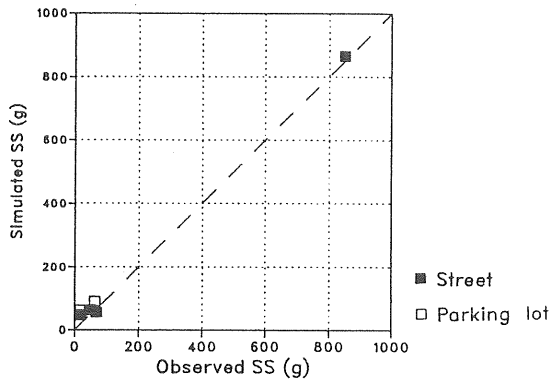

Figure 7.7 Simulated sediment mass compared to observed mass for four runoffs from the street and two from the parking lot.

As seen from Fig 7.7 there is a good agreement between simulated mass and observed mass. However, looking at the peak value and the time of occurence, the precision is not as good as for the mass. Still, both peak value and time to peak are fairly well simulated by the model, as can be seen from Fig. 7.8 and Fig. 7.9.

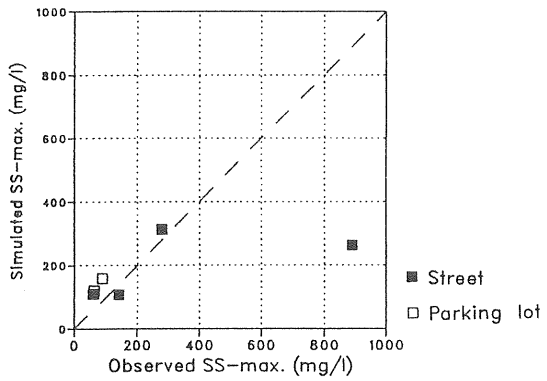

Figure 7.8 Simulated peak sediment concentrations compared to observed peak concentrations for four runoffs from the street and two from the parking lot.

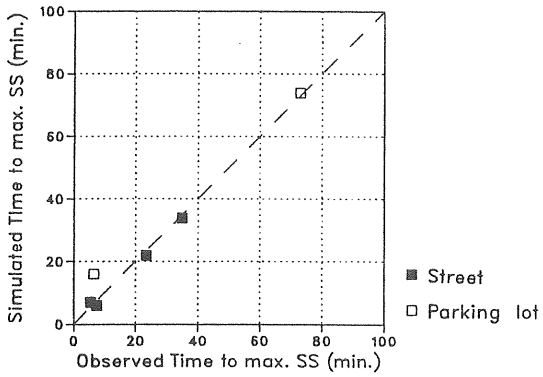

Figure 7.9 Simulated time to peak compared to observed peak for four runoffs from the street and two from the parking lot.

To demonstrate the goodness of the fit between the simulated concentrations and the observed concentrations, two runoff events, one from the street and one from the parking lot have been choosen. It is seen from Fig. 7.10 and Fig. 7.11 that the

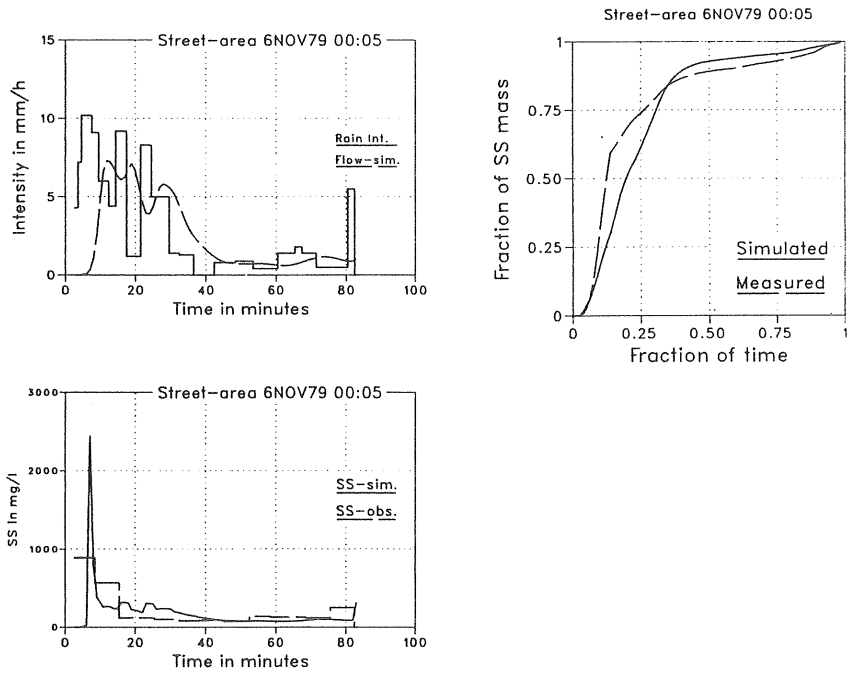

Figure 7.10 Simulated and observed concentrations for the street runoff 6 Nov. 79.

peaks are hit but that the simulated peak values are greater than the observed ones. One explanation may be that the observed concentration curve has a time resolution, which is as short as three minutes and most often around six minutes.

Looking at the fraction graphs in Fig. 7.10 and Fig. 7.11, the simulated curve and the observed curve follow each other well. They also demonstrate that for this kind of storm about 75% of the sediment mass is transported during the first 25% of the runoff duration.

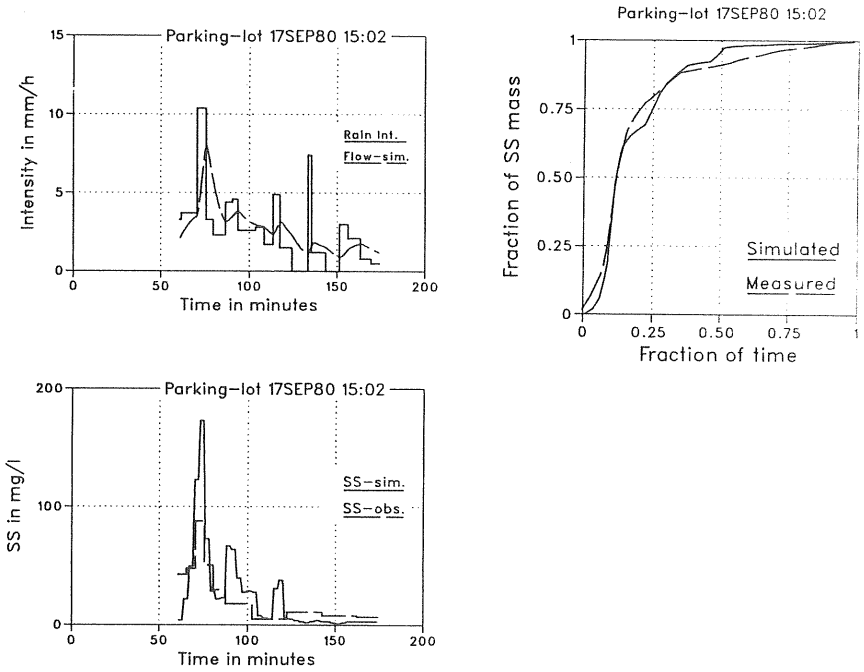

Figure 7.11 Simulated and observed concentrations for the parking lot runoff 17 Sep. 80.

8. AN IMPROVED MODEL FOR THE SIMULATION OF HEAVY METAL TRANSPORT WITH SURFACE RUNOFF

8.1 Simulation of dissolved heavy metals

According to Chap. 6.6.3 the observed dissolved metal concentrations show different concentration levels for different storms. Within storms, however, the concentration levels are relatively constant. The variation between storms can partly be explained by variations in the pH-value. The lower the pH-value is the higher the dissolved metal concentration will be. Plotting observed dissolved metal concentrations versus pH-value gives, however, no distinct picture of this relationship, which is shown in Fig. 8.1.

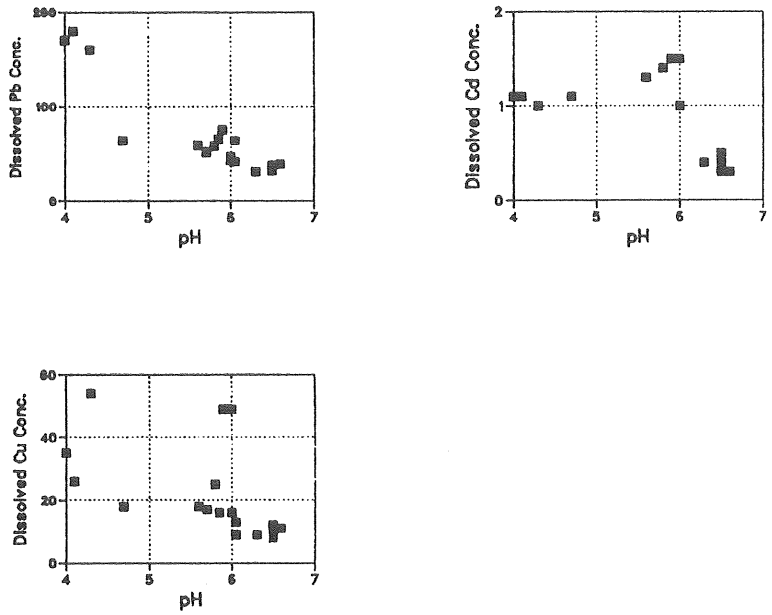

Figure 8.1 Dissolved metal concentrations of Pb, Cd and Cu plotted versus pH-value.

Since the dissolved metal concentrations are relatively constant compared to the solids associated concentrations within storms, the dissolved metal concentrations are treated as constants for simulation purposes. The dissolved concentrations used are given in Table 8.1.

Table 8.1 Dissolved metal concentrations of Pb, Cd and Cu used for simulation purposes.

Pb (µg/l)	Cd (µg/l)	Cu (µg/l)
20.0	0.60	25.0

An improvement of the simulation model would be to incorporate a relationship between pH and dissolved metal concentration. However, forecasting of pH-values is difficult and simulations affected by changes in pH-value would be interesting when simulating annual loads for example. The storms could in this case be ranked according to pH-value.

8.2 Solids associated metals

8.2.1 Developement of a model

The analysis in Chap. 6 of the observed runoffs from the street and the parking lot gave, as a result, suggestions of how to simulate solids associated metals.

In principal, it has been shown, that the concentrations of solids associated metals, expressed as mass of metal per mass of solid, can be explained by using a constant metal load per unit area of solids and assuming spheric particles. The general equations derived are Eq. (6.6) and Eq. (6.7). They are written below in a form which allows for calculations for different particle sizes.

$$SA_i = 3.34\frac{1}{d_i} \qquad (8.1)$$

SA_i = specific area (mm^2/mg)
d_i = mean diameter of the i:th particle fraction (mm)

$$MESS_i = MESSA \times SA_i \qquad (8.2)$$

$MESS_i$=solids associated metal (µg/mg)
MESSA=metal load per unit area (µg/mm^2)

The constant MESSA have been estimated in three different ways, which are described in Table 6.16. Three storms from the parking lot were collected and the solids separated into size fractions. These particle size dependent data have been used to determine MESSA by regression and by calculating the arithmetic means for all data, thus disregarding the size fractions. The third method of calculation was by regression analysis of six storms from the street. These samples were mixed with respect to particle sizes.

The three sets of MESSA-constants are used for the further simulations and referred to as Model 1, Model 2 and Model 3. The constants are tabulated below Table 8.2 with the appropriate reference.

Table 8.2 Estimates of metal load per unit area, MESSA, for Model 1, Model 2 and Model 3.

Data from		Pb	Cd	Cu	Zn
			(µg/mm^2)		
Parking lot	Model 1	0.0022	0.000038	0.0088	0.0020
- " -	Model 2	0.0011	0.000057	0.0066	0.0022
Street area	Model 3	0.0052	0.000017	0.0006	-

8.2.2 A subroutine for solids associated metals

The routine for calculation of solids associated metal concentrations uses Eq. (8.1) and Eq. (8.2), thus making a calculation for each particle size choosen. However, the runoff and solids transport calculations are time dependent. The solids concentration will vary with time and so will the metal concentrations. This time dependency is reflected in Eq. (8.3), which is the equation for the calculation of metal concentration for one particle size fraction.

$$MEC_i(t) = MESSA \times SA \times SS_i(t) \tag{8.3}$$

$MEC_i(t)$=time and particle size dependent metal concentration (mg/m^3)

The total concentration is achieved by summing up for all particle sizes.

$$MEC(t) = \sum MEC_i(t) \tag{8.4}$$

MEC(t)=time dependent metal concentration (mg/m^3)

To obtain the metal mass flow it is necessary to introduce the runoff flow, Q(t), which is done in Eq. (8.5).

$$MEM(t) = Q(t) \times MEC(t) \tag{8.5}$$

MEM(t)=time dependent metal mass flow (mg/s)
Q(t) =runoff flow (m^3/s)

For the runoff event, the transported metal mass is calculated by integration over time.

$$MEM = \int MEM(t)dt \tag{8.6}$$

MEM=total metal mass for the event (mg)

A flow chart for the solids associated metals subroutine is given in Fig. 8.2. The equations used for the calculations are the equations given in this chapter.

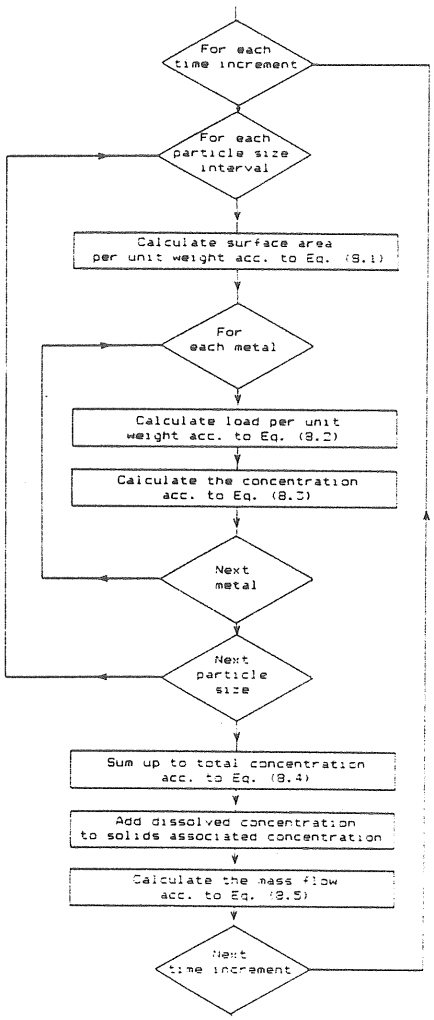

Figure 8.2 Flow chart for the solids associated metals subroutine.

8.3 A model for simulation of total concentrations

The total concentrations, mass flows or event masses are achieved simply by adding dissolved metal to solids associated.

The model for total metal concentrations is described by the flowchart in Fig. 8.2. The only difference is that the dissolved concentrations are added.

8.4 Verification for selected rainfalls

8.4.1 Dependent runoff events with respect to metals

Model 3, for which the solids associated metal constant was derived from six runoff events from the street, have been checked towards these events. The events are given in Table 8.3 together with some charecteristics of the rainfalls.

Table 8.3 Characteristics of six runoff events, which are dependent with respect to solids associated metals.

Date	Rainfall Characteristics			Type
	Volume (mm)	Mean Intensity (mm/h)	Max. Intensity (mm/h)	
17SEP79a	0.60	1.98	5.70	Street
17SEP79b	0.70	1.11	3.30	Street
6NOV79	3.70	2.80	10.2	Street
16NOV79	3.70	1.80	10.2	Street
26NOV79	2.70	2.32	17.6	Street
2JUN80	0.60	9.42	12.6	Street

Fig. 8.3 shows that there is good agreement between observed and simulated sediment yield for these runoff events.

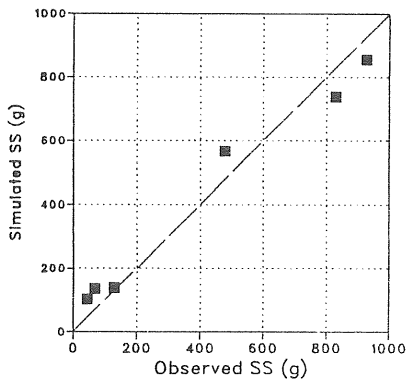

Figure 8.3 Simulated and observed sediment mass for six runoff events from the street.

The simulated metal masses are also close to the observed masses, which is seen from Fig. 8.4. With respect to total masses the model reflects what has been observed.

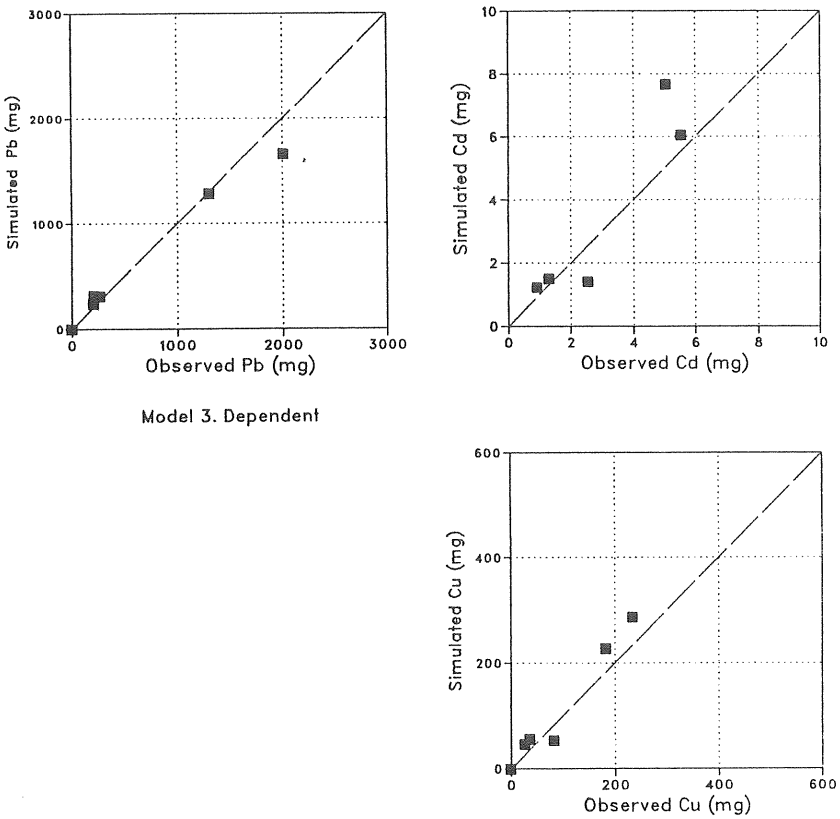

Figure 8.4 Simulated and observed metal masses for six dependent runoff events from the street.

The time dependent simulated and observed concentrations have been plotted in Fig. 8.5 to see if the model is capable of simulating the dynamics of a runoff event.

The comparisons between observed and simulated masses as well as observed and simulated concentrations demonstrate that the model reflects the physical processes with respect to solids and metals. However, the metal load per unit area of solids was

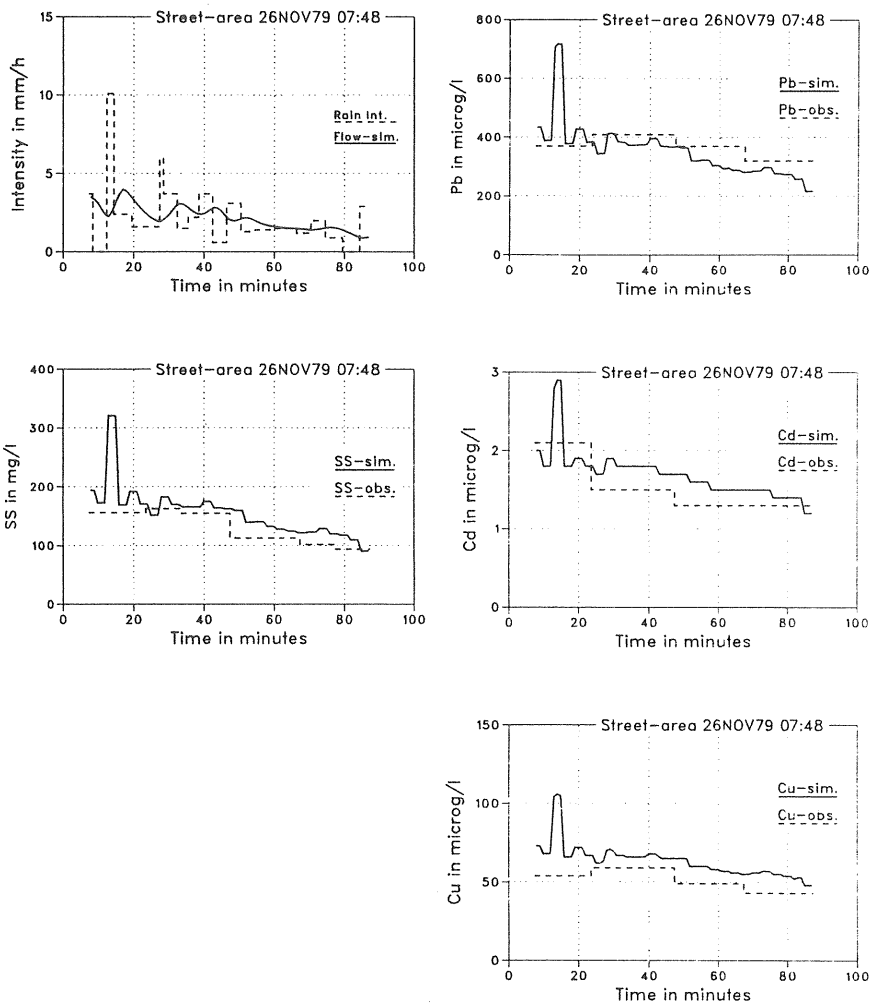

Figure 8.5 Simulated and observed concentrations for the runoff event 26 Nov. 79.

derived from the same set of rainfalls, as the simulations were made with. A true verification has to be made with independent rainfalls, which is described below.

8.4.2 Independent runoff events with respect to metals

It has been possible to select five independent runoff events from the database of observed runoffs. Three from the street and two from the parking lot. The rainfalls and their characteristics are described in Table 8.4.

Table 8.4 Characteristics of five rainfall events from the street and the parking lot. All of them independent with respect to solids and metals.

Date	Rainfall Characteristics			Type
	Volume (mm)	Mean Intensity (mm/h)	Max. Intensity (mm/h)	
16AUG80	0.90	1.28	16.6	Street
28AUG80	0.50	1.25	6.0	Street
17SEP80	5.30	1.90	14.7	Street
16AUG80	0.70	1.46	16.6	Parking lot
17SEP80	4.80	1.90	14.7	Parking lot

The verification is made for Model 1, Model 2 and Model 3 separately and the results with respect to masses are compared metal by metal. It is expected, that Model 1 and 2 would not give as good results for the street as for the parking lot, since the metal loads per unit area are derived from runoffs from the parking lot for these models. Fig. 8.6 and Fig. 8.7 verify this. In conclusion, Model 1 and Model 2 underestimate the Pb masses and overestimate the Cd and Cu masses for the street. The masses from the parking lot are well simulated except for Cu, which is overestimated.

Model 3, derived from observed runoffs from the street, gives the best agreement between observed and simulated masses for all metals and for both surfaces. The Cd masses are simulated with an accuracy which is better than +/- 10%. The Pb and Cu masses are simulated within +/- 30%, which is acceptable.

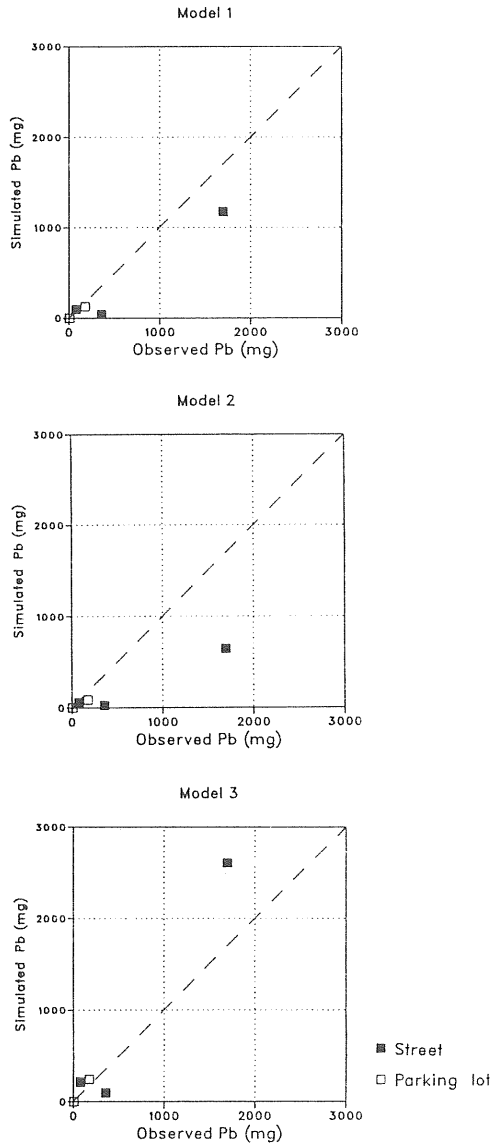

Figure 8.6 Comparison between simulated and observed masses of Pb for Models 1, 2 and 3.

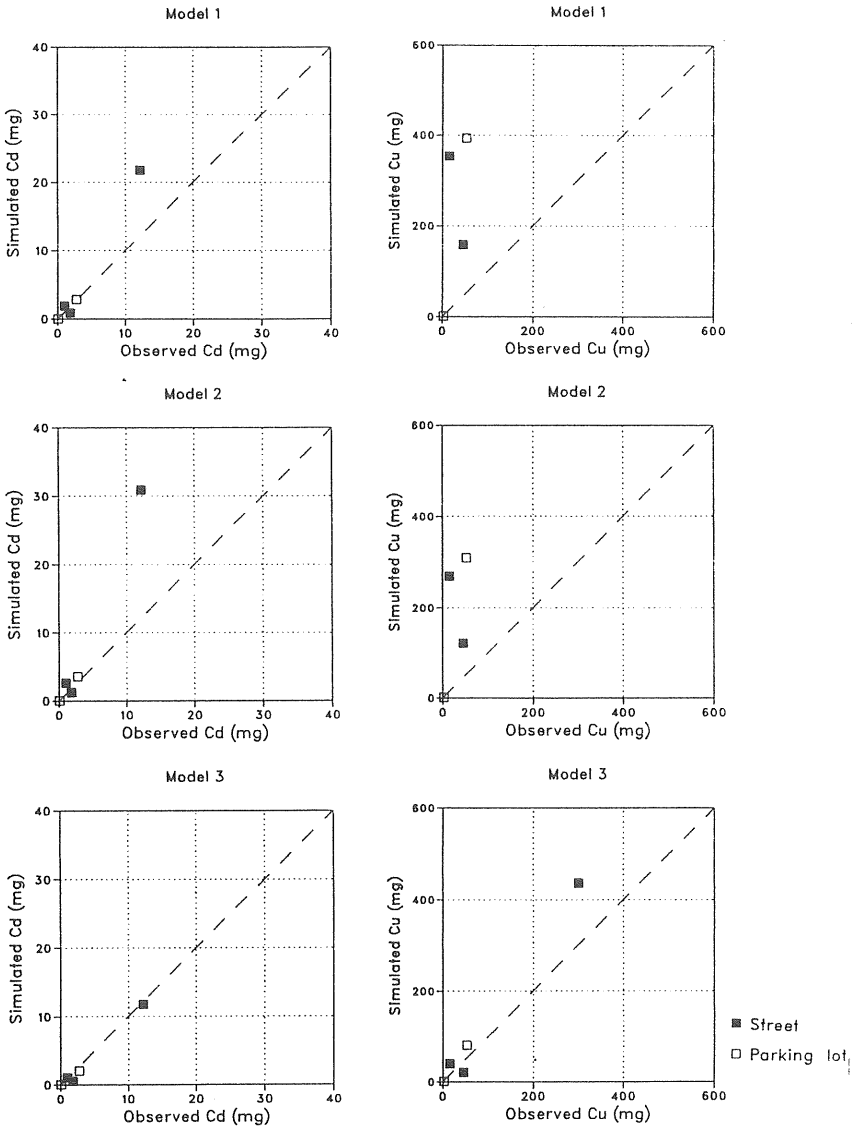

Figure 8.7 Comparison between simulated and observed masses of Cd and Cu for Models 1,2 and 3.

A demonstration of how well Model 3 reflects the dynamics of the runoff event is given in Fig. 8.8 and Fig. 8.10, where the same runoff event, 17 Sep. 80, is shown for both areas.

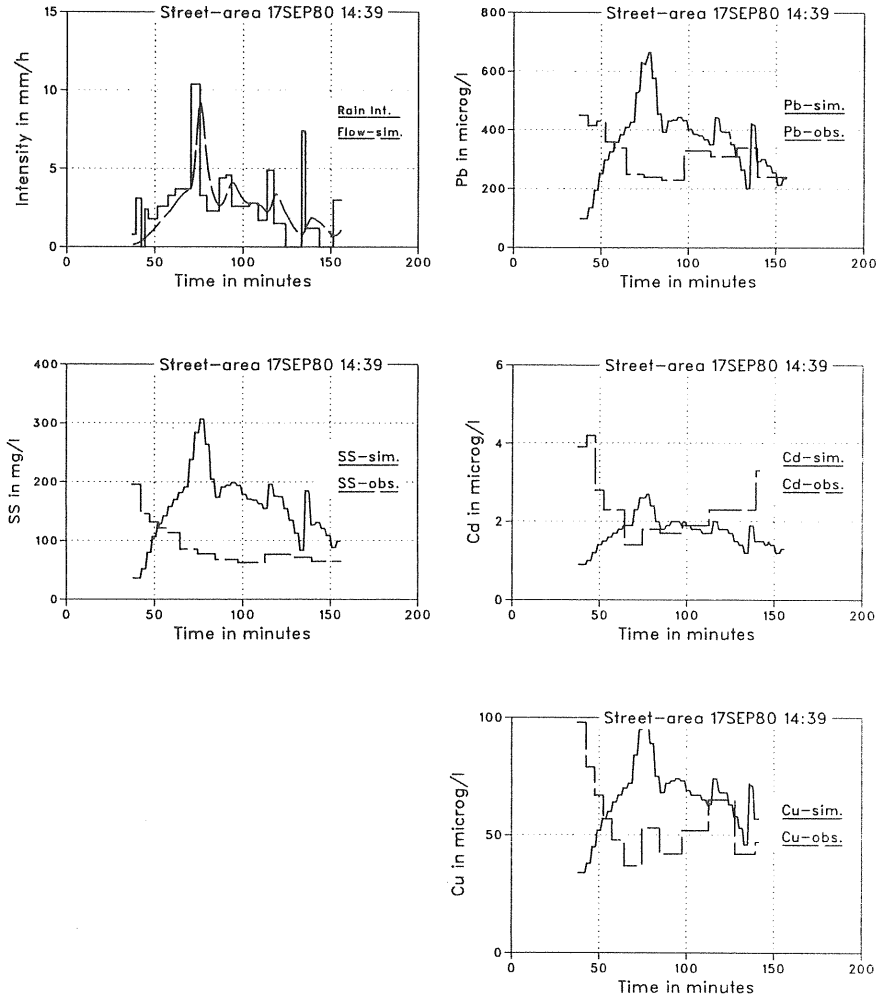

Figure 8.8 Simulated and observed graphs for the street area 17 Sep. 80. Simulations with Model 3.

As seen from Fig. 8.8, the solids are poorly simulated. There seems to be some timing error, which cannot be explained. The fraction graphs in Fig. 8.9 give the same message, too low simulated concentrations in the beginning of the runoff and to high later during the runoff event. The simulated solids mass is

overestimated with a factor of 1.4. The conclusion is, that if the solids are poorly simulated, the metals will also be poorly simulated.

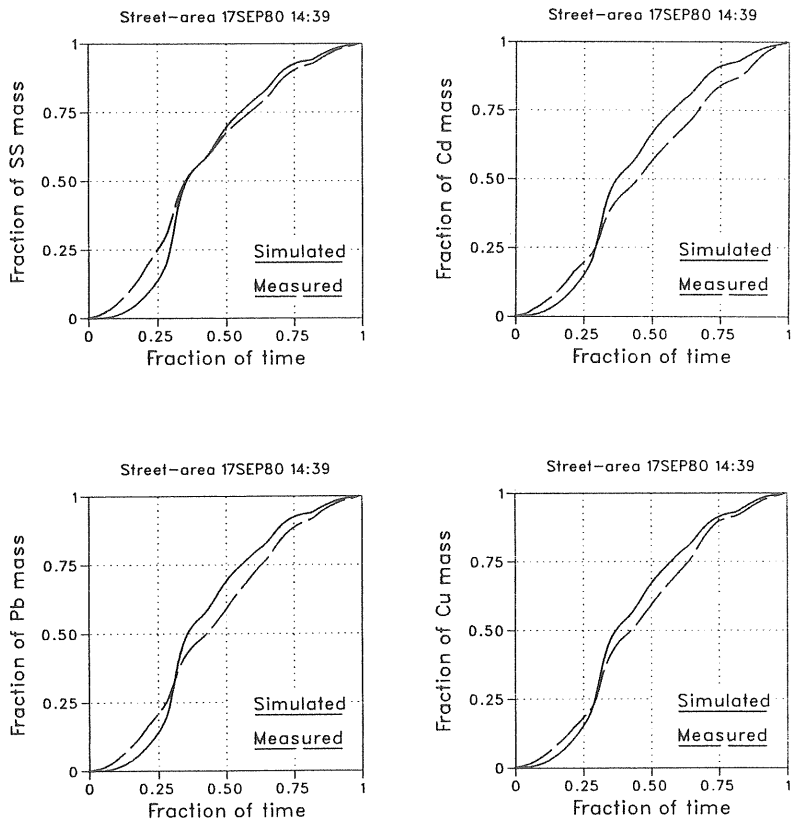

Figure 8.9 Fraction graphs for the street runoff event 17 Sep. 80.

The parking lot event in Fig 8.10 displays a good simulation of solids. The peak value is overestimated compared to the observed peak value. This is however partly expected due to the sampling procedure, which did not allow for better resolution than 3-9 minutes. The second and the third peaks are not showed by the observed curve, but these are contained in one sample each.

The metals are also well simulated, the highest peak is hit on time, but for Pb and Cu the peak value is overestimated.

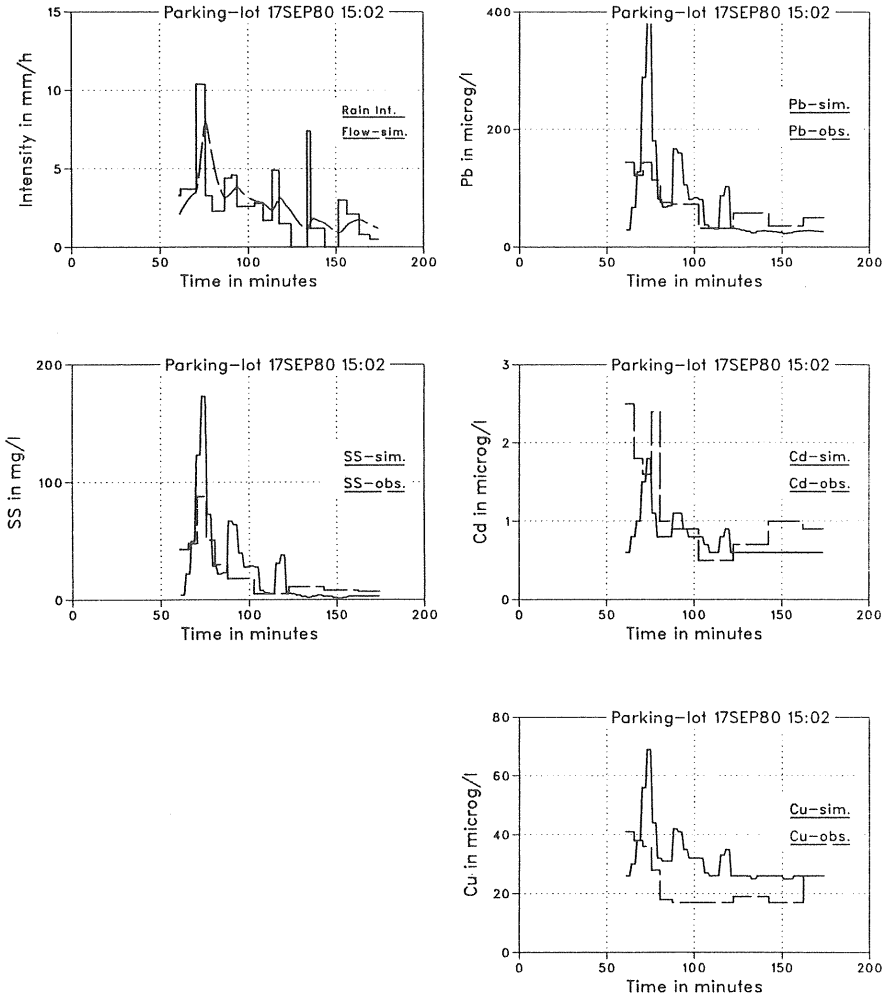

Figure 8.10 Simulated and observed graphs for the parking lot 17 Sep. 80. Simulations with Model 3.

The fraction graphs in Fig. 8.11 give, compared to Fig. 8.9, an impression that the difference between the simulations for the two runoff events is neglectable. This type of graph is useful as a compliment to the comparison of masses. Given that the masses correspond, the fraction graph gives a good view of the dynamics of the runoff event.

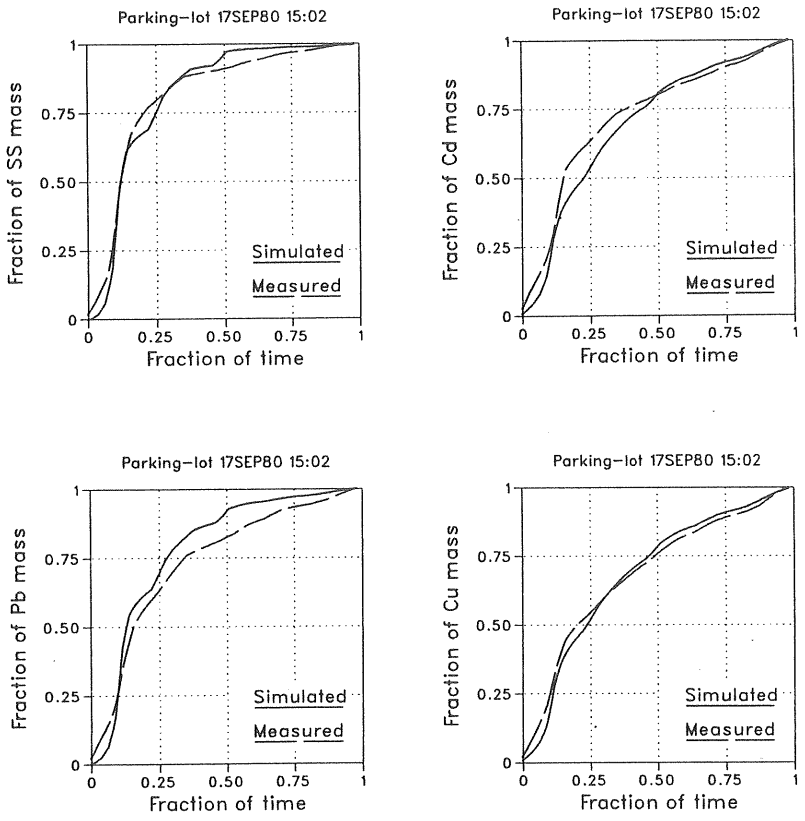

Figure 8.11 Fraction graphs for the parking lot runoff event 17 Sep. 80.

9. DISCUSSION

9.1 A synthetic rainfall for the discussion and analyses of particle transport

To be able to point out the difficulties with particle transport modelling and differences between modelling approaches two synthetic rainfall events were derived. Both of them with the same volume, duration and peak intensity but with different shapes. The rainfall events are described in Table 9.1 and shown in Fig. 9.1. They are simply called: Rain 1 and Rain 2 and labeled R12 (Rain 1 followed by Rain 2) or R21 (Rain 2 followed by Rain 1).

Table 9.1 Characteristics of two synthetic rainfall events.

	Rain 1	Rain 2
Volume (mm)	6.67	6.67
Duration (min)	60	60
Peak Intensity (mm/h)	25.0	25.0

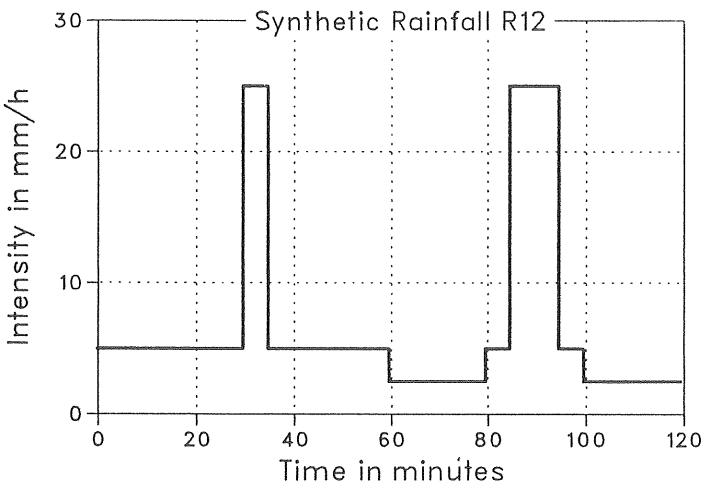

Figure 9.1 Description of the synthetic rainfall events Rain 1 and Rain 2, labeled R12.

The simulations are carried out for two different particle size distributions. The normal one which has been used for all the simulations described in Chap. 7 and Chap. 8 and a special one with fewer small particles. Both are given in Fig. 9.2.

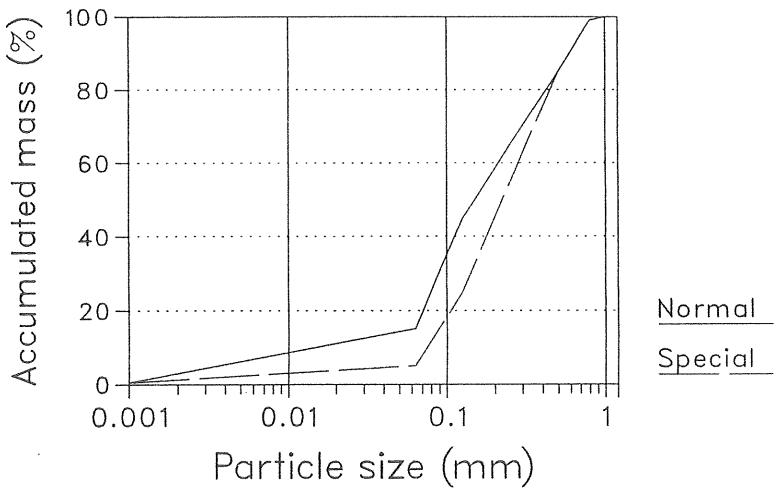

Figure 9.2 Description of two particle size distributions

9.2 Effects of particle size distribution on transported solids

9.2.1 Solids loads and concentrations for the synthetic rainfall events

The derived solids and metal transport model does not take into account any limitations of the surface solids load. However, the simulation results reportedin Chap. 7 and Chap. 8, are believed not to be affected to a great extent by this fact. This is because the storms with long duration before sampling started have been excluded. The surface solids load should not for this reason be a limiting factor for these storms.

The capability of the model to calculate solids and metal transport for different particle size fractions can however prove to be very important to the simulation results.

A simulation with the two synthetic rainfall events for the normal particle size distribution is shown in Fig. 9.3. Looking at the concentrations the same peak concentrations are met for both events but Rain 2, whose peak has a longer duration, gives higher concentrations with a longer duration.

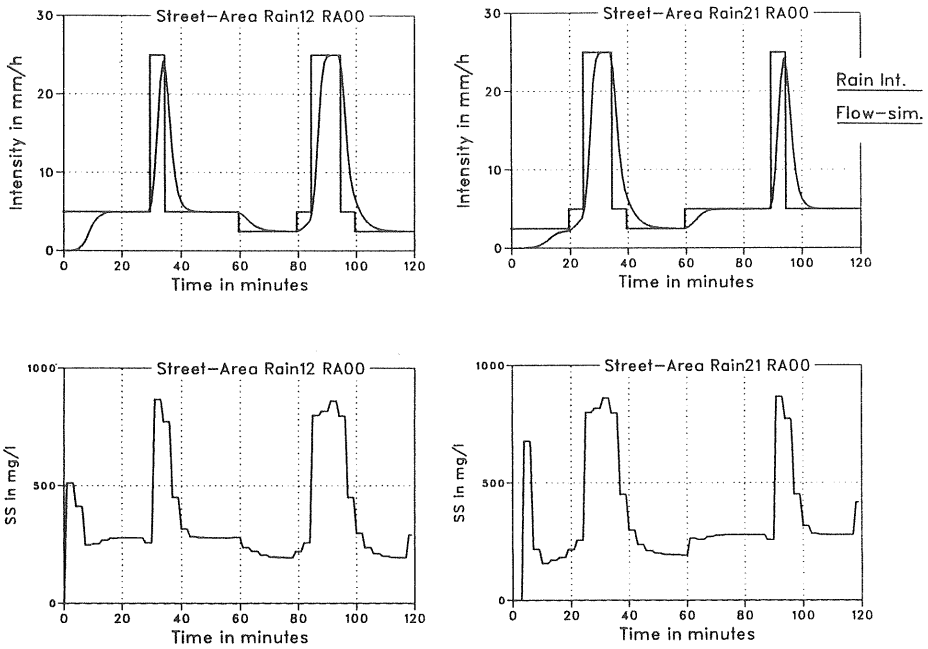

Figure 9.3 Solids concentrations for the synthetic rainfall events Rain 12 and Rain 21.

The higher concentrations for Rain 2 are also reflected in the loads, as shown in Fig. 9.4. For all fractions Rain 2 gives higher loads than does Rain 1 give, despite the fact that the rain events have the same characteristics. Obviously the duration with the high intensity for Rain 2 is not compensated by the higher intensity before and after the peak for Rain 1.

The importance of being able to simulate the transport capacity of different particle size fractions is demonstrated in Fig. 9.4. Looking at the finest fraction the difference between the

two event loads is only about 30 %, but for the coarsest fraction the difference is about 100 %. If for example the intensities were too low to transport particles coarser than 0.063 mm, the difference between the two rain events would have been ignored.

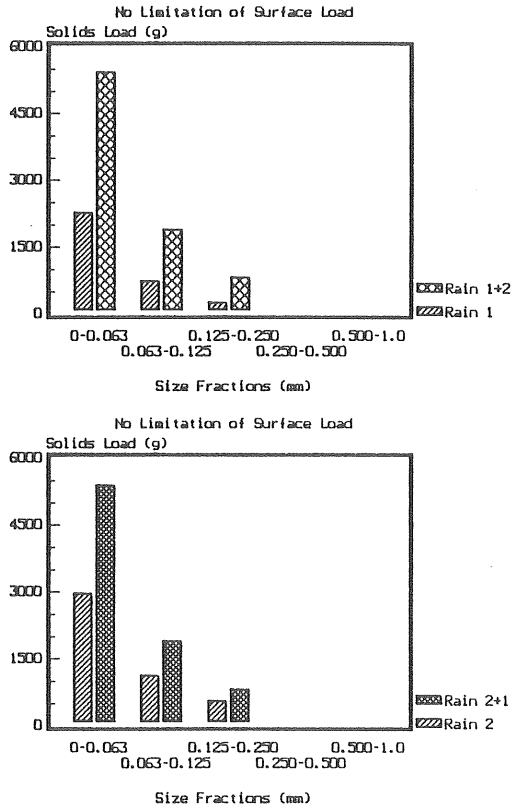

Figure 9.4 Solids loads for different particle size fractions for the two synthetic rainfall events.

Also, as seen both from the concentrations and the loads, the order of the rainfall events makes no difference. This would not be expected since there is no limitation of surface load.

9.2.2 Comparisons between the developed model and SWMM.

The Storm Water Management Model (SWMM), Huber et al. (1981) uses an exponential decay function for calculating the runoff mass flow. It is often written in the form given in Eq. (9.1).

$$P_0 - P = P_0 A(1 - e^{-krt}) \tag{9.1}$$

P = mass of solids on surface
t = time
k = coefficient
r = runoff rate (depth/time)
A = availability factor

The availability factor is an equation of the form:

$$A = a + br^c \tag{9.2}$$

where a, b and c are constants. For solids the following formula is given: $A = 0.057 + 1.4\ r^{1.1}$. An assumption often used is that 0.5 inch (12.7 mm) of rainfall causes 90 % reduction of solids on the surface. This gives a k-value of 4.6 per inch.

Using Eq. (9.1) and the constants given here together with an original load of 5.0 g/m^2 produces mass flows for the synthetic rainfalls as shown in Fig. 9.5. The calculations are made for the rainfall intensity instead of runoff intensity, which affects the shape of the mass flow curve, but not the main features of it.

The mass flow curve produced for the normal particle size distribution, also shown in Fig. 9.5, is in agreement with the SWMM-curve for the first event but not for the second one. When the large peak comes first the difference is more marked. The reason is that SWMM calculates the wash off according to the surface load, which surely is reduced when the second event comes. The herein developed model has the potential to estimate too high mass flows for the second event since the surface load will be a limiting factor for this kind of events.

However, with the same conditions, except for the particle size distribution, the same exercise is made again. Now with the special particle size distribution, which has less small particles. The result is shown in Fig. 9.6, which displays the same

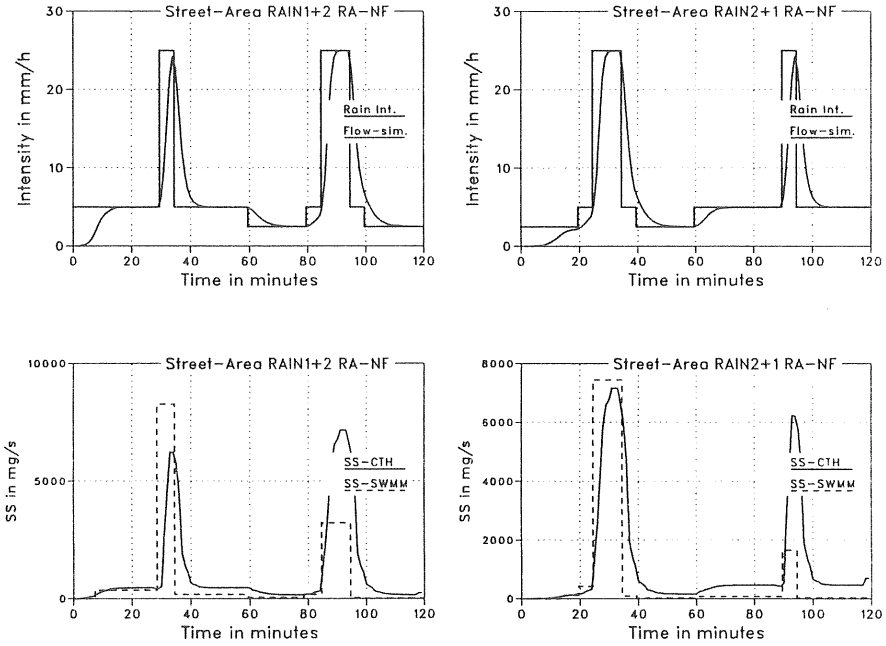

Figure 9.5 Solids flow curves for the synthetic rainfall events derived by the developed model and the SWMM-model.

SWMM-curve as before but lower mass flows for the developed model. Now the best agreement is achieved for the second event. The SWMM-curve shows mass flows that are too high for the first event, because SWMM takes into account only the total surface load, which is the same for both cases, and not the particle size distribution.

Simulations with the SWMM-form solids transport relationship would give mass flows in agreement with the developed model for moderate rainfall intensities, when only the finest particle size fraction is moved. However, if followed by a high intensity rainfall, the SWMM relationship would fail to reflect the increase in mass flow which would be expected.

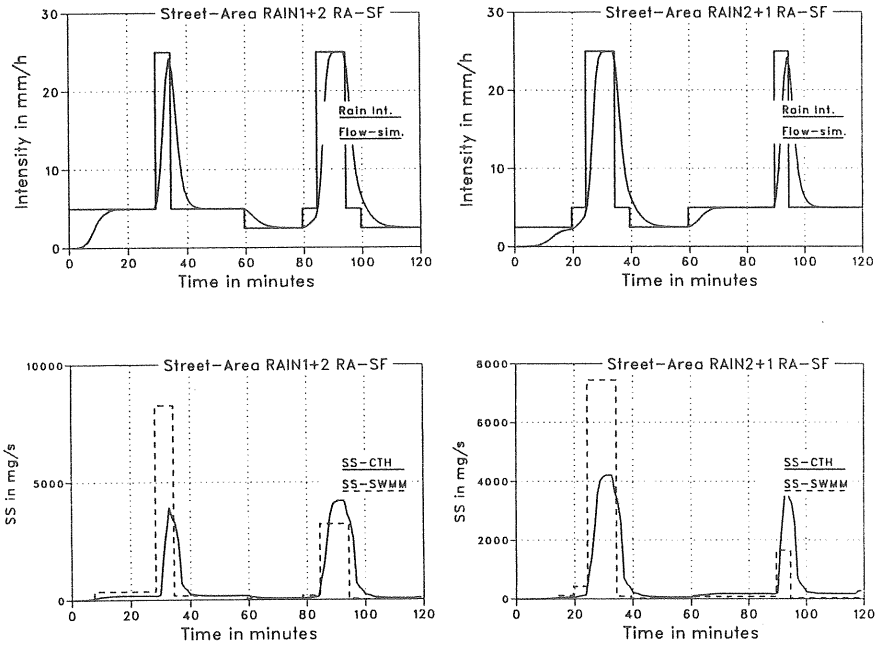

Figure 9.6 Solids flow curves derived by the developed model and the SWMM-model for the special particle size distribution.

A model with a dynamic particle size distribution would reflect reality better. This means that as solids are washed off the surface the particle size distribution changes for the remaining solids and should be reflected by a model.

9.3 Effects of limited surface load

9.3.1 An improved model with surface load masss balance

The model developed has been modified with respect to the particle size distribution, which has been made dynamic, see Fig. 9.7. At the beginning of a rainfall event the normal distribution is used for the solids resting on the surface. During the washoff of solids the distribution is corrected in a way that it always reflects the distribution of the remaining surface load.

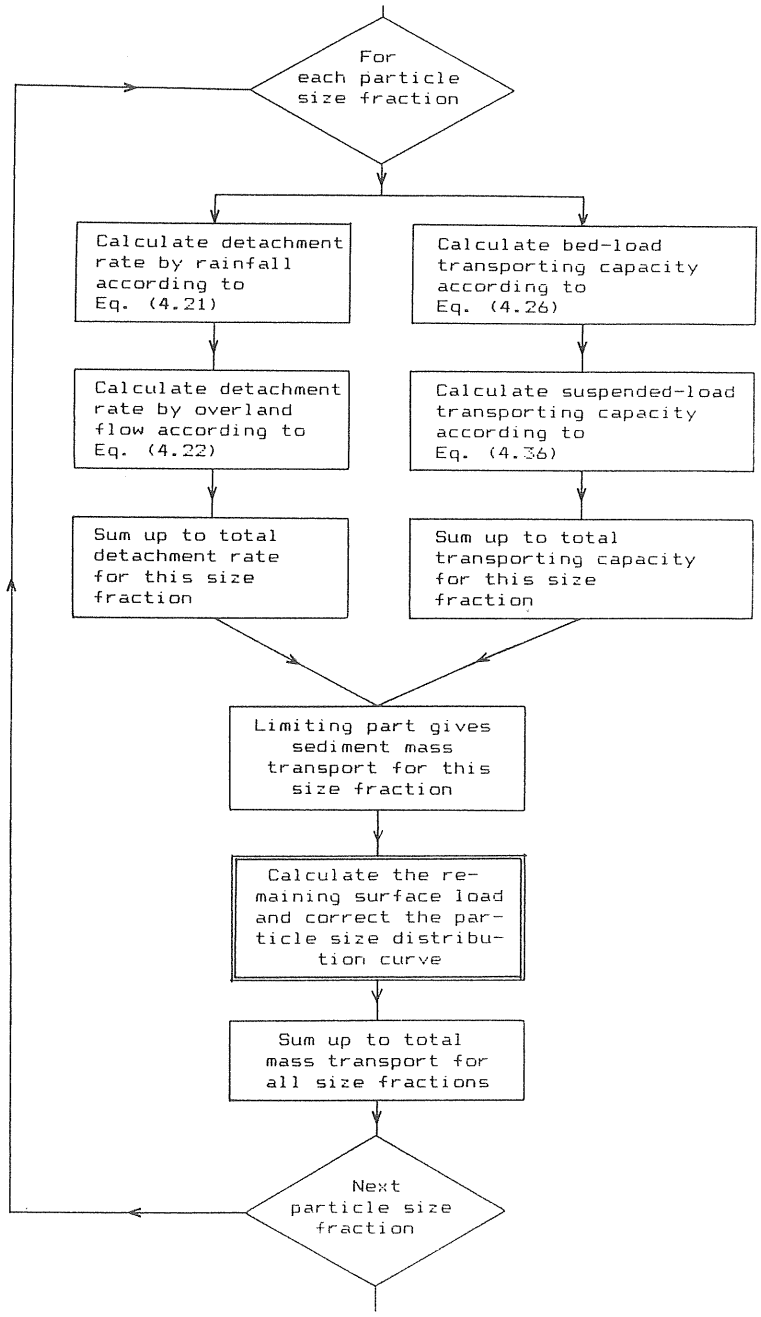

Figure 9.7 Flowchart for the sediment transport model with surface load mass balance.

A simulation with the two synthetic rainfall events for a surface load of 5.0 g/m^2 results in solids concentrations, which are decreasing as the event proceeds. In Fig. 9.8 the simulated solids concentrations are shown for Rain 1 followed by Rain 2 and vice versa. The difference between the first and the second peak is more marked when Rain 2 comes first, since Rain 2 has a greater solids transport than Rain 1 has. The surface load is obviously a limiting factor in both cases for the second peak.

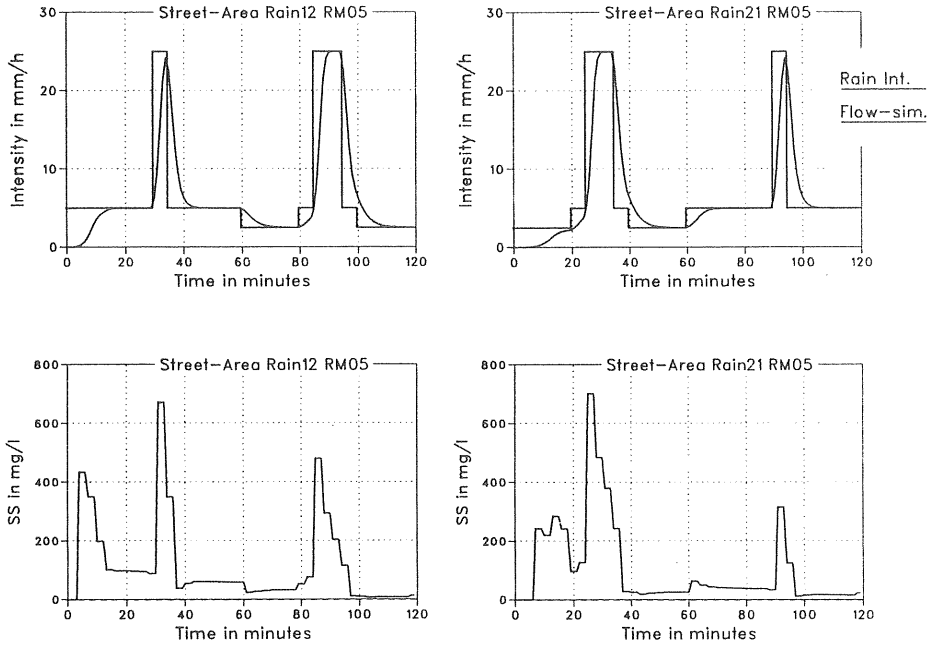

Figure 9.8 Solids concentrations simulated with the modified model for two synthetic rainfall events.

The transported solids loads for the different particle size fractions are shown for the two cases in Fig. 9.9. In the case of Rain 1 coming first, between 35 % and 70 % of the total transported load is removed by the first event. Almost 100 % of the finest fraction is transported during the total event but nothing of the two coarsest fractions. The other case of Rain 2 coming first removes from 70 % to 80 % of the total solids load during the first part of the event. Again almost all of the

finest fraction is removed while nothing of the two coarsest fractions is moved. The total transported load does not differ between the two cases partly because of the limited supply of solids for the finer fractions.

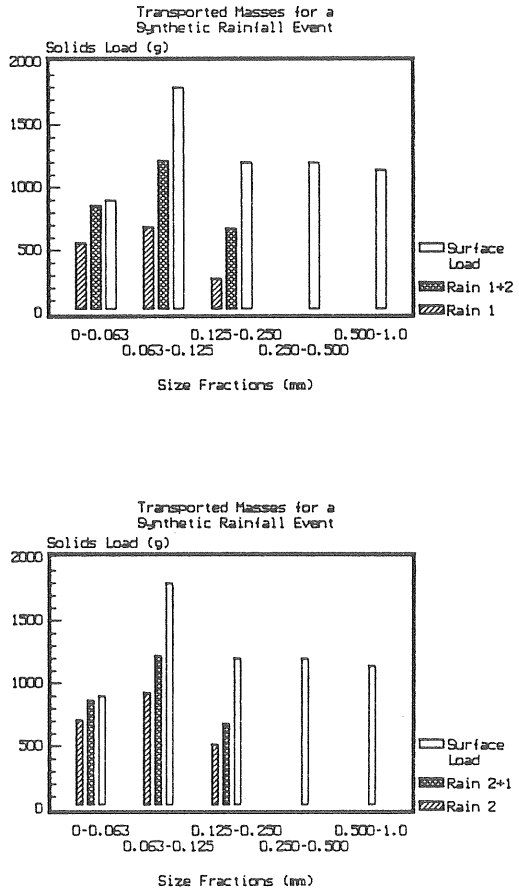

Figure 9.9 Transported solids loads for the different particle size fractions simulated by the improved model.

As seen from Fig. 9.9 the more limited the supply is, the more reduced the transport will be. To investigate the effect of the limited supply another simulation was made with a total surface load of 10.0 g/m^2. The solids concentrations are shown in Fig. 9.10, which has a larger second peak compared to the simulation with 5.0 g/m^2.

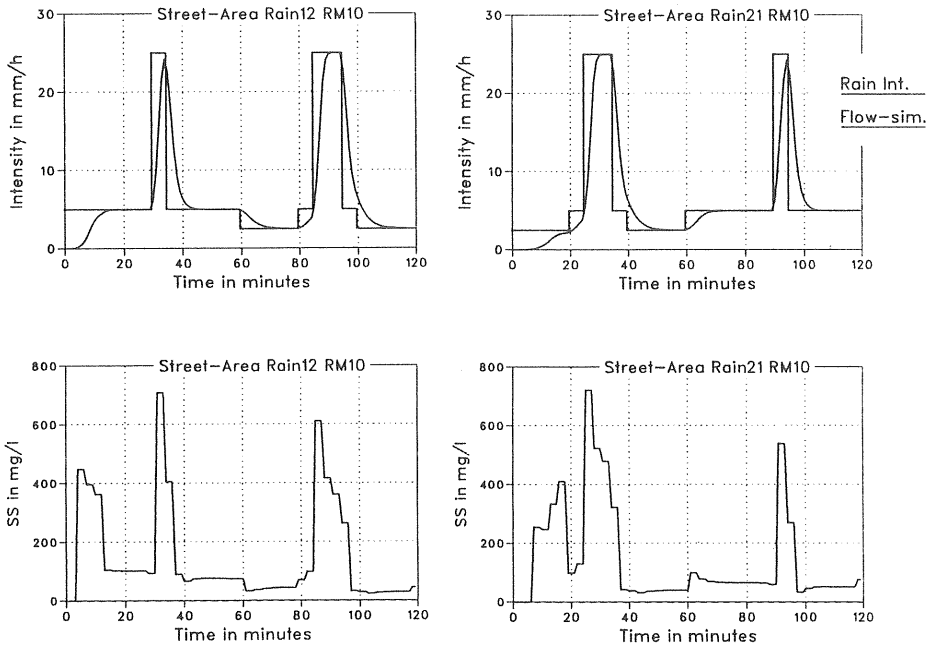

Figure 9.10 Simulated solids concentrations for a surface load of 10.0 g/m^2.

Looking at the loads, shown in Fig. 9.11 in the case of Rain 1 coming first, this peak removes only between 15 % and 40 % of the total load. In the case of Rain 2 coming first the corresponding figures are 20 % and 45 %. There are still solids on the surface in every fraction after the total event.

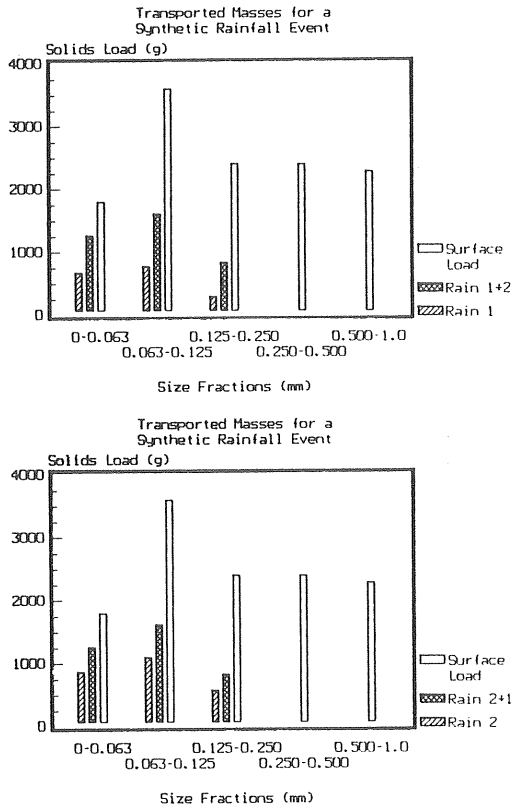

Figure 9.11 Transported solids loads for the different particle size fractions simulated for a surface load of 10.0 g/m^2.

The difference between the two surface loads is better described by Fig. 9.12, where Rain 1 is compared to Rain 1 preceeded by Rain 2 and Rain 2 compared to Rain 2 preceeded by Rain 1. If there were no changes of the particle size distribution during the event the bars should be of the same height. This is not the case since the particle size distribution of the surface load is changed due to the transported solids. However, with increasing surface load, both totally and for each particle size fraction, the effect is less noticeable.

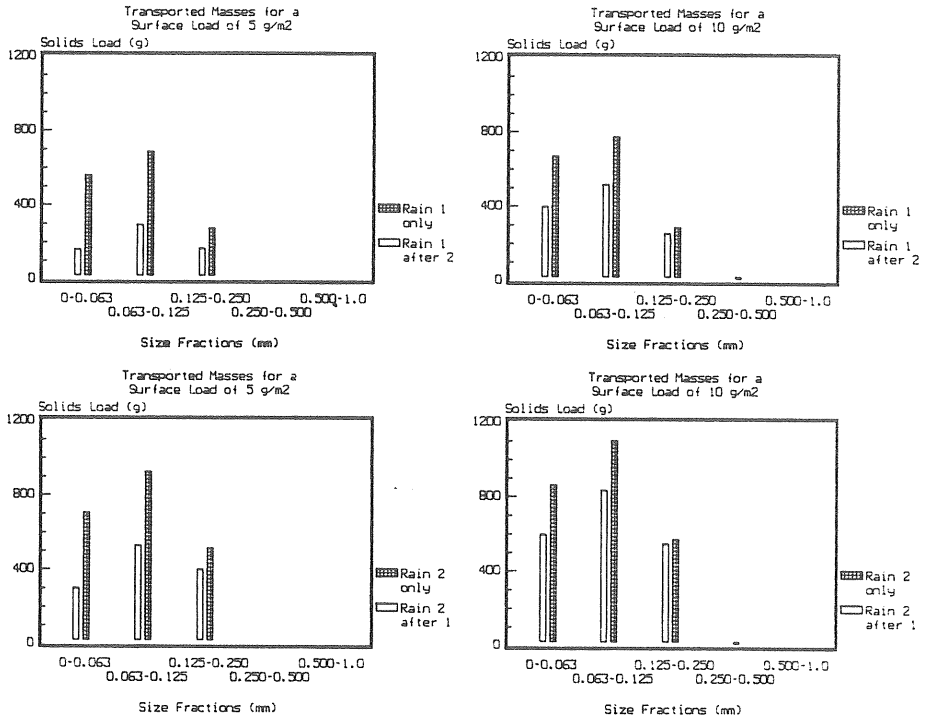

Figure 9.12 Comparison between transported solids loads for a single rain event and the same event preceeded by another event.

9.3.2 Comparisons between the improved model and SWMM

Using the improved model with a surface load of 5.0 g/m^2 and the normal particle size distribution to simulate the solids mass flow for the the two rainfall events, produces the graphs shown in Fig. 9.13. As a comparison, again the solids mass flow calculated with the SWMM-formula is also displayed in Fig. 9.13.

The model developed here gives lower mass flows for the second peak than does the SWMM-formula give. The mass flows of the SWMM- formula are however much higher for the first peak, which

could be adjusted by the calibration coefficients in the SWMM-formula. The availability factor could for example be reduced. This could bring the SWMM-curve to match the curve of the developed model.

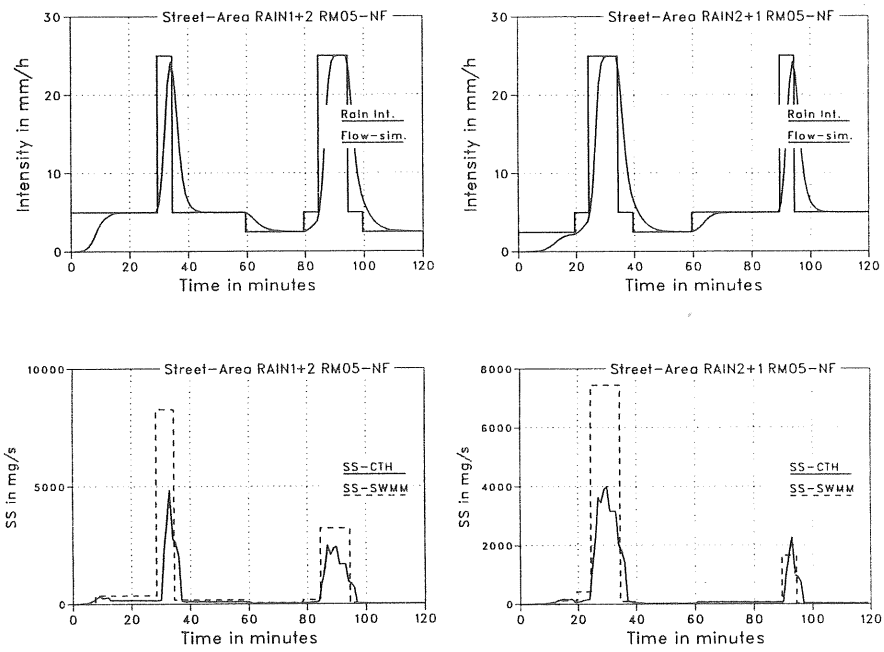

Figure 9.13 Simulated mass flow with the developed model and with SWMM for two synthetic rainfall events.

A small change of the particle size distribution is reflected by the developed model but not by the SWMM-formula, which leads to a larger difference between the two simulation curves. The simulation with the special particle size distribution is shown in Fig. 9.14.

Another way of changing the mass flow of solids is to simulate an area with a different slope. The parking lot is not as steep as the street and will give particle transport mainly for the finest fraction. The SWMM-formula will however give the same mass flow irrespective of the change in slope, which is shown in Fig. 9.15

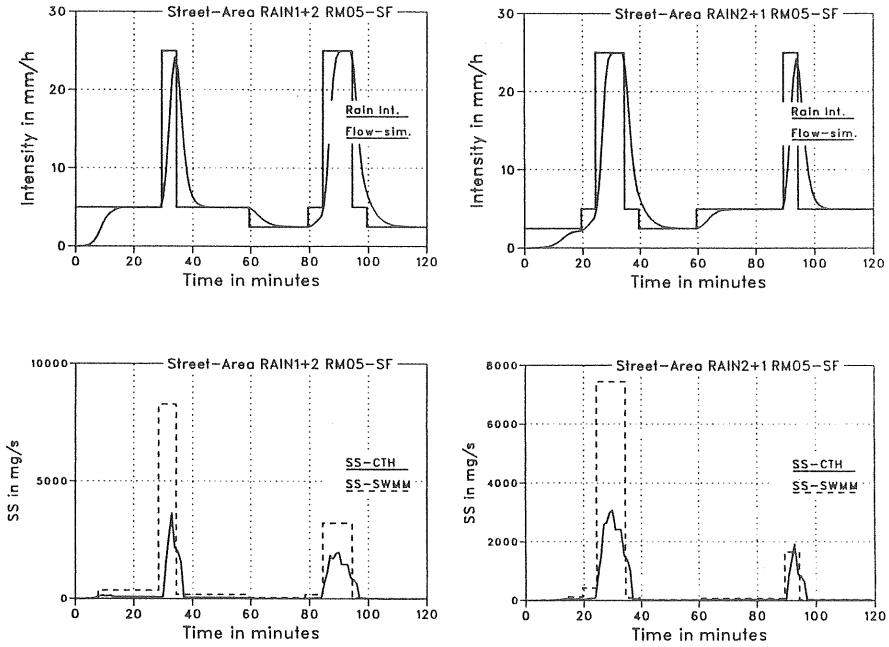

Figure 9.14 Simulated mass flow with the developed model and with SWMM for the special particle size distribution.

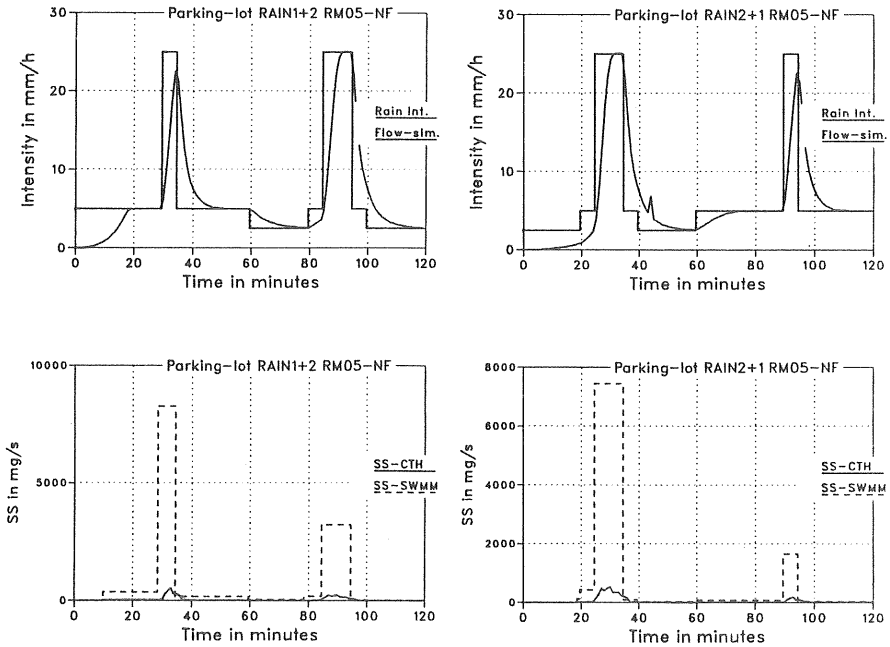

Figure 9.15 Simulated mass flow with the developed model and with SWMM for the parking lot.

9.4 Simulations with the improved model for some observed storms

Simulations were made for the observed storms and compared to the observed concentrations in Chap. 7 and Chap. 8. To compare the simulation results of the improved model to those of the originally developed model, a few storms will be displayed again.

The runoff from the street 6 Nov.79 was displayed in Fig. 7.10 and showed good agreement between observed and simulated concentrations except for the first peak which was overestimated. The improved model simulates the variations of the concentration graph better, shown in Fig. 9.16, but the total surface load has to be increased to 60 g/m^2 to get a very good fit.

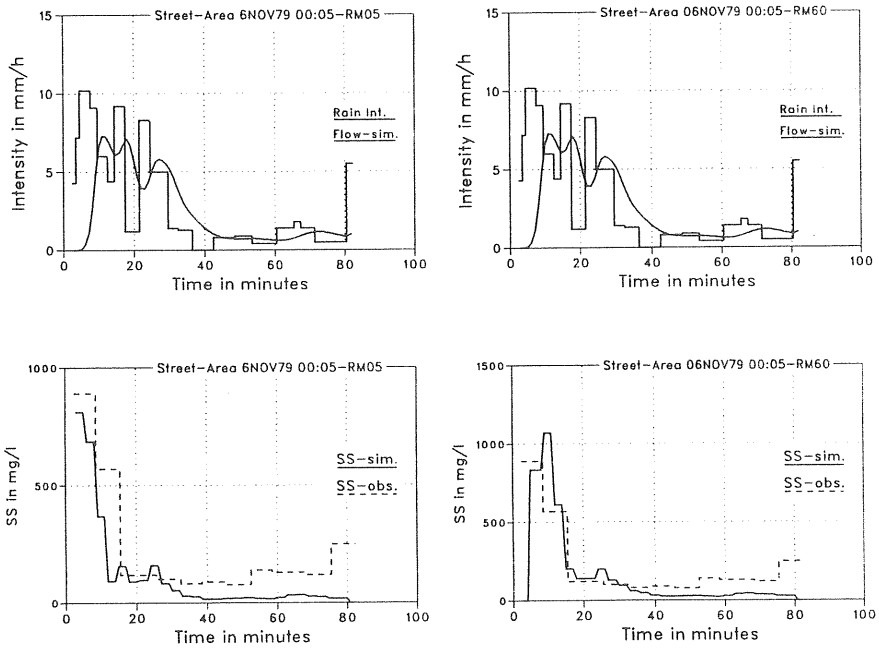

Figure 9.16 Simulated and observed concentrations with the improved model for the street runoff 6 Nov. 79.

In Chap. 8 the storm of 17 Sep. 80 was displayed both for the street area and the parking lot area, Fig. 8.8 and 8.9. The simulations for the parking lot are good but for the street area

the simulated curve has a completely different form than the observed one. The cause could be a limited supply of solids, which causes the observed solids concentration to decrease even if the runoff intensity is increasing.

New simulations are made by the improved model which are displayed in Fig. 9.17 for the street area and Fig. 9.18 for the parking lot. The variations for the street area in the observed curves both for solids and metal concentrations are much better simulated in this case.

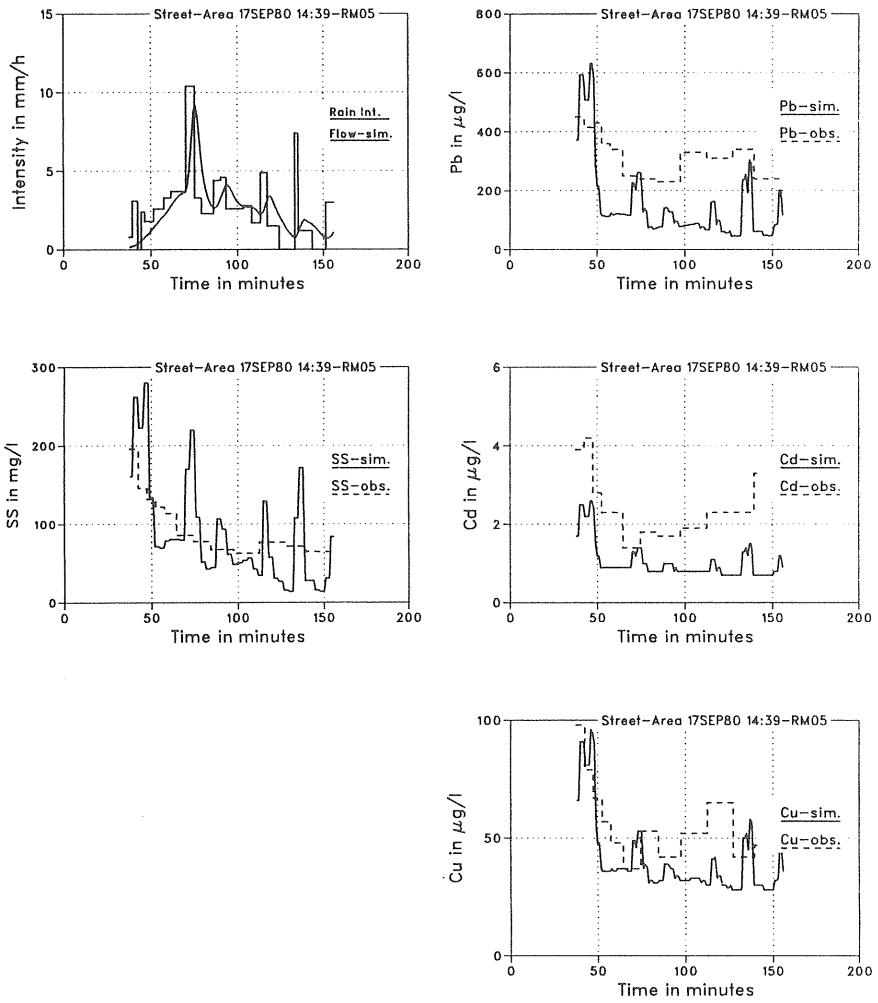

Figure 9.17 Simulated and observed concentrations with the improved model for the street runoff 17 Sep. 80.

For the parking lot the differences between the originally simulated curves and the curves simulated by the improved model are small. The fit is still good.

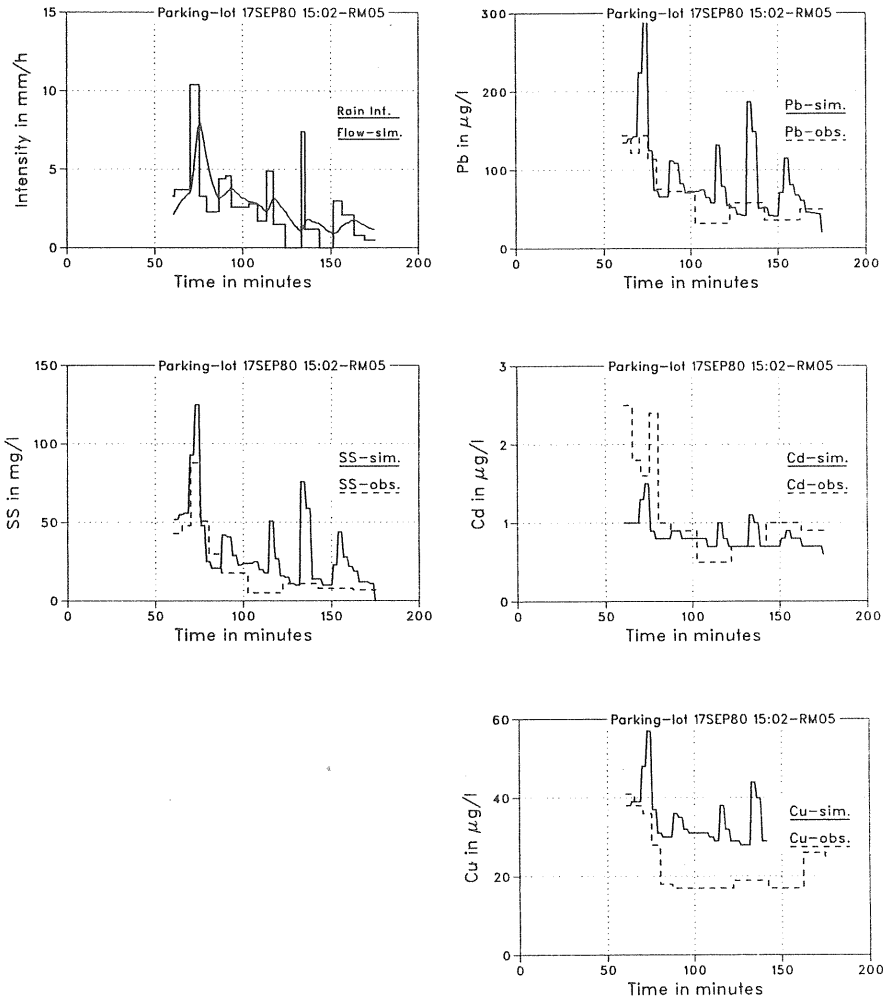

Figure 9.18 Simulated and observed concentrations with the improved model for the parking lot runoff 17 Sep. 80.

With regard to loads the differences between the two models are tabulated in Table 9.2

Table 9.2 Observed and simulated solids and metals loads for the originally developed model and the improved model.

Date	Type	Model	Surface load (g/m^2)	SS obs. (g)	SS sim. (g)	Pb obs. (mg)	Pb sim. (mg)	Cd obs. (mg)	Cd sim. (mg)	Cu obs. (mg)	Cu sim (mg)
6NOV79	S	OM	-	930	860	-	-	-	-	-	-
		IM	5.0	930	470	-	-	-	-	-	-
		IM	60.0	930	1100	-	-	-	-	-	-
17SEP80	S	OM	-	480	1200	1700	2600	12.0	12.0	300	440
		IM	5.0	480	520	1700	770	12.0	5.8	300	230
17SEP80	P	OM	-	63	91	180	240	2.7	2.0	53	81
		IM	5.0	63	90	180	240	2.7	2.0	53	81

S = Street Area
P = Parking Lot
OM = Originally Developed Model
IM = Improved Model

9.5 Recommendations on further research and development

The model devloped in the context of this work should be further tested. One area that has not been investigated is simulations with simplified sediment transport equations and the effect on the simulation results. Another area is the application of the model for larger catchments through a simplified areal description of a catchment. This will probably affect the simulations seriously since the sediment transport is very sensitive to the simulated velocities and these can be expected not to be simulated as accurate for a large catchment with a rough areal description as for a small one.

To make the model appropriate for use in urban drainage planning and sewer network analysis it has to be integrated in an urban runoff and sewer network simulation package. This can be done as long as the overland flow simulation routine feeds the sediment transport model with water depths and velocities.

The simulation of sediment transport in sewers and through different hydraulic structures, i.e. overflows, detention basins, is an area where improved simulation models will come. Simulation with the model developed here will serve as an input to simulations with sewer network sediment transport models.

In the area of substances associated to solids there has to be further research to establish relationships between solids and other substances than Pb, Cd and Cu which have been investigated here.

10 CONCLUSIONS

Urban runoff solids concentration curves can be simulated using theories on sediment transport in open channels. The simulations require an overland flow model based on the kinematic wave theory as an input to the solids concentration calculations.

Particles are detached from the ground by raindrop energy input and overland flow shear forces. The potential transport rate is governed by flow conditions and particle properties. The limiting one of the detachment rate and the potential transport rate determines the actual transporting rate.

The potential transport rate over a given surface is strongly dependent on the particle sizes. Each particle size has its own critical flow above which it will be transported. As the flow varies the potential transport rate will vary.

The solids particle size distribution curve can be represented by the geometrical mean particle size of a number of size fractions.

The solids supply of a surface can be a limiting factor for some particle size fractions. Since the smaller particle sizes always are transported, if there is a runoff, the surface will for some storms run out of supply for these particle sizes.

The original particle size distribution curve for a surface at the beginning of a runoff event has to be corrected continously during the runoff with respect to the transported mass of particles.

A first flush effect for a runoff event is logical and is caused by small particles which are readily transported but limited in supply.

There is a linear relationship between solids associated metal concentrations and surface area of the particles. The particle shape can be approximated by a sphere, thus creating an inverse relationship between solids associated metal concentrations and particle diameter.

The dissolved metal concentrations vary less than do the solids associated metal concentrations and can be approximated by a constant concentration. The variations in the dissolved concentrations can only partly be explained by changes of the pH-value.

Simulations of solids transport using the Storm Water Management Model reflect the limited supply of small particles. The SWMM gives reasonable results for not too steep areas and low to moderate runoff intensities, when only the smaller particles are transported.

REFERENCES

Alley, W.M. and Smith, P.E. (1982). Multi-Event Urban Runoff Quality Model. U.S. Geological Survey Open File Report, 82-764, Reston, VA.

American Public Works Association, APWA. (1969). Water Pollution Aspects of Urban Runoff. Federal Water Pollution Control Administration, Contact WP-20-15, Washington, DC.

Arnell, V. and Asp, T. (1979). Nederbördens varaktighet och mängd vid Lundby i Göteborg 1921-1939. Chalmers University of Technology, Urban Geohydrological Research Group, Meddelande nr 44, Göteborg

Arnell, V. (1982). Rainfall Data for the Design of Sewer Pipe Systems. Chalmers University of Technology, Department of Hydraulics, Report Series A:8, Göteborg.

Dever, R.J., Roesner, L.A. and Aldrich, J.A. (1983). Urban Highway Storm Drainage Model Vol. 4, Surface Runoff Program User's Manual and Documentation. FHWA/RD-83/044, Federal Highway Administration, Washington, DC.

Einstein, H.A. (1950). The Bedload Function for Sediment Transportation in Open Channel Flows. U.S. Dept. of Agr., Soil Cons. Service, Technical Bull. No. 1026.

Environmental Protection Agency (EPA). 1983). Results of the Nationwide Urban Runoff Program, Volume I Final Report. NTIS PB84-1855552, EPA, Washington, DC.

Falk, J. and Niemczynowicz, J. (1979). Modelling of Runoff from Impermeable Surfaces. Lund Institute of Technology, Dept. of Water Res. Eng., Report No. 3024, Lund.

Geiger, W.F. (1975). Urban Runoff Pollution Derived from Long-Time Simulation. Proceedings National Symposium on Urban Hydrology and Sediment Control, 259-270. University of Kentucky, Lexington, KY.

Geiger, W.F. (1984). Characteristics of Combined Sewer Runoff. Proceedings of the Third International Conference on Urban Storm Drainage, Vol. III, 851-860, Chalmers University of Technology, Göteborg.

Hjulström, F. (1935). Studies of the Morphological Acivity of Rivers as Illustrated by the River Fyris. Bulletin, Geol. Inst. of Uppsala, Vol. 25, Uppsala.

Hogland, W. (1986). Rural and Urban Water Budgets. A Description and Characterization of Different Parts of the Water Budgets with Special Emphasis on Combined Sewer Overflows. Lund University, Dept. of Water Res. Eng., Report No. 1006, Lund.

Huber, W.C. (1986). Deterministic Modeling of Urban Runoff Quality. In Urban Runoff Pollution, NATO ASI Series, Series G: Ecological Sciences, Vol. 10, 167-242, Springer Verlag, Berlin Heidelberg.

Huber, W.C., Heany, J.P., Nix, S.J., Dickinson, R.E. and Polmann, D.J. (1981). Storm Water Management Model Users Manual, Version III. EPA-600/2-84-109a. Environmental Protection Agency, Cincinnati, OH.

Johansson, R.C., Imhoff, J.C. and Davis, H.H. (1980). Users Manual for Hydrological Simulation Program - FORTRAN (HSPF). EPA-600/9-80-015, Environmental Protection Agency, Athens, GA.

Kinori, B.Z. and Mevorach, J. (1984). Manual of Surface Drainage Engineering. Volume II: Stream Flow Engineering and Flood Protection. Elsevier Science Publishers B.V., Amsterdam.

Li, R.M. (1974). Mathematical Modeling of Response from Small Watersheds. Ph.D. Dissertation, Dept. of Civil Eng., Colorado State University, Ft. Collins, Colorado.

Li, R.M., Simons, D.B. and Stevens, M.A. (1975). Nonlinear Kinematic Wave Approximation for Water Routing. Water Resources Research, Vol. 11, No. 2.

Lighthill, M.J. and Whitham, G.B. (1955). On Kinematic Waves: I. Flood Movement in Long Rivers. Proc. Royal Soc. of London, Ser. A, Vol. 229.

Lindberg, S. and Jörgensen, T.W. (1986). Modelling of Urban Storm Sewer Systems. In Urban Drainage Modeling, Eds. Maksimovic, C. and Radojkovic, M., Proceedings of the International Symposium on Comparion of Urban Drainage Models with Real Catchment Data, UDM '86 Dubrovnik', Yugoslavia, Pergamon Press, Oxford.

Lindholm, O. (1975). Valg av Modellregn. (The Selection of Model Storms). Projektkomitéen for rensing av avlöpsvann, Report PRA 6, Oslo. (In Norwegian).

Lindholm, O.G. (1978). Modelling of Sewerage Systems. In Mathematical Models in Water Pollution Control, Chap. 10, 227-246. A. James, Ed. John Wiley and Sons, New York.

Lisper, P. (1974). Om dagvattnets sammansättning och dess variationer. Chalmers Tekniska Högskola. Doktorsavhandling, Göteborg

Lyngfelt, S. (1985). On Urban Runoff Modelling. The Application of Numerical Models Based on Kinematic Wave Theory. Chalmers University of Technology, Department of Hydraulics, Report Series A:13, Göteborg.

Malmqvist, P.A. and Svensson, G. (1974). Dagvattnets beskaffenhet och egenskaper. Sammansättning av utförda dagvattenundersökningar i Stockholm och Göteborg 1969-1972. English Summary, Urban Geohydrology Research Group, Chalmers University of Technology, Report No. 11, Göteborg.

Malmqvist, P.A. (1983). Urban Stormwater Pollutant Sources. An Analysis of Inflows and Outflows of Nitrogen, Phosphorous, Lead, Zinc and Copper in Urban Areas. Chalmers University of Technology, Dept. of Sanitary Engineering, Göteborg.

Metcalf and Eddy, Inc., University of Florida and Water Resources Engineers, Inc. (1971). Stormwater Management Model, Volume I - Final Report, EPA Report 11024DOC07/71, Environmental Protection Agency, Washington, DC.

Meyer, L.D. (1971). Soil Erosion by Water on Upland Areas. River Mechanics, Volume II, Edited by H.W. Shen, Ft. Collins, Colorado.

Meyer-Peter, E. and Müller, R. (1948). Formulas for Bedload Transport. Int. Assoc. for Hydr. Res., 2nd Meeting, Stockholm.

Morrison, G.M. (1985). Metal Speciation in Urban Runoff. Ph. D. Thesis, Middlesex Polytechnic, London.

Nittim,R. (1977). Overland Flow on Impervious Surface. Water Research Laboratory, University of New South Wales, Report No. 151, Australia

Phelps, H.O. (1975). Shallow Laminar Flows over Rough Granular Surfaces. Jornal of the Hydraulics Division, ASCE, HY12, December.

Price, R.K. and Mance, G. (1978). A Suspended Solids Model for Storm Water Runoff. Proceedings of the International Conference on Urban Storm Drainage, 546-555, University of Southampton. Pentech Press, London.

Roesner, L.A. Nichandros, H.M., Shubinski, R.P., Feldman, A.D., Abbott, J.N. and Friedland, A.O. (1974). A Model for Evaluating Runoff Quality in Metropolitan Master Planning. ASCE Urban Water Resources Research Program. Technical Memorandum No. 23, American Society of Civil Engineers, New York.

Rouse, H. (1937). Modern Conceptions of the Mechanics of Turbulence. Trans. ASCE, 102.

Sartor, J.D. and Boyd, G.B. (1972). Water Pollution Aspects of Street Surface Contaminants. EPA-R2-72-081, Environmental Protection Agency, Washington, DC.

Schoklitsch, A. (1934). Der Geschiebetrieb und die Geschiebefracht. Wasserkraft und Wasserwirtschaft, 29(4).

Shields, A. (1936). Anwendung der Ähnlichkeitsmechanik und Turbulenzforshung auf die Geschiebebewegung. Mitt. Preuss. Versuchsanstalt f˝r Wasser, Erd und Schiffbau, no. 26, Berlin.

Shulits, S. (1968). Bedload Formulas, Part A: A Selection of Bedload Formulas. Penn. State University, U.S. Dept. of Comm.

Simons, D.B. Li, R.M. and Ward, T.J. (1977a). Simple Method for Estimating On-Site Soil Erosion. Dept. of Civil Eng., Colorado State University, Ft. Collins, Colorado.

Simons, D.B. Li, R.M. and Ward, T.J. (1977b). A Simple Procedure for Estimating On-Site Soil Erosion. Proceedings, International Symposium on Urban Hydrology, Hydraulics and Sediment Control, University of Kentucky, Lexington, KY.

Simons, D.B. Li, R.M., Shiao, L.Y. and Eggert, K.G. (1977c). Storm Water and Sediment Runoff Simulation for Upland Watersheds Using Analytical Routing Techniques. Dept. of Civil Eng., Colorado State University, Ft. Collins, Colorado.

Sutherland, R.C. and Ellis, F.W. (1979). An Approach to Urban Pollutant Washoff Modeling. Proceedings International Symposium on Urban Stormwater Management, University of Kentucky, Lexington, KY.

Söderlund, G., Lehtinen, H. and Friberg, S. (1970). Physico-chemical and Microbiological Properties of Urban Stormwater Runoff. 5th International Water Pollution Research Conference, July-August.

Woolhiser, D.A. and Ligget, J.A. (1967). Unsteady, One-Dimensional Flow over a Plane - the Rising Hydrograph. Water Resources Research, Vol. 3, No. 3.

Åkerlindh, G. (1950). Regnvädersavrinningens beskaffenhet. Nordisk hygienisk tidskrift 31, No. 1, Stockholm.

LIST OF SYMBOLS

The system of units used throughout the text is the SI-system, if not outwritten.

A	cross section of flow (L^2)
A	availability factor
A_b	constant in bed load formula
A_s	surface area fraction covered with sediment
ASS	accumulated mass of suspended solids (M)
a	distance of reference plane from the bed (L)
a	constant
B	width of channel (L)
B_s	constant in the critical shear stress formula
b	parameter in the momentum equation of flow
b	constant
CDSS	solids associated cadmium, weight per weight (M/M)
CUSS	solids associated copper, weight per weight (M/M)
c	local concentration (M/L^3)
c	constant
c_a	concentration at distance a from bed (M/L^3)
D	duration of rainfall (T)
D_f	detachment coefficient for overland or guttter flow
D_r	detachment coefficient for rainfall
d	water depth (L)
d_i	geometric mean diameter of i:th particle fraction (L)
d_s	particle diameter (L)
F	Froude number
f	Darcy-Weissbach friction factor
g	acceleration of gravity (L/T^2)
h	V-notch water depth (L)
i	rain intensity (L/T)
i_d	rain intensity constant (L/T)
i_e	effective rain intensity (L/T)
i_p	ponding intensity (L/T)
i_u	upstream inflow intensity to a catchment (L/T)
K	friction parameter

K_b constant in bed load formula

K_g friction parameter due to grain resistance

k constant

k_s roughness height (L)

k_1 constant in suspended load equation

k_2 constant in suspended load equation

L length in direction of flow (L)

MEC metal concentration (M/L^3)

MEM total metal mass for an event (M)

MESS solids associated metal load (M/M)

MESSA solids associated metal load per unit area (M/L^2)

M_s bed load discharge (M/T L)

MEC_i metal concentration for i:th particle fraction (M/L^3)

$MESS_i$ solids associated metal load for i:th particle fraction (M/M)

N number of observations

n Manning roughness coefficient

n_b Manning coefficient for bed roughness

n_g Manning coefficient for grain roughness

P wetted perimeter

P mass of solids on a surface (M)

P_o mass of solids on a surface at the start of an event (M)

PBSS solids associated lead (M/M)

Q flow (L^3/T)

q water discharge (L^2/T)

q_b bed load discharge (M/T L)

q_c critical water (L^2/T)

q_r runoff rate (L^2/T)

q_{sb} suspended bed load discharge (M/T L)

q_{ss} suspended load discharge (M/T L)

q_{st} total suspended load discharge (M/T L)

R hydraulic radius (L)

R_b hydraulic radius with respect to the bed (L)

Re Reynolds' number

r runoff intensity (L/T)

r regression coefficient

S slope (L/L)

SS	suspended solids concentration (M/L^3)
SA	specific surface area (L^2/M)
S_c	channel slope (L/L)
S_f	friction slope (L/L)
S_0	surface slope (L/L)
SA_i	specific surface area for i:th particle fraction (L^2/M)
T	channel width at water surface (L)
t	time (T)
u	velocity (L/T)
u_*	shear velocity (L/T)
v	velocity
v_c	critical velocity
V_{sa}	total detached sediment volume per unit of time (L^3/T)
V_{sf}	sediment volume detached by flow per unit of time (L^3/T)
V_{sr}	sediment volume detached by rain per unit of time (L^3/T)
W	width (L)
w	settling velocity (L/T)
x	coordinate (L)
Y_w	runoff volume (L^3)
y	depth (L)
y'	relative depth, y/d (L/L)
y'_a	relative depth, y/a (L/L)
z	parameter in suspended load transport equation,= $w/\kappa u_*$
γ	specific weight of water (F/L^3)
γ_s	specific weight of sediments (F/L^3)
κ	von Karman constant
ν	kinematic viscosity (L^2/T)
ρ_s	density of sediment (M/L^3)
ρ_w	density of water (M/L^3)
σ	standard deviation
τ	shear stress (F/L^2)
τ_c	critical shear stress (F/L^2)
Φ	porosity of sediment

LIST OF FIGURES

LIST OF TABLES

LIST OF APPENDICES

APPENDIX 1

In Appendix 1 is the rainfall intensity for some events 0.0 which means not observed. In the case of a substance having the value -1.0 this means not analysed.

Roof area 79 08 01 00:26

Time min	P mm/h	R l/s	pH	Cond mS/m	SS mg/l	Cd µg/l	Pb µg/l	Cu µg/l	Zn µg/l
1	0.0	0.00	4.8	93	24	-1.0	35	28	180
2	0.0	0.00	4.8	93	24	-1.0	35	28	180
3	0.0	0.02	4.8	93	24	-1.0	35	28	180
4	0.0	0.04	4.4	68	12	-1.0	49	16	130
5	0.0	0.07	4.4	68	12	-1.0	49	16	130
6	0.0	0.08	4.4	68	12	-1.0	49	16	130
7	0.0	0.08	4.4	64	4	-1.0	49	36	120
8	0.0	0.08	4.4	64	4	-1.0	49	36	120
9	0.0	0.11	4.4	64	4	-1.0	49	36	120
10	0.0	0.17	4.4	64	4	-1.0	49	36	120
11	0.0	0.23	4.4	60	4	-1.0	44	11	94
12	0.0	0.27	4.4	60	4	-1.0	44	11	94
13	0.0	0.26	4.4	60	4	-1.0	44	11	94
14	0.0	0.20	4.4	57	2	-1.0	41	46	110
15	0.0	0.15	4.4	57	2	-1.0	41	46	110
16	0.0	0.14	4.4	57	2	-1.0	41	46	110
17	0.0	0.14	4.5	54	4	-1.0	42	20	85
18	0.0	0.12	4.5	54	4	-1.0	42	20	85
19	0.0	0.09	4.5	54	4	-1.0	42	20	85
20	0.0	0.08	4.5	54	4	-1.0	42	20	85
21	0.0	0.08	4.5	54	4	-1.0	42	20	85
22	0.0	0.08	4.5	54	4	-1.0	42	20	85
23	0.0	0.08	4.5	54	4	-1.0	42	20	85
24	0.0	0.07	4.5	41	9	-1.0	25	10	66
25	0.0	0.06	4.5	41	9	-1.0	25	10	66
26	0.0	0.05	4.5	41	9	-1.0	25	10	66
27	0.0	0.05	4.5	26	4	-1.0	16	10	19
28	0.0	0.05	4.5	26	4	-1.0	16	10	19
29	0.0	0.04	4.5	26	4	-1.0	16	10	19
30	0.0	0.04	4.5	26	4	-1.0	16	10	19
31	0.0	0.03	4.6	21	1	-1.0	15	3	19
32	0.0	0.03	4.6	21	1	-1.0	15	3	19
33	0.0	0.03	4.6	21	1	-1.0	15	3	19

Roof area 79 08 08 20:48

Time min	P mm/h	R l/s	pH	Cond mS/m	SS mg/l	Cd µg/l	Pb µg/l	Cu µg/l	Zn µg/l
1	0.0	0.00	4.5	170	26	-1.0	44	50	370
2	0.0	0.01	4.5	170	26	-1.0	44	50	370
3	0.0	0.08	4.5	170	26	-1.0	44	50	370
4	0.0	0.09	4.2	142	12	-1.0	46	52	180
5	0.0	0.11	4.2	142	12	-1.0	46	52	180
6	0.0	0.13	4.2	142	12	-1.0	46	52	180
7	0.0	0.56	4.2	128	2	-1.0	46	52	180
8	0.0	0.84	4.2	128	2	-1.0	46	52	180
9	0.0	0.93	4.2	128	2	-1.0	46	52	180
10	0.0	1.05	4.2	128	2	-1.0	46	52	180
11	0.0	1.06	4.1	128	1	-1.0	49	60	140
12	0.0	1.01	4.1	128	1	-1.0	49	60	140
13	0.0	0.95	4.1	128	1	-1.0	49	60	140
14	0.0	0.85	4.2	127	1	-1.0	49	60	140
15	0.0	0.73	4.2	127	1	-1.0	49	60	140
16	0.0	0.63	4.2	127	1	-1.0	49	60	140
17	0.0	0.55	4.3	115	2	-1.0	40	70	140
18	0.0	0.47	4.3	115	2	-1.0	40	70	140
19	0.0	0.44	4.3	115	2	-1.0	40	70	140
20	0.0	0.45	4.3	115	2	-1.0	40	70	140
21	0.0	0.40	4.3	120	2	-1.0	40	70	140
22	0.0	0.35	4.3	120	2	-1.0	40	70	140
23	0.0	0.33	4.3	120	2	-1.0	40	70	140
24	0.0	0.31	4.3	122	1	-1.0	44	56	200
25	0.0	0.29	4.3	122	1	-1.0	44	56	200
26	0.0	0.27	4.3	122	1	-1.0	44	56	200
27	0.0	0.24	4.2	126	3	-1.0	44	56	200
28	0.0	0.21	4.2	126	3	-1.0	44	56	200
29	0.0	0.18	4.2	126	3	-1.0	44	56	200
30	0.0	0.18	4.2	126	3	-1.0	44	56	200
31	0.0	0.18	4.3	110	1	-1.0	30	60	140
32	0.0	0.19	4.3	110	1	-1.0	30	60	140
33	0.0	0.17	4.3	110	1	-1.0	30	60	140
34	0.0	0.15	4.3	94	1	-1.0	30	60	140
35	0.0	0.15	4.3	94	1	-1.0	30	60	140
36	0.0	0.15	4.3	94	1	-1.0	30	60	140
37	0.0	0.14	4.4	94	1	-1.0	26	58	110
38	0.0	0.15	4.4	94	1	-1.0	26	58	110
39	0.0	0.27	4.4	94	1	-1.0	26	58	110
40	0.0	0.33	4.4	94	1	-1.0	26	58	110
41	0.0	0.36	4.4	76	1	-1.0	26	58	110
42	0.0	0.36	4.4	76	1	-1.0	26	58	110
43	0.0	0.33	4.4	76	1	-1.0	26	58	110
44	0.0	0.29	4.5	45	4	-1.0	12	58	38
45	0.0	0.27	4.5	45	4	-1.0	12	58	38

Roof area 79 08 19 00:04

Time min	P mm/h	R l/s	pH	Cond mS/m	SS mg/l	Cd µg/l	Pb µg/l	Cu µg/l	Zn µg/l
1	0.0	0.00	5.2	69	62	-1.0	44	24	180
2	0.0	0.02	5.2	69	62	-1.0	44	24	180
3	0.0	0.15	5.2	69	62	-1.0	44	24	180
4	0.0	0.34	5.2	42	17	-1.0	20	4	76
5	0.0	0.41	5.2	42	17	-1.0	20	4	76
6	0.0	0.35	5.2	42	17	-1.0	20	4	76
7	0.0	0.29	4.9	34	18	-1.0	20	4	76
8	0.0	0.22	4.9	34	18	-1.0	20	4	76
9	0.0	0.13	4.9	34	18	-1.0	20	4	76
10	0.0	0.09	4.9	34	18	-1.0	20	4	76
11	0.0	0.09	5.2	22	17	-1.0	10	2	48
12	0.0	0.12	5.2	22	17	-1.0	10	2	48
13	0.0	0.26	5.2	22	17	-1.0	10	2	48
14	0.0	0.40	5.5	34	16	-1.0	10	2	48
15	0.0	0.53	5.5	34	16	-1.0	10	2	48
16	0.0	0.65	5.5	34	16	-1.0	10	2	48
17	0.0	0.71	5.6	11	7	-1.0	5	2	28
18	0.0	0.72	5.6	11	7	-1.0	5	2	28
19	0.0	0.67	5.6	11	7	-1.0	5	2	28
20	0.0	0.62	5.6	11	7	-1.0	5	2	28
21	0.0	0.50	5.8	10	4	-1.0	5	2	28
22	0.0	0.37	5.8	10	4	-1.0	5	2	28
23	0.0	0.25	5.8	10	4	-1.0	5	2	28
24	0.0	0.16	5.7	10	1	-1.0	5	2	28
25	0.0	0.10	5.7	10	1	-1.0	5	2	28
26	0.0	0.05	5.7	10	1	-1.0	5	2	28

Roof area 79 08 08 20:48

Time min	P mm/h	R l/s	pH	Cond mS/m	SS mg/l	Cd µg/l	Pb µg/l	Cu µg/l	Zn µg/l
46	0.0	0.30	4.5	45	4	-1.0	12	58	38
47	0.0	0.31	4.6	30	4	-1.0	12	58	38
48	0.0	0.31	4.6	30	4	-1.0	12	58	38
49	0.0	0.33	4.6	30	4	-1.0	12	58	38
50	0.0	0.35	4.6	30	4	-1.0	12	58	38
51	0.0	0.39	4.8	17	5	-1.0	8	12	28
52	0.0	0.47	4.8	17	5	-1.0	8	12	28
53	0.0	0.64	4.8	17	5	-1.0	8	12	28
54	0.0	1.04	4.9	14	5	-1.0	8	12	28
55	0.0	1.69	4.9	14	5	-1.0	8	12	28
56	0.0	2.46	4.9	14	5	-1.0	8	12	28
57	0.0	3.04	4.9	13	4	-1.0	6	12	28
58	0.0	3.12	4.9	13	4	-1.0	6	12	28
59	0.0	3.15	4.9	13	4	-1.0	6	12	28
60	0.0	3.07	4.9	13	4	-1.0	6	12	28
61	0.0	3.13	5.0	13	2	-1.0	6	12	28
62	0.0	3.22	5.0	13	2	-1.0	6	12	28
63	0.0	3.32	5.0	13	2	-1.0	6	12	28
64	0.0	3.35	5.0	13	1	-1.0	18	24	28
65	0.0	3.42	5.0	13	1	-1.0	18	24	28
66	0.0	3.56	5.0	13	1	-1.0	18	24	28
67	0.0	3.72	4.9	16	2	-1.0	18	24	28
68	0.0	3.61	4.9	16	2	-1.0	18	24	28
69	0.0	3.51	4.9	16	2	-1.0	18	24	28
70	0.0	3.44	4.9	16	2	-1.0	18	24	28
71	0.0	3.20	5.0	16	1	-1.0	10	32	10
72	0.0	3.00	5.0	16	1	-1.0	10	32	10
73	0.0	2.77	5.0	16	1	-1.0	10	32	10
74	0.0	2.25	5.0	18	1	-1.0	10	32	10
75	0.0	1.96	5.0	18	1	-1.0	10	32	10
76	0.0	1.70	5.0	18	1	-1.0	10	32	10
77	0.0	1.48	5.0	19	1	-1.0	10	32	10
78	0.0	1.37	5.0	19	1	-1.0	10	32	10
79	0.0	1.26	5.0	19	1	-1.0	10	32	10
80	0.0	1.15	5.0	19	1	-1.0	10	32	10

Roof area 79 08 21 16:54

Time min	P mm/h	R l/s	pH	Cond mS/m	SS mg/l	Cd µg/l	Pb µg/l	Cu µg/l	Zn µg/l
1	0.0	0.00	4.2	55	8	-1.0	18	13	64
2	0.0	0.02	4.2	55	8	-1.0	18	13	64
3	0.0	0.04	4.2	55	8	-1.0	18	13	64
4	0.0	0.06	4.1	57	4	-1.0	16	8	48
5	0.0	0.09	4.1	57	4	-1.0	16	8	48
6	0.0	0.13	4.1	57	4	-1.0	16	8	48
7	0.0	0.13	4.0	58	1	-1.0	16	8	48
8	0.0	0.11	4.0	58	1	-1.0	16	8	48
9	0.0	0.09	4.0	58	1	-1.0	16	8	48
10	0.0	0.06	4.0	58	1	-1.0	16	8	48
11	0.0	0.03	4.1	57	1	-1.0	15	9	80
12	0.0	0.01	4.1	57	1	-1.0	15	9	80
13	0.0	0.01	4.1	57	1	-1.0	15	9	80
14	0.0	0.01	4.2	56	1	-1.0	15	9	80
15	0.0	0.01	4.2	56	1	-1.0	15	9	80
16	0.0	0.01	4.2	56	1	-1.0	15	9	80
17	0.0	0.01	4.3	37	1	-1.0	8	6	48
18	0.0	0.01	4.3	37	1	-1.0	8	6	48
19	0.0	0.01	4.3	37	1	-1.0	8	6	48
20	0.0	0.01	4.3	37	1	-1.0	8	6	48
21	0.0	0.01	4.2	32	1	-1.0	8	6	48
22	0.0	0.01	4.2	32	1	-1.0	8	6	48
23	0.0	0.01	4.2	32	1	-1.0	8	6	48
24	0.0	0.01	4.4	33	1	-1.0	10	8	40
25	0.0	0.01	4.4	33	1	-1.0	10	8	40
26	0.0	0.01	4.4	33	1	-1.0	10	8	40
27	0.0	0.01	4.3	33	1	-1.0	10	8	40
28	0.0	0.01	4.3	33	1	-1.0	10	8	40
29	0.0	0.01	4.3	33	1	-1.0	10	8	40
30	0.0	0.01	4.3	33	1	-1.0	10	8	40
31	0.0	0.01	4.3	34	1	-1.0	10	8	40
32	0.0	0.02	4.3	34	1	-1.0	10	8	40
33	0.0	0.02	4.3	34	1	-1.0	10	8	40

Parking lot 79 09 02 18:41

Time min	P mm/h	R l/s	pH	Cond mS/m	SS mg/l	Cd µg/l	Pb µg/l	Cu µg/l	Zn µg/l
1	33.4	0.60	3.6	107	140	2.2	160	73	-1
2	35.7	0.47	3.6	107	140	2.2	160	73	-1
3	35.7	0.41	3.6	107	140	2.2	160	73	-1
4	30.3	0.88	3.5	107	100	1.5	110	71	-1
5	30.3	1.74	3.5	107	100	1.5	110	71	-1
6	18.9	2.46	3.5	107	100	1.5	110	71	-1
7	18.9	2.78	3.5	115	69	1.5	110	71	-1
8	18.9	2.70	3.5	115	69	1.5	110	71	-1
9	27.3	2.76	3.5	115	69	1.5	110	71	-1
10	30.1	3.04	3.5	115	69	1.5	110	71	-1
11	30.1	2.13	3.5	109	110	0.7	99	47	-1
12	34.0	1.81	3.5	109	110	0.7	99	47	-1
13	34.0	1.72	3.5	109	110	0.7	99	47	-1
14	91.0	2.36	3.6	86	75	0.7	99	47	-1
15	12.9	2.80	3.6	86	75	0.7	99	47	-1
16	12.9	3.12	3.6	86	75	0.7	99	47	-1
17	11.4	3.27	3.7	87	28	0.7	99	47	-1
18	11.4	3.33	3.7	87	28	0.7	99	47	-1
19	11.4	3.30	3.7	87	28	0.7	99	47	-1
20	5.6	3.10	3.7	87	28	0.7	99	47	-1

Parking lot 79 09 11 09:23

Time min	P mm/h	R l/s	pH	Cond mS/m	SS mg/l	Cd µg/l	Pb µg/l	Cu µg/l	Zn µg/l
1	1.1	0.05	3.9	240	46	8.3	280	88	-1
2	1.1	0.07	3.9	240	46	8.3	280	88	-1
3	1.1	0.08	3.9	240	46	8.3	280	88	-1
4	1.1	0.09	3.9	240	46	8.3	280	88	-1
5	1.9	0.09	3.9	240	46	8.3	280	88	-1
6	1.9	0.10	3.9	240	46	8.3	280	88	-1
7	1.9	0.10	3.8	225	23	6.0	230	75	-1
8	1.9	0.11	3.8	225	23	6.0	230	75	-1
9	0.0	0.13	3.8	225	23	6.0	230	75	-1
10	0.0	0.15	3.8	225	23	6.0	230	75	-1
11	0.0	0.16	3.8	225	23	6.0	230	75	-1
12	0.0	0.16	3.8	225	23	6.0	230	75	-1
13	0.0	0.16	3.8	225	23	6.0	230	75	-1
14	0.0	0.16	3.9	192	17	4.8	180	61	-1
15	0.0	0.17	3.9	192	17	4.8	180	61	-1
16	0.0	0.17	3.9	192	17	4.8	180	61	-1
17	3.4	0.17	3.9	192	17	4.8	180	61	-1
18	3.4	0.18	3.9	192	17	4.8	180	61	-1
19	3.4	0.18	3.9	192	17	4.8	180	61	-1
20	3.4	0.20	3.9	192	17	4.8	180	61	-1
21	0.6	0.23	3.9	192	17	4.8	180	61	-1
22	0.6	0.21	3.9	192	17	4.8	180	61	-1
23	0.6	0.19	3.9	192	17	4.8	180	61	-1
24	0.6	0.19	3.9	192	17	4.8	180	61	-1
25	0.6	0.20	3.9	192	17	4.8	180	61	-1
26	0.6	0.21	3.9	192	17	4.8	180	61	-1
27	0.6	0.17	3.9	192	17	4.8	180	61	-1
28	0.6	0.17	3.9	192	17	4.8	180	61	-1
29	0.6	0.17	3.9	192	17	4.8	180	61	-1
30	0.4	0.16	3.9	192	17	4.8	180	61	-1

Parking lot 79 09 11 10:27

Time min	P mm/h	R l/s	pH	Cond mS/m	SS mg/l	Cd µg/l	Pb µg/l	Cu µg/l	Zn µg/l
1	0.0	0.09	4.1	108	16	4.8	150	33	-1
2	0.0	0.09	4.1	108	16	4.8	150	33	-1
3	0.0	0.09	4.1	108	16	4.8	150	33	-1
4	0.0	0.09	4.1	108	16	4.8	150	33	-1
5	0.0	0.09	4.1	108	16	4.8	150	33	-1
6	0.0	0.09	4.1	108	16	4.8	150	33	-1
7	2.1	0.09	4.1	94	30	4.8	150	33	-1
8	2.1	0.09	4.1	94	30	4.8	150	33	-1
9	2.1	0.09	4.1	94	30	4.8	150	33	-1
10	2.1	0.09	4.1	94	30	4.8	150	33	-1
11	2.1	0.10	4.2	76	15	2.8	72	22	-1
12	2.8	0.11	4.2	76	15	2.8	72	22	-1
13	2.8	0.13	4.2	76	15	2.8	72	22	-1
14	2.8	0.16	4.2	76	15	2.8	72	22	-1
15	3.4	0.19	4.2	76	15	2.8	72	22	-1
16	3.4	0.22	4.2	76	15	2.8	72	22	-1
17	0.7	0.25	4.2	76	15	2.8	72	22	-1
18	0.7	0.27	4.2	76	15	2.8	72	22	-1
19	0.7	0.28	4.2	76	15	2.8	72	22	-1
20	0.8	0.28	4.2	76	15	2.8	72	22	-1
21	0.8	0.27	4.2	58	10	2.8	72	22	-1
22	0.8	0.25	4.2	58	10	2.8	72	22	-1
23	0.6	0.22	4.2	58	10	2.8	72	22	-1
24	0.6	0.23	4.2	58	10	2.8	72	22	-1
25	0.6	0.25	4.2	58	10	2.8	72	22	-1
26	0.6	0.26	4.2	58	10	2.8	72	22	-1
27	0.6	0.28	4.2	58	10	2.8	72	22	-1
28	4.6	0.29	4.2	58	10	2.8	72	22	-1
29	4.6	0.30	4.2	58	10	2.8	72	22	-1
30	4.6	0.31	4.2	58	10	2.8	72	22	-1
31	4.6	0.36	4.4	45	8	1.0	54	18	-1
32	2.2	0.34	4.4	45	8	1.0	54	18	-1
33	2.2	0.32	4.4	45	8	1.0	54	18	-1
34	2.2	0.30	4.4	45	8	1.0	54	18	-1
35	2.2	0.30	4.4	45	8	1.0	54	18	-1
36	0.7	0.30	4.4	45	8	1.0	54	18	-1
37	0.7	0.29	4.4	45	8	1.0	54	18	-1
38	0.7	0.28	4.4	45	8	1.0	54	18	-1
39	0.7	0.27	4.4	45	8	1.0	54	18	-1
40	0.7	0.25	4.4	45	8	1.0	54	18	-1
41	0.7	0.22	4.4	45	8	1.0	54	18	-1
42	0.7	0.20	4.4	45	8	1.0	54	18	-1
43	0.7	0.21	4.4	45	8	1.0	54	18	-1

Parking lot 79 09 17 17:37

Time min	P mm/h	R l/s	pH	Cond mS/m	SS mg/l	Cd µg/l	Pb µg/l	Cu µg/l	Zn µg/l
1	0.0	0.00	4.5	70	78	5.0	140	45	-1
2	0.0	0.00	4.5	70	78	5.0	140	45	-1
3	0.0	0.00	4.5	70	78	5.0	140	45	-1
4	0.0	0.02	4.5	70	78	5.0	140	45	-1
5	3.9	0.14	4.5	70	78	5.0	140	45	-1
6	4.2	0.19	4.5	70	78	5.0	140	45	-1
7	4.2	0.22	4.5	70	78	5.0	140	45	-1
8	5.7	0.23	4.5	70	78	5.0	140	45	-1
9	5.7	0.26	4.5	70	78	5.0	140	45	-1
10	2.2	0.29	4.5	70	78	5.0	140	45	-1
11	2.2	0.31	4.2	65	30	1.1	97	38	-1
12	1.1	0.32	4.2	65	30	1.1	97	38	-1
13	1.1	0.30	4.2	65	30	1.1	97	38	-1
14	1.2	0.29	4.3	62	24	1.5	85	30	-1
15	1.2	0.27	4.3	62	24	1.5	85	30	-1
16	1.9	0.26	4.3	62	24	1.5	85	30	-1
17	1.9	0.25	4.3	59	22	2.2	81	35	-1
18	1.9	0.24	4.3	59	22	2.2	81	35	-1
19	0.0	0.22	4.3	59	22	2.2	81	35	-1
20	0.0	0.20	4.3	59	22	2.2	81	35	-1
21	0.0	0.18	4.3	59	22	2.2	81	35	-1
22	0.0	0.16	4.3	59	22	2.2	81	35	-1
23	0.0	0.14	4.3	59	22	2.2	81	35	-1
24	0.0	0.13	4.2	60	6	2.6	81	35	-1
25	0.0	0.13	4.2	60	6	2.6	81	35	-1
26	0.0	0.13	4.2	60	6	2.6	81	35	-1
27	0.0	0.13	4.2	60	6	2.6	81	35	-1
28	0.0	0.12	4.2	60	6	2.6	81	35	-1
29	0.0	0.10	4.2	60	6	2.6	81	35	-1
30	0.0	0.10	4.2	60	6	2.6	81	35	-1

Parking lot 79 11 06 00:06

Time min	P mm/h	R l/s	pH	Cond mS/m	SS mg/l	Cd µgl	Pb µg/l	Cu µg/l	Zn µg/l
1	7.2	0.00	4.5	56	62	-1.0	-1	-1	-1
2	10.2	0.00	4.5	56	62	-1.0	-1	-1	-1
3	10.2	0.01	4.5	56	62	-1.0	-1	-1	-1
4	10.2	0.04	4.5	56	62	-1.0	-1	-1	-1
5	9.1	0.06	4.5	56	62	-1.0	-1	-1	-1
6	9.1	0.07	4.5	56	62	-1.0	-1	-1	-1
7	6.0	0.19	4.5	39	30	-1.0	-1	-1	-1
8	6.0	0.43	4.5	39	30	-1.0	-1	-1	-1
9	6.0	0.55	4.5	39	30	-1.0	-1	-1	-1
10	4.4	0.67	4.5	39	30	-1.0	-1	-1	-1
11	4.4	0.72	4.7	29	25	-1.0	-1	-1	-1
12	9.2	0.67	4.7	29	25	-1.0	-1	-1	-1
13	9.2	0.64	4.7	29	25	-1.0	-1	-1	-1
14	9.2	0.64	4.7	29	25	-1.0	-1	-1	-1
15	1.2	0.58	4.7	29	25	-1.0	-1	-1	-1
16	1.2	0.52	4.7	29	25	-1.0	-1	-1	-1
17	1.2	0.47	3.5	113	7	-1.0	-1	-1	-1
18	1.2	0.44	3.5	113	7	-1.0	-1	-1	-1
19	8.3	0.42	3.5	113	7	-1.0	-1	-1	-1
20	8.3	0.41	3.5	113	7	-1.0	-1	-1	-1
21	8.3	0.40	3.5	113	7	-1.0	-1	-1	-1
22	5.0	0.42	3.5	113	7	-1.0	-1	-1	-1
23	5.0	0.45	3.5	113	7	-1.0	-1	-1	-1
24	5.0	0.46	3.5	113	7	-1.0	-1	-1	-1
25	5.0	0.41	3.5	113	7	-1.0	-1	-1	-1
26	5.0	0.37	3.5	113	7	-1.0	-1	-1	-1
27	1.4	0.37	3.5	113	7	-1.0	-1	-1	-1
28	1.4	0.37	3.5	113	7	-1.0	-1	-1	-1
29	1.4	0.37	3.5	113	7	-1.0	-1	-1	-1
30	1.3	0.37	3.5	113	7	-1.0	-1	-1	-1
31	1.3	0.34	3.5	113	7	-1.0	-1	-1	-1
32	1.3	0.31	0.0	0	0	0.0	0	0	0
33	1.3	0.27	0.0	0	0	0.0	0	0	0
34	0.0	0.24	0.0	0	0	0.0	0	0	0
35	0.0	0.20	0.0	0	0	0.0	0	0	0
36	0.0	0.17	0.0	0	0	0.0	0	0	0
37	0.0	0.14	0.0	0	0	0.0	0	0	0
38	0.0	0.14	0.0	0	0	0.0	0	0	0
39	0.0	0.13	0.0	0	0	0.0	0	0	0
40	0.8	0.13	0.0	0	0	0.0	0	0	0
41	0.8	0.13	0.0	0	0	0.0	0	0	0
42	0.8	0.13	0.0	0	0	0.0	0	0	0
43	0.8	0.13	0.0	0	0	0.0	0	0	0
44	0.8	0.10	4.0	46	15	-1.0	-1	-1	-1
45	0.8	0.09	4.0	46	15	-1.0	-1	-1	-1

Parking lot 79 11 06 00:06

Time min	P mm/h	R l/s	pH	Cond mS/m	SS mg/l	Cd µgl	Pb µg/l	Cu µg/l	Zn µg/l
46	0.9	0.10	4.0	46	15	-1.0	-1	-1	-1
47	0.9	0.10	4.0	46	15	-1.0	-1	-1	-1
48	0.9	0.10	4.0	46	15	-1.0	-1	-1	-1
49	0.9	0.09	4.0	46	15	-1.0	-1	-1	-1
50	0.9	0.09	4.0	46	15	-1.0	-1	-1	-1
51	0.4	0.08	4.0	46	15	-1.0	-1	-1	-1
52	0.4	0.08	4.0	46	15	-1.0	-1	-1	-1
53	0.4	0.07	4.0	46	15	-1.0	-1	-1	-1
54	0.4	0.07	4.0	46	15	-1.0	-1	-1	-1
55	0.4	0.07	4.0	46	15	-1.0	-1	-1	-1
56	0.4	0.07	4.0	46	15	-1.0	-1	-1	-1
57	0.4	0.08	4.0	46	15	-1.0	-1	-1	-1
58	1.4	0.08	4.0	46	15	-1.0	-1	-1	-1
59	1.4	0.08	4.0	46	15	-1.0	-1	-1	-1
60	1.4	0.08	4.0	46	15	-1.0	-1	-1	-1
61	1.4	0.07	4.0	46	15	-1.0	-1	-1	-1
62	1.4	0.07	4.0	46	15	-1.0	-1	-1	-1
63	1.8	0.07	4.0	46	15	-1.0	-1	-1	-1
64	1.8	0.07	4.0	46	15	-1.0	-1	-1	-1
65	1.4	0.08	4.0	46	15	-1.0	-1	-1	-1
66	1.4	0.10	4.0	46	15	-1.0	-1	-1	-1
67	1.4	0.11	4.0	46	15	-1.0	-1	-1	-1
68	1.4	0.12	4.0	46	15	-1.0	-1	-1	-1
69	0.5	0.12	4.0	46	15	-1.0	-1	-1	-1
70	0.5	0.13	4.0	46	15	-1.0	-1	-1	-1
71	0.5	0.10	4.0	46	15	-1.0	-1	-1	-1
72	0.5	0.09	4.0	46	15	-1.0	-1	-1	-1
73	0.5	0.09	4.0	46	15	-1.0	-1	-1	-1
74	0.5	0.10	4.0	46	15	-1.0	-1	-1	-1
75	0.5	0.10	4.0	46	15	-1.0	-1	-1	-1
76	0.5	0.11	4.0	46	15	-1.0	-1	-1	-1

Parking lot 80 08 16 22:23

Time min	P mm/h	R l/s	pH	Cond mS/m	SS mg/l	Cd µg/l	Pb µg/l	Cu µg/l	Zn µg/l
1	16.6	0.03	5.3	79	-1	1.4	140	47	-1
2	16.6	0.05	5.3	79	-1	1.4	140	47	-1
3	0.0	0.09	5.3	79	-1	1.4	140	47	-1
4	0.0	0.14	5.3	79	-1	1.4	140	47	-1
5	0.0	0.20	5.3	79	-1	1.4	140	47	-1
6	0.0	0.22	5.3	79	-1	1.4	140	47	-1
7	0.0	0.25	5.3	79	-1	1.4	140	47	-1
8	0.0	0.27	5.3	79	-1	1.4	140	47	-1
9	0.8	0.26	5.3	79	-1	1.4	140	47	-1
10	0.8	0.26	5.3	79	-1	1.4	140	47	-1
11	0.8	0.25	4.4	69	-1	1.2	130	50	-1
12	0.8	0.23	4.4	69	-1	1.2	130	50	-1
13	0.8	0.21	4.4	69	-1	1.2	130	50	-1
14	0.0	0.20	4.4	69	-1	1.2	130	50	-1
15	0.0	0.19	4.4	69	-1	1.2	130	50	-1
16	0.0	0.18	4.3	72	-1	1.2	100	51	-1
17	0.0	0.16	4.3	72	-1	1.2	100	51	-1
18	0.0	0.15	4.3	72	-1	1.2	100	51	-1
19	0.5	0.14	4.3	72	-1	1.2	100	51	-1
20	0.5	0.13	4.3	72	-1	1.2	100	51	-1
21	0.5	0.13	4.3	72	-1	1.2	100	51	-1
22	0.5	0.12	4.3	72	-1	1.2	100	51	-1
23	0.5	0.11	4.3	72	-1	1.2	100	51	-1
24	0.5	0.11	4.3	72	-1	1.2	100	51	-1
25	0.5	0.10	4.3	72	-1	1.2	100	51	-1

Parking lot 80 08 16 23:48

Time min	P mm/h	R l/s	pH	Cond mS/m	SS mg/l	Cd µg/l	Pb µg/l	Cu µg/l	Zn µg/l
1	7.3	1.15	4.6	55	-1	0.6	70	43	-1
2	7.3	1.06	4.6	55	-1	0.6	70	43	-1
3	6.1	0.97	4.6	55	-1	0.6	70	43	-1
4	4.0	0.92	4.6	55	-1	0.6	70	43	-1
5	3.4	0.86	4.6	55	-1	0.6	70	43	-1
6	3.4	0.82	4.6	55	-1	0.6	70	43	-1
7	3.4	0.79	4.6	55	-1	0.6	70	43	-1
8	8.1	0.77	4.5	48	-1	0.6	66	39	-1
9	8.1	0.75	4.5	48	-1	0.6	66	39	-1
10	8.1	0.75	4.5	48	-1	0.6	66	39	-1
11	7.3	0.76	4.5	48	-1	0.6	66	39	-1
12	7.3	0.77	4.5	48	-1	0.6	66	39	-1
13	4.0	0.77	4.5	48	-1	0.6	66	39	-1
14	4.0	0.78	4.5	48	-1	0.6	66	39	-1
15	8.6	0.80	4.5	48	-1	0.6	66	39	-1
16	8.6	0.83	4.5	48	-1	0.6	66	39	-1
17	8.6	0.91	4.5	48	-1	0.6	66	39	-1
18	8.6	1.00	4.5	38	-1	0.4	67	32	-1
19	6.1	1.06	4.5	38	-1	0.4	67	32	-1
20	6.1	1.04	4.5	38	-1	0.4	67	32	-1
21	16.6	1.02	4.5	38	-1	0.4	67	32	-1
22	6.1	0.99	4.5	38	-1	0.4	67	32	-1
23	9.2	0.99	4.5	38	-1	0.4	67	32	-1
24	9.2	0.95	4.5	38	-1	0.4	67	32	-1
25	4.0	0.90	4.5	38	-1	0.4	67	32	-1
26	12.3	0.85	4.5	38	-1	0.4	67	32	-1
27	12.3	0.78	4.5	38	-1	0.4	67	32	-1
28	6.1	0.69	5.0	17	-1	0.4	42	24	-1
29	6.1	0.67	5.0	17	-1	0.4	42	24	-1
30	6.1	0.65	5.0	17	-1	0.4	42	24	-1
31	4.0	0.64	5.0	17	-1	0.4	42	24	-1
32	4.0	0.60	5.0	17	-1	0.4	42	24	-1
33	3.0	0.58	5.0	17	-1	0.4	42	24	-1
34	3.0	0.60	5.0	17	-1	0.4	42	24	-1
35	6.1	0.57	5.0	17	-1	0.4	42	24	-1

Parking lot 80 08 20 12:28

Time min	P mm/h	R l/s	pH	Cond mS/m	SS mg/l	Cd µg/l	Pb µg/l	Cu µg/l	Zn µg/l
1	10.7	0.56	4.9	14	-1	1.9	23	5	-1
2	10.7	0.49	4.9	14	-1	1.9	23	5	-1
3	4.0	0.45	4.9	14	-1	1.9	23	5	-1
4	4.0	0.42	4.9	14	-1	1.9	23	5	-1
5	4.0	0.35	4.9	14	-1	1.9	23	5	-1
6	12.2	0.28	4.9	14	-1	1.9	23	5	-1
7	0.0	0.27	4.9	14	-1	1.9	23	5	-1
8	0.0	0.27	4.9	14	-1	1.9	23	5	-1
9	0.0	0.27	4.9	14	-1	1.9	23	5	-1
10	12.2	0.27	4.9	14	-1	1.9	23	5	-1
11	0.0	0.28	4.9	17	-1	0.4	17	21	-1
12	0.0	0.30	4.9	17	-1	0.4	17	21	-1
13	0.0	0.27	4.9	17	-1	0.4	17	21	-1
14	0.0	0.31	4.9	17	-1	0.4	17	21	-1
15	0.0	0.26	4.9	17	-1	0.4	17	21	-1
16	2.1	0.22	4.9	17	-1	0.4	17	21	-1
17	2.1	0.22	4.9	17	-1	0.4	17	21	-1
18	2.1	0.19	4.9	17	-1	0.4	17	21	-1
19	2.1	0.14	4.9	17	-1	0.4	17	21	-1
20	1.9	0.12	4.9	17	-1	0.4	17	21	-1
21	1.9	0.10	4.9	17	-1	0.4	17	21	-1
22	1.9	0.08	4.9	17	-1	0.4	17	21	-1
23	1.9	0.08	4.9	17	-1	0.4	17	21	-1
24	1.9	0.10	4.9	17	-1	0.4	17	21	-1
25	1.7	0.10	4.9	17	-1	0.4	17	21	-1
26	1.7	0.09	4.8	19	-1	0.4	23	10	-1
27	1.7	0.08	4.8	19	-1	0.4	23	10	-1
28	1.7	0.08	4.8	19	-1	0.4	23	10	-1
29	1.7	0.08	4.8	19	-1	0.4	23	10	-1
30	1.7	0.08	4.8	19	-1	0.4	23	10	-1
31	1.7	0.09	4.8	19	-1	0.4	23	10	-1
32	1.7	0.08	4.8	19	-1	0.4	23	10	-1
33	2.9	0.07	4.8	19	-1	0.4	23	10	-1
34	2.9	0.08	4.8	19	-1	0.4	23	10	-1
35	2.9	0.09	4.8	19	-1	0.4	23	10	-1
36	2.9	0.11	4.8	19	-1	0.4	23	10	-1
37	2.9	0.12	4.8	19	-1	0.4	23	10	-1
38	3.1	0.14	4.8	19	-1	0.4	23	10	-1
39	3.1	0.15	4.8	19	-1	0.4	23	10	-1
40	3.1	0.14	4.8	19	-1	0.4	23	10	-1
41	3.1	0.14	4.7	25	-1	1.6	22	15	-1
42	3.1	0.13	4.7	25	-1	1.6	22	15	-1
43	0.0	0.12	4.7	25	-1	1.6	22	15	-1
44	0.0	0.12	4.7	25	-1	1.6	22	15	-1
45	0.0	0.11	4.7	25	-1	1.6	22	15	-1

Parking lot 80 08 20 12:28

Time min	P mm/h	R l/s	pH	Cond mS/m	SS mg/l	Cd µg/l	Pb µg/l	Cu µg/l	Zn µg/l
46	0.0	0.10	4.7	25	-1	1.6	22	15	-1
47	0.0	0.10	4.7	25	-1	1.6	22	15	-1
48	0.0	0.09	4.7	25	-1	1.6	22	15	-1
49	0.8	0.09	4.7	25	-1	1.6	22	15	-1
50	0.8	0.09	4.7	25	-1	1.6	22	15	-1
51	0.8	0.08	4.7	25	-1	1.6	22	15	-1
52	0.8	0.08	4.7	25	-1	1.6	22	15	-1
53	0.8	0.08	4.7	25	-1	1.6	22	15	-1
54	0.0	0.08	4.7	25	-1	1.6	22	15	-1
55	0.0	0.07	4.7	25	-1	1.6	22	15	-1
56	0.0	0.07	4.7	29	-1	0.9	19	12	-1
57	0.0	0.07	4.7	29	-1	0.9	19	12	-1
58	0.0	0.06	4.7	29	-1	0.9	19	12	-1
59	0.0	0.04	4.7	29	-1	0.9	19	12	-1
60	1.8	0.04	4.7	29	-1	0.9	19	12	-1
61	1.8	0.04	4.7	29	-1	0.9	19	12	-1
62	1.8	0.05	4.7	29	-1	0.9	19	12	-1
63	1.8	0.05	4.7	29	-1	0.9	19	12	-1
64	1.8	0.05	4.7	29	-1	0.9	19	12	-1
65	1.7	0.07	4.7	29	-1	0.9	19	12	-1
66	1.7	0.05	4.7	29	-1	0.9	19	12	-1
67	1.7	0.04	4.7	29	-1	0.9	19	12	-1
68	1.7	0.04	4.7	29	-1	0.9	19	12	-1
69	1.7	0.04	4.7	29	-1	0.9	19	12	-1
70	1.7	0.04	4.7	29	-1	0.9	19	12	-1
71	0.7	0.04	4.7	29	-1	0.9	19	12	-1
72	0.7	0.04	4.7	29	-1	0.9	19	12	-1
73	0.7	0.03	4.7	29	-1	0.9	19	12	-1
74	0.7	0.03	4.7	29	-1	0.9	19	12	-1
75	0.7	0.03	4.7	29	-1	0.9	19	12	-1
76	0.7	0.03	4.7	29	-1	0.9	19	12	-1
77	1.9	0.02	4.7	29	-1	0.9	19	12	-1
78	1.9	0.02	4.7	29	-1	0.9	19	12	-1
79	1.9	0.02	4.7	29	-1	0.9	19	12	-1
80	1.9	0.02	4.7	29	-1	0.9	19	12	-1
81	1.9	0.02	4.7	29	-1	0.9	19	12	-1
82	1.9	0.02	4.7	29	-1	0.9	19	12	-1
83	1.9	0.03	4.7	29	-1	0.9	19	12	-1
84	1.9	0.04	4.7	29	-1	0.9	19	12	-1
85	2.9	0.05	4.7	29	-1	0.9	19	12	-1
86	1.6	0.04	4.5	33	-1	0.8	58	21	-1
87	1.6	0.03	4.5	33	-1	0.8	58	21	-1
88	1.6	0.04	4.5	33	-1	0.8	58	21	-1
89	1.6	0.04	4.5	33	-1	0.8	58	21	-1
90	1.6	0.03	4.5	33	-1	0.8	58	21	-1

Parking lot 80 08 20 12:28

Time min	P mm/h	R l/s	pH	Cond mS/m	SS mg/l	Cd µg/l	Pb µg/l	Cu µg/l	Zn µg/l
91	1.6	0.03	4.5	33	-1	0.8	58	21	-1
92	1.6	0.03	4.5	33	-1	0.8	58	21	-1
93	1.6	0.04	4.5	33	-1	0.8	58	21	-1
94	1.6	0.05	4.5	33	-1	0.8	58	21	-1
95	0.0	0.06	4.5	33	-1	0.8	58	21	-1
96	0.0	0,07	4.5	33	-1	0.8	58	21	-1
97	0.0	0.07	4.5	33	-1	0.8	58	21	-1
98	5.1	0.06	4.5	33	-1	0.8	58	21	-1
99	5.1	0.07	4.5	33	-1	0.8	58	21	-1
100	5.1	0.10	4.5	33	-1	0.8	58	21	-1
101	4.0	0.09	4.6	25	-1	0.6	28	19	-1
102	4.0	0.16	4.6	25	-1	0.6	28	19	-1
103	9.1	0.22	4.6	25	-1	0.6	28	19	-1
104	9.1	0.25	4.6	25	-1	0.6	28	19	-1
105	1.9	0.26	4.6	25	-1	0.6	28	19	-1
106	1.9	0.28	4.6	25	-1	0.6	28	19	-1
107	3.4	0.27	4.6	25	-1	0.6	28	19	-1
108	3.4	0.25	4.6	25	-1	0.6	28	19	-1
109	3.4	0.23	4.6	25	-1	0.6	28	19	-1
110	2.9	0.23	4.6	25	-1	0.6	28	19	-1
111	2.9	0.22	4.6	25	-1	0.6	28	19	-1
112	2.9	0.21	4.6	25	-1	0.6	28	19	-1
113	6.0	0.19	4.7	22	-1	2.7	23	11	-1
114	6.0	0.16	4.7	22	-1	2.7	23	11	-1
115	0.0	0.14	4.7	22	-1	2.7	23	11	-1
116	0.0	0.11	4.7	22	-1	2.7	23	11	-1
117	0.0	0.09	4.7	22	-1	2.7	23	11	-1
118	0.0	0.08	4.7	22	-1	2.7	23	11	-1
119	0.0	0.07	4.7	22	-1	2.7	23	11	-1
120	0.0	0.06	4.7	22	-1	2.7	23	11	-1

Parking lot 80 08 28 20:40

Time min	P mm/h	R l/s	pH	Cond mS/m	SS mg/l	Cd µg/l	Pb µg/l	Cu µg/l	Zn µg/l
1	1.1	0.15	3.5	230	19	3.5	300	117	-1
2	1.1	0.15	3.5	230	19	3.5	300	117	-1
3	0.0	0.15	3.5	230	19	3.5	300	117	-1
4	0.0	0.15	3.5	230	19	3.5	300	117	-1
5	1.4	0.15	3.5	230	19	3.5	300	117	-1
6	1.4	0.15	3.5	230	19	3.5	300	117	-1
7	1.4	0.15	3.5	230	19	3.5	300	117	-1
8	1.6	0.14	3.5	230	15	3.7	310	121	-1
9	1.6	0.14	3.5	230	15	3.7	310	121	-1
10	1.6	0.13	3.5	230	15	3.7	310	121	-1
11	0.0	0.13	3.5	230	15	3.7	310	121	-1
12	0.0	0.13	3.5	230	15	3.7	310	121	-1
13	0.0	0.12	3.5	230	15	3.7	310	121	-1
14	0.0	0.12	3.5	230	15	3.7	310	121	-1
15	0.0	0.11	3.5	230	15	3.7	310	121	-1
16	0.0	0.11	3.5	230	15	3.7	310	121	-1
17	0.2	0.11	3.5	230	15	3.7	310	121	-1
18	0.2	0.10	3.5	230	15	3.7	310	121	-1
19	0.2	0.10	3.5	230	15	3.7	310	121	-1
20	0.2	0.11	3.5	230	15	3.7	310	121	-1
21	0.2	0.11	3.4	235	8	2.8	300	125	-1
22	0.2	0.12	3.4	235	8	2.8	300	125	-1
23	0.2	0.12	3.4	235	8	2.8	300	125	-1
24	0.2	0.13	3.4	235	8	2.8	300	125	-1
25	0.2	0.13	3.4	235	8	2.8	300	125	-1
26	0.2	0.14	3.4	235	8	2.8	300	125	-1
27	0.2	0.15	3.4	235	8	2.8	300	125	-1
28	0.2	0.16	3.4	235	8	2.8	300	125	-1
29	0.2	0.16	3.4	235	8	2.8	300	125	-1
30	0.2	0.17	3.4	235	8	2.8	300	125	-1
31	0.2	0.18	3.4	235	8	2.8	300	125	-1
32	0.2	0.19	3.4	235	8	2.8	300	125	-1
33	0.2	0.19	3.3	240	11	2.7	300	125	-1
34	0.2	0.19	3.3	240	11	2.7	300	125	-1
35	0.2	0.20	3.3	240	11	2.7	300	125	-1
36	0.2	0.22	3.3	240	11	2.7	300	125	-1
37	0.2	0.24	3.3	240	11	2.7	300	125	-1
38	0.2	0.25	3.3	240	11	2.7	300	125	-1
39	0.2	0.27	3.3	240	11	2.7	300	125	-1
40	0.2	0.29	3.3	240	11	2.7	300	125	-1
41	0.2	0.30	3.3	240	11	2.7	300	125	-1
42	0.2	0.31	3.3	240	11	2.7	300	125	-1

Parking lot 80 09 17 15:02

Time min	P mm/h	R l/s	pH	Cond mS/m	SS mg/l	Cd µg/l	Pb µg/l	Cu µg/l	Zn µg/l
1	3.3	0.42	4.1	120	43	2.5	144	41	-1
2	3.7	0.50	4.1	120	43	2.5	144	41	-1
3	3.7	0.52	4.1	120	43	2.5	144	41	-1
4	3.7	0.51	4.1	120	43	2.5	144	41	-1
5	3.7	0.51	4.1	120	43	2.5	144	41	-1
6	3.8	0.50	4.1	100	48	1.8	122	38	-1
7	3.8	0.50	4.1	100	48	1.8	122	38	-1
8	3.8	0.50	4.1	100	48	1.8	122	38	-1
9	3.8	0.53	4.1	100	48	1.8	122	38	-1
10	3.8	0.56	4.1	100	48	1.8	122	38	-1
11	10.4	0.60	4.2	90	88	1.6	144	36	-1
12	10.4	0.65	4.2	90	88	1.6	144	36	-1
13	10.4	0.70	4.2	90	88	1.6	144	36	-1
14	10.4	0.73	4.2	90	88	1.6	144	36	-1
15	10.4	0.77	4.2	90	88	1.6	144	36	-1
16	3.3	0.81	4.2	70	51	2.4	114	28	-1
17	3.3	0.82	4.2	70	51	2.4	114	28	-1
18	3.3	0.83	4.2	70	51	2.4	114	28	-1
19	3.3	0.84	4.2	70	51	2.4	114	28	-1
20	2.3	0.88	4.2	70	51	2.4	114	28	-1
21	2.3	0.93	4.3	47	30	1.0	76	18	-1
22	2.3	0.97	4.3	47	30	1.0	76	18	-1
23	2.3	0.93	4.3	47	30	1.0	76	18	-1
24	2.3	0.89	4.3	47	30	1.0	76	18	-1
25	2.3	0.85	4.3	47	30	1.0	76	18	-1
26	2.3	0.82	4.3	47	30	1.0	76	18	-1
27	4.4	0.78	4.3	47	30	1.0	76	18	-1
28	4.4	0.74	4.3	34	18	0.9	73	17	-1
29	4.4	0.70	4.3	34	18	0.9	73	17	-1
30	4.4	0.69	4.3	34	18	0.9	73	17	-1
31	4.6	0.70	4.3	34	18	0.9	73	17	-1
32	4.6	0.71	4.3	34	18	0.9	73	17	-1
33	4.6	0.70	4.3	34	18	0.9	73	17	-1
34	2.6	0.68	4.3	34	18	0.9	73	17	-1
35	2.6	0.67	4.3	34	18	0.9	73	17	-1
36	2.6	0.66	4.3	34	18	0.9	73	17	-1
37	2.6	0.65	4.3	34	18	0.9	73	17	-1
38	2.6	0.64	4.3	34	18	0.9	73	17	-1
39	2.6	0.63	4.3	34	18	0.9	73	17	-1
40	2.6	0.62	4.3	34	18	0.9	73	17	-1
41	2.6	0.61	4.3	34	18	0.9	73	17	-1
42	2.6	0.60	4.3	34	18	0.9	73	17	-1
43	2.6	0.56	4.2	28	5	0.5	32	17	-1
44	2.8	0.52	4.2	28	5	0.5	32	17	-1
45	2.8	0.53	4.2	28	5	0.5	32	17	-1

Parking lot 80 09 17 15:02

Time min	P mm/h	R l/s	pH	Cond mS/m	SS mg/l	Cd µg/l	Pb µg/l	Cu µg/l	Zn µg/l
46	2.8	0.53	4.2	28	5	0.5	32	17	-1
47	2.8	0.54	4.2	28	5	0.5	32	17	-1
48	2.8	0.54	4.2	28	5	0.5	32	17	-1
49	1.7	0.54	4.2	28	5	0.5	32	17	-1
50	1.7	0.54	4.2	28	5	0.5	32	17	-1
51	1.7	0.55	4.2	28	5	0.5	32	17	-1
52	1.7	0.58	4.2	28	5	0.5	32	17	-1
53	1.7	0.60	4.2	28	5	0.5	32	17	-1
54	4.9	0.62	4.2	28	5	0.5	32	17	-1
55	4.9	0.55	4.2	28	5	0.5	32	17	-1
56	4.9	0.49	4.2	28	5	0.5	32	17	-1
57	4.9	0.47	4.2	28	5	0.5	32	17	-1
58	1.5	0.48	4.2	28	5	0.5	32	17	-1
59	1.5	0.49	4.2	28	5	0.5	32	17	-1
60	1.5	0.50	4.2	28	5	0.5	32	17	-1
61	1.5	0.50	4.2	28	5	0.5	32	17	-1
62	1.5	0.51	4.2	28	5	0.5	32	17	-1
63	1.5	0.52	4.2	30	11	0.7	58	19	-1
64	1.5	0.52	4.2	30	11	0.7	58	19	-1
65	0.0	0.51	4.2	30	11	0.7	58	19	-1
66	0.0	0.50	4.2	30	11	0.7	58	19	-1
67	0.0	0.49	4.2	30	11	0.7	58	19	-1
68	0.0	0.49	4.2	30	11	0.7	58	19	-1
69	0.0	0.48	4.2	30	11	0.7	58	19	-1
70	0.0	0.47	4.2	30	11	0.7	58	19	-1
71	0.0	0.47	4.2	30	11	0.7	58	19	-1
72	0.0	0.47	4.2	30	11	0.7	58	19	-1
73	0.0	0.47	4.2	30	11	0.7	58	19	-1
74	7.4	0.48	4.2	30	11	0.7	58	19	-1
75	7.4	0.49	4.2	30	11	0.7	58	19	-1
76	1.2	0.50	4.2	30	11	0.7	58	19	-1
77	1.2	0.52	4.2	30	11	0.7	58	19	-1
78	1.2	0.54	4.2	30	11	0.7	58	19	-1
79	1.2	0.51	4.2	30	11	0.7	58	19	-1
80	1.2	0.50	4.2	30	11	0.7	58	19	-1
81	1.2	0.52	4.2	30	11	0.7	58	19	-1
82	1.2	0.54	4.2	30	11	0.7	58	19	-1
83	1.2	0.56	4.1	32	8	1.0	36	17	-1
84	0.0	0.57	4.1	32	8	1.0	36	17	-1
85	0.0	0.53	4.1	32	8	1.0	36	17	-1
86	0.0	0.50	4.1	32	8	1.0	36	17	-1
87	0.0	0.47	4.1	32	8	1.0	36	17	-1
88	0.0	0.48	4.1	32	8	1.0	36	17	-1
89	0.0	0.49	4.1	32	8	1.0	36	17	-1
90	0.0	0.49	4.1	32	8	1.0	36	17	-1

Parking lot 80 09 17 15:02

Time min	P mm/h	R l/s	pH	Cond mS/m	SS mg/l	Cd µg/l	Pb µg/l	Cu µg/l	Zn µg/l
91	0.0	0.48	4.1	32	8	1.0	36	17	-1
92	3.0	0.47	4.1	32	8	1.0	36	17	-1
93	3.0	0.46	4.1	32	8	1.0	36	17	-1
94	3.0	0.45	4.1	32	8	1.0	36	17	-1
95	3.0	0.43	4.1	32	8	1.0	36	17	-1
96	3.0	0.40	4.1	32	8	1.0	36	17	-1
97	2.1	0.37	4.1	32	8	1.0	36	17	-1
98	2.1	0.34	4.1	32	8	1.0	36	17	-1
99	2.1	0.36	4.1	32	8	1.0	36	17	-1
100	2.1	0.38	4.1	32	8	1.0	36	17	-1
101	2.1	0.36	4.1	32	8	1.0	36	17	-1
102	2.1	0.36	4.1	32	8	1.0	36	17	-1
103	2.1	0.36	4.1	36	7	0.9	50	26	-1
104	0.8	0.36	4.1	36	7	0.9	50	26	-1
105	0.8	0.35	4.1	36	7	0.9	50	26	-1
106	0.8	0.35	4.1	36	7	0.9	50	26	-1
107	0.8	0.34	4.1	36	7	0.9	50	26	-1
108	0.8	0.34	4.1	36	7	0.9	50	26	-1
109	0.8	0.34	4.1	36	7	0.9	50	26	-1
110	0.5	0.35	4.1	36	7	0.9	50	26	-1
111	0.5	0.36	4.1	36	7	0.9	50	26	-1
112	0.5	0.38	4.1	36	7	0.9	50	26	-1
113	0.5	0.38	4.1	36	7	0.9	50	26	-1
114	0.5	0.38	4.1	36	7	0.9	50	26	-1
115	0.5	0.37	4.1	36	7	0.9	50	26	-1

Street area 79 08 19 00:03

Time min	P mm/h	R l/s	pH	Cond mS/m	SS mg/l	Cd µg/l	Pb µg/l	Cu µg/l	Zn µg/l
1	0.0	0.0	5.7	83	170	-1.0	160	56	580
2	0.0	0.16	5.7	83	170	-1.0	160	56	580
3	0.0	0.86	5.7	83	170	-1.0	160	56	580
4	0.0	1.80	6.0	44	56	-1.0	120	30	140
5	0.0	2.50	6.0	44	56	-1.0	120	30	140
6	0.0	2.54	6.0	44	56	-1.0	120	30	140
7	0.0	2.28	6.3	31	48	-1.0	120	30	140
8	0.0	1.93	6.3	31	48	-1.0	120	30	140
9	0.0	1.53	6.3	31	48	-1.0	120	30	140
10	0.0	1.18	6.3	31	48	-1.0	120	30	140
11	0.0	0.92	6.6	24	41	-1.0	130	50	120
12	0.0	0.89	6.6	24	41	-1.0	130	50	120
13	0.0	0.98	6.6	24	41	-1.0	130	50	120
14	0.0	1.55	6.5	29	48	-1.0	130	50	120
15	0.0	2.20	6.5	29	48	-1.0	130	50	120
16	0.0	2.68	6.5	29	48	-1.0	130	50	120

Street area 79 08 21 16:53

Time min	P mm/h	R l/s	pH	Cond mS/m	SS mg/l	Cd µg/l	Pb µg/l	Cu µg/l	Zn µg/l
1	0.0	0.00	5.2	57	190	-1.0	360	67	340
2	0.0	0.01	5.2	57	190	-1.0	360	67	340
3	0.0	0.02	5.2	57	190	-1.0	360	67	340
4	0.0	0.07	5.2	51	130	-1.0	290	46	250
5	0.0	0.32	5.2	51	130	-1.0	290	46	250
6	0.0	1.01	5.2	51	130	-1.0	290	46	250
7	0.0	1.13	5.4	50	89	-1.0	240	47	220
8	0.0	0.91	5.4	50	89	-1.0	240	47	220
9	0.0	0.72	5.4	50	89	-1.0	240	47	220
10	0.0	0.56	5.4	50	89	-1.0	240	47	220
11	0.0	0.45	5.2	45	69	-1.0	190	36	200
12	0.0	0.38	5.2	45	69	-1.0	190	36	200
13	0.0	0.37	5.2	45	69	-1.0	190	36	200
14	0.0	0.35	5.3	47	79	-1.0	220	130	230
15	0.0	0.33	5.3	47	79	-1.0	220	130	230
16	0.0	0.31	5.3	47	79	-1.0	220	130	230
17	0.0	0.32	5.3	47	81	-1.0	200	42	220
18	0.0	0.35	5.3	47	81	-1.0	200	42	220
19	0.0	0.32	5.3	47	81	-1.0	200	42	220
20	0.0	0.31	5.3	47	81	-1.0	200	42	220
21	0.0	0.30	5.5	46	120	-1.0	300	60	260
22	0.0	0.29	5.5	46	120	-1.0	300	60	260
23	0.0	0.28	5.5	46	120	-1.0	300	60	260
24	0.0	0.25	5.9	48	120	-1.0	300	60	260
25	0.0	0.21	5.9	48	120	-1.0	300	60	260
26	0.0	0.21	5.9	48	120	-1.0	300	60	260
27	0.0	0.22	5.5	43	110	-1.0	260	56	220
28	0.0	0.27	5.5	43	110	-1.0	260	56	220
29	0.0	0.30	5.5	43	110	-1.0	260	56	220
30	0.0	0.32	5.5	43	110	-1.0	260	56	220
31	0.0	0.34	5.6	43	110	-1.0	260	56	220
32	0.0	0.34	5.6	43	110	-1.0	260	56	220
33	0.0	0.38	5.6	43	110	-1.0	260	56	220
34	0.0	0.44	5.6	43	120	-1.0	200	59	220
35	0.0	0.48	5.6	43	120	-1.0	200	59	220
36	0.0	0.51	5.6	43	120	-1.0	200	59	220
37	0.0	0.54	5.5	41	81	-1.0	200	59	220
38	0.0	0.53	5.5	41	81	-1.0	200	59	220
39	0.0	0.51	5.5	41	81	-1.0	200	59	220
40	0.0	0.48	5.5	41	81	-1.0	200	59	220
41	0.0	0.44	5.5	37	65	-1.0	190	38	160
42	0.0	0.41	5.5	37	65	-1.0	190	38	160
43	0.0	0.39	5.5	37	65	-1.0	190	38	160
44	0.0	0.39	5.5	30	69	-1.0	190	38	160
45	0.0	0.39	5.5	30	69	-1.0	190	38	160
46	0.0	0.39	5.5	30	69	-1.0	190	38	160

Street area 79 09 02 10:30

Time min	P mm/h	R l/s	pH	Cond mS/m	SS mg/l	Cd µg/l	Pb µg/l	Cu µg/l	Zn µg/l
1	5.7	0.00	4.9	137	160	-1.0	72	160	-1
2	2.0	0.00	4.9	137	160	-1.0	72	160	-1
3	6.4	0.10	4.9	137	160	-1.0	72	160	-1
4	6.4	0.46	4.0	76	280	-1.0	970	130	-1
5	0.0	0.62	4.0	76	280	-1.0	970	130	-1
6	0.0	0.56	4.0	76	280	-1.0	970	130	-1
7	0.0	0.43	4.2	200	81	-1.0	970	130	-1
8	0.0	0.32	4.2	200	81	-1.0	970	130	-1
9	0.0	0.22	4.2	200	81	-1.0	970	130	-1
10	0.0	0.18	4.2	200	81	-1.0	970	130	-1
11	0.0	0.15	4.3	194	41	-1.0	680	130	-1
12	0.0	0.11	4.3	194	41	-1.0	680	130	-1
13	0.0	0.09	4.3	194	41	-1.0	680	130	-1
14	0.0	0.08	4.3	200	35	-1.0	680	130	-1
15	0.0	0.07	4.3	200	35	-1.0	680	130	-1
16	0.0	0.06	4.3	200	35	-1.0	680	130	-1
17	0.0	0.05	4.3	200	150	-1.0	880	130	-1
18	0.0	0.04	4.3	200	150	-1.0	880	130	-1
19	0.0	0.04	4.3	200	150	-1.0	880	130	-1
20	0.0	0.04	4.3	200	150	-1.0	880	130	-1
21	0.0	0.03	4.2	147	150	-1.0	880	130	-1
22	0.0	0.03	4.2	147	150	-1.0	880	130	-1
23	0.0	0.03	4.2	147	150	-1.0	880	130	-1

Street area 79 09 02 12:04

Time min	P mm/h	R l/s	pH	Cond mS/m	SS mg/l	Cd µg/l	Pb µg/l	Cu µg/l	Zn µg/l
1	5.8	0.00	4.3	110	220	-1.0	-1	-1	-1
2	12.9	0.03	4.3	110	220	-1.0	-1	-1	-1
3	12.6	0.19	4.3	110	220	-1.0	-1	-1	-1
4	2.6	0.56	4.4	88	140	-1.0	-1	-1	-1
5	9.1	1.20	4.4	88	140	-1.0	-1	-1	-1
6	9.1	2.16	4.4	88	140	-1.0	-1	-1	-1
7	0.0	2.08	4.4	84	73	-1.0	-1	-1	-1
8	0.0	1.64	4.4	84	73	-1.0	-1	-1	-1
9	0.0	1.11	4.4	84	73	-1.0	-1	-1	-1
10	0.0	0.70	4.4	84	73	-1.0	-1	-1	-1
11	0.0	0.53	4.8	85	100	-1.0	-1	-1	-1
12	0.0	0.41	4.8	85	100	-1.0	-1	-1	-1
13	0.0	0.32	4.8	85	100	-1.0	-1	-1	-1
14	0.0	0.25	4.8	94	69	-1.0	-1	-1	-1
15	0.0	0.20	4.8	94	69	-1.0	-1	-1	-1
16	0.0	0.16	4.8	94	69	-1.0	-1	-1	-1
17	0.0	0.14	4.8	94	69	-1.0	-1	-1	-1
18	0.0	0.12	4.8	94	69	-1.0	-1	-1	-1
19	0.0	0.09	4.8	94	69	-1.0	-1	-1	-1
20	0.0	0.07	4.8	94	69	-1.0	-1	-1	-1
21	0.0	0.06	4.7	110	110	-1.0	-1	-1	-1
22	0.0	0.07	4.7	110	110	-1.0	-1	-1	-1
23	0.0	0.06	4.7	110	110	-1.0	-1	-1	-1
24	0.0	0.05	4.8	105	150	-1.0	-1	-1	-1
25	0.0	0.04	4.8	105	150	-1.0	-1	-1	-1
26	0.0	0.04	4.8	105	150	-1.0	-1	-1	-1

Street area 79 09 11 09:30

Time min	P mm/h	R l/s	pH	Cond mS/m	SS mg/l	Cd µg/l	Pb µg/l	Cu µg/l	Zn µg/l
1	1.9	0.15	5.3	187	140	-1.0	620	80	-1
2	0.0	0.18	5.3	187	140	-1.0	620	80	-1
3	0.0	0.19	5.3	187	140	-1.0	620	80	-1
4	0.0	0.15	5.3	187	140	-1.0	620	80	-1
5	0.0	0.15	5.3	187	140	-1.0	620	80	-1
6	0.0	0.14	5.3	187	140	-1.0	620	80	-1
7	0.0	0.13	5.0	159	130	-1.0	580	91	-1
8	0.0	0.13	5.0	159	130	-1.0	580	91	-1
9	0.0	0.11	5.0	159	130	-1.0	580	91	-1
10	3.4	0.11	5.0	159	130	-1.0	580	91	-1
11	3.4	0.11	5.0	159	130	-1.0	580	91	-1
12	3.4	0.11	5.0	159	130	-1.0	580	91	-1
13	3.4	0.11	5.0	159	130	-1.0	580	91	-1
14	0.6	0.12	4.9	129	100	-1.0	550	88	-1
15	0.6	0.15	4.9	129	100	-1.0	550	88	-1
16	0.6	0.17	4.9	129	100	-1.0	550	88	-1
17	0.6	0.17	5.0	115	140	-1.0	530	85	-1
18	0.6	0.16	5.0	115	140	-1.0	530	85	-1
19	0.6	0.14	5.0	115	140	-1.0	530	85	-1
20	0.6	0.13	5.0	115	140	-1.0	530	85	-1
21	0.6	0.12	5.0	115	140	-1.0	530	85	-1
22	0.6	0.10	5.0	115	140	-1.0	530	85	-1
23	0.4	0.09	5.0	115	140	-1.0	530	85	-1

Street area 79 09 11 10:10

Time min	P mm/h	R l/s	pH	Cond mS/m	SS mg/l	Cd µg/l	Pb µg/l	Cu µg/l	Zn µg/l
1	0.4	0.01	5.2	92	86	-1.0	320	71	-1
2	0.4	0.01	5.2	92	86	-1.0	320	71	-1
3	0.4	0.01	5.2	92	86	-1.0	320	71	-1
4	0.0	0.01	5.2	92	86	-1.0	320	71	-1
5	0.0	0.01	5.2	92	86	-1.0	320	71	-1
6	0.0	0.01	5.2	92	86	-1.0	320	71	-1
7	0.0	0.01	5.5	70	130	-1.0	390	67	-1
8	0.0	0.01	5.5	70	130	-1.0	390	67	-1
9	0.0	0.02	5.5	70	130	-1.0	390	67	-1
10	0.0	0.01	5.5	70	130	-1.0	390	67	-1
11	0.3	0.01	5.5	58	99	-1.0	390	67	-1
12	0.3	0.01	5.5	58	99	-1.0	390	67	-1
13	0.3	0.01	5.5	58	99	-1.0	390	67	-1
14	0.3	0.01	5.6	51	81	-1.0	310	52	-1
15	0.3	0.01	5.6	51	81	-1.0	310	52	-1
16	0.3	0.01	5.6	51	81	-1.0	310	52	-1
17	0.3	0.01	5.7	46	94	-1.0	310	52	-1
18	0.0	0.01	5.7	46	94	-1.0	310	52	-1
19	0.0	0.01	5.7	46	94	-1.0	310	52	-1
20	0.0	0.01	5.7	46	94	-1.0	310	52	-1
21	0.0	0.01	5.8	42	92	-1.0	310	52	-1
22	0.0	0.00	5.8	42	92	-1.0	310	52	-1
23	0.0	0.01	5.8	42	92	-1.0	310	52	-1
24	2.1	0.01	5.8	42	92	-1.0	310	52	-1
25	2.1	0.01	5.8	42	92	-1.0	310	52	-1
26	2.1	0.01	5.8	42	92	-1.0	310	52	-1
27	2.1	0.01	5.8	42	92	-1.0	310	52	-1
28	2.1	0.02	5.8	42	92	-1.0	310	52	-1
29	2.8	0.03	5.8	42	92	-1.0	310	52	-1
30	2.8	0.09	5.8	42	92	-1.0	310	52	-1

Street area 79 09 17 17:37

Time min	P mm/h	R l/s	pH	Cond mS/m	SS mg/l	Cd µg/l	Pb µg/l	Cu µg/l	Zn µg/l
1	0.0	0.01	5.7	53	82	1.1	330	41	-1
2	0.0	0.01	5.7	53	82	1.1	330	41	-1
3	0.0	0.02	5.7	53	82	1.1	330	41	-1
4	0.0	0.03	5.7	53	82	1.1	330	41	-1
5	3.9	0.09	5.7	53	82	1.1	330	41	-1
6	4.2	0.19	5.7	53	82	1.1	330	41	-1
7	4.2	0.25	5.8	66	87	1.5	310	46	-1
8	5.7	0.24	5.8	66	87	1.5	310	46	-1
9	5.7	0.24	5.8	66	87	1.5	310	46	-1
10	2.2	0.25	5.8	66	87	1.5	310	46	-1
11	2.2	0.22	5.8	66	87	1.5	310	46	-1
12	1.1	0.18	5.8	66	87	1.5	310	46	-1
13	1.1	0.14	5.8	66	87	1.5	310	46	-1
14	1.2	0.15	6.0	49	72	1.5	280	36	-1
15	1.2	0.16	6.0	49	72	1.5	280	36	-1
16	1.9	0.17	6.0	49	72	1.5	280	36	-1
17	1.9	0.12	6.0	49	72	1.5	280	36	-1
18	1.9	0.07	6.0	49	72	1.5	280	36	-1
19	0.0	0.06	6.0	49	72	1.5	280	36	-1
20	0.0	0.06	6.0	49	72	1.5	280	36	-1
21	0.0	0.06	6.0	49	72	1.5	280	36	-1
22	0.0	0.05	6.0	49	72	1.5	280	36	-1
23	0.0	0.05	6.0	49	72	1.5	280	36	-1
24	0.0	0.04	6.0	49	72	1.5	280	36	-1
25	0.0	0.04	6.0	49	72	1.5	280	36	-1
26	0.0	0.03	6.0	49	72	1.5	280	36	-1

Street area 79 09 17 18:47

Time min	P mm/h	R l/s	pH	Cond mS/m	SS mg/l	Cd µg/l	Pb µg/l	Cu µg/l	Zn µg/l
1	1.5	0.02	5.9	45	99	1.3	270	46	-1
2	1.5	0.03	5.9	45	99	1.3	270	46	-1
3	1.5	0.03	5.9	45	99	1.3	270	46	-1
4	2.7	0.04	5.9	45	99	1.3	270	46	-1
5	2.7	0.07	5.9	45	99	1.3	270	46	-1
6	3.3	0.10	5.9	45	99	1.3	270	46	-1
7	3.3	0.12	6.0	38	63	0.7	310	34	-1
8	2.7	0.15	6.0	38	63	0.7	310	34	-1
9	2.7	0.18	6.0	38	63	0.7	310	34	-1
10	2.7	0.16	6.0	38	63	0.7	310	34	-1
11	0.8	0.14	6.0	38	63	0.7	310	34	-1
12	0.8	0.16	6.0	38	63	0.7	310	34	-1
13	0.8	0.15	6.0	38	63	0.7	310	34	-1
14	1.4	0.14	6.1	34	39	1.3	200	27	-1
15	1.4	0.12	6.1	34	39	1.3	200	27	-1
16	1.4	0.12	6.1	34	39	1.3	200	27	-1
17	0.5	0.11	6.1	34	39	1.3	200	27	-1
18	0.5	0.09	6.1	34	39	1.3	200	27	-1
19	0.5	0.07	6.1	34	39	1.3	200	27	-1
20	0.5	0.07	6.1	34	39	1.3	200	27	-1
21	0.5	0.07	6.1	34	39	1.3	200	27	-1
22	2.4	0.06	6.1	34	39	1.3	200	27	-1
23	2.4	0.05	6.1	34	39	1.3	200	27	-1
24	1.6	0.06	6.1	34	39	1.3	200	27	-1
25	0.5	0.07	6.1	34	39	1.3	200	27	-1
26	0.5	0.08	6.1	34	39	1.3	200	27	-1
27	0.5	0.09	6.1	34	39	1.3	200	27	-1
28	0.5	0.08	6.1	34	39	1.3	200	27	-1
29	0.5	0.08	6.1	34	39	1.3	200	27	-1
30	0.5	0.07	6.1	34	39	1.3	200	27	-1

Street area 79 10 31 19:16

Time min	P mm/h	R l/s	pH	Cond mS/m	SS mg/l	Cd µg/l	Pb µg/l	Cu µg/l	Zn µg/l
1	0.0	0.02	3.9	510	56	-1.0	1000	160	-1
2	0.0	0.04	3.9	510	56	-1.0	1000	160	-1
3	0.0	0.04	3.9	510	56	-1.0	1000	160	-1
4	0.0	0.06	3.9	510	56	-1.0	1000	160	-1
5	0.0	0.10	3.9	510	56	-1.0	1000	160	-1
6	0.0	0.11	3.9	510	56	-1.0	1000	160	-1
7	0.0	0.15	5.2	360	54	-1.0	920	130	-1
8	0.0	0.22	5.2	360	54	-1.0	920	130	-1
9	0.0	0.25	5.2	360	54	-1.0	920	130	-1
10	0.0	0.27	5.2	360	54	-1.0	920	130	-1
11	0.0	0.28	5.2	308	42	-1.0	800	110	-1
12	0.0	0.32	5.2	308	42	-1.0	800	110	-1
13	0.0	0.35	5.2	308	42	-1.0	800	110	-1
14	0.0	0.36	5.3	248	37	-1.0	700	99	-1
15	0.0	0.36	5.3	248	37	-1.0	700	99	-1
16	0.0	0.37	5.3	248	37	-1.0	700	99	-1
17	0.0	0.37	5.2	195	33	-1.0	620	89	-1
18	0.0	0.43	5.2	195	33	-1.0	620	89	-1
19	0.0	0.48	5.2	195	33	-1.0	620	89	-1
20	0.0	0.47	5.2	195	33	-1.0	620	89	-1
21	0.0	0.46	5.3	155	27	-1.0	510	69	-1
22	0.0	0.46	5.3	155	27	-1.0	510	69	-1
23	0.0	0.46	5.3	155	27	-1.0	510	69	-1
24	0.0	0.45	5.6	128	66	-1.0	560	68	-1
25	0.0	0.44	5.6	128	66	-1.0	560	68	-1
26	0.0	0.44	5.6	128	66	-1.0	560	68	-1
27	0.0	0.41	5.6	128	66	-1.0	560	68	-1
28	0.0	0.36	5.6	128	66	-1.0	560	68	-1
29	0.0	0.35	5.6	128	66	-1.0	560	68	-1
30	0.0	0.34	5.6	128	66	-1.0	560	68	-1

Street area 79 11 06 00:05

Time min	P mm/h	R l/s	pH	Cond mS/m	SS mg/l	Cd µg/l	Pb µg/l	Cu µg/l	Zn µg/l
1	4.3	0.0	5.9	130	890	-1.0	-1	-1	-1
2	7.2	0.00	5.9	130	890	-1.0	-1	-1	-1
3	10.2	0.01	5.9	130	890	-1.0	-1	-1	-1
4	10.2	0.04	5.9	130	890	-1.0	-1	-1	-1
5	10.2	0.09	5.9	130	890	-1.0	-1	-1	-1
6	9.1	0.84	5.9	130	890	-1.0	-1	-1	-1
7	9.1	2.00	5.9	73	570	-1.0	-1	-1	-1
8	6.0	2.77	5.9	73	570	-1.0	-1	-1	-1
9	6.0	3.18	5.9	73	570	-1.0	-1	-1	-1
10	6.0	3.36	5.9	73	570	-1.0	-1	-1	-1
11	4.4	3.36	5.9	73	570	-1.0	-1	-1	-1
12	4.4	3.39	5.9	73	570	-1.0	-1	-1	-1
13	9.2	3.47	5.9	73	570	-1.0	-1	-1	-1
14	9.2	3.52	4.1	62	120	-1.0	-1	-1	-1
15	9.2	3.47	4.1	62	120	-1.0	-1	-1	-1
16	1.2	3.41	4.1	62	120	-1.0	-1	-1	-1
17	1.2	3.05	4.1	62	120	-1.0	-1	-1	-1
18	1.2	2.71	4.1	62	120	-1.0	-1	-1	-1
19	1.2	2.44	4.1	62	120	-1.0	-1	-1	-1
20	8.3	2.15	4.1	62	120	-1.0	-1	-1	-1
21	8.3	2.01	4.1	62	120	-1.0	-1	-1	-1
22	8.3	2.00	4.1	62	120	-1.0	-1	-1	-1
23	5.0	2.05	4.1	62	120	-1.0	-1	-1	-1
24	5.0	2.26	6.4	17	100	-1.0	-1	-1	-1
25	5.0	2.39	6.4	17	100	-1.0	-1	-1	-1
26	5.0	2.30	6.4	17	100	-1.0	-1	-1	-1
27	5.0	2.16	6.4	17	100	-1.0	-1	-1	-1
28	1.4	2.03	6.4	17	100	-1.0	-1	-1	-1
29	1.4	1.86	6.4	17	100	-1.0	-1	-1	-1
30	1.4	1.71	6.4	17	100	-1.0	-1	-1	-1
31	1.3	1.60	4.2	48	81	-1.0	-1	-1	-1
32	1.3	1.44	4.2	48	81	-1.0	-1	-1	-1
33	1.3	1.22	4.2	48	81	-1.0	-1	-1	-1
34	1.3	1.04	4.2	48	81	-1.0	-1	-1	-1
35	0.0	0.80	4.2	48	81	-1.0	-1	-1	-1
36	0.0	0.67	4.2	48	81	-1.0	-1	-1	-1
37	0.0	0.68	3.5	132	89	-1.0	-1	-1	-1
38	0.0	0.66	3.5	132	89	-1.0	-1	-1	-1
39	0.0	0.57	3.5	132	89	-1.0	-1	-1	-1
40	0.0	0.49	3.5	132	89	-1.0	-1	-1	-1
41	0.8	0.46	3.5	132	89	-1.0	-1	-1	-1
42	0.8	0.45	3.5	132	89	-1.0	-1	-1	-1
43	0.8	0.43	3.5	132	89	-1.0	-1	-1	-1
44	0.8	0.40	3.7	102	77	-1.0	-1	-1	-1
45	0.8	0.36	3.7	102	77	-1.0	-1	-1	-1

Street area 79 11 06 00:05

Time min	P mm/h	R l/s	pH	Cond mS/m	SS mg/l	Cd µg/l	Pb µg/l	Cu µg/l	Zn µg/l
46	0.8	0.35	3.7	102	77	-1.0	-1	-1	-1
47	0.9	0.34	3.7	102	77	-1.0	-1	-1	-1
48	0.9	0.34	3.7	102	77	-1.0	-1	-1	-1
49	0.9	0.34	3.7	102	77	-1.0	-1	-1	-1
50	0.9	0.34	3.7	102	77	-1.0	-1	-1	-1
51	0.9	0.34	3.9	82	140	-1.0	-1	-1	-1
52	0.4	0.35	3.9	82	140	-1.0	-1	-1	-1
53	0.4	0.35	3.9	82	140	-1.0	-1	-1	-1
54	0.4	0.35	3.9	82	140	-1.0	-1	-1	-1
55	0.4	0.34	3.9	82	140	-1.0	-1	-1	-1
56	0.4	0.34	3.9	82	140	-1.0	-1	-1	-1
57	0.4	0.34	6.2	34	130	-1.0	-1	-1	-1
58	0.4	0.27	6.2	34	130	-1.0	-1	-1	-1
59	1.4	0.21	6.2	34	130	-1.0	-1	-1	-1
60	1.4	0.21	6.2	34	130	-1.0	-1	-1	-1
61	1.4	0.21	6.2	34	130	-1.0	-1	-1	-1
62	1.4	0.25	6.2	34	130	-1.0	-1	-1	-1
63	1.4	0.27	6.2	34	130	-1.0	-1	-1	-1
64	1.8	0.28	6.2	34	130	-1.0	-1	-1	-1
65	1.8	0.30	6.2	34	130	-1.0	-1	-1	-1
66	1.4	0.34	6.2	34	130	-1.0	-1	-1	-1
67	1.4	0.39	6.4	34	120	-1.0	-1	-1	-1
68	1.4	0.44	6.4	34	120	-1.0	-1	-1	-1
69	1.4	0.48	6.4	34	120	-1.0	-1	-1	-1
70	0.5	0.48	6.4	34	120	-1.0	-1	-1	-1
71	0.5	0.44	6.4	34	120	-1.0	-1	-1	-1
72	0.5	0.41	6.4	34	120	-1.0	-1	-1	-1
73	0.5	0.44	6.4	34	120	-1.0	-1	-1	-1
74	0.5	0.47	4.3	60	250	-1.0	-1	-1	-1
75	0.5	0.48	4.3	60	250	-1.0	-1	-1	-1
76	0.5	0.52	4.3	60	250	-1.0	-1	-1	-1
77	0.5	0.63	4.3	60	250	-1.0	-1	-1	-1
78	0.5	0.65	4.3	60	250	-1.0	-1	-1	-1
79	5.5	0.64	4.3	60	250	-1.0	-1	-1	-1
80	5.5	0.70	4.3	60	250	-1.0	-1	-1	-1

Street area 79 11 16 07:47

Time min	P mm/h	R l/s	pH	Cond mS/m	SS mg/l	Cd µg/l	Pb µg/l	Cu µg/l	Zn µg/l
1	1.7	0.70	5.6	36	280	1.3	720	81	-1
2	1.7	0.66	5.6	36	280	1.3	720	81	-1
3	2.4	0.65	5.6	36	280	1.3	720	81	-1
4	2.4	0.69	5.6	36	280	1.3	720	81	-1
5	2.4	0.75	5.6	36	280	1.3	720	81	-1
6	2.4	0.82	5.6	36	280	1.3	720	81	-1
7	2.4	0.86	5.6	36	280	1.3	720	81	-1
8	2.4	0.91	5.6	36	280	1.3	720	81	-1
9	2.4	0.90	5.6	36	280	1.3	720	81	-1
10	1.7	0.76	5.6	36	280	1.3	720	81	-1
11	1.7	0.90	6.4	29	290	1.6	770	78	-1
12	1.7	0.91	6.4	29	290	1.6	770	78	-1
13	1.7	0.87	6.4	29	290	1.6	770	78	-1
14	1.7	0.87	6.4	29	290	1.6	770	78	-1
15	1.7	0.87	6.4	29	290	1.6	770	78	-1
16	1.5	0.84	6.4	29	290	1.6	770	78	-1
17	1.5	0.83	6.4	29	290	1.6	770	78	-1
18	1.5	0.85	6.4	29	290	1.6	770	78	-1
19	0.8	0.85	6.4	29	290	1.6	770	78	-1
20	0.8	0.83	6.4	29	290	1.6	770	78	-1
21	0.8	0.80	4.0	62	300	1.6	770	78	-1
22	0.8	0.92	4.0	62	300	1.6	770	78	-1
23	0.8	0.97	4.0	62	300	1.6	770	78	-1
24	0.8	1.00	4.0	62	300	1.6	770	78	-1
25	2.3	0.98	4.0	62	300	1.6	770	78	-1
26	2.3	0.90	4.0	62	300	1.6	770	78	-1
27	2.3	0.94	4.0	62	300	1.6	770	78	-1
28	2.3	0.90	4.0	62	300	1.6	770	78	-1
29	2.3	0.82	4.0	62	300	1.6	770	78	-1
30	2.3	0.95	4.0	62	300	1.6	770	78	-1
31	0.2	0.85	6.3	28	220	1.3	490	64	-1
32	1.9	0.94	6.3	28	220	1.3	490	64	-1
33	1.9	0.99	6.3	28	220	1.3	490	64	-1
34	1.9	0.93	6.3	28	220	1.3	490	64	-1
35	1.9	1.03	6.3	28	220	1.3	490	64	-1
36	1.9	0.95	6.3	28	220	1.3	490	64	-1
37	1.9	0.88	6.3	28	220	1.3	490	64	-1
38	1.9	0.88	6.3	28	220	1.3	490	64	-1
39	1.4	0.93	6.3	28	220	1.3	490	64	-1
40	1.4	0.95	6.3	28	220	1.3	490	64	-1
41	1.4	0.95	4.7	32	210	1.3	490	64	-1
42	2.3	0.94	4.7	32	210	1.3	490	64	-1
43	2.3	0.93	4.7	32	210	1.3	490	64	-1
44	2.3	0.93	4.7	32	210	1.3	490	64	-1
45	2.3	0.93	4.7	32	210	1.3	490	64	-1

Street area 79 11 16 07:47

Time min	P mm/h	R l/s	pH	Cond mS/m	SS mg/l	Cd µg/l	Pb µg/l	Cu µg/l	Zn µg/l
46	2.3	0.94	4.7	32	210	1.3	490	64	-1
47	3.5	0.96	4.3	37	180	1.3	490	64	-1
48	3.5	0.98	4.3	37	180	1.3	490	64	-1
49	3.5	1.09	4.3	37	180	1.3	490	64	-1
50	3.5	1.12	4.3	37	180	1.3	490	64	-1
51	3.5	1.11	4.3	37	180	1.3	490	64	-1
52	2.1	1.15	4.3	37	180	1.3	490	64	-1
53	2.1	1.19	4.3	37	180	1.3	490	64	-1
54	2.1	1.19	6.3	18	210	1.3	490	64	-1
55	5.5	1.20	6.3	18	210	1.3	490	64	-1
56	5.5	1.26	6.3	18	210	1.3	490	64	-1
57	5.5	1.31	6.3	18	210	1.3	490	64	-1
58	4.5	1.35	6.3	18	210	1.3	490	64	-1
59	4.5	1.46	6.3	18	210	1.3	490	64	-1
60	4.5	1.63	6.3	18	210	1.3	490	64	-1
61	4.1	1.81	3.8	56	130	0.9	270	30	-1
62	4.1	1.89	3.8	56	130	0.9	270	30	-1
63	4.1	1.99	3.8	56	130	0.9	270	30	-1
64	2.8	1.92	3.8	56	130	0.9	270	30	-1
65	2.8	1.71	3.8	56	130	0.9	270	30	-1
66	2.8	1.69	3.8	56	130	0.9	270	30	-1
67	4.0	1.59	6.3	14	115	0.9	270	30	-1
68	4.0	1.54	6.3	14	115	0.9	270	30	-1
69	4.0	1.57	6.3	14	115	0.9	270	30	-1
70	4.0	1.60	6.3	14	115	0.9	270	30	-1
71	4.0	1.70	6.3	14	115	0.9	270	30	-1
72	2.9	1.83	6.3	14	115	0.9	270	30	-1
73	2.9	1.80	6.3	14	115	0.9	270	30	-1
74	2.9	1.72	6.3	18	120	0.9	270	30	-1
75	2.9	1.75	6.3	18	120	0.9	270	30	-1
76	4.4	1.76	6.3	18	120	0.9	270	30	-1
77	4.4	1.59	6.3	18	120	0.9	270	30	-1
78	4.4	1.45	6.3	18	120	0.9	270	30	-1
79	4.4	1.43	6.3	18	120	0.9	270	30	-1
80	4.4	1.42	6.3	18	120	0.9	270	30	-1

Street area 79 11 26 07:48

Time min	P mm/h	R l/s	pH	Cond mS/m	SS mg/l	Cd µg/l	Pb µg/l	Cu µg/l	Zn µg/l
1	3.7	0.52	6.5	23	156	2.1	370	54	-1
2	0.0	0.50	6.5	23	156	2.1	370	54	-1
3	0.0	0.49	6.5	23	156	2.1	370	54	-1
4	0.0	0.49	6.5	23	156	2.1	370	54	-1
5	0.0	0.49	6.5	23	156	2.1	370	54	-1
6	10.1	0.49	6.5	23	156	2.1	370	54	-1
7	10.1	0.47	6.5	23	156	2.1	370	54	-1
8	2.4	0.45	6.5	23	156	2.1	370	54	-1
9	2.4	0.49	6.5	23	156	2.1	370	54	-1
10	2.4	0.48	6.5	23	156	2.1	370	54	-1
11	2.4	0.47	6.5	23	156	2.1	370	54	-1
12	2.4	0.47	6.5	23	156	2.1	370	54	-1
13	1.6	0.45	6.5	23	156	2.1	370	54	-1
14	1.6	0.42	6.5	23	156	2.1	370	54	-1
15	1.6	0.43	6.5	23	156	2.1	370	54	-1
16	1.6	0.45	6.5	23	156	2.1	370	54	-1
17	1.6	0.46	6.5	21	163	1.5	410	59	-1
18	1.6	0.47	6.5	21	163	1.5	410	59	-1
19	1.6	0.47	6.5	21	163	1.5	410	59	-1
20	1.6	0.47	6.5	21	163	1.5	410	59	-1
21	6.0	0.47	6.5	21	163	1.5	410	59	-1
22	3.7	0.47	6.5	21	163	1.5	410	59	-1
23	3.7	0.45	6.5	21	163	1.5	410	59	-1
24	3.7	0.42	6.5	21	163	1.5	410	59	-1
25	3.7	0.44	6.5	21	163	1.5	410	59	-1
26	1.5	0.45	6.5	21	163	1.5	410	59	-1
27	1.5	0.46	6.6	23	155	1.5	410	59	-1
28	1.5	0.45	6.6	23	155	1.5	410	59	-1
29	2.3	0.41	6.6	23	155	1.5	410	59	-1
30	2.3	0.35	6.6	23	155	1.5	410	59	-1
31	2.3	0.34	6.6	23	155	1.5	410	59	-1
32	3.7	0.34	6.6	23	155	1.5	410	59	-1
33	3.7	0.33	6.6	23	155	1.5	410	59	-1
34	3.7	0.32	6.6	23	155	1.5	410	59	-1
35	3.7	0.35	6.6	23	155	1.5	410	59	-1
36	0.6	0.37	6.6	23	155	1.5	410	59	-1
37	0.6	0.35	6.6	23	155	1.5	410	59	-1
38	0.6	0.33	6.6	23	155	1.5	410	59	-1
39	0.6	0.31	6.6	23	155	1.5	410	59	-1
40	3.1	0.30	6.6	23	155	1.5	410	59	-1
41	3.1	0.29	6.6	24	113	1.3	370	49	-1
42	3.1	0.28	6.6	24	113	1.3	370	49	-1
43	3.1	0.28	6.6	24	113	1.3	370	49	-1
44	1.3	0.28	6.6	24	113	1.3	370	49	-1
45	1.3	0.28	6.6	24	113	1.3	370	49	-1

Street area 79 11 26 07:48

Time min	P mm/h	R l/s	pH	Cond mS/m	SS mg/l	Cd µg/l	Pb µg/l	Cu µg/l	Zn µg/l
46	1.3	0.27	6.6	24	113	1.3	370	49	-1
47	1.3	0.27	6.5	25	113	1.3	370	49	-1
48	1.4	0.26	6.5	25	113	1.3	370	49	-1
49	1.4	0.25	6.5	25	113	1.3	370	49	-1
50	1.4	0.26	6.5	25	113	1.3	370	49	-1
51	1.4	0.26	6.5	25	113	1.3	370	49	-1
52	1.4	0.25	6.5	25	113	1.3	370	49	-1
53	1.5	0.26	6.5	25	113	1.3	370	49	-1
54	1.5	0.25	6.5	25	113	1.3	370	49	-1
55	1.5	0.23	6.5	25	113	1.3	370	49	-1
56	1.5	0.23	6.5	25	113	1.3	370	49	-1
57	1.5	0.23	6.5	25	113	1.3	370	49	-1
58	1.5	0.23	6.5	25	113	1.3	370	49	-1
59	1.5	0.23	6.5	25	113	1.3	370	49	-1
60	1.2	0.23	6.5	25	113	1.3	370	49	-1
61	1.2	0.23	6.6	26	102	1.3	320	43	-1
62	1.2	0.24	6.6	26	102	1.3	320	43	-1
63	1.2	0.25	6.6	26	102	1.3	320	43	-1
64	2.1	0.24	6.6	26	102	1.3	320	43	-1
65	2.1	0.23	6.6	26	102	1.3	320	43	-1
66	2.1	0.21	6.6	26	102	1.3	320	43	-1
67	2.1	0.21	6.6	26	102	1.3	320	43	-1
68	0.9	0.22	6.6	26	102	1.3	320	43	-1
69	0.9	0.23	6.6	26	102	1.3	320	43	-1
70	0.9	0.23	6.6	26	102	1.3	320	43	-1
71	0.9	0.23	6.5	27	94	1.3	320	43	-1
72	0.9	0.24	6.5	27	94	1.3	320	43	-1
73	0.0	0.23	6.5	27	94	1.3	320	43	-1
74	0.0	0.22	6.5	27	94	1.3	320	43	-1
75	0.0	0.18	6.5	27	94	1.3	320	43	-1
76	0.0	0.19	6.5	27	94	1.3	320	43	-1
77	0.0	0.21	6.5	27	94	1.3	320	43	-1
78	2.9	0.21	6.5	27	94	1.3	320	43	-1
79	2.9	0.20	6.5	27	94	1.3	320	43	-1
80	2.9	0.19	6.5	27	94	1.3	320	43	-1

Street area 80 06 02 22:15

Time min	P mm/h	R l/s	pH	Cond mS/m	SS mg/l	Cd µg/l	Pb µg/l	Cu µg/l	Zn µg/l
1	0.7	0.09	5.7	230	260	5.4	320	170	-1
2	3.5	0.11	5.7	230	260	5.4	320	170	-1
3	3.5	0.12	5.7	230	260	5.4	320	170	-1
4	3.5	0.12	5.7	230	260	5.4	320	170	-1
5	0.0	0.16	5.7	230	260	5.4	320	170	-1
6	0.0	0.26	5.7	230	260	5.4	320	170	-1
7	12.6	0.37	5.7	230	260	5.4	320	170	-1
8	4.2	0.47	6.0	110	132	2.4	280	80	-1
9	1.0	0.57	6.0	110	132	2.4	280	80	-1
10	1.0	0.64	6.0	110	132	2.4	280	80	-1
11	1.0	0.60	6.0	110	132	2.4	280	80	-1
12	0.6	0.51	6.0	110	132	2.4	280	80	-1
13	0.6	0.39	6.0	110	132	2.4	280	80	-1
14	0.6	0.30	6.0	110	132	2.4	280	80	-1
15	0.6	0.27	6.0	110	132	2.4	280	80	-1

Street area 80 08 16 22:21

Time min	P mm/h	R l/s	pH	Cond mS/m	SS mg/l	Cd µg/l	Pb µg/l	Cu µg/l	Zn µg/l
1	0.0	0.00	4.8	40	-1	2.0	185	59	-1
2	0.0	0.01	4.8	40	-1	2.0	185	59	-1
3	16.6	0.33	4.8	40	-1	2.0	185	59	-1
4	16.6	1.04	4.8	40	-1	2.0	185	59	-1
5	0.0	1.62	4.8	40	-1	2.0	185	59	-1
6	0.0	2.04	4.9	26	-1	1.5	160	38	-1
7	0.0	1.87	4.9	26	-1	1.5	160	38	-1
8	0.0	1.69	4.9	26	-1	1.5	160	38	-1
9	0.0	1.51	4.9	26	-1	1.5	160	38	-1
10	0.0	1.36	4.9	26	-1	1.5	160	38	-1
11	0.8	1.20	5.1	18	-1	0.9	130	25	-1
12	0.8	1.05	5.1	18	-1	0.9	130	25	-1
13	0.8	0.89	5.1	18	-1	0.9	130	25	-1
14	0.8	0.75	5.1	18	-1	0.9	130	25	-1
15	0.8	0.63	5.1	18	-1	0.9	130	25	-1
16	0.0	0.63	5.1	18	-1	0.9	130	25	-1
17	0.0	0.54	5.1	18	-1	0.9	130	25	-1
18	0.0	0.46	5.3	12	-1	1.9	95	17	-1
19	0.0	0.43	5.3	12	-1	1.9	95	17	-1
20	0.0	0.41	5.3	12	-1	1.9	95	17	-1
21	0.5	0.38	5.3	12	-1	1.9	95	17	-1
22	0.5	0.35	5.3	12	-1	1.9	95	17	-1
23	0.5	0.31	5.3	12	-1	1.9	95	17	-1
24	0.5	0.27	5.3	12	-1	1.9	95	17	-1
25	0.5	0.24	5.3	12	-1	1.9	95	17	-1
26	0.5	0.23	5.3	12	-1	1.9	95	17	-1
27	0.5	0.24	5.3	12	-1	1.9	95	17	-1
28	0.5	0.25	5.3	14	-1	1.5	77	14	-1
29	0.8	0.25	5.3	14	-1	1.5	77	14	-1
30	0.8	0.27	5.3	14	-1	1.5	77	14	-1
31	0.8	0.29	5.3	14	-1	1.5	77	14	-1
32	0.8	0.29	5.3	14	-1	1.5	77	14	-1
33	0.8	0.29	5.3	14	-1	1.5	77	14	-1
34	0.8	0.30	5.3	14	-1	1.5	77	14	-1
35	0.6	0.33	5.3	14	-1	1.5	77	14	-1
36	0.6	0.33	5.3	14	-1	1.5	77	14	-1
37	0.6	0.33	5.3	14	-1	1.5	77	14	-1
38	0.6	0.34	5.5	12	-1	1.2	100	14	-1
39	0.6	0.32	5.5	12	-1	1.2	100	14	-1
40	0.6	0.27	5.5	12	-1	1.2	100	14	-1
41	0.6	0.27	5.5	12	-1	1.2	100	14	-1
42	0.7	0.27	5.5	12	-1	1.2	100	14	-1
43	0.7	0.27	5.5	12	-1	1.2	100	14	-1
44	0.7	0.26	5.5	12	-1	1.2	100	14	-1
45	0.7	0.23	5.5	12	-1	1.2	100	14	-1
46	0.7	0.21	5.5	12	-1	1.2	100	14	-1
47	0.7	0.19	5.5	12	-1	1.2	100	14	-1

Street area 80 08 28 20:32

Time min	P mm/h	R l/s	pH	Cond mS/m	SS mg/l	Cd µg/l	Pb µg/l	Cu µg/l	Zn µg/l
1	2.9	0.24	3.4	160	47	4.7	820	113	-1
2	2.9	0.24	3.4	160	47	4.7	820	113	-1
3	2.9	0.25	3.4	160	47	4.7	820	113	-1
4	2.9	0.26	3.4	160	47	4.7	820	113	-1
5	2.9	0.23	3.4	160	47	4.7	820	113	-1
6	2.9	0.20	3.4	160	47	4.7	820	113	-1
7	1.1	0.18	3.4	160	47	4.7	820	113	-1
8	1.1	0.17	3.4	220	60	5.1	1100	128	-1
9	1.1	0.20	3.4	220	60	5.1	1100	128	-1
10	1.1	0.22	3.4	220	60	5.1	1100	128	-1
11	0.0	0.20	3.4	220	60	5.1	1100	128	-1
12	0.0	0.20	3.4	220	60	5.1	1100	128	-1
13	1.4	0.22	3.5	170	48	3.5	790	95	-1
14	1.4	0.19	3.5	170	48	3.5	790	95	-1
15	1.4	0.18	3.5	170	48	3.5	790	95	-1
16	1.6	0.17	3.5	170	48	3.5	790	95	-1
17	1.6	0.16	3.5	170	48	3.5	790	95	-1
18	1.6	0.16	3.6	150	27	3.5	560	88	-1
19	0.0	0.15	3.6	150	27	3.5	560	88	-1
20	0.0	0.14	3.6	150	27	3.5	560	88	-1
21	0.0	0.14	3.6	150	27	3.5	560	88	-1
22	0.0	0.13	3.6	150	27	3.5	560	88	-1

Street area 80 09 17 14:39

Time min	P mm/h	R l/s	pH	Cond mS/m	SS mg/l	Cd µg/l	Pb µg/l	Cu µg/l	Zn µg/l
1	0.8	0.05	4.8	150	196	3.9	450	98	-1
2	0.8	0.07	4.8	150	196	3.9	450	98	-1
3	3.1	0.07	4.8	150	196	3.9	450	98	-1
4	3.1	0.09	4.8	150	196	3.9	450	98	-1
5	3.1	0.12	4.8	150	196	3.9	450	98	-1
6	0.0	0.14	5.0	120	146	4.2	415	79	-1
7	0.0,	0.18	5.0	120	146	4.2	415	79	-1
8	2.4	0.21	5.0	120	146	4.2	415	79	-1
9	2.4	0.30	5.0	120	146	4.2	415	79	-1
10	1.8	0.46	5.0	120	146	4.2	415	79	-1
11	1.8	0.58	5.1	840	132	2.8	430	67	-1
12	1.8	0.62	5.1	840	132	2.8	430	67	-1
13	1.8	0.67	5.1	840	132	2.8	430	67	-1
14	1.8	0.77	5.1	840	132	2.8	430	67	-1
15	2.6	0.78	5.1	840	132	2.8	430	67	-1
16	2.6	0.80	5.2	650	122	2.3	360	57	-1
17	2.6	0.85	5.2	650	122	2.3	360	57	-1
18	2.6	0.97	5.2	650	122	2.3	360	57	-1
19	2.6	1.16	5.2	650	122	2.3	360	57	-1
20	2.6	1.19	5.2	650	122	2.3	360	57	-1
21	3.3	1.14	5.2	480	114	2.3	340	48	-1
22	3.3	1.12	5.2	480	114	2.3	340	48	-1
23	3.3	1.12	5.2	480	114	2.3	340	48	-1
24	3.3	1.12	5.2	480	114	2.3	340	48	-1
25	3.7	1.13	5.2	480	114	2.3	340	48	-1
26	3.7	1.14	5.2	480	114	2.3	340	48	-1
27	3.7	1.15	5.2	480	114	2.3	340	48	-1
28	3.7	1.17	5.3	290	86	1.4	250	37	-1
29	3.8	1.22	5.3	290	86	1.4	250	37	-1
30	3.8	1.27	5.3	290	86	1.4	250	37	-1
31	3.8	1.32	5.3	290	86	1.4	250	37	-1
32	3.8	1.38	5.3	290	86	1.4	250	37	-1
33	3.8	1.43	5.3	290	86	1.4	250	37	-1
34	10.4	1.61	5.3	290	86	1.4	250	37	-1
35	10.4	1.81	5.3	290	86	1.4	250	37	-1
36	10.4	2.01	5.3	290	86	1.4	250	37	-1
37	10.4	2.23	5.3	290	86	1.4	250	37	-1
38	10.4	2.30	5.5	290	78	1.8	240	53	-1
39	3.3	2.30	5.5	290	78	1.8	240	53	-1
40	3.3	2.31	5.5	290	78	1.8	240	53	-1
41	3.3	2.34	5.5	290	78	1.8	240	53	-1
42	3.3	2.37	5.5	290	78	1.8	240	53	-1
43	2.3	2.40	5.5	290	78	1.8	240	53	-1
44	2.3	2.54	5.5	290	78	1.8	240	53	-1
45	2.3	2.69	5.5	290	78	1.8	240	53	-1

Street area 80 09 17 14:39

Time min	P mm/h	R l/s	pH	Cond mS/m	SS mg/l	Cd µg/l	Pb µg/l	Cu µg/l	Zn µg/l
46	2.3	2.54	5.5	290	78	1.8	240	53	-1
47	2.3	2.42	5.5	290	78	1.8	240	53	-1
48	2.3	2.34	5.6	270	68	1.7	230	42	-1
49	2.3	2.26	5.6	270	68	1.7	230	42	-1
50	4.4	2.17	5.6	270	68	1.7	230	42	-1
51	4.4	2.08	5.6	270	68	1.7	230	42	-1
52	4.4	2.00	5.6	270	68	1.7	230	42	-1
53	4.4	1.91	5.6	270	68	1.7	230	42	-1
54	4.6	1.83	5.6	270	68	1.7	230	42	-1
55	4.6	1.75	5.6	270	68	1.7	230	42	-1
56	4.6	1.68	5.6	270	68	1.7	230	42	-1
57	2.6	1.87	5.6	270	68	1.7	230	42	-1
58	2.6	2.03	5.6	270	68	1.7	230	42	-1
59	2.6	2.05	5.6	270	68	1.7	230	42	-1
60	2.6	2.07	5.6	270	68	1.7	230	42	-1
61	2.6	1.88	5.0	415	63	1.9	330	52	-1
62	2.6	1.80	5.0	415	63	1.9	330	52	-1
63	2.6	1.78	5.0	415	63	1.9	330	52	-1
64	2.6	1.77	5.0	415	63	1.9	330	52	-1
65	2.6	1.75	5.0	415	63	1.9	330	52	-1
66	2.6	1.73	5.0	415	63	1.9	330	52	-1
67	2.8	1.68	5.0	415	63	1.9	330	52	-1
68	2.8	1.60	5.0	415	63	1.9	330	52	-1
69	2.8	1.53	5.0	415	63	1.9	330	52	-1
70	2.8	1.49	5.0	415	63	1.9	330	52	-1
71	2.8	1.46	5.0	415	63	1.9	330	52	-1
72	1.7	1.48	5.0	415	63	1.9	330	52	-1
73	1.7	1.52	5.0	415	63	1.9	330	52	-1
74	1.7	1.62	5.0	415	63	1.9	330	52	-1
75	1.7	1.59	5.0	415	63	1.9	330	52	-1
76	1.7	1.52	5.4	340	77	2.3	310	65	-1
77	4.9	1.64	5.4	340	77	2.3	310	65	-1
78	4.9	1.62	5.4	340	77	2.3	310	65	-1
79	4.9	1.55	5.4	340	77	2.3	310	65	-1
80	4.9	1.62	5.4	340	77	2.3	310	65	-1
81	1.5	1.72	5.4	340	77	2.3	310	65	-1
82	1.5	1.83	5.4	340	77	2.3	310	65	-1
83	1.5	1.89	5.4	340	77	2.3	310	65	-1
84	1.5	1.69	5.4	340	77	2.3	310	65	-1
85	1.5	1.62	5.4	340	77	2.3	310	65	-1
86	1.5	1.57	5.4	340	77	2.3	310	65	-1
87	1.5	1.53	5.4	340	77	2.3	310	65	-1
88	0.0	1.50	5.4	340	77	2.3	310	65	-1
89	0.0	1.47	5.4	340	77	2.3	310	65	-1
90	0.0	1.44	5.4	340	77	2.3	310	65	-1

Street area 80 09 17 14:39

Time min	P mm/h	R l/s	pH	Cond mS/m	SS mg/l	Cd µg/l	Pb µg/l	Cu µg/l	Zn µg/l
91	0.0	1.44	5.4	340	72	2.3	340	42	-1
92	0.0	1.42	5.4	340	72	2.3	340	42	-1
93	0.0	1.36	5.4	340	72	2.3	340	42	-1
94	0.0	1.32	5.4	340	72	2.3	340	42	-1
95	0.0	1.31	5.4	340	72	2.3	340	42	-1
96	0.0	1.23	5.4	340	72	2.3	340	42	-1
97	7.4	1.22	5.4	340	72	2.3	340	42	-1
98	7.4	1.27	5.4	340	72	2.3	340	42	-1
99	1.2	1.33	5.4	340	72	2.3	340	42	-1
100	1.2	1.44	5.4	340	72	2.3	340	42	-1
101	1.2	1.49	5.4	340	72	2.3	340	42	-1
102	1.2	1.54	5.4	340	72	2.3	340	42	-1
103	1.2	1.59	5.6	400	65	3.3	240	47	-1
104	1.2	1.65	5.6	400	65	3.3	240	47	-1
105	1.2	1.64	5.6	400	65	3.3	240	47	-1
106	1.2	1.57	5.6	400	65	3.3	240	47	-1
107	0.0	1.51	5.6	400	65	3.3	240	47	-1
108	0.0	1.41	5.6	400	65	3.3	240	47	-1
109	0.0	1.43	5.6	400	65	3.3	240	47	-1
110	0.0	1.43	5.6	400	65	3.3	240	47	-1
111	0.0	1.17	5.6	400	65	3.3	240	47	-1
112	0.0	1.24	5.6	400	65	3.3	240	47	-1
113	0.0	1.32	5.6	400	65	3.3	240	47	-1
114	0.0	1.40	5.6	400	65	3.3	240	47	-1
115	3.0	1.35	5.6	400	65	3.3	240	47	-1
116	3.0	1.22	5.6	400	65	3.3	240	47	-1
117	3.0	1.16	5.6	400	65	3.3	240	47	-1
118	3.0	1.10	5.6	400	65	3.3	240	47	-1
119	3.0	1.03	5.6	400	65	3.3	240	47	-1
120	2.1	0.97	5.6	400	65	3.3	240	47	-1

Appendix 2.1 Street area total and dissolved concentrations for observed storms

Date	Time fr. start min.	Pb Tot. µg/l	Pb Dis. µg/l	Cu Tot. µg/l	Cu Dis. µg/l	Cd Tot. µg/l	Cd Dis. µg/l	pH
17SEP79	3.0	330	52	41	17	1.1	-	5.7
17SEP79	10.0	310	58	46	25	1.5	1.4	5.8
17SEP79	20.0	280	43	36	16	1.5	1.0	6.0
17SEP79	-	270	65	46	16	1.3	-	5.9
17SEP79	-	310	64	34	13	0.7	-	6.1
17SEP79	-	200	42	27	9	1.3	-	6.1
06NOV79	3.0	4500	75	230	49	3.9	1.5	5.9
06NOV79	18.0	500	180	40	26	1.7	1.1	4.1
06NOV79	76.0	800	160	103	54	2.1	1.0	4.3
16NOV79	5.0	720	59	81	18	1.3	1.3	5.6
16NOV79	25.0	770	170	78	35	1.6	1.1	4.0
16NOV79	43.0	490	64	64	18	1.3	1.1	4.7
16NOV79	70.0	270	31	30	9	0.9	0.4	6.3
26NOV79	8.5	370	32	54	8	2.1	0.3	6.5
26NOV79	33.5	410	39	59	11	1.5	0.3	6.6
26NOV79	53.5	370	38	49	10	1.3	0.4	6.5
26NOV79	75.0	320	38	43	12	1.3	0.5	6.5
02JUN80	2.5	320	51	170	100	-	-	5.7
02JUN80	7.5	280	47	82	49	2.4	1.5	6.0
16JUN80	-	75	40	33	33	1.3	1.0	4.6
16JUN80	-	110	38	31	28	1.0	0.8	5.1
16JUN80	-	140	46	43	42	1.5	1.2	5.2

Appendix 2.2 Parking lot total and dissolved concentrations for observed storms

Date	Time fr. start min.	Pb Tot. µg/l	Pb Dis. µg/l	Cu Tot. µg/l	Cu Dis. µg/l	Cd Tot. µg/l	Cd Dis. µg/l	pH
06NOV79	3	160	66	27	27	-	-	4.5
06NOV79	30	35	21	12	6	0.8	0.5	3.5
06NOV79	65	51	27	8	7	0.9	0.4	4.0
16JUN80	-	86	9	18	13	0.8	0.4	5.3
16JUN80	-	38	10	26	20	0.9	0.5	4.8
16JUN80	-	45	10	16	16	0.9	0.5	4.7
16JUN80	-	69	19	24	17	0.8	0.6	4.6

APPENDIX 2

Appendix 2.3 Roof area lot total and dissolved concentrations for observed storms

Date	Time fr. start min.	Pb Tot. µg/l	Pb Dis. µg/l	Cu Tot. µg/l	Cu Dis. µg/l	Cd Tot. µg/l	Cd Dis. µg/l	pH
01AUG79	1.5	35	26	29	29	-	-	4.8
01AUG79	4.5	49	36	18	18	-	-	4.4
01AUG79	8.5	49	44	36	18	-	-	4.4
01AUG79	11.5	44	35	-	-	-	-	4.4
01AUG79	15.0	41	38	46	20	-	-	4.4
09AUG79	1.5	44	29	50	35	-	-	4.5
09AUG79	8.5	46	43	52	26	-	-	4.2

Appendix 2.4 Parking lot total and dissolved metals concentrations for different particle size fractions.

Date	Particle size µm	Pb Tot. µg/l	Pb Dis. µg/l	Cd Tot. µg/l	Cd Dis. µg/l	Cu Tot. µg/l	Cu Dis. µg/l	Zn Tot. µg/l	Zn Dis. µg/l
01NOV82	10	37.0	16.00	0.86	1.15	29.0	27.0	248	228
01NOV82	25	36.0	17.00	0.70	1.16	27.0	26.0	256	248
01NOV82	50	42.0	16.00	4.00	0.82	30.0	26.0	280	256
01NOV82	100	55.0	17.00	1.04	0.95	29.0	30.0	284	248
01NOV82	200	42.0	20.00	1.02	1.42	27.0	27.0	248	248
17NOV82	10	18.0	5.00	3.18	2.50	258.0	101.0	218	195
17NOV82	25	25.2	4.90	3.10	2.28	320.0	93.0	226	191
17NOV82	50	28.0	4.70	3.22	2.28	366.0	105.0	218	188
17NOV82	100	29.6	4.50	3.16	2.34	370.0	106.0	218	180
17NOV82	200	30.8	3.80	3.90	3.30	365.0	87.0	188	164
22NOV82	10	16.9	4.00	1.58	1.42	81.0	55.0	164	164
22NOV82	25	18.3	4.10	1.50	1.70	66.5	50.5	94	110
22NOV82	50	19.9	4.10	1.64	1.46	82.0	60.0	117	110
22NOV82	100	20.9	4.30	1.50	1.18	82.0	55.0	110	102
22NOV82	200	20.5	3.80	1.36	1.12	71.0	49.5	62	78
06DEC82	10	71.0	8.20	1.22	1.00	253.0	104.0	264	226
06DEC82	25	79.0	7.50	1.46	1.00	272.0	103.0	280	234
06DEC82	50	77.0	7.20	1.54	1.18	280.0	131.0	288	234
06DEC82	100	79.0	8.75	1.08	1.12	286.0	132.0	288	250
06DEC82	200	76.0	7.00	1.08	0.90	272.0	101.0	250	202

Appendix 2.5 Parking lot solids associated metals concentrations for different particle size fractions. Weight of metal per weight of solids.

Date	Particle size µm	Pb µg/mg	Cd µg/mg	Cu µg/mg	Zn µg/mg
17NOV82	10	0.433	0.0227	5.23	0.767
17NOV82	25	0.178	0.00342	1.71	0.293
17NOV82	50	0.0625	0.00250	0.708	0.000
17NOV82	100	0.0333	0.0000	0.0556	0.148
17NOV82	200	0.03654	0.000000	0.26923	0.00000
22NOV82	10	0.92143	0.011429	1.85714	0.00000
22NOV82	25	0.07647	0.000000	0.00000	0.00000
22NOV82	50	0.07619	0.018095	0.28571	1.09524
22NOV82	100	0.03810	0.006667	0.23810	0.04762
22NOV82	200	0.00526	0.000000	0.00000	0.00000
06DEC82	10	1.06441	0.003729	2.52542	0.64407
06DEC82	25	0.14032	0.003871	0.32258	0.12903
06DEC82	50	0.00000	0.000000	0.00000	0.11111
06DEC82	100	0.00511	0.000000	0.05682	0.00000
06DEC82	200	0.00000	0.003014	0.23288	0.13699

Appendix 2.6 Parking lot solids associated metals concentrations for different particle size fractions. Weight of metal per solids surface area.

Date	Particle size µm	Pb $\mu g/mm^2$	Cd $\mu g/mm^2$	Cu $\mu g/mm^2$	Zn $\mu g/mm^2$
17NOV82	10	0.00130	0.000068	0.01572	0.00230
17NOV82	25	0.00134	0.000026	0.01284	0.00220
17NOV82	50	0.00093	0.000037	0.01057	0.00000
17NOV82	100	0.00101	0.000000	0.00168	0.00449
17NOV82	200	0.00219	0.000000	0.01612	0.00000
22NOV82	10	0.00277	0.000034	0.00558	0.00000
22NOV82	25	0.00058	0.000000	0.00000	0.00000
22NOV82	50	0.00114	0.000270	0.00426	0.01635
22NOV82	100	0.00115	0.000202	0.00721	0.00144
22NOV82	200	0.00032	0.000000	0.00000	0.00000
06DEC82	10	0.00320	0.000011	0.00758	0.00193
06DEC82	25	0.00106	0.000029	0.00243	0.00097
06DEC82	50	0.00000	0.000000	0.00000	0.00166
06DEC82	100	0.00016	0.000000	0.00172	0.00000
06DEC82	200	0.00000	0.000180	0.01394	0.00820

Appendix 3.1 Street area mean concentrations for observed storms.

Date	Duration min.	SS mg/l	Cd µg/l	Pb µg/l	Cu µg/l	Zn µg/l
19AUG79	16	56	-	129	39	155
21AUG79	46	91	-	223	52	211
02SEP79	23	189	-	998	145	-
02SEP79	26	106	-	-	-	-
11SEP79	23	124	-	541	80	-
11SEP79	30	92	-	320	56	-
17SEP79	26	71	1.50	264	36	-
17SEP79	30	45	1.00	207	26	-
31OCT79	30	42	-	607	82	-
06NOV79	80	236	-	-	-	-
16NOV79	80	197	1.20	480	55	-
26NOV79	80	139	1.62	376	53	-
02JUN80	15	162	3.00	288	101	-
16AUG80	47	-	1.43	129	29	-
28AUG80	22	39	3.66	702	91	-
17SEP80	120	77	2.16	284	49	-

Appendix 3.2 Parking lot mean concentrations for observed storms.

Date	Duration min.	SS mg/l	Cd µg/l	Pb µg/l	Cu µg/l
02SEP79	20	69	1.04	104	56
11SEP79	30	19	5.00	184	61
11SEP79	43	10	2.16	66	19
17SEP79	30	37	3.00	110	39
06NOV79	76	15	-	-	-
16AUG80	25	-	5.33	540	200
20AUG80	120	-	-	24	14
28AUG80	42	13	3.25	310	130
17SEP80	115	22	1.05	68	22

Appendix 3.3 Roof area mean concentrations for observed storms.

Date	Duration min.	SS mg/l	Cd µg/l	Pb µg/l	Cu µg/l	Zn µg/l
01AUG79	33	4.0	-	37	20	84
02AUG79	20	8.0	-	21	22	97
08AUG79	80	2.2	-	17	29	47
19AUG79	26	11.0	-	10	3	45
21AUG79	33	1.0	-	9	5	31

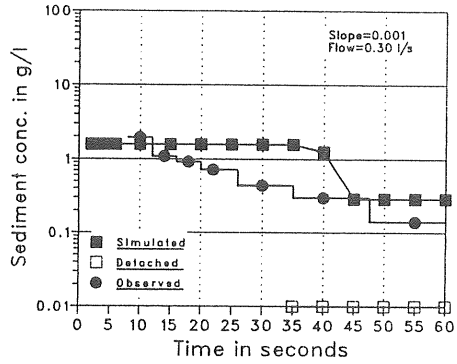

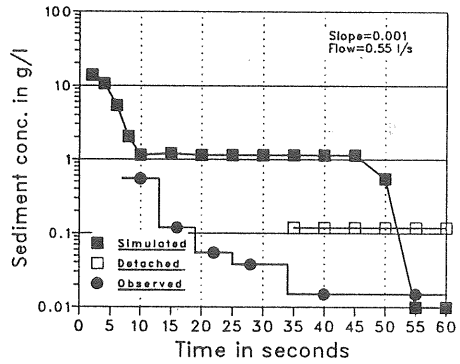

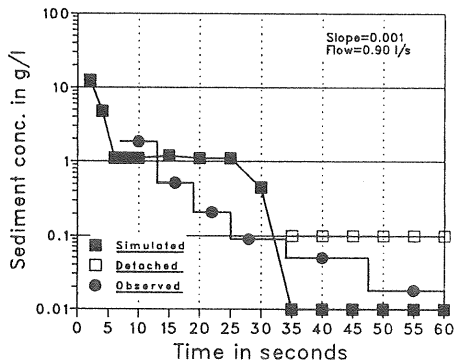

Appendix 4.1 Simulated and observed sediment concentrations for a 0.001 surface slope.

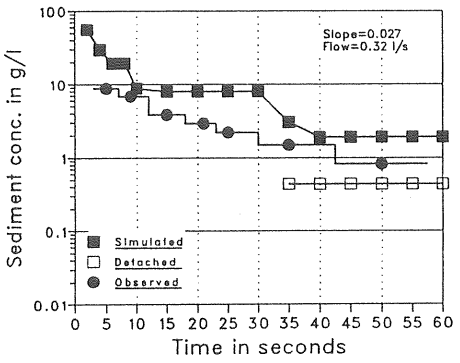

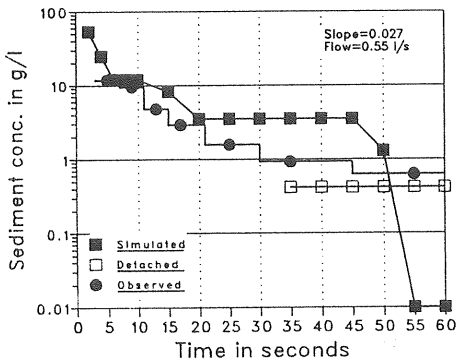

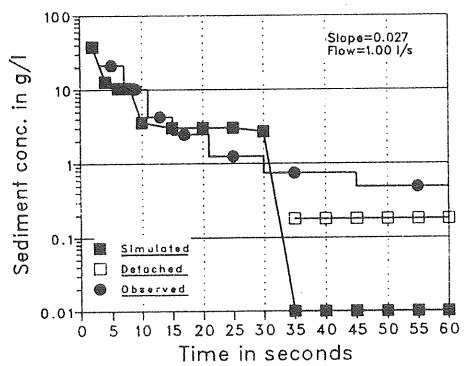

Appendix 4.2 Simulated and observed sediment concentrations for a 0.027 surface slope.

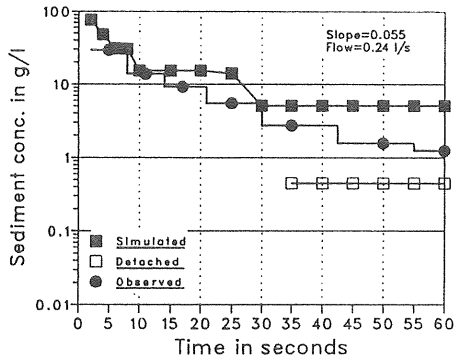

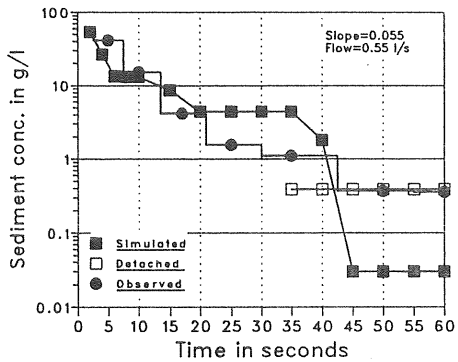

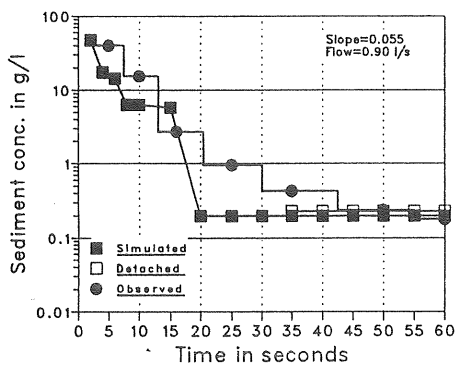

Appendix 4.3 Simulated and observed sediment concentrations for a 0.055 surface slope.

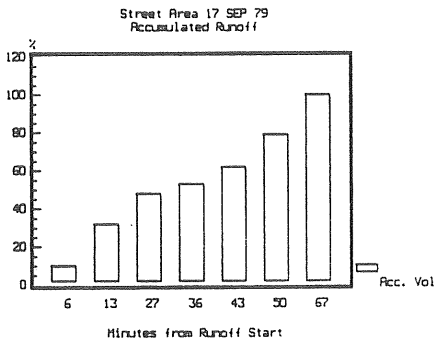

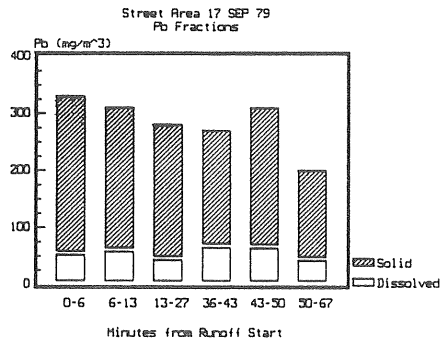

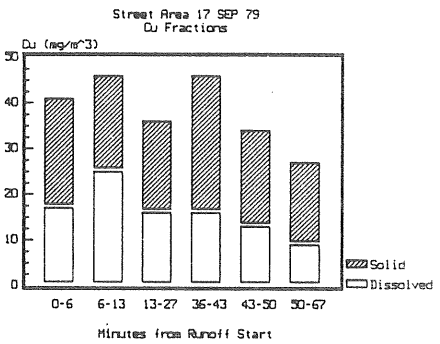

Appendix 5.1 Accumulated volume and dissolved and solids associated concentrations of Pb and Cu for the event 17 Sep. 79.

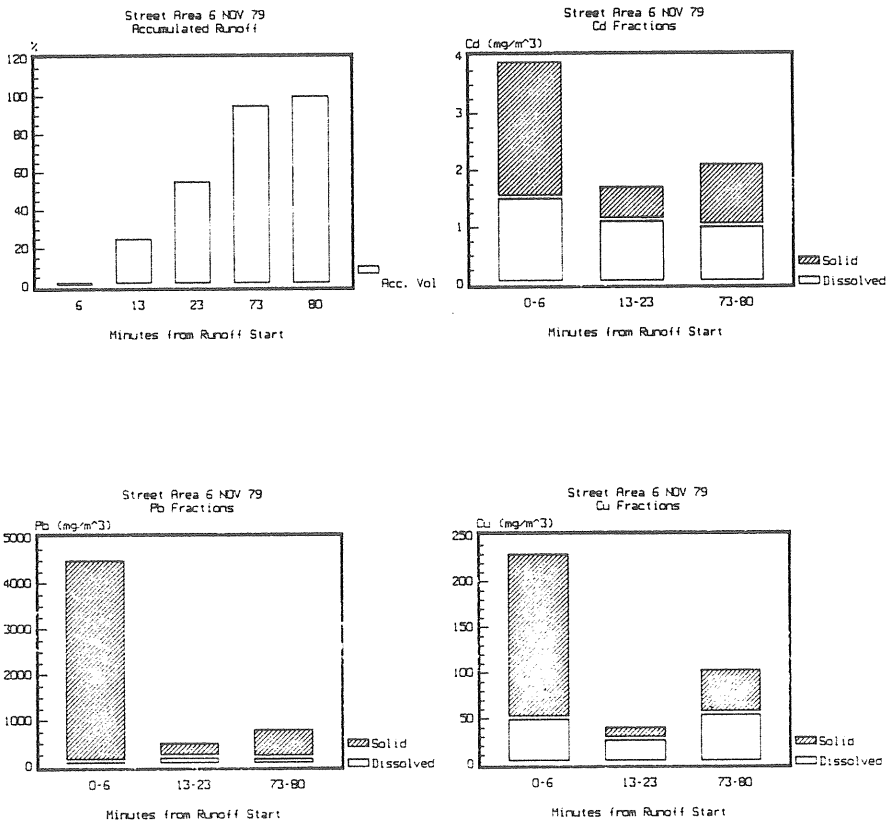

Appendix 5.2 Accumulated volume and dissolved and solids associated concentrations for Pb, Cd and Cu for the event 6 Nov. 79.

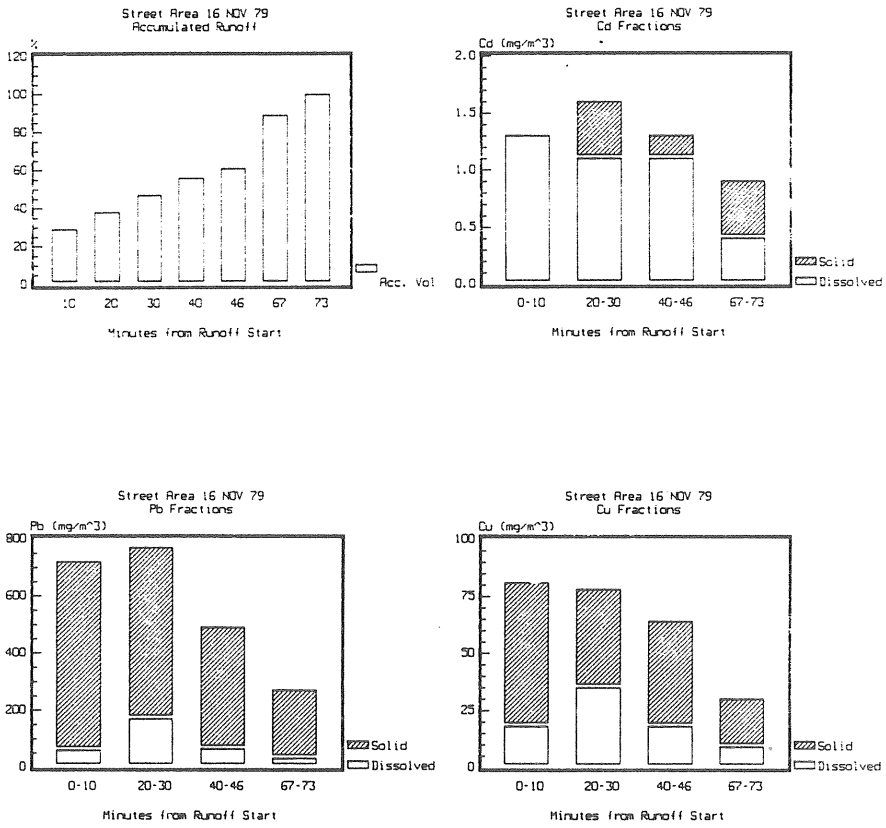

Appendix 5.3 Accumulated volume and dissolved and solids associated concentrations of Pb, Cd and Cu for the event 16 Nov. 79.

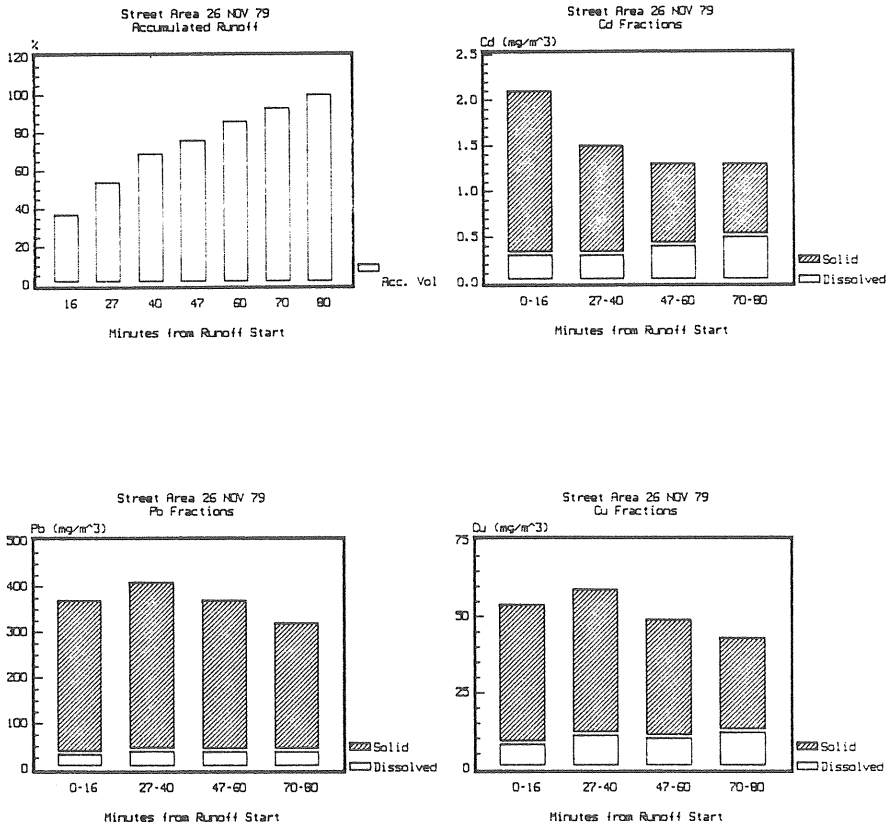

Appendix 5.4 Accumulated volume and dissolved and solids associated concentrations of Pb, Cd and Cu for the event 26 Nov. 79.

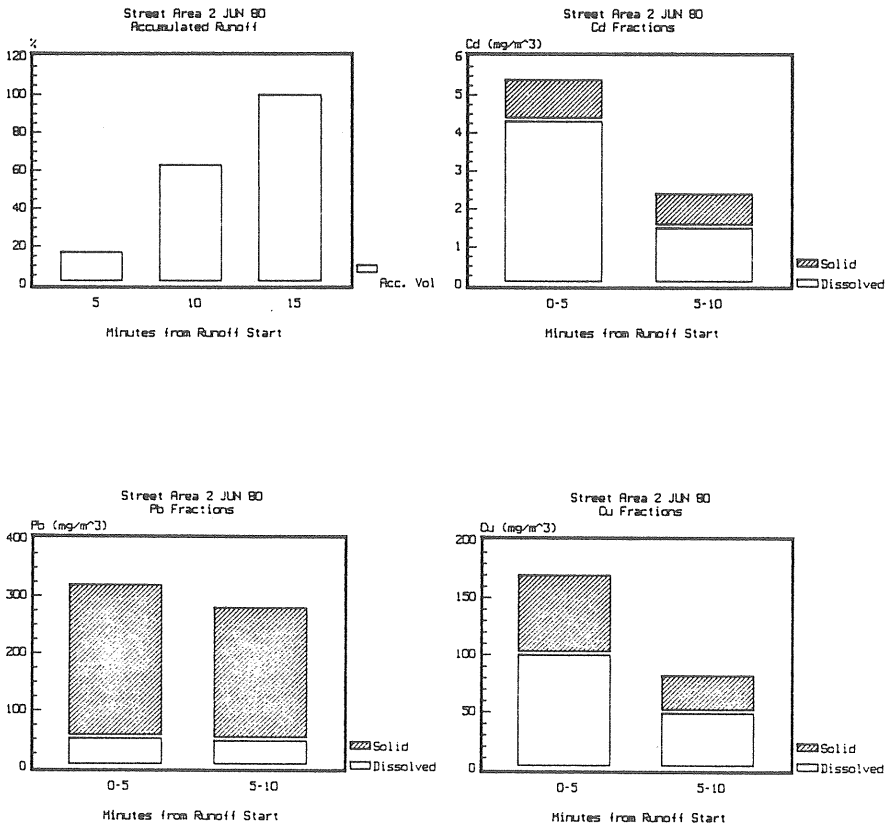

Appendix 5.5 Accumulated volume and dissolved and solids associated concentrations of Pb, Cd and Cu for the event 2 Jun. 80.

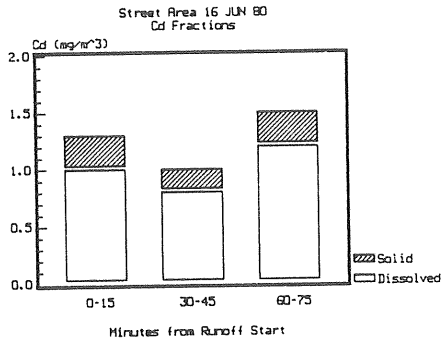

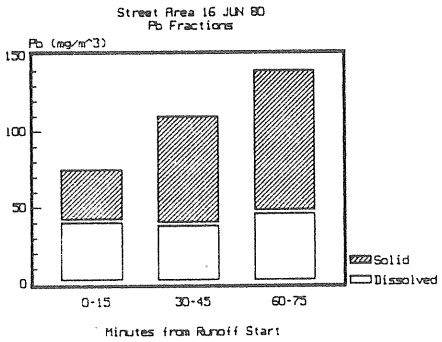

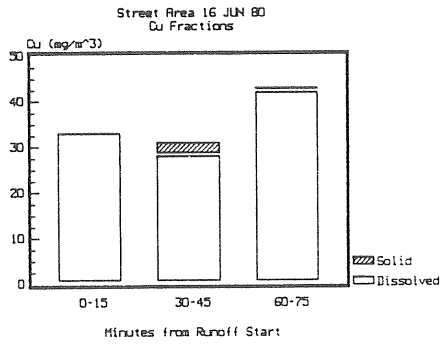

Appendix 5.6 Accumulated volume and dissolved and solids associated concentrations of Pb, Cd and Cu for the event 16 Jun. 80.